Structure-activity Relationships of Niclosamide to Overcome Colistin Resistance

by

Liam Berry

A thesis submitted to the Faculty of Graduate Studies of
The University of Manitoba
in partial fulfillment of the requirements for the degree of

DOCTOR OF PHILOSOPHY

Department of Chemistry
University of Manitoba
Winnipeg, Manitoba, Canada

Copyright © 2024 by Liam Berry

Abstract

Antibacterial resistance poses a significant threat to global healthcare systems, particularly against Gram-negative bacteria (GNB). Addressing this challenge requires urgent development of new therapies, especially given the emergence of resistance even to last-resort antibiotics like colistin. However, rising rates of colistin resistance highlight the need for alternative strategies. One promising approach involves repurposing existing drugs, such as the anthelmintic niclosamide, known to enhance colistin activity in combination therapy. Despite its potential, niclosamide faces limitations due to poor solubility, bioavailability, and off-target toxicity. Thus, repurposing it as an antibacterial agent necessitates the synthesis of new derivatives capable of overcoming these challenges. Additionally, a comprehensive exploration of niclosamide's structure–activity relationship (SAR) against GNB remains unexplored. We synthesized a series of niclosamide analogs to address these gaps, focusing on three main objectives: mitigating toxicity by replacing the nitro group, modifying the central amide moiety, and designing niclosamide-based hybrid antibiotics. Our SAR investigation led to the discovery of several lead compounds with comparable colistin-potentiating activity to niclosamide but with reduced cytotoxicity. Notably, we also identified synergy with antibiotics beyond colistin, including cefiderocol and bacitracin. Overall, our work provides critical insights into synthetic strategies for developing new niclosamide derivatives. We also demonstrate that toxicity to mammalian cells can be minimized while maintaining colistin potentiation and reveal promising avenues for repurposing niclosamide in combating antibacterial resistance.

Acknowledgements

This thesis would not be possible without the help of many others. I would like to thank the following people for their invaluable support during this journey:

My advisor, Dr. Frank Schweizer: I am grateful for the opportunity to be a part of this lab, for having the freedom to explore my own research ambitions, and for your guidance, encouragement, and support throughout this journey. Your expertise, mentorship, and constructive feedback have been instrumental in shaping the direction of my research.

My committee members, Dr. Rebecca Davis, Dr. George Zhanel, and Dr. Ayush Kumar: I extend my appreciation to each member of my thesis committee for their time, expertise, and insightful comments. Your diverse perspectives and challenging questions during committee meetings have enriched the quality of this work.

Colleagues and peers: I would like to thank every member of the Schweizer research group who I have had the pleasure to work alongside over the years, and for the undergraduate students I have had the opportunity to mentor. Our discussions, debates, and friendly chats have helped me to grow as a scientist and kept me sane during this process. Special thanks to my mentor, Dr. Ronald Domalaon, for training me as an undergraduate student and always being available to chat about research or life.

Family, Mom, Dad, and Dylan: Thank you for always being there for me, for helping me throughout my undergraduate and graduate studies, and for always asking me about my research, even when my explanations made little sense. Your support has been invaluable during this process.

Shin: You have been an amazing source of support and motivation. Your love, companionship and belief in me have fueled my determination. You were my rock during challenging times. This achievement is as much yours as it is mine, and I am grateful for the journey we have shared together.

There are many other people, too numerous to list here, who have helped me during this journey. Thank you. I am humbled by the support I have received.

But most of all, I would like to thank my dog, Tucker. Thank you for forcing me to get outside and move after hours hunched over a computer, and for being an endless bundle of joy.

Table of Contents

List of Figures

List of Tables

CHAPTER ONE:
Colistin as a therapeutic agent against Gram-negative bacteria

1.1: The problem of antimicrobial resistance and ESKAPE pathogens

The widespread and ever-increasing threat of antimicrobial resistant (AMR) "superbugs" presents a significant danger to the global healthcare system.[1] A recent report has estimated that in 2019, 1.27 million deaths globally were directly attributable to bacterial AMR, with 4.95 million deaths associated with AMR.[2] The World Health Organization (WHO), in 2017, compiled a comprehensive inventory of priority pathogens with a focus on 12 bacterial families. This roster was segmented into three stratifications: critical, high, and medium. Among these, *Enterococcus faecium, Staphylococcus aureus, Klebsiella pneumoniae, Acinetobacter baumannii, Pseudomonas aeruginosa*, and various Enterobacter species, collectively referred to as ESKAPE pathogens[3], were designated "priority status".[4]

Gram-negative bacteria (GNB) have garnered particular attention due to their highly restrictive outer membrane (OM) structure which limits the entry of many antibiotics into the cell, relative to Gram-positive bacteria. This results in Gram-negative bacteria being intrinsically resistant to many antibiotics that are active against Gram-positive bacteria.[5] Other forms of intrinsic resistance include the presence of efflux pumps: transmembrane proteins that expel antibiotics out of the cell rendering them ineffective.[6] Entering the intracellular environment of GNB is thus challenging for many molecules.

In addition to intrinsic resistance mechanisms, bacteria are also able to develop resistance to antibiotics by producing enzymes which modify the antibiotic, rendering it inactive. The most common examples of these are the β-lactamases and the aminoglycoside-modifying enzymes.[7] β-lactamases degrade β-lactam antibiotics such as penicillin by hydrolyzing the key β-lactam ring, preventing the drug from binding to penicillin binding proteins. β-lactamases are grouped into four classes: A, B, C, and D. Class A, C and D β-lactamases are serine-dependent and typically have a narrow substrate spectrum whereas class

B β-lactamases (metallo-β-lactamases) typically employ zinc in the active site and are able to hydrolyze virtually all β-lactam antibiotics.[8,9] Aminoglycoside-modifying enzymes confer resistance to aminoglycosides such as tobramycin by modifying the aminoglycoside structure including phosphorylation, N-acylation and others thereby preventing the aminoglycoside from binding to the ribosome.[10,11]

Modification of the target of an antibiotic is another method of inducing antibiotic resistance. Ribosomal modification can alter the structure of the ribosome in such a way that aminoglycosides or tetracyclines are no longer able to bind to the ribosome, while ribosomal function is maintained.[12] Similarly, DNA gyrase and topoisomerase IV modification can lead to resistance to fluoroquinolone antibiotics.[13]

In light of the looming threat of AMR, new therapeutic options are being explored. Given the lack of antibiotic development in recent decades,[14] clinicians have been forced to utilize a variety of therapeutic approaches. Combination therapy, where two or more antibiotics are administered simultaneously, is one such approach.[15] Antibiotics that were once considered too toxic have also seen increased usage in the clinic as current treatment options fall short, such as the antimicrobial peptide colistin.[16–18]

1.2: Clinical use of polymyxin antibiotics and colistin

The emergence and widespread occurrence of multidrug-resistant (MDR) bacterial infections has led to a lack of effective antibiotics in the clinic. [19] Additionally, limited success of drug development programs to develop new classes of antibiotics has led to the re-introduction of colistin as a drug of last resort.[20] Colistin is a cyclic cationic lipopeptide

antibiotic, originally isolated in the 1940's from *Paenibacillus polymyxa* and first introduced in the clinic in the 1950's. However, clinical usage of colistin was limited due to severe side effects such as nephrotoxicity and neurotoxicity. Colistin usage gradually increased in the 1990's to combat rising rates of MDR infections, as existing treatment options were rendered less effective.[21] Colistin is part of the polymyxin family of antimicrobial peptides and is also known as polymyxin E. The polymyxins are a structurally diverse family of antibiotics and a consensus as to whether clinically significant differences in toxicity and efficacy exist between members of this family has not been established.[22] Regardless, colistin (primarily as an intravenous formulation) and polymyxin B (primarily as a topical formulation) are the only polymyxins currently used clinically.[17]

Colistin was first used in the clinic in the 1940s when few treatment options existed for GNB relative to Gram-positive organisms but was abandoned in the 1970s due to severe side effects including nephrotoxicity and neurotoxicity.[23] As rates of MDR GNB increased and treatment options for problematic pathogens such as *A. baumannii, P. aeruginosa* and *K. pneumoniae* dwindled (and understanding of pharmacokinetics and proper dosing of colistin increased), clinical use of colistin has re-emerged. Colistin is administered parenterally as the inactive prodrug colistin methanesulfonate (CMS) which incorporates sulfomethyl groups appended to the primary amine side chains of Dab.[24] This prodrug formulation is significantly less toxic than colistin and the sulfomethyl groups are hydrolyzed *in vivo* after administration. [23] One of the reasons that understanding of colistin toxicity and dosing has improved in recent years is due to improved bioanalytical methods that are able to differentiate between CMS and colistin and monitor the conversion over time *in vivo.* [24]

The structures of several members of the polymyxin family including colistin

(polymyxin E) are shown in **Figure 1.1**. Polymyxins consist of a ten amino acid sequence, interestingly incorporating several L-2,4-diaminobutyric acid (Dab) moieties and a lipid tail acylated to the N-terminus.[25] They are cyclic peptides, cyclized via amide bond formation between the primary amine on the Dab4 side chain and the C-terminus on Thr10 forming a cyclic heptapeptide core and a linear tripeptide tail. The amino acid sequence is mostly conserved between polymyxins, with differences occurring at position 6 (D-Phe in polymyxin B, D-Leu in polymyxin E) and at the lipid tail, which vary in structure. As polymyxins are natural products isolated from living organisms with very small differences in chemical structure (Polymyxin E_1 differs from E_2 by a single carbon atom in its lipid tail) they are typically difficult to separate and are referred to as asingular entity (such as colistin). Significant differences in activity or toxicity between polymyxin E_1 and E_2 has not been observed and therefore colistin is administered as a mixture of variable composition.[22]

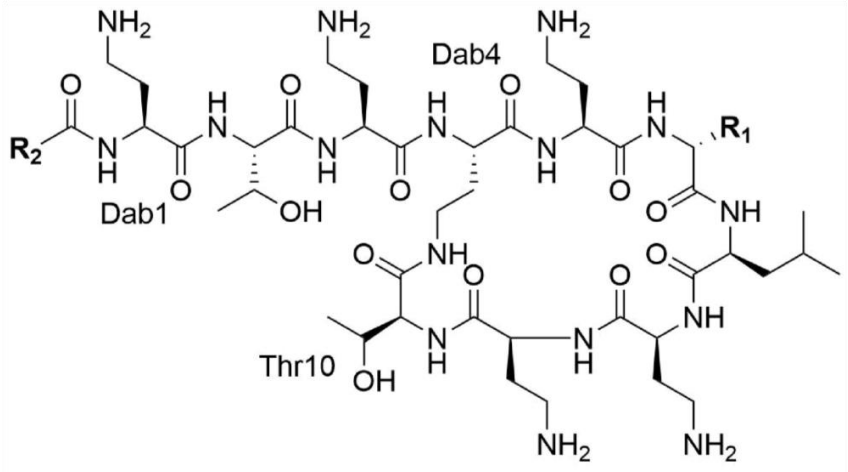

Polymyxin	R_1	R_2
B_1	D-Phe	(*S*)-6-methyloctanoyl
B_2	D-Phe	6-methylheptanoyl
E_1	D-Leu	(*S*)-6-methyloctanoyl
E_2	D-Leu	6-methylheptanoyl

Figure 1.1 Structure of polymyxins B_1, B_2, E_1 and E_2.

Colistin is completely inactive against Gram-positive bacteria and some species of GNB that are intrinsically resistant (such as *Burkholderia cepacia*) but possesses potent activity against most wild-type and MDR strains of *P. aeruginosa*, *A. baumannii* and Enterobacteriaceae. [26] Current Clinical and Laboratory Standards Institute (CLSI) guidelines have established intermediate and resistance breakpoints of ≤2 μg/mL and ≥4 μg/mL respectively for *P. aeruginosa* and *A. baumannii*, but do not recommend breakpoints for Enterobacteriaceae,instead defining colistin MICs of ≤2 μg/mL as wild-type and ≥4 μg/mL as non-wild-type.[27] The only suitable reference method for MIC determination is broth microdilution. A recent discovery that complicates *in vitro* MIC data is that can bind to many laboratory materials including glass, polystyrene, and polypropylene. This binding is non-specific and highly variable, decreasing effective colistin concentration in solution anywhere from 4%-62% and casting doubt as to how translatable *in vitro* susceptibility data is to *in vivo* results.[28] However, *in vivo* results reveal that colistin is bactericidal at concentrations higher than 0.5 x MIC, displaying rapid concentration-dependent killing.[29]

The plasma concentration over time of both CMS and colistin in healthy volunteers has been studied.[24] After a 1 hour intravenous infusion of 80 mg CMS, CMS plasma concentrations peaked at 4.8 mg/L before declining with a half-life of 0.5 h. 2 h after infusion started, the active compound colistin concentration peaked before declining with a half-life of 3 h, significantly higher than the half-life of CMS indicating that CMS is converted to colistin much faster than colistin is eliminated. [23] Colistin distribution has been shown to be restricted to the extracellular space, as it has a large molecular weight and is highly charged leading to challenges crossing cellular membranes.[30] Although colistin is a peptide, it is surprisingly stable to exopeptidases

and has a longer half-life than most peptides, mainly due to its cyclic structure and hydrophobic lipid tail.[24] Colistin renal clearance is very low (1.9 mL/min) primarily due to extensive tubular reabsorption. This is thought to be due to the polycationic nature of colistin and is presumed to explain part of colistin's nephrotoxicity.[31] Improvements in bioanalytical methods have improved the utility of colistin and have resulted in much safer administration, lowering rates of nephrotoxicity from 50% in older studies to 15-25% in recent times. [31]

Despite the use of colistin as a last line of defense against MDR infections and its potent bactericidal activity, colistin resistance has emerged and is a growing threat.[32] If this trend continues, and if drug development programs fail to discover novel antibiotics, humanity may be left with no effective agents with which to combat MDR bacterial infections.

1.3: Colistin mechanism of action and resistance

The key structural features that contribute to colistin's antibacterial activity are its overall amphiphilic structure and the basic Dab amino acids.[25] The primary amine side chains are basic and protonizeable at physiological pH, conferring a net positive charge to colistin. The positively charged amine groups are able to electrostatically interact with the lipid A portion of lipopolysaccharide (LPS) embedded in the outer membrane of Gram-negative bacteria. Lipid A contains negatively charged phosphate groups which are normally bridged by divalent cations such as Mg^{2+} and Ca^{2+}.[33] The electrostatic interaction between the cationic colistin and the anionic phosphate groups leads to displacement of these divalent cations, resulting in outer membrane destabilization. The lipid tail of colistin is then able to interact with the phospholipid bilayer of the membrane, further compromising its integrity. The hydrophilic Thr and

hydrophobic Leu side chains are also important in this interaction as colistin adopts a very specific 3-dimensional conformation, such that the polar and non-polar domains form two distinct faces, leading to increased LPS binding affinity.[25] After this interaction occurs, colistin ruptures the outer membrane and transits the periplasmic space via a self-promoted uptake mechanism, leading to inner membrane destabilization and eventual cell lysis and cell death.[34]

Although the interaction between colistin and lipid A has been well studied and thoroughly documented, other hypotheses about how colistin is able to disrupt the inner membrane of GNB exist. The previously described mechanism, the "membrane lysis" mechanism, is currently the most accepted mechanism. However, a "vesicle-vesicle contact" mechanism has also been proposed, where the action of colistin binding to LPS induces contact between the periplasmic surfaces of the outer and inner membranes.[35] This contact promotes phospholipid exchange between membranes, resulting in membrane destabilization and an osmatic imbalance resulting in cell death.

In addition to membrane lysis and vesicle-vesicle contact mechanisms, secondary targets for colistin have also been proposed in recent years. Recently, Deris *et al.* have reported that colistin is also able to inhibit bacterial respiration via inhibition of type 2 nicotinamide adenine dinucleotide dehydrogenase (NDH-2).[36] Although the precise mechanism for this interaction is unknown, NDH-2 is embedded in the inner membrane of bacteria and once colistin disrupts this membrane it may also affect the structure and function of NDH-2.

Another secondary mechanism of action that is under some dispute involves the formation ofhydroxyl radicals (OH•). Sampson *et al.* proposed that colistin induces rapid killing of *Acinetobacter baumannii* via a hydroxyl radical death pathway.[37] However, Brochmann et al.were unable to confirm these results and showed that prevention of OH•

accumulation in *P. aeruginosa* did not prevent colistin from killing the bacteria.[29] Alternative mechanisms of action for colistin are currently not well studied, and more work needs to be done in order to decipher the precise mechanism(s) of bactericidal activity.

Despite colistin's use as a drug of last resort, resistance has been observed and rates are increasing.[38] In fact, pandrug-resistant infections that are completely untreatable with conventional antibiotics have already claimed the lives of several patients.[39] It is imperative that colistin resistance is studied, monitored, and understood. As the fundamental target for colistin's action, LPS modification is implicated in the majority of colistin resistance mechanisms.[40] Removing the negative charge on the phosphate groups of lipid A prevents the cationic colistin from electrostatically interacting with the cell surface. The phosphate groups are typically alkylated with basic moieties such as 4-amino-L-arabinose, phosphoethanolamine or galactosamine, conferring an overall positive charge which effectively repels colistin molecules.[41] Typically, addition of 4-amino-L-arabinose results in an increase in colistin minimum inhibitory concentration (MIC) to 512 μg/ml, while addition of phosphoethanolamine confers lower levels of resistance, decreasing colistin susceptibly by between 4- and 128-fold. The expression of the genes required for addition of these groups is regulated differently between species but is primarily controlled by the action of two-component signal transduction systems PmrAB and PhoPQ.[42] In *P. aeruginosa* these systems can be activated in response to many factors such as low Mg^{2+} conditions, the presence of antimicrobial peptides (such as colistin), and changes in intracellular pH. In *E. coli*, modification of LPS with cationic residues can be triggered [38]

Other modifications to LPS, although rare, have been reported to increase resistance to colistin. Recently, a novel resistance mechanism has been observed in *P. aeruginosa* which is

characterized by the deacylation of lipid A.[43] The amount of penta-acylated lipid A, in comparison to the normally hexa-acylated lipid A, was found to increase substantially in both colistin susceptible and colistin resistant *P. aeruginosa* after exposure to colistin. This results in denser packing of the penta-acylated lipid A headgroups and a reduced ability for the hydrophobic tail of colistin to interact with the fatty acyl chains of lipid A. Overall, lipid A deacylation results in resistance to colistin, especially in combination with the previously mentioned addition of cationic residues to the phosphate groups of lipid A.[43]

Another drastic method of colistin resistance which has only been observed in *A. baumannii* is the complete loss of LPS and lipid A from the cell surface. [44] Unsurprisingly, this results in extremely high levels of colistin resistance (>256 µg/ml) as colistin is now completely unable to interact with the outer membrane. Loss of LPS can occur as a result of mutations in several genes involved inLPS biosynthesis, particularly lpxA, lpxC and lpxD. These mutations have been observed in a small number of clinical isolates of colistin resistant *A. baumannii* but are also associated with an overall decrease in virulence and bacterial fitness. This mechanism of resistance is also not clinically significant as the loss of LPS makes the outer membrane of *A. baumannii* highly permeable, increasing susceptibility towards many other classes of antibiotics. Nonetheless, this resistance mechanism reveals that bacteria are able to adopt drastic changes in physiology in order to survive in the presence of colistin. New resistance mechanisms to colistin are expected to emerge or may even be undiscovered in current isolates and must be studied in order to maintain colistin's effectiveness as a drug of last resort for MDR infections. [45]

In order to solve the challenges of colistin resistance, extensive effort in recent years has been devoted to developing new polymyxin antibiotics. The goals of these programs are to

enhance activity, overcome polymyxin resistance and reduce toxicity.

1.4: Recent advancements in new polymyxins

The increase in colistin usage in recent years as well as rising rates of resistance has led to several new drug development programs aimed at producing the next generation of polymyxin-like lipopeptides.[46] Extensive structure activity relationship (SAR) studies have revealed key structural features on the colistin molecular scaffold, indicating which groups are amenable to modification. Briefly, most amino acids cannot be modified without losing activity, with the exception of Dab1 and the hydrophobic amino acids at position 6 and 7 (D-Leu for colistin) which can be replaced by other hydrophobic moieties. The N-terminal lipid tail can also be modified with a wide variety of groups.[25]

Incorporating this SAR knowledge and considering the previously discussed resistance mechanisms, namely modification of LPS to reduce the negative charge, rational design of a new polymyxin derivative at Monash University produced an agent (FADDI-002) which is effective against colistin-resistant *P. aeruginosa, A. baumannii* and *K. pneumoniae.*[46] (**Figure 1.2**). FADDI-002 contains the non-natural amino acid L-octylglycine at position 7, conferring additional hydrophobicity relative to polymyxin B, which presumably enhances hydrophobic interactions with lipid A and overcomes the disruption in polymyxin-LPS interactions in resistant strains. Interestingly, FADDI-002 and other related molecules also possess activity against Gram- positive organisms (MICs of 4-8 μg/mL against vancomycin-resistant *Enterococcus faecium* andmethicillin-resistant *Staphylococcus aureus*) which is not seen in other polymyxins.

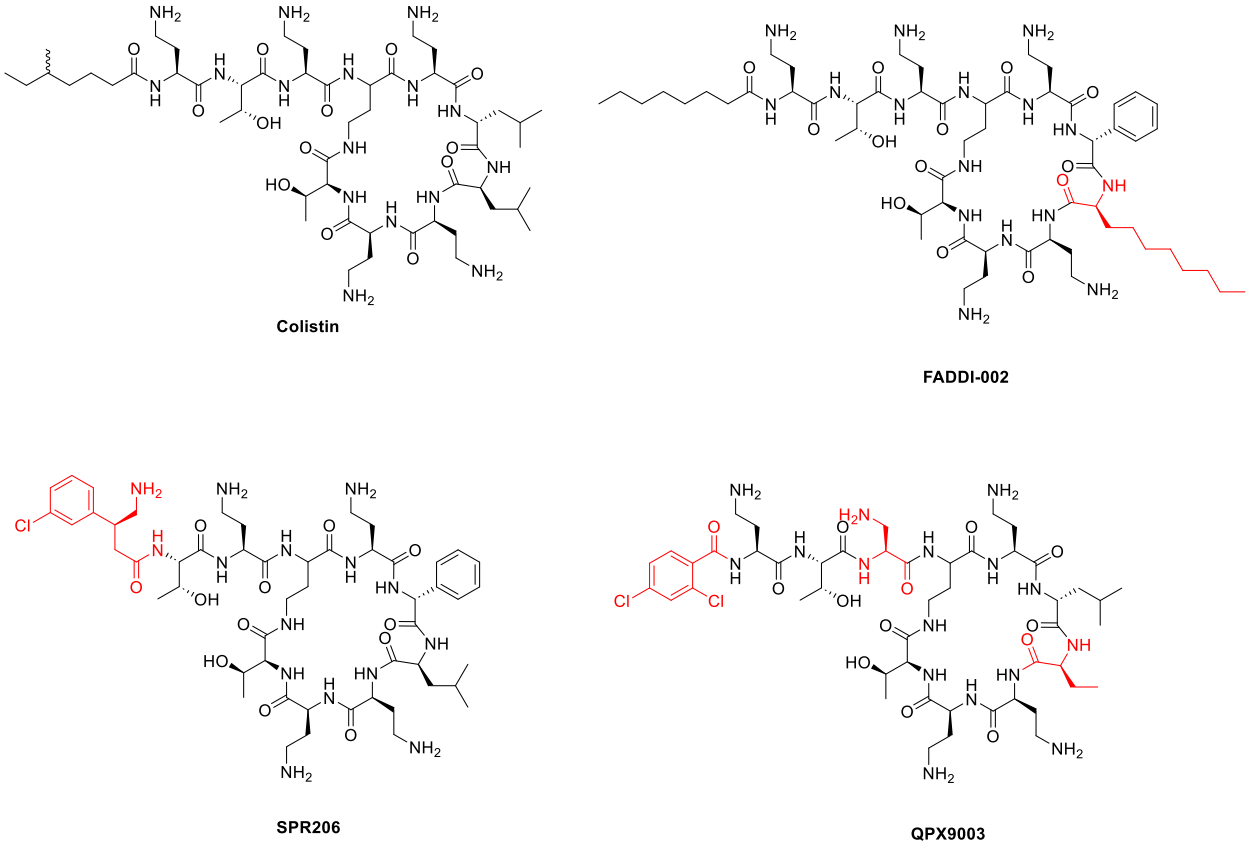

Figure 1.2: Structure of colistin and novel derivatives FADDI-002, SPR206 and QPX9003. Structural differences from existing polymyxins are highlighted in red.

SPR206 is another novel polymyxin derivative, currently in development by Spero Therapeutics.[47] The goal of this program was to enhance antibacterial potency while reducing nephrotoxicity. The key modification that SPR206 incorporates is the replacement of the Dab1 residue and the fatty-acyl chain with an aminobutyrate N-terminus, substituted at the *β*-position with a chlorobenzyl moiety. SPR206 showed slightly enhanced (2-fold) activity compared to colistin, but with drastically reduced kidney accumulation. A successful phase-1 trial was reported[48] where no appreciable accumulation occurred with repeated dosing of SPR206. In addition, no evidence of nephrotoxicity was observed over 14 days of a dosing regimen anticipated to exceed requirements for clinical efficacy.

The Li lab at the University of Melbourne has also reported a series of novel polymyxins by optimizing for multiple parameters simultaneously: antibacterial activity, nephrotoxicity, acute toxicity, lung drug exposure, and lung surfactant binding.[49] They also developed a mouse model to screen for nephrotoxicity, which is more reliable than cell-based toxicity assays. The culmination of their efforts resulted in a novel polymyxin analog that is currently being developed by Qpex Biopharma, QPX9003. This molecule incorporates changes at positions 3, 6 and 7 when compared to colistin, and subtle structural changes at these positions led to pronounced changes in potency and toxicity. The N-terminal lipid was replaced by a dichlorophenyl moiety, Dab3 was replaced by Dap3, and Leu7 was replaced by Abu7. Diaminopropionic acid (Dap) differs from Dab by the loss of a single methylene unit in the side chain. Aminobutyric acid (Abu) differs from Leu by the loss of an isobutyl group. Overall, it was found that reducing hydrophobicity in the amino acid side chains results in a reduction in toxicity. (**Figure 1.2**). Phase 1 clinical trials of QPX9003 are ongoing (NCT04808414).

Another approach that is being explored is the use of polymyxin-based adjuvants (molecules which increase the activity of other drugs when used in combination therapy) to treat MDR GNB infections.[50] The most well-known of such adjuvants is polymyxin B nonapeptide (PMBN) which is generated from cleavage of the Dab1 residue and the lipid tail from polymyxin B.[51] Although this compound lacks inherent antimicrobial activity due to the absence of the lipid tail which is key for outer membrane lysis, it is still able to bind strongly to LPS and disrupt its integrity, rendering the outer membrane more permeable to other antibiotics. In fact, PMBN is one of the best-known membrane permeabilizing agents for GNB.[52] The removal of the hydrophobic lipid tail removes the amphiphilic nature of the molecule, which results in a significant reduction in acute toxicity and nephrotoxicity. Reducing the amount of

positive charges (from 5 in colistin to 4 in PMBN) also appears to play a role in nephrotoxicity. Spero Therapeutics has recently developed a similar polymyxin derivative for adjuvant therapy, SPR-741, which replaces Dab1 and the lipid tail of polymyxin B with an acetyl group and replaces Dab3 with a Ser residue in an effort to further reduce nephrotoxicity (**Figure 1.3)**. The renal clearance of SPR-741 is ~400-fold higher than that of colistin, and SPR-741 is now in clinical development as an antibiotic potentiator.[53,54] SPR-741 has shown the ability to enhance the potency of more than 20 existing antibiotics against GNB in combination therapy and has completed phase 1a and 1b clinical trials.

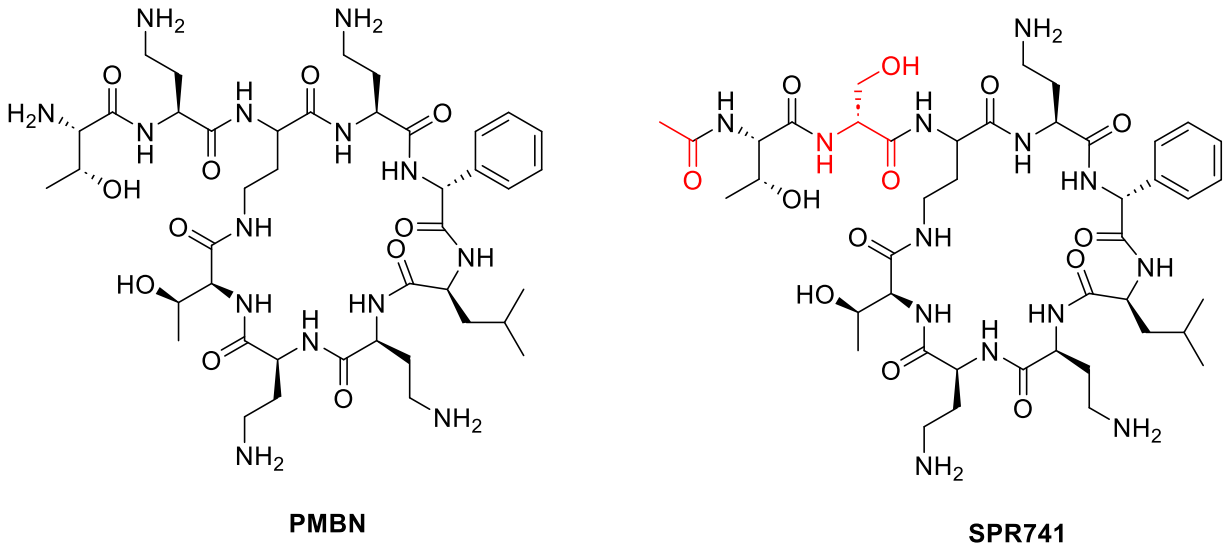

Figure 1.3: Structure of PMBN and SPR741. Structural differences are highlighted in red.

New derivatives of colistin and new approaches (such as combination therapy) may hold the key to overcoming colistin resistance when combined with proper antimicrobial stewardship to prevent resistance rates from increasing further.

1.5: Combination and adjuvant therapy with colistin

As an alternative to developing new polymyxin derivatives, colistin-based combination therapy has also been explored. The goal of combination therapy is to enhance the activity of colistin by using an additional antibiotic treatment, which may overcome resistance to colistin, suppress resistance development and allow for lower dosages of colistin and thus less toxic side effects.[55] Several colistin combinations that display in *vitro synergy* have been explored clinically including colistin + meropenem, colistin + rifampicin, and colistin + minocycline.[56] Colistin + meropenem was shown in one study to result in lower mortality rates and higher microbial eradication of carbapenem-resistant *MDR A. baumannii.*[57]

Another form of colistin combination therapy that has gained prominence in recent years, is the use of adjuvant therapy. Adjuvants are enhancer molecules that increase the activity of other antibiotics when used in combination therapy, and several classes of adjuvants for various antibiotics have been reported.[58,59] Adjuvants are usually inhibitors of efflux pumps, inhibitors of degradation enzymes or membrane permeabilizers. Ideally, the adjuvant should be devoid of potent intrinsic antibacterial activity to reduce the risk of selecting for resistance. Overall, the function of an adjuvant is to augment activity and ideally efficacy of a partner antibiotic.[50] A class of adjuvants with widespread clinical success are β-lactamase inhibitors, which are now usually proscribed in combination with β-lactam antibiotics.[60]

Adjuvant therapy for colistin has generated much interest, with several classes of molecules being reported that are able to overcome colistin resistance in combination therapy and/or enhance the activity of colistin such that lower doses can be used with reduced toxicity.[61]

One prominent strategy involves inhibiting fatty acid synthesis of GNB in combination with colistin. Carfrae et al. have reported the ability of the biotin biosynthesis inhibitor, MAC13772, to synergize with colistin exclusively against colistin-resistant bacteria.[62]

Inhibiting fatty acid biosynthesis was shown to lead to changes in phospholipid composition of the OM, restoring colistin sensitivity in colistin-resistant organisms.[62] Other fatty acid synthesis inhibitors were also shown to be efficacious in combination with colistin, potentially opening a new target in the search for new colistin adjuvants.[62]

Another interesting class of molecules are 2-aminoimidazole based adjuvants which are able to down regulate the PmrAB two-component signaling system in *A. baumannii*. [63] This downregulation is responsible for reversal of lipid A modification, and thus breaking colistin-resistance in *mcr-1* positive strains. Lead compounds enabled a 1000-fold reduction in the minimum inhibitory concentration of colistin in vitro, and showed efficacy in a *Galleria mellonella* infection model, demonstrating the potential therapeutic utility of these molecules. [63]

ArnT, a cytoplasmic membrane enzyme, was recently shown to be responsible for lipid A aminoarabinosylation and was thus selected for virtual screening for potential colistin adjuvants.[64] A potential inhibitor, BBN149 was discovered and was demonstrated to synergize with colistin against colistin-resistant *P. aeruginosa*, restoring activity. ArnT was also used a target for medicinal chemistry efforts to develop the *ent*-beyerane diterpene scaffold as a colistin adjuvant.[65]

One of the most promising colistin adjuvants reported to date is the anthelmintic drug niclosamide, approved for the treatment of tapeworm infections, which has recently been shown to have antimicrobial activity against Gram-positive bacteria, as well as synergizing with colistin against Gram-negative bacteria.[66–68] The combination of niclosamide and colistin has been found to be synergistic across a wide variety of colistin-susceptible and colistin-resistant Gram-negative bacteria. Our group has previously reported that niclosamide is able to enhance

colistin activity by up to 2048-fold against *P. aeruginosa*, overcoming resistance in all strains tested.[67] The following chapter will explore niclosamide as a potential target for drug repurposing programs against a variety of diseases, and describe the utility of niclosamide as an adjuvant to overcome colistin resistance.

1.6: Conclusions

The rising threat of AMR infections and the dwindling antibiotic pipeline has resulted in the resurrection of colistin, which was once considered too toxic for clinical use. However, as scientific breakthroughs led to an increased understanding of colistin's mechanism of action, pharmacokinetics, and bacterial resistance mechanisms, colistin can now be effectively used to combat infections with no remaining treatment options. Rates of colistin resistance must be controlled where possible, and resistance mechanisms must be studied in order to design new derivatives of colistin that are effective even against bacteria that have developed resistance to all conventional antibiotics. Recent years have shown the development of a number of promising polymyxin derivatives that may overcome the challenges of toxicity and colistin resistance. Combination therapy of colistin with adjuvant molecules will likely play a role in future development of colistin therapies, especially as rates of AMR increase globally. Several classes of potential colistin adjuvants have been reported, with niclosamide demonstrating particular interest for future development.

1.7: References

1. Thabit, A. K.; Crandon, J. L.; Nicolau, D. P. *Expert Opin Pharmacother* **2015**, *16* (2), 159–177.

2. Murray, C. J. L.; Ikuta, K. S.; Sharara, F.; Swetschinski, L.; Robles Aguilar, G.; Gray, A.; Han, C.; Bisignano, C.; Rao, P.; Wool, E.; Johnson, S. C.; Browne, A. J.; Chipeta, M. G.; Fell, F.; Hackett, S.; Haines-Woodhouse, G.; Kashef Hamadani, B. H.; Kumaran, E. A. P.; McManigal, B.; Achalapong, S.; Agarwal, R.; Akech, S.; Albertson, S.; Amuasi, J.; Andrews, J.; Aravkin, A.; Ashley, E.; Babin, F.-X.; Bailey, F.; Baker, S.; Basnyat, B.; Bekker, A.; Bender, R.; Berkley, J. A.; Bethou, A.; Bielicki, J.; Boonkasidecha, S.; Bukosia, J.; Carvalheiro, C.; Castañeda-Orjuela, C.; Chansamouth, V.; Chaurasia, S.; Chiurchiù, S.; Chowdhury, F.; Clotaire Donatien, R.; Cook, A. J.; Cooper, B.; Cressey, T. R.; Criollo-Mora, E.; Cunningham, M.; Darboe, S.; Day, N. P. J.; De Luca, M.; Dokova, K.; Dramowski, A.; Dunachie, S. J.; Duong Bich, T.; Eckmanns, T.; Eibach, D.; Emami, A.; Feasey, N.; Fisher-Pearson, N.; Forrest, K.; Garcia, C.; Garrett, D.; Gastmeier, P.; Giref, A. Z.; Greer, R. C.; Gupta, V.; Haller, S.; Haselbeck, A.; Hay, S. I.; Holm, M.; Hopkins, S.; Hsia, Y.; Iregbu, K. C.; Jacobs, J.; Jarovsky, D.; Javanmardi, F.; Jenney, A. W. J.; Khorana, M.; Khusuwan, S.; Kissoon, N.; Kobeissi, E.; Kostyanev, T.; Krapp, F.; Krumkamp, R.; Kumar, A.; Kyu, H. H.; Lim, C.; Lim, K.; Limmathurotsakul, D.; Loftus, M. J.; Lunn, M.; Ma, J.; Manoharan, A.; Marks, F.; May, J.; Mayxay, M.; Mturi, N.; Munera-Huertas, T.; Musicha, P.; Musila, L. A.; Mussi-Pinhata, M. M.; Naidu, R. N.; Nakamura, T.; Nanavati, R.; Nangia, S.; Newton, P.; Ngoun, C.; Novotney, A.; Nwakanma, D.; Obiero, C. W.; Ochoa, T. J.; Olivas-Martinez, A.; Olliaro, P.; Ooko, E.; Ortiz-Brizuela, E.; Ounchanum, P.; Pak, G. D.; Paredes, J. L.; Peleg, A. Y.; Perrone, C.; Phe, T.; Phommasone, K.; Plakkal, N.; Ponce-de-Leon, A.; Raad, M.; Ramdin, T.; Rattanavong, S.; Riddell, A.; Roberts, T.; Robotham, J. V.; Roca, A.; Rosenthal, V. D.; Rudd, K. E.; Russell, N.; Sader, H. S.; Saengchan, W.; Schnall, J.; Scott, J. A. G.; Seekaew, S.; Sharland, M.; Shivamallappa, M.; Sifuentes-Osornio, J.; Simpson, A. J.; Steenkeste, N.; Stewardson, A. J.; Stoeva, T.; Tasak, N.; Thaiprakong, A.; Thwaites, G.; Tigoi, C.; Turner, C.; Turner, P.; van Doorn, H. R.; Velaphi, S.; Vongpradith, A.; Vongsouvath, M.; Vu, H.; Walsh, T.; Walson, J. L.; Waner, S.; Wangrangsimakul, T.; Wannapinij, P.; Wozniak, T.; Young Sharma, T. E. M. W.; Yu, K. C.; Zheng, P.; Sartorius, B.; Lopez, A. D.; Stergachis, A.; Moore, C.; Dolecek, C.; Naghavi, M. *The Lancet* **2022**, *399* (10325), 629–655.

3. Boucher, H. W.; Talbot, G. H.; Bradley, J. S.; Edwards, J. E.; Gilbert, D.; Rice, L. B.; Scheld, M.; Spellberg, B.; Bartlett, J. *Clinical Infectious Diseases* **2009**, *48* (1), 1–12.

4. Gulland, A. *BMJ* **2014**, *348* (may01 6), g3062–g3062.

5. Zgurskaya, H. I.; López, C. A.; Gnanakaran, S. *ACS Infect Dis* **2016**, *1* (11), 512–522.

6. Willers, C.; Wentzel, J. F.; du Plessis, L. H.; Gouws, C.; Hamman, J. H. *Expert Opin Ther Targets* **2017**, *21* (1), 23–36.

7. Pang, Z.; Raudonis, R.; Glick, B. R.; Lin, T. J.; Cheng, Z. *Biotechnol Adv* **2019**, *37* (1), 177–192.

8. King, A. M.; Reid-Yu, S. A.; Wang, W.; King, D. T.; De Pascale, G.; Strynadka, N. C.; Walsh, T. R.; Coombes, B. K.; Wright, G. D. *Nature* **2014**, *510* (7506), 503–506.

9. Wilke, M. S.; Lovering, A. L.; Strynadka, N. C. J. *Curr Opin Microbiol* **2005**, *8* (5), 525–533.

10. Welch, K. T.; Virga, K. G.; Whittemore, N. A.; Özen, C.; Wright, E.; Brown, C. L.; Lee, R. E.; Serpersu, E. H. *Bioorg Med Chem* **2005**, *13* (22), 6252–6263.

11. Szychowski, J.; Kondo, J.; Zahr, O.; Auclair, K.; Westhof, E.; Hanessian, S.; Keillor, J. W. *ChemMedChem* **2011**, *6* (11), 1961–1966.

12. Fosso, M. Y.; Li, Y.; Garneau-Tsodikova, S. *Med. Chem. Commun.* **2014**, *5* (8), 1075–1091.

13. Redgrave, L. S.; Sutton, S. B.; Webber, M. A.; Piddock, L. J. V. *Trends in Micro*. **2014**, 438–445.

14. Fernandes, P.; Martens, E. *Biochem Pharmacol* **2017**, *133*, 152–163.

15. Tyers, M.; Wright, G. D. *Nat. Rev. Microbio*. **2019**, 141–155.

16. Karvanen, M. Uppsala Universitet, **2013**.

17. Nation, R. L.; Li, J.; Cars, O.; Couet, W.; Dudley, M. N.; Kaye, K. S.; Mouton, J. W.; Paterson, D. L.; Tam, V. H.; Theuretzbacher, U.; Tsuji, B. T.; Turnidge, J. D. *Lancet Infect Dis*. Elsevier February 1, 2015, pp 225–234.

18. Gales, A. C.; Jones, R. N.; Sader, H. S. *Journal of Antimicrobial Chemotherapy* **2011**, *66* (9), 2070–2074.

19. Butler, M. S.; Blaskovich, M. A.; Cooper, M. A. *Journal of Antibiotics* **2017**, *70* (1), 3–24.

20. Li, J.; Nation, R. L.; Turnidge, J. D.; Milne, R. W.; Coulthard, K.; Rayner, C. R.; Paterson, D. L. *Lancet Infect Dis* **2006**, *6* (9), 589–601.

21. Yahav, D.; Farbman, L.; Leibovici, L.; Paul, M. *Clinical Microbiology and Infection* **2012**, *18* (1), 18–29.

22. Sivanesan, S.; Roberts, K.; Wang, J.; Chea, S.-E.; Thompson, P. E.; Li, J.; Nation, R. L.; Velkov, T. *J Nat Prod* **2017**, *80* (1), 225–229.

23. Tigen, E. T.; Koltka, E. N.; Dogru, A.; Gura, M.; Vahabaoglu, H. *I. J. of Crit. Care Med.* **2016**, *20* (6), 353–356.

24. Grégoire, N.; Aranzana-Climent, V.; Magréault, S.; Marchand, S.; Couet, W. *Clin Pharmacokinet* **2017**, *56* (12), 1441–1460.

25. Velkov, T.; Thompson, P. E.; Nation, R. L.; Li, J. *J Med Chem* **2010**, *53* (5), 1898–1916.

26. Bialvaei, A. Z.; Samadi Kafil, H. *Curr Med Res Opin* **2015**, *31* (4), 707–721.

27. Clinical and Laboratory Standards Institute. 28th ed.; Clin. Lab. Stand Institute: Wayne, PA, 2018.

28. Li, J., Nation, R. L., Kaye, K. S., Eds.; Advances in Experimental Medicine and Biology; Springer International Publishing: Cham, **2019**, *1145*.

29. Brochmann, R. P.; Toft, A.; Ciofu, O.; Briales, A.; Kolpen, M.; Hempel, C.; Bjarnsholt, T.; Høiby, N.; Jensen, P. Ø. *Int J Antimicrob Agents* **2014**, *43* (2), 140–147.

30. Vaara, M.; Fox, J.; Loidl, G.; Siikanen, O.; Apajalahti, J.; Hansen, F.; Frimodt-Møller, N.; Nagai, J.; Takano, M.; Vaara, T. *Antimicrob Agents Chemother* **2008**, *52* (9), 3229–3236.

31. Zavascki, A. P.; Nation, R. L. *Antimicrob Agents Chemother* **2017**, *61* (3).

32. Caniaux, I.; van Belkum, A.; Zambardi, G.; Poirel, L.; Gros, M. F. *Eur J of Clin Micro* **2017**, *36* (3), 415–420.

33. Wang, X.; Quinn, P. J. *Prog Lipid Res* **2010**, *49* (2), 97–107.

34. Hancock, R. E.; Bell, A. *Eur J Clin Microbiol Infect Dis* **1988**, *7* (6), 713–720.

35. Cajal, Y.; Rogers, J.; Berg, O. G.; Jain, M. K. *Biochemistry* **1996**, *35* (1), 299–308.

36. Deris, Z. Z.; Akter, J.; Sivanesan, S.; Roberts, K. D.; Thompson, P. E.; Nation, R. L.; Li, J.; Velkov, T. *J Antibiot (Tokyo)* **2014**, *67* (2), 147–151.

37. Sampson, T. R.; Liu, X.; Schroeder, M. R.; Kraft, C. S.; Burd, E. M.; Weiss, D. S. *Antimicrob Agents Chemother* **2012**, *56* (11), 5642–5649.

38. Jeannot, K.; Bolard, A.; Plésiat, P. *Int J Antimicrob Agents* **2017**, *49* (5), 526–535.

39. Abat, C.; Fournier, P.-E.; Jimeno, M.-T.; Rolain, J.-M.; Raoult, D. *European Journal of Clinical Microbiology & Infectious Diseases* **2018**, *37* (9), 1687–1697.

40. Moffatt, J. H.; Harper, M.; Boyce, J. D. In *Polymyxin Antibiotics: From Laboratory Bench to Bedside*; Li, J., Nation, R., K, K., Eds.; Springer, Cham, 2019; pp 55–71.

41. Liu, Y. Y.; Wang, Y.; Walsh, T. R.; Yi, L. X.; Zhang, R.; Spencer, J.; Doi, Y.; Tian, G.; Dong, B.; Huang, X.; Yu, L. F.; Gu, D.; Ren, H.; Chen, X.; Lv, L.; He, D.; Zhou, H.; Liang, Z.; Liu, J. H.; Shen, J. *Lancet Infect Dis* **2016**, *16* (2), 161–168.

42. Lee, J.-Y.; Ko, K. S. *Diagn Microbiol Infect Dis* **2014**, *78* (3), 271–276.

43. Han, M.-L.; Velkov, T.; Zhu, Y.; Roberts, K. D.; Le Brun, A. P.; Chow, S. H.; Gutu, A. D.; Moskowitz, S. M.; Shen, H.-H.; Li, J. *ACS Chem Biol* **2018**, *13* (1), 121–130.

44. Moffatt, J. H.; Harper, M.; Harrison, P.; Hale, J. D. F.; Vinogradov, E.; Seemann, T.; Henry, R.; Crane, B.; St Michael, F.; Cox, A. D.; Adler, B.; Nation, R. L.; Li, J.; Boyce, J. D. *Antimicrob Agents Chemother* **2010**, *54* (12), 4971–4977.

45. Trebosc, V.; Gartenmann, S.; Tötzl, M.; Lucchini, V.; Schellhorn, B.; Pieren, M.; Lociuro, S.; Gitzinger, M.; Tigges, M.; Bumann, D.; Kemmer, C. *mBio* **2019**, *10* (4).

46. Velkov, T.; Roberts, K. D.; Nation, R. L.; Wang, J.; Thompson, P. E.; Li, J. *ACS Chem Biol* **2014**, *9* (5), 1172–1177.

47. Brown, P.; Abbott, E.; Abdulle, O.; Boakes, S.; Coleman, S.; Divall, N.; Duperchy, E.; Moss, S.; Rivers, D.; Simonovic, M.; Singh, J.; Stanway, S.; Wilson, A.; Dawson, M. J. *ACS Infect Dis* **2019**, *5* (10), 1645–1656.

48. Jon, B.; Troy, L.; K, G. V.; Emily, S.; Lisa, M.; Yang, L.; David, M. *Antimicrob Agents Chemother* **2021**, *65* (10)

49. Roberts, K. D.; Zhu, Y.; Azad, M. A. K.; Han, M.-L.; Wang, J.; Wang, L.; Yu, H. H.; Horne, A. S.; Pinson, J.-A.; Rudd, D.; Voelcker, N. H.; Patil, N. A.; Zhao, J.; Jiang, X.; Lu, J.; Chen, K.; Lomovskaya, O.; Hecker, S. J.; Thompson, P. E.; Nation, R. L.; Dudley, M. N.; Griffith, D. C.; Velkov, T.; Li, J. *Nat Commun* **2022**, *13* (1), 1625.

50. Douafer, H.; Andrieu, V.; Phanstiel, O.; Brunel, J. M. *J Med Chem* **2019**, *62* (19), 8665–8681.

51. Vaara, M.; Viljanen, P. *Antimicrob Agents Chemother* **1985**, *27* (4), 548–554.

52. Tsubery, H.; Ofek, I.; Cohen, S.; Fridkin, M. *J Med Chem* **2000**, *43* (16), 3085–3092.

53. French, S.; Farha, M. A.; Ellis, M. J.; Sameer, Z.; J. P.; Cotroneo, N.; Lister, T.; Rubio, A.; Brown, E. D. *ACS Infect Dis* **2020** *6* (6), 1405-1412

54. Zurawski DV, Reinhart AA, A.; YA, Pucci MJ, Si Y, Abu-Taleb R, S. J.; Demons ST, Tyner SD, L. T. *Antimicrob Agents Chemother* **2017**, *61* (12), 1–6.

55. Li, Y.; Lin, X.; Yao, X.; Huang, Y.; Liu, W.; Ma, T.; Fang, B. *Antimicrob Agents Chemother* **2018**, *62* (12), e01631-18.

56. S, K. K.; Dror, M.; Visanu, T.; Yehuda, C.; Cheng-Hsun, C.; George, D.; Sorabh, D.; Emanuele, D.-M.; Achilles, G.; Anastasia, K.; Mical, P.; Emmanuelle, R.; Michael, R.; Michael, S.; Matthew, S.; Dora, T.; Sotirios, T.; Daniel, K.; Gopi, P.; David, C.; Leonard, L.; Laura, P.; Sylvia, M.-P.; Kurt, S.; Laura, S.; Katie, L.; Jolene, D.; Christine, C.; W, D. G.; Varduhi, G.; M, P. J. *NEJM Evidence* **2022**, *2* (1), EVIDoa2200131.

57. Paul, M.; Daikos, G. L.; Durante-Mangoni, E.; Yahav, D.; Carmeli, Y.; Benattar, Y. D.; Skiada, A.; Andini, R.; Eliakim-Raz, N.; Nutman, A.; Zusman, O.; Antoniadou, A.; Pafundi, P. C.; Adler, A.; Dickstein, Y.; Pavleas, I.; Zampino, R.; Daitch, V.; Bitterman, R.; Zayyad, H.; Koppel, F.; Levi, I.; Babich, T.; Friberg, L. E.; Mouton, J. W.; Theuretzbacher, U.; Leibovici, L. *Lancet Infect Dis* **2018**, *18* (4), 391–400.

58. Pieren, M.; Tigges, M. *Curr Opin Pharmacol* **2012**, *12* (5), 551–555.

59. Wright, G. D. *Trends Microbiol* **2016**, *24* (11), 862–871.

60. Papp-Wallace, K. M.; Bonomo, R. A. *Infectious Disease Clinics of North America*, **2016**, 441–464.

61. MacNair, C. R.; Stokes, J. M.; Carfrae, L. A.; Fiebig-Comyn, A. A.; Coombes, B. K.; Mulvey, M. R.; Brown, E. D. *Nat Commun* **2018**, *9* (1), 458.

62. Carfrae, L. A.; Rachwalski, K.; French, S.; Gordzevich, R.; Seidel, L.; Tsai, C. N.; Tu, M. M.; MacNair, C. R.; Ovchinnikova, O. G.; Clarke, B. R.; Whitfield, C.; Brown, E. D. *Nat Microbiol* **2023**, *8* (6), 1026–1038.

63. Minrovic, B. M.; Hubble, V. B.; Barker, W. T.; Jania, L. A.; Melander, R. J.; Koller, B. H.; Melander, C. *ACS Med Chem Lett* **2019**, *10* (5), 828–833.

64. Ghirga, F.; Stefanelli, R.; Cavinato, L.; Lo Sciuto, A.; Corradi, S.; Quaglio, D.; Calcaterra, A.; Casciaro, B.; Loffredo, M. R.; Cappiello, F.; Morelli, P.; Antonelli, A.; Rossolini, G. M.; Mangoni, M.; Mancone, C.; Botta, B.; Mori, M.; Ascenzioni, F.; Imperi, F. *Journal of Antimicrobial Chemotherapy* **2020**, *75* (9), 2564–2572.

65. Quaglio, D.; Mangoni, M. L.; Stefanelli, R.; Corradi, S.; Casciaro, B.; Vergine, V.; Lucantoni, F.; Cavinato, L.; Cammarone, S.; Loffredo, M. R.; Cappiello, F.; Calcaterra, A.; Erazo, S.; Ghirga, F.; Mori, M.; Imperi, F.; Ascenzioni, F.; Botta, B. *J Org Chem* **2020**, *85* (16), 10891–10901.

66. Ayerbe-Algaba, R.; Gil-Marqués, M. L.; Jiménez-Mejías, M. E.; Sánchez-Encinales, V.; Parra-Millán, R.; Pachón-Ibáñez, M. E.; Pachón, J.; Smani, Y. *Front Cell Infect Microbiol* **2018**, *8*, 348.

67. Domalaon, R.; Malaka De Silva, P.; Kumar, A.; Zhanel, G. G.; Schweizer, F. *Antimicrob Agents Chemother* **2019**, *63* (4), e02574-18.

68. Xu, J.; Pachón-Ibáñez, M. E.; Cebrero-Cangueiro, T.; Chen, H.; Sánchez-Céspedes, J.; Zhou, J. *Bioorg Med Chem Lett* **2019**, *29* (11), 1399–1402.

CHAPTER TWO:
Repurposing niclosamide as an adjuvant for colistin

2.1: Drug repurposing towards overcoming antibiotic resistance

A significant barrier to the development of new antibiotics is the challenging and costly drug approval process. It can cost up to $1,000,000,000 to develop a new drug and bring it to market, with much of this cost being associated with clinical trials to demonstrate the safety and efficacy of the drug.[1] This combined with limited return on investment for treating rare AMR infections has stagnated the development of new antibiotics.[2] One method to overcome this significant challenge is to repurpose existing, FDA approved, nonantibiotic drugs towards the fight against AMR bacteria.[3] The already established toxicity and pharmacokinetic profiles of these drugs may streamline the approval process. In recent years, drug repurposing has gained traction as a viable approach to discovering new antimicrobial agents.

The most direct and efficient method for detecting currently unknown antibacterial properties of nonantibiotic drugs is to assess whether a molecule in a library is able to inhibit the growth of pathogenic bacteria.[4] Recent advances in cell-based high-throughput screening (HTS) have allowed researchers to rapidly test libraries of thousands of FDA approved drugs for latent antibacterial activity. This method of screening is typically fast, reproducible, and easily interpreted, with hits characterized as inhibition of visible growth at a certain concentration. However, cell-based HTS techniques typically provide no insight as to the precise mechanism of action of any lead compounds, requiring further biochemical study in order to decipher molecular targets for inhibition of growth. Growth inhibition screens of FDA approved drugs have resulted in several promising candidates for new antibiotics. Auranofin (**Fig. 2.1A**), in clinical use to treat rheumatoid arthritis, has recently been found to display many off-target effects including treatment of amoebiasis, inhibition of *Giardia lamlia* growth and attachment, as well as potent inhibition of *Staphylococcus aureus*.[5]

Another strategy for screening potential drug repurposing candidates is to search for drugs known as adjuvants, molecules that are able to improve the activity of existing antibiotics in combination therapy. Interest in new adjuvants with novel methods of potentiation has increased in recent years as rates of antibiotic resistance has risen.[6] HTS screens for repurposed drugs as adjuvants either look for growth inhibition at varying concentrations of FDA approved drugs in combination with a fixed concentration of a known antibiotic, or for specific target interactions such as disabling efflux pumps.[4] An interesting application for these repurposing screens is the

discovery of agents which are able to permeabilize the outer membrane of Gram-negative bacteria. As Gram-negative bacteria possess a highly restrictive outer membrane, relative to Gram-positive bacteria, many hydrophobic antibiotics have difficulty penetrating the cell and are thus only active against Gram-positive bacteria.[7] Membrane permeabilizing drugs may be identified by screening for adjuvant molecules which potentiate the effects of Gram-positive antibiotics such as rifampicin and novobiocin against Gram-negative bacteria. Recently, Stokes et. al. screened 1500+ FDA approved drugs for synergy with rifampicin, novobiocin and erythromycin against *Escherichia coli*[8]. The screen revealed that pentamidine (**Fig 2.1B**), used to treat pneumocystis pneumonia, was able to permeabilize the outer membrane of *E. coli* and render these antibiotics effective.

Other, less conventional, screening strategies are also used that provide more information than simple growth inhibition. Target-based HTS techniques typically monitor for specific phenotypic changes, expression of particular genes, or other biochemical markers that provide insight into the mechanism of action of any hits.[4] This approach is significantly more complex and relies on having a clearly defined target but can provide valuable information towards understanding precisely how a repurposed drug may affect bacterial cells. In fact,
target-based screens can reveal promising candidates that are unable to directly inhibit bacterial growth but may possess other activity such as anti-virulence properties or the ability to inhibit quorum-sensing. Diflunisal (**Fig. 2.1C**), an FDA-approved nonsteroidal anti-inflammatory drug, was discovered via HTS to supress the production of virulence factors in *S. aureus*.[9]

Another example of repurposing a nonantibiotic drug as an anti-virulence agent is the anthelmintic drug Niclosamide (**Fig. 2.1D**). In an HTS screen designed to discover inhibitors of quorum-sensing, niclosamide was found to interfere with the transcription of many genes involved in quorum-sensing and production of virulence factors in *Pseudomonas aeruginosa*.[10] At a concentration of 20 μM, niclosamide was also found to significantly alter the transcription of 258 different genes, with most alterations characterized by a reduction in transcription of genes involved in the production of virulence factors. In addition, 5 to 10 μM of niclosamide was found to dramatically reduce production of both pyocyanin and elastase (by 85-90%), two important virulence factors. At a concentration of 15 μM, niclosamide was found to almost completely protect *G. mellonella* worms against a lethal dose of a hypervirulent strain of *P. aeruginosa,* despite displaying no growth inhibition whatsoever at this concentration *in vitro.* This effect was attributed primarily to virulence inhibition, allowing the innate immune response of *G. mellonella* to

overcome the infection. Niclosamide has also been shown to have antibacterial activity against Gram-positive bacteria[11] and synergize with colistin against Gram-negative bacteria[12,13] making it a promising repurposing candidate towards fighting bacterial infections.

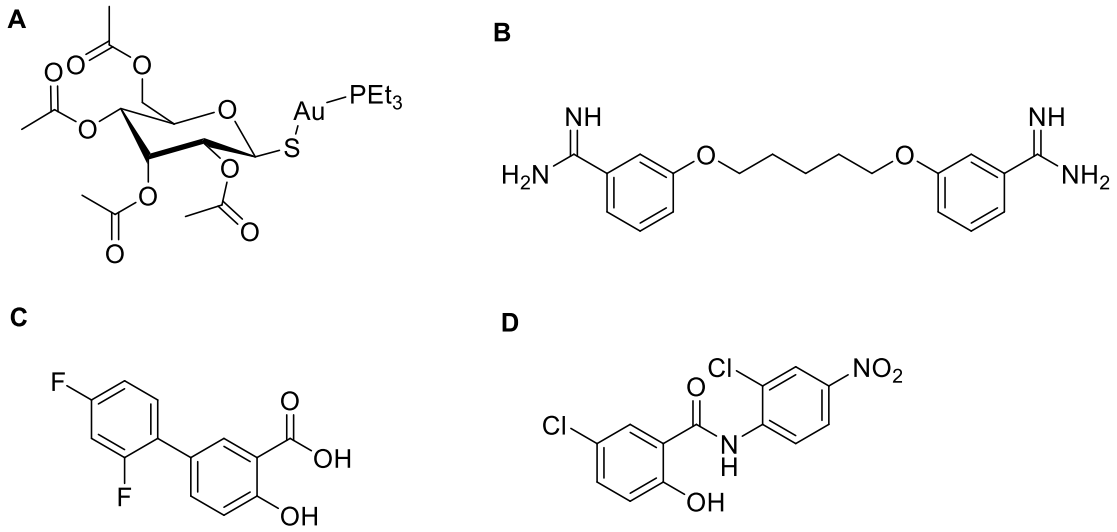

Figure 2.1 Structures of auranofin (A), Pentamidine (B), Diflunisal (C), and Niclosamide (D)

2.2: Niclosamide as a candidate for drug-repurposing

Niclosamide belongs to the salicylanilide family of drugs (consisting of salicylic acid joined to aniline via an amide linkage), and is a promising candidate for drug-repurposing for a variety of diseases. Initially discovered in the early 1950s as a molluscicid[14], niclosamide was later found to be effective against human tapeworm infections in and approved by the FDA in 1982.[15] Niclosamide is now on the World Health Organization's essential list of medicines. Despite its widespread use as an anthelmintic drug, the mechanism of action of niclosamide is not fully understood.[16] The anthelmintic activity of niclosamide is likely due to uncoupling of oxidative phosphorylation as niclosamide can disrupt the proton motive force.[17] As efforts in repurposing niclosamide towards treating other diseases have increased, a wide variety of other biological activities have also been discovered.

Niclosamide has recently been shown to regulate multiple signaling pathways and biological processes, outside of its original FDA approved indication.[16] Niclosamide has been reported to inhibit Wnt/β-catenin signaling and mTORC1 signaling.[18] This may be a promising target for repurposing niclosamide as an anti-cancer agent, such as against triple-negative breast

cancer.[19] Niclosamide was also shown to disrupt STAT3 signaling pathways,[20] inhibit Notch signaling, and downregulate AR-V7 protein expression, all of which are promising targets for treating various cancers including lung cancer, leukemia, and prostate cancer.[21–23] It is currently unclear whether specific interactions with biological targets, an indirect mechanism, or combinations of both are occurring. More research is needed to identify any biological targets that niclosamide is binding to in order to develop more selective derivatives of niclosamide.[16]

The outbreak of coronavirus disease 2019 (COVID-19) has driven the develop of many novel antiviral treatments, including through drug repurposing efforts.[24] Niclosamide was discovered in a screen of 3000 FDA-approved drugs to be a potent inhibitor of severe acute respiratory syndrome coronavirus 2 (SARS-CoV-2), the virus that causes COVID-19. (ref) A human airways epithelial model demonstrated strong antiviral activity for niclosamide, and an inhaled niclosamide formulation was developed and tested in a murine infection model of SARS-CoV-2, displaying improved survival and reduced viral loads.[24] Several clinical trials of niclosamide against COVID-19 have been conducted, with mixed results. Challenges for repurposing niclosamide as an anti-SARS-CoV-2 agent include poor systemic delivery of niclosamide attributed to low oral bioavailability.[24]

Niclosamide has also demonstrated other biological effects. For example, niclosamide has been shown to anti-viral activity to other viruses such as Zika virus[25], the ability to depolarize mitochondrial membranes in vascular smooth muscle cells (which may be useful as an anti-hypertensive drug)[26], and may even play a roll in regulating metabolic diseases such as type 2 diabetes mellitus[27] and nonalcoholic fatty liver disease.[28] The multifunctional nature of niclosamide suggests that it is able to regulate many signalling pathways and biological processes, and in the future, it may be repurposed towards other diseases.[16] Indeed, niclosamide is currently undergoing clinical trials for colorectal cancer treatment[29], with trials for other treatments expected to follow soon.

2.3: Niclosamide as an antibacterial agent

The utility of niclosamide as an antibacterial agent is of particular interest, with considerable effort devoted to studying this phenomenon. For instance, niclosamide has been shown to be an effective antimicrobial agent against methicillin-resistant *Staphylococcus aureus* (MRSA)[30] and vancomycin-resistant *Enterococci* (VRE).[11] It has also shown to be effective at

eradicating gut pathogens such as *Helicobacter pylori*[31] and *Clostridium difficile*[32], the pharmacokinetic properties that allow niclosamide to be an effective anthelmintic may prove useful in treating gut pathogens.

The suggested mechanism of action of niclosamide towards parasitic infections is primarily due to uncoupling of oxidative phosphorylation.[33] Niclosamide suggestively interferes with the electron transport chain to ATP synthase, primarily through dissipation of the proton motive force. This results in the inability of tapeworms to synthesize adenosine tri-phosphate (ATP) and a disruption in their metabolism.. Niclosamide has also been shown to reduce *C. difficile* virulence as well as protect mammalian cells from *C. difficile* endotoxins, suggestively via a dose-dependent decrease in endosomal pH.[34] Taken together, these data indicate that niclosamide is able to disrupt the proton motive force of many organisms. This dissipation of the proton gradient and membrane potential is most likely how niclosamide is able to inhibit the growth of Gram-positive bacteria, although other mechanisms of action have not been ruled out.

These extremely interesting biological effects are not unique to niclosamide, with other salicylanilides displaying similar properties. Oxyclozanide, rafoxanide and closantel are other anthelmintic salicylanilides that are FDA approved for veterinary use and have been extensively studied for off-label use. The structures of these molecules are outlined in **Fig 2**. Clearly, there is significant structural diversity within the salicylanilide family, and all of these salicylanilides have been shown to exhibit similar or even superior antimicrobial effects when compared to niclosamide. For instance, oxyclozanide was found to be just as effective as niclosamide against MRSA but was much less toxic to HepG2 human liver carcinoma cells.[30] However, against *H. pylori,* niclosamide found to be the most active salicylanilide with an MIC of 0.25 μg/mL compared to MICs of 2.0, 4.0 and 16.0 μg/mL for oxyclozanide, rafoxanide and closantel, respectively.[31] Against VRE, niclosamide and closantel were similar in effectiveness, inhibiting the growth of fifteen clinical isolates of *Enterococcus faecium* at concentrations ranging from 1 to 8 μg/ml.[11] Oxyclozanide and rafoxanide were much less effective, with MICs ranging from 4 to 32 μg/ml. Interestingly, all salicylanilides with the exception of closantel tested were ineffective against *Enterococcus faecalis* with MICs between 32 to 128 μg/ml. Closantel was able to inhibit the growth of several strains of *E. faecalis* at concentrations of 1-2 μg/ml.

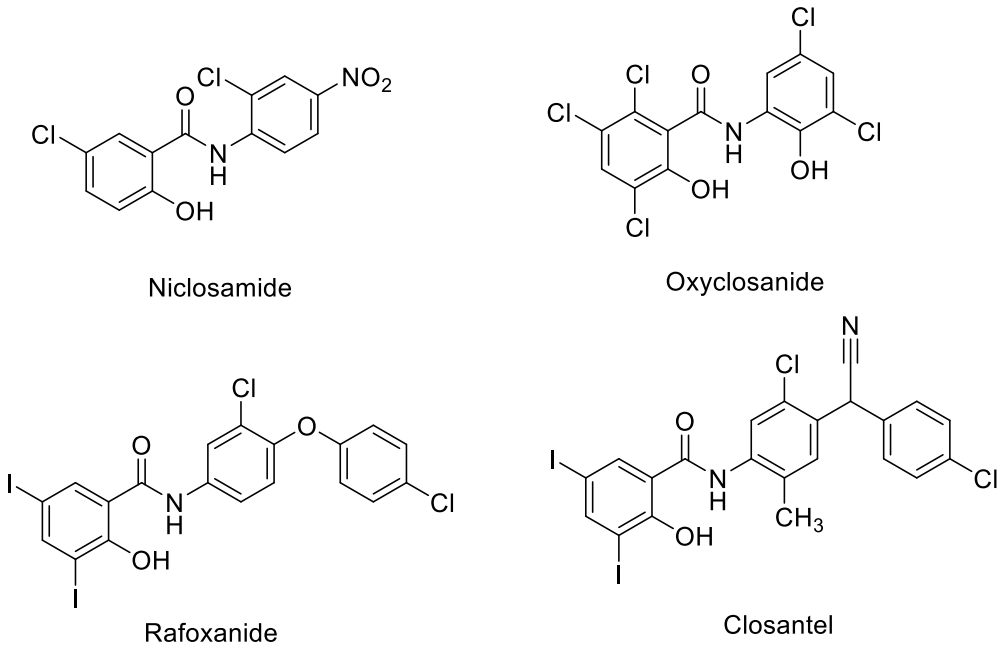

Figure 2.2. Structures of niclosamide, oxyclozanide, rafoxanide, and closantel.

Notably however, niclosamide has demonstrated poor activity against Gram-negative organisms. This has primarily been attributed to the poor outer membrane penetration of niclosamide against these organisms, as Gram-negative bacteria possess an additional highly restrictive outer membrane relative to Gram-positive bacteria.[7] Niclosamide can become active against Gram-negative organisms in combination with agents that permeabilize the outer membrane, such as polymyxin B nonapeptide (PMBN).[35] More interesting however, is the synergy observed between niclosamide and colistin, especially against colistin-resistant Gram-negative bacteria.[13]

2.4: Niclosamide as an adjuvant for colistin

The combination of niclosamide and colistin has been found to be synergistic across a wide variety of colistin-susceptible and colistin-resistant Gram-negative bacteria. Our group has previously reported that niclosamide is able to synergize selectively with colistin against wild-type *Pseudomonas aeruginosa*.[13] At a concentration of 1 μg/mL of niclosamide, the minimum inhibitory concentration (MIC) of colistin was lowered from 1 μg/mL to 0.125 μg/ml, corresponding to a 8-

fold reduction in MIC. This effect was also observed in other Gram-negative bacteria, with synergistic interactions between niclosamide and colistin found for wild-type and multidrug-resistant (but colistin susceptible) strains of *Acinetobacter baumannii, Klebsiella pneumoniae, Escherichia coli,* and *Enterobacter cloacae,* all of which are prominent human pathogens. Surprisingly, niclosamide also appears to rescue the activity of colistin against colistin-resistant Gram-negative bacteria. A panel of colistin-resistant Gram-negative bacterial isolates (MIC of colistin ranged from 4 to 1024 μg/ml) was exposed to combination therapy of niclosamide and colistin. In all thirteen isolates tested, 1 μg/mL of niclosamide was able to lower the MIC of colistin below the susceptibility breakpoint (≤2 μg/ml) as defined by the Clinical and Laboratory Standards Institute (CLSI).[36] A time-kill kinetics assay also confirmed that niclosamide was able to enhance bacterial killing of colistin against various strains of *P. aeruginosa*, and addition of niclosamide to colistin therapy was demonstrated to supress resistance development over several passages.

Similar results were also observed in other studies with niclosamide displaying the same ability to potentiate colistin against fourteen colistin-resistant strains of *A. baumannii* and four colistin-resistant strains of *K. pneumoniae.*[12] Niclosamide was also shown to enhance bacterial killing in colistin-resistant and colistin-susceptible strains of *A. baumannii* in time-kill kinetic assays. Interestingly, the authors observed a drastic reduction in the MIC of colistin against resistant organisms at a concentration of 2 μM of niclosamide (0.66 μg/ml). This concentration was able to lower the MIC of colistin in all strains of *A. baumannii* and *K. pneumoniae* tested below 2 μg/ml. Different organisms appeared to be more susceptible to niclosamide, 1 μM of niclosamide (0.33 μg/ml) was found to make all four colistin-resistant strains of *K. pneumoniae* susceptible to colistin in combination therapy, but only one out of fourteen strains of *A. baumannii.*

Closantel, oxyclozanide and rafoxanide were also shown to overcome colistin resistance in combination therapy with colistin.[37] Against colistin-susceptible clinical isolates of *P. aeruginosa* all combinations of colistin and salicylanilide were synergistic, with the exception of two strains in which the combinations were additive. Rafoxanide appeared to be the best potentiator of colistin, followed by closantel and then oxyclozanide. At 1 μg/ml, rafoxanide was able to reduce the MIC of colistin between 4-fold and 32-fold in most strains, lowering the MIC from 0.25 to 0.008 μg/mL (a 32-fold reduction) against PA095. This synergy was also observed against other colistin-susceptible Gram-negative bacteria, with all combinations of salicylanilides

and colistin resulting in synergistic interactions against five multi-drug resistant clinical isolates of *A. baumannii,* and 4 strains of *Enterobacteriaceae*. Similar to niclosamide, all three salicylanilides were able to overcome colistin resistance against most colistin-resistant multidrug-resistant Gram-negative clinical isolates tested. Interestingly, oxyclozanide and rafoxanide displayed similar potency against colistin-resistant organisms, followed by closantel. These results indicate the potential for new derivatives of niclosamide to be synthesized for the purpose of overcoming colistin resistance in combination therapy, as the salicylanilides which were quite structurally diverse possessed similar activity. Despite these results, niclosamide was still the most potent salicylanilide in most cases, able to overcome colistin resistance in all clinical isolates tested so far at 1 μg/mL which none of the other salicylanilides were able to accomplish. Closantel has also been shown to enhance Polymyxin b killing of *A baumannii* in a separate study.[39]

The mechanism of action for niclosamide as an adjuvant for colistin was recently explored by Copp *et al*.[40] It was discovered that Gram-negative bacteria possess two innate resistance mechanisms which explain niclosamide's lack of stand-alone activity. Resistance was primarily mediated via multidrug efflux pumps, with a secondary mechanism of nitroreduction. When efflux was compromised, niclosamide was able to dissipate the proton motive force (PMF), increase oxidative stress and reduce ATP production. The observed synergy between colistin and niclosamide may result from outer membrane disruption by colistin increasing niclosamide entry into the cell, followed by the inhibition of PMF-dependent efflux by niclosamide. This results in even further increased concentration niclosamide entering the cell, increasing oxygen consumption and decreasing ATP production. The authors also validated the niclosamide-colistin combination *in vivo* using a murine abscess model.[40]

Other mechanisms of action may be possible however, Li *et al.*[41] have recently reported that niclosamide as well as benzimidazole analogues are capable of increasing the production of reactive oxygen species (ROS). Given that polymyxin antibiotics may also induce cell death by generating ROS, niclosamide and colistin may be synergistically killing bacteria through several simultaneous pathways. Further investigation is required to determine the exact mechanism of action and specific targets of niclosamide as an adjuvant for colistin.

2.5: Conclusions

Drug repurposing of nonantibiotic drugs towards overcoming bacterial infections, facilitated through rapid advancements in HTS methods, is gaining traction as a viable method of drug discovery. Several promising FDA-approved candidates for drug repurposing have been discovered in recent years, including the anthelmintic agent niclosamide. Niclosamide has been investigated as a drug that can be repurposed towards treating a variety of diseases. In particular, niclosamide displays promising activity against Gram-positive bacteria, and can synergize with colistin against Gram-negative bacteria. Niclosamide holds potential as a solution to solve the rising threat of colistin resistance. However, as niclosamide is optimized for treating parasitic infections in the gut, it has extremely poor oral bioavailability and systemic distribution, which may present a challenge for treating bacterial infections.[41,42] In addition, the propensity for niclosamide to interact with so many varied biological systems may also be a downside, resulting in unwanted off-target side effects. Therefore, there is an urgent need to design novel niclosamide derivatives with specific and targeted biological functions.

2.6: References

1. Prasad, V.; Mailankody, S. *JAMA Intern Med* **2017**, *177* (11), 1569.
2. Fernandes, P.; Martens, E. *Biochem Pharmacol* **2017**, *133*, 152–163.
3. Ejim, L.; Farha, M. A.; Falconer, S. B.; Wildenhain, J.; Coombes, B. K.; Tyers, M.; Brown, E. D.; Wright, G. D. *Nat Chem Biol* **2011**, *7* (6), 348–350.
4. Farha, M. A.; Brown, E. D. *Nat Microbiol* **2019**, *4* (4), 565–577.
5. Roder, C.; Thomson, M. J. *Drugs in R and D* **2015**, *15* (1), 13–20.
6. Pieren, M.; Tigges, M. *Curr Opin Pharmacol* **2012**, *12* (5), 551–555.
7. Zgurskaya, H. I.; López, C. A.; Gnanakaran, S. *ACS Infect Dis* **2016**, *1* (11), 512–522.
8. Stokes, J. M.; Macnair, C. R.; Ilyas, B.; French, S.; Côté, J. P.; Bouwman, C.; Farha, M. A.; Sieron, A. O.; Whitfield, C.; Coombes, B. K.; Brown, E. D. *Nat Microbiol* **2017**, *2* (5), 17028.
9. Khodaverdian, V.; Pesho, M.; Truitt, B.; Bollinger, L.; Patel, P.; Nithianantham, S.; Yu, G.; Delaney, E.; Jankowsky, E.; Shoham, M. *Antimicrob Agents Chemother* **2013**, *57* (8), 3645–3652.
10. Imperi, F.; Massai, F.; Pillai, C. R.; Longo, F.; Zennaro, E.; Rampioni, G.; Visc, P.; Leoni, L. *Antimicrob Agents Chemother* **2013**, *57* (2), 996–1005.
11. Mohammad, H.; AbdelKhalek, A.; Abutaleb, N. S.; Seleem, M. N. *Int J Antimicrob Agents* **2018**, *51* (6), 897–904.
12. Ayerbe-Algaba, R.; Gil-Marqués, M. L.; Jiménez-Mejías, M. E.; Sánchez-Encinales, V.; Parra-Millán, R.; Pachón-Ibáñez, M. E.; Pachón, J.; Smani, Y. *Front Cell Infect Microbiol* **2018**, *8*, 348.
13. Domalaon, R.; Malaka De Silva, P.; Kumar, A.; Zhanel, G. G.; Schweizer, F. *Antimicrob Agents Chemother* **2019**, *63* (4), e02574-18.
14. Andrews, P.; Thyssen, J.; Lorke, D. *Pharmacol Ther* **1982**, *19* (2), 245–295.
15. Pearson, R. D.; Hewlett, E. L. *Ann Intern Med* **1985**, *102* (4), 550–551.
16. Chen, W.; Mook, R. A.; Premont, R. T.; Wang, J. *Cell Signal* **2018**, *41*, 89–96.
17. Kadri, H.; Lambourne, O. A.; Mehellou, Y. *ChemMedChem* **2018**, *13* (11), 1088–1091.
18. Wang, J.; Ren, X.; Piao, H.; Zhao, S.; Osada, T.; Premont, R. T.; Mook, R. A.; Morse, M. A.; Lyerly, H. K.; Chen, W. *Biochemical Journal* **2019**, *476* (3), 535–546.
19. Liu, J.; Chen, X.; Ward, T.; Pegram, M.; Shen, K. *Tumor Biology* **2016**, *37* (7), 9825–9835.
20. Gyamfi, J.; Lee, Y.-H.; Min, B. S.; Choi, J. *Sci Rep* **2019**, *9* (1), 11336.
21. Li, Y.; Li, P.-K.; Roberts, M. J.; Arend, R. C.; Samant, R. S.; Buchsbaum, D. J. *Cancer Lett* **2014**, *349* (1), 8–14.

22. Wang, Y.-C.; Chao, T.-K.; Chang, C.-C.; Yo, Y.-T.; Yu, M.-H.; Lai, H.-C. *PLoS One* **2013**, *8* (9), e74538-.

23. Shangguan, F.; Liu, Y.; Ma, L.; Qu, G.; Lv, Q.; An, J.; Yang, S.; Lu, B.; Cao, Q. *J Cancer* **2020**, *11* (12), 3454–3466.

24. Singh, S.; Weiss, A.; Goodman, J.; Fisk, M.; Kulkarni, S.; Lu, I.; Gray, J.; Smith, R.; Sommer, M.; Cheriyan, J. *Br J Pharmacol* **2022**, *179* (13), 3250–3267.

25. Li, Z.; Brecher, M.; Deng, Y.-Q.; Zhang, J.; Sakamuru, S.; Liu, B.; Huang, R.; Koetzner, C. A.; Allen, C. A.; Jones, S. A.; Chen, H.; Zhang, N.-N.; Tian, M.; Gao, F.; Lin, Q.; Banavali, N.; Zhou, J.; Boles, N.; Xia, M.; Kramer, L. D.; Qin, C.-F.; Li, H. *Cell Res* **2017**, *27* (8), 1046–1064.

26. Xiao, X.-L.; Hu, N.; Zhang, X.-Z.; Jiang, M.; Chen, C.; Ma, R.; Ma, Z.-G.; Gao, J.-L.; Xuan, X.-C.; Sun, Z.-J.; Dong, D.-L. *Br J Pharmacol* **2018**, *175* (10), 1707–1718.

27. Bhagat, H. A.; Compton, S. A.; Musso, D. L.; Laudeman, C. P.; Jackson, K. M. P.; Yi, N. Y.; Nierobisz, L. S.; Forsberg, L.; Brenman, J. E.; Sexton, J. Z. *PLoS One* **2018**, *13* (10), e0204605.

28. Tao, H.; Zhang, Y.; Zeng, X.; Shulman, G. I.; Jin, S. *Nat Med* **2014**, *20* (11), 1263–1269.

29. Burock, S.; Daum, S.; Keilholz, U.; Neumann, K.; Walther, W.; Stein, U. *BMC Cancer* **2018**, *18* (1), 297.

30. Rajamuthiah, R.; Fuchs, B. B.; Conery, A. L.; Kim, W.; Jayamani, E.; Kwon, B.; Ausubel, F. M.; Mylonakis, E. *PLoS One* **2015**, *10* (4), e0124595.

31. Tharmalingam, N.; Port, J.; Castillo, D.; Mylonakis, E. *Sci Rep* **2018**, *8* (1), 3701.

32. Gooyit, M.; Janda, K. D. *Sci Rep* **2016**, *6* (1), 33642.

33. Weinbach, E. C.; Garbus, J. *Nature* **1969**, *221* (5185), 1016–1018.

34. Tharmalingam, N.; Jayamani, E.; Rajamuthiah, R.; Castillo, D.; Fuchs, B. B.; Kelso, M. J.; Mylonakis, E. *Future Med Chem* **2017**, *9* (12), 1401–1411.

35. Domalaon, R.; Berry, L.; Tays, Q.; Zhanel, G. G.; Schweizer, F. *Bioorg Chem* **2018**, *80*, 639–648.

36. Clinical and Laboratory Standards Institute. 28th ed.; Clin. Lab. Stand Institute: Wayne, PA, 2018.

37. Domalaon, R.; Okunnu, O.; Zhanel, G. G.; Schweizer, F. *J Antibiot (Tokyo)* **2019**. *75* (10), 707–718

38. Tran, T. B.; Cheah, S.-E.; Yu, H. H.; Bergen, P. J.; Nation, R. L.; Creek, D. J.; Purcell, A.; Forrest, A.; Doi, Y.; Song, J.; Velkov, T.; Li, J. *J Antibiot (Tokyo)* **2016**, *69* (6), 415–421.

39. Copp, J. N.; Pletzer, D.; Brown, A. S.; Van der Heijden, J.; Miton, C. M.; Edgar, R. J.; Rich, M. H.; Little, R. F.; Williams, E. M.; Hancock, R. E. W.; Tokuriki, N.; Ackerley, D. F. *mBio* **2020**, *11* (5), 1–14.

40. Li, H.; Mattingly, A. E.; Jania, L. A.; Smith, R.; Melander, R. J.; Ernst, R. K.; Koller, B. H.; Melander, C. *ACS Infect Dis* **2021**, *7* (12), 3303–3313.

41. Chen, H.; Yang, Z.; Ding, C.; Chu, L.; Zhang, Y.; Terry, K.; Liu, H.; Shen, Q.; Zhou, J. *ACS Med Chem Lett* **2013**, *4* (2), 180–185.

42. Xu, J.; Pachón-Ibáñez, M. E.; Cebrero-Cangueiro, T.; Chen, H.; Sánchez-Céspedes, J.; Zhou, J. *Bioorg Med Chem Lett* **2019**, *29* (11), 1399–1402.

CHAPTER THREE:
Thesis Objectives

Despite the remarkable potential for niclosamide as a drug repurposing agent described in the previous chapter, significant barriers to clinical usage of niclosamide as an adjuvant for colistin. Niclosamide is quite hydrophobic and therefore poorly absorbed into the bloodstream and poorly bioavailable.[1] A useful property for treating parasitic infections in the GI tract, but a significant hinderance for treating systemic bacterial infections. In addition, niclosamide is extensively (>99%) protein-bound in blood plasma, further limiting its bioavailability.[2] The potent anti-cancer activity of niclosamide is also a significant drawback for antibacterial repurposing programs, as it represents toxicity against human cells.[3] In order to solve these challenges, new derivatives of niclosamide must be made which are more bioavailable and less toxic. To further complicate this problem however, a thorough structure-activity relationship of niclosamide as an adjuvant for colistin has yet to be examined.

The objective of this thesis was therefore to perform a structure-activity relationship study of niclosamide, with an emphasis on designing new analogues that solve the challenges described above. Additional aims included designing more potent colistin adjuvants, expanding the spectrum of antibiotics that niclosamide can potentiate, and harnessing the pleotropic biological activities of niclosamide for novel antibacterial purposes. This was accomplished with three major goals:

a) **Perform a structure-activity relationship study of niclosamide**. First, a library of niclosamide analogues was synthesized to examine how the niclosamide scaffold can be modified while maintaining synergy with colistin. The target molecules for this project are outlined in **Fig 3.1**. The two main sites of modification are the aryl nitro group, which has been associated with toxicity[4], and the central amide moiety, which has previously been replaced with benzimidazole bioisosteres.[5] The initial library of compounds focused on attaching amide and triazole scaffolds (Chapter 4). If these scaffolds can successfully be synthesized, they can rapidly be derivatized with a wide variety of hydrophilic moieties, including short peptides. The amide in niclosamide was also replaced with a sulfonamide group (Chapter 6). Niclosamide's extremely poor solubility, even in organic solvents, represents a challenge both chemically and biologically. This has been previously associated with the planar structure of niclosamide, which contributes to aggregation in solution.[6] Introducing more globularity and hydrogen-bond accepting sites via sulfonamide replacement may be a viable strategy to improve solubility. [6]

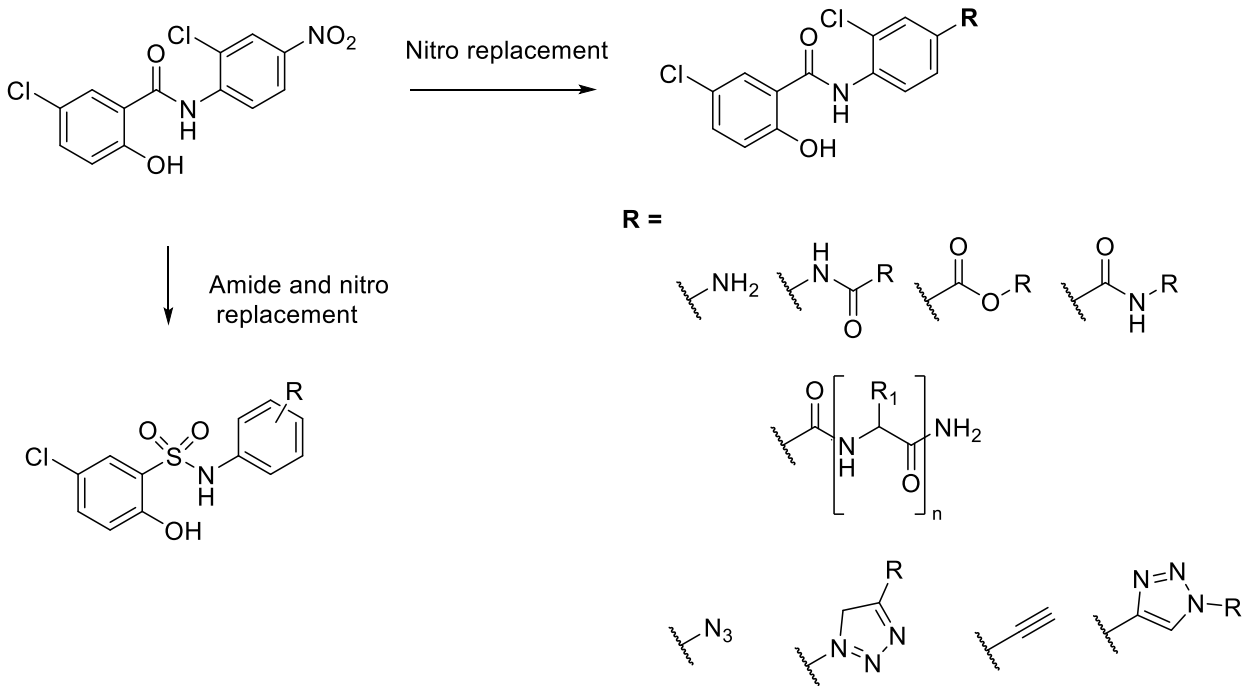

Figure 3.1 Target molecules for the initial structure-activity relationship study of niclosamide

b) **Synthesize niclosamide-based hybrid antibiotics.** After the initial structure-activity relationship study, the next goal for this project was to synthesize hybrid antibiotics, where niclosamide is covalently linked to existing antibiotics (Chapter 5). If the short peptide analogs of niclosamide retain colistin-potentiating activity, a niclosamide-colistin hybrid molecule will be synthesized using solid-phase peptide synthesis (**Fig 3.2**). Ideally, this molecule will incorporate both niclosamide and colistin modes of action simultaneously, potentially resulting in a single molecule that is effective against colistin-resistant bacteria. This hybrid approach has previously been used on the tobramycin scaffold to develop novel membrane-permeabilizing agents. Given that niclosamide faces significant challenges crossing the membrane in Gram-negative bacteria[7], attaching niclosamide to tobramycin may allow increased intracellular penetration by hijacking tobramycin's self-promoted uptake mechanism.[8,9] **(Fig 3.2)** This molecule was synthesized via copper-assisted azide-alkyne cycloaddition (CuAAC)[10] based on the triazole scaffold. The pleotropic biological activities of niclosamide described in Chapter 2 also resulted in a tobramycin-based conjugate with novel activity.

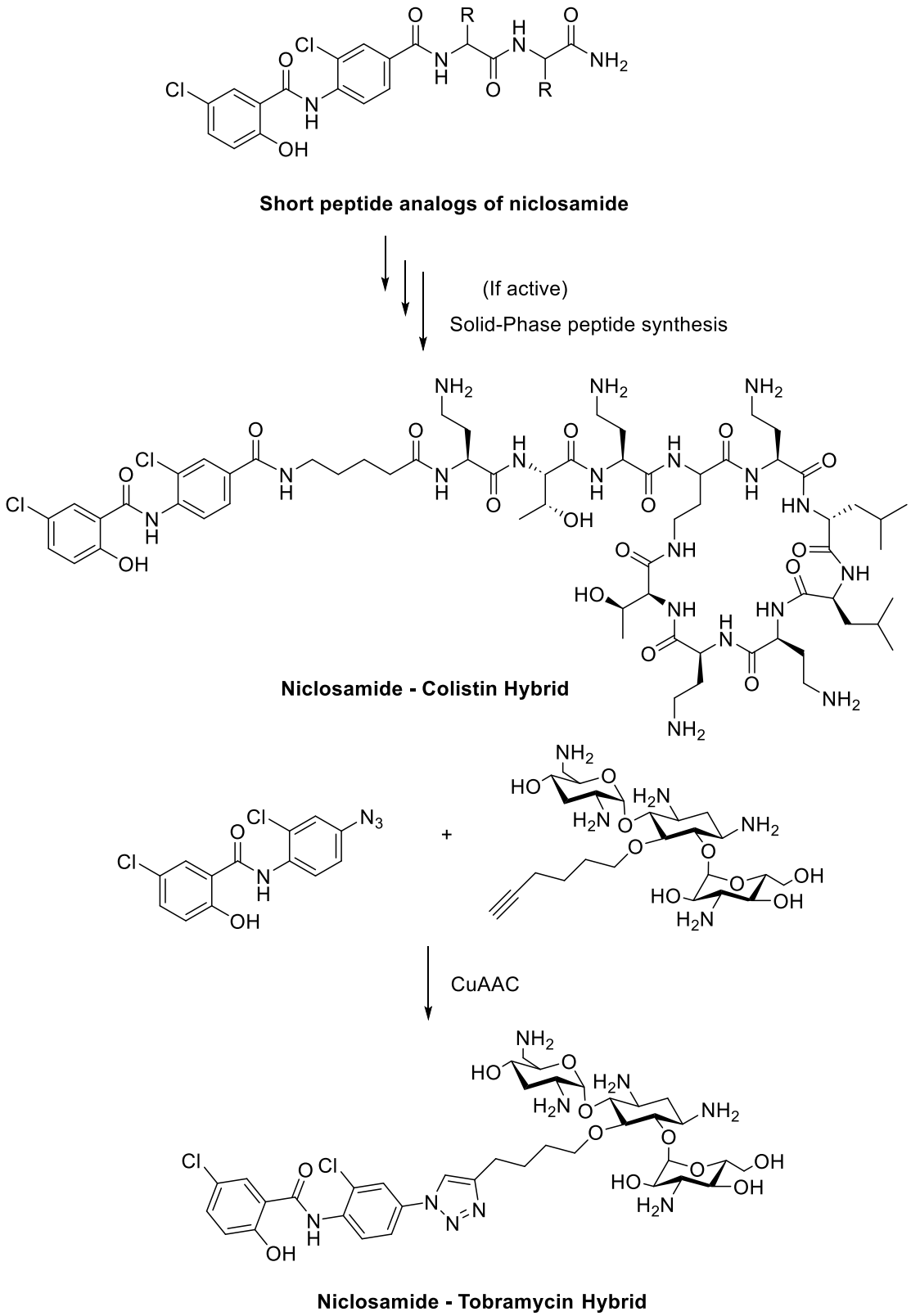

Figure 3.2. Structures of proposed niclosamide-colistin and niclosamide-tobramycin hybrid molecules

c) **Carry out extensive biological evaluations of novel niclosamide derivatives.** All of the novel analogues of niclosamide were then tested for a variety of biological activities. The primary outcome measured was colistin potentiation against Gram-negative bacteria. Human cell toxicity, stand-alone activity against Gram-positive bacteria, and synergy with other antibiotics against both Gram-negative and Gram-positive bacteria was also assessed.

The overall hypothesis for this thesis is that the structure of niclosamide can be modified through a variety of approaches to reduce toxicity, enhance solubility, and enhance niclosamide potency as an adjuvant for colistin and other antibiotics.

3.1: References

1. Chen, H.; Yang, Z.; Ding, C.; Chu, L.; Zhang, Y.; Terry, K.; Liu, H.; Shen, Q.; Zhou, J. *ACS Med Chem Lett* **2013**, *4* (2), 180–185.
2. Jara, M. O.; Warnken, Z. N.; Sahakijpijarn, S.; Thakkar, R.; Kulkarni, V. R.; Christensen, D. J.; Koleng, J. J.; Williams, R. O. *Pharmaceutics* **2022**, *14* (12).
3. Li, Y.; Li, P.-K.; Roberts, M. J.; Arend, R. C.; Samant, R. S.; Buchsbaum, D. J. *Cancer Lett* **2014**, *349* (1), 8–14.
4. Ngai, T. W.; Elfar, G. A.; Yeo, P.; Phua, N.; Hor, J. H.; Chen, S.; Ho, Y. S.; Cheok, C. F. *Int J Mol Sci* **2021**, *22* (19).
5. Li, H.; Mattingly, A. E.; Jania, L. A.; Smith, R.; Melander, R. J.; Ernst, R. K.; Koller, B. H.; Melander, C. *ACS Infect Dis* **2021**, *7* (12), 3303–3313.
6. Vuai, S. A. H.; Sahini, M. G.; Onoka, I.; Kiruri, L. W.; Shadrack, D. M. *RSC Adv* **2021**, *11* (52), 33136–33147.
7. Copp, J. N.; Pletzer, D.; Brown, A. S.; Van der Heijden, J.; Miton, C. M.; Edgar, R. J.; Rich, M. H.; Little, R. F.; Williams, E. M.; Hancock, R. E. W.; Tokuriki, N.; Ackerley, D. F. *mBio* **2020**, *11* (5), 1–14.
8. Hancock, R. E.; Bell, A. *Eur J Clin Microbiol Infect Dis* **1988**, *7* (6), 713–720.
9. Zhang, L.; Dhillon, P.; Yan, H.; Farmer, S.; Hancock, R. E. W. *Antimicrob Agents Chemother* **2000**, *44* (12), 3317–3321.
10. Huisgen, R. *Angew.Chem.,Int.Ed.Engl.* **1963**, *2* (10), 565–598.

CHAPTER FOUR:
Exploring structure-activity relationships of niclosamide-based colistin potentiators in colistin-resistant Gram-negative bacteria

The work presented in this chapter has been previously published in:

Liam Berry, Quinn Neale, Rajat Arora, Danyel Ramirez, Marc Brizuela, Ronald Domalaon, Gilbert Arthur, Frank Schweizer. *Antibiotics* **2024,** *13,* 43

4.1: Preface

As described in previous chapters, novel strategies to develop new antibiotics must be developed. Colistin, typically a last-resort antibiotic for highly resistant Gram-negative bacteria (GNB) infections, faces a growing challenge with increasing rates of resistance. The anthelmintic drug niclosamide shows promise in combination therapy, boosting colistin's effectiveness. However, little is known about how niclosamide interacts with GNB in terms of its structure-activity relationship (SAR).

To fill this gap, we conducted a study, synthesizing various niclosamide analogs to explore their SAR. The aim was to uncover the specific molecular factors that enhance colistin activity when combined with niclosamide. The results not only contribute to a better understanding of how colistin is potentiated but also have implications for improving therapeutic strategies.

In the course of our research, a notable finding emerged—replacing the nitro group of niclosamide with a methyl ester in compound **5a** resulted in a promising lead candidate. This compound displayed colistin-potentiating activity similar to niclosamide but with reduced cytotoxicity. This discovery not only validates the effectiveness of niclosamide in combination therapy but also suggests the possibility of refining drug candidates to minimize harm to mammalian cells.

Beyond its immediate impact, our work offers insights into synthetic strategies for developing new niclosamide derivatives. The ability to adjust the structure of these derivatives, as revealed by SAR analysis, provides a potential path for tailoring compounds with improved therapeutic characteristics. Additionally, demonstrating that toxicity to mammalian cells can be lessened without compromising colistin potentiation suggests the practical application of this research in creating safer and more effective antimicrobial treatments. Overall, this study advances

our understanding of how niclosamide and colistin interact and sets the stage for further synthesis of new niclosamide analogs.

4.2: Abstract

Colistin is primarily used as a last resort antibiotic against highly resistant Gram-negative bacteria (GNB). Rising rates of colistin resistance, however, may limit future use of this agent. The anthelmintic drug niclosamide has been shown to enhance colistin activity in combination therapy, but a detailed structure-activity relationship (SAR) for niclosamide against GNB has yet to be studied. A series of niclosamide analogs were synthesized to perform an SAR, leading to the discovery of a lead compound that displayed comparable colistin-potentiating activity to niclosamide with reduced cytotoxicity. Overall, this work provides important insights into synthetic strategies for the future development of novel niclosamide derivatives and demonstrates that toxicity to mammalian cells can be reduced while maintaining colistin potentiation.

4.3: Introduction

The widespread and ever-increasing threat of antimicrobial-resistant (AMR) "superbugs" presents a significant danger to the healthcare system and to the entire world.[1,2] Indeed, a substantial increase in infections caused by AMR Gram-negative bacteria (GNB) has led to the increase in usage of last resort antibiotics such as colistin. However, rising rates of colistin resistance have resulted in bacterial infections that are resistant to all currently used antibiotics, leading to the deaths of several patients.[3] If no new treatments for these challenging infections are developed, humanity may be left with no effective agents with which to eradicate these "superbugs".

A significant barrier to the development of new antibiotics is the challenging and costly drug approval process.[4] This combined with limited return on investment for treating rare AMR

infections has stagnated the development of new antibiotics.[5] One method to overcome this significant challenge is to repurpose existing FDA-approved drugs towards the fight against AMR bacteria.[6] The already established toxicity and pharmacokinetic profiles of these drugs may streamline and potentially truncate the development and approval process for such agents, rendering a quick pathway for their much needed use in the clinic. An example of such is the anthelmintic drug niclosamide approved for the treatment of tapeworm infections, which has been shown to exhibit antibacterial activity against Gram-positive bacteria[7], inhibit quorum sensing in Gram-negative bacteria[8], and able to synergize with colistin against GNB[9] to combat the development of colistin resistance.

Despite being a promising candidate for repurposing as a drug against AMR infections, niclosamide has notable limitations. In particular, niclosamide has an extremely poor bioavailability primarily due to its low solubility.[10] Toxicity to mammalian cells has also been observed which has spurred interest in repurposing niclosamide as an anticancer agent[11] but is a significant hindrance for developing it as a selective and safe antibacterial agent. In order to further develop niclosamide as an adjuvant capable of augmenting colistin and overcome colistin resistance, novel derivatives must be synthesized, and their structure-activity relationships need to be studied. Several publications have reported novel niclosamide analogs for combating colistin resistance[12], as well as a detailed mechanistic understanding of niclosamide in combination with colistin[13].

The aim of this study is to synthesize derivatives of niclosamide with a goal of reducing toxicity to human cells while retaining synergy with colistin. Niclosamide is composed of a 5-chlorosalicylic acid ring linked to a 2-chloro-4-nitroaniline ring via an amide bond. The nitro group has been demonstrated to contribute to genotoxicity[14], as well as serving as a target for bacterial

nitroreductases resulting in resistance to niclosamide[13]. These factors, in addition to reports that structurally similar salicylanilides such as rafoxanide (**Figure 1**) which lack the nitro group can also synergize with colistin[15], led to us targeting this site for most of our modifications. Our initial synthetic goal was the replacement of the nitro group with an amide moiety, which would allow rapid synthesis of a small library of amide analogs incorporating various functional groups. We also explored attaching azide and alkyne functional groups to the niclosamide scaffold with the goal of producing a small library of triazole-containing compounds via copper-assisted azide-alkyne cycloaddition (CuACC)[16].

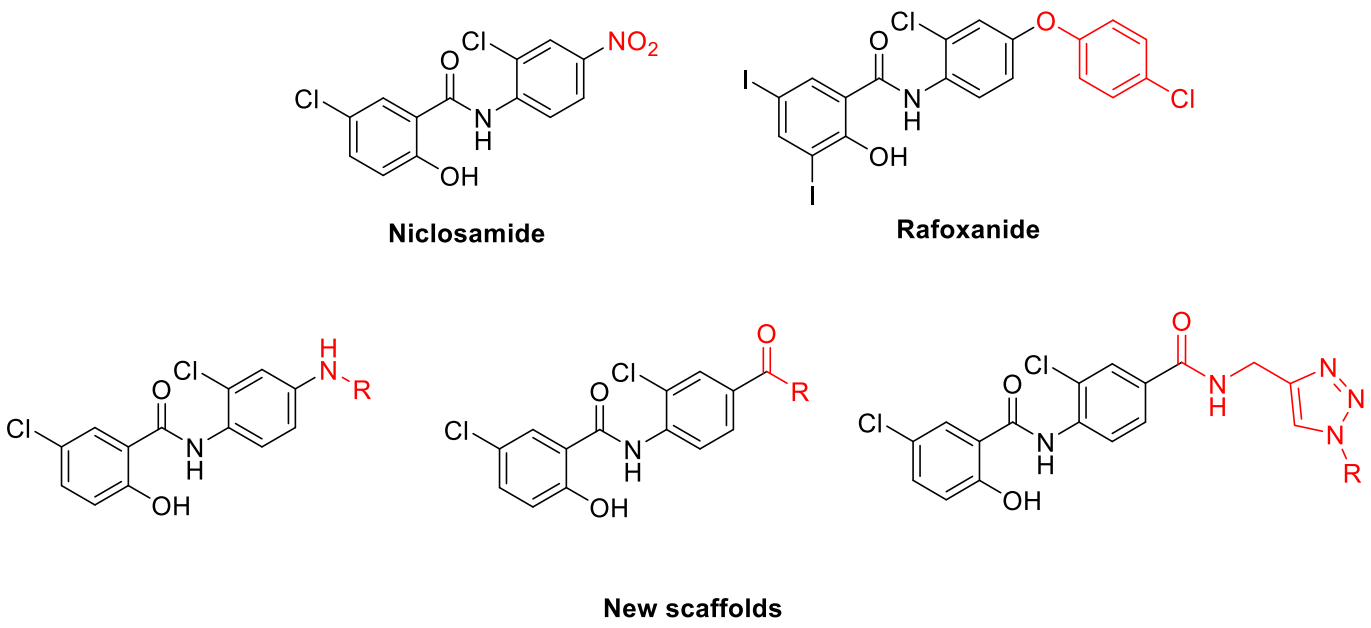

Figure 4.1. Structures of niclosamide, rafoxanide and proposed new scaffolds. The initial site of modification is highlighted.

In this work, it was found that the nitro group in niclosamide could be replaced with a methyl ester, an azide, or (to a lesser extent) a primary amine while retaining synergy with colistin against colistin-resistant GNB. We also show that replacement of the nitro group can result in novel

derivatives of niclosamide with lower cytotoxicity against human cells. Overall, this work provides important insights towards future development and optimization of niclosamide for overcoming colistin resistance.

4.4: Results and Discussion

4.3.1 Synthesis of target comounds

The nitro group on niclosamide was chosen as an initial site for modification. We initially sought to synthesize two series of amide analogs, one of which linked the amide to the salicylanilide scaffold via the nitrogen and one that was linked via the carbonyl group. The first series of derivatives resulted from treating niclosamide with zinc dust in the presence of NH_4Cl, yielding primary amine derivative **1**. As an initial study, the amine was further acylated and alkylated to produce compounds **2** and **3** (**Figure 4.2**).

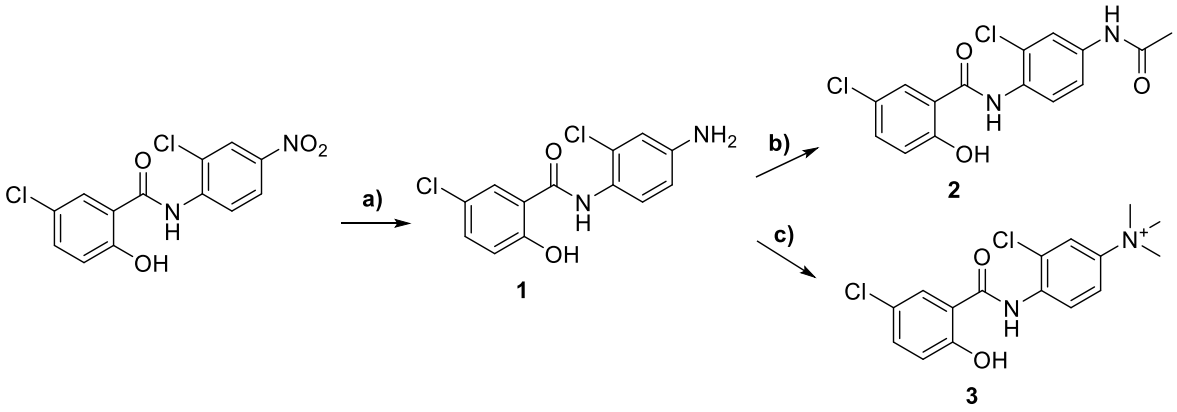

Figure 4.2. Synthesis of amine derivatives of niclosamide (a) Zn, NH_4Cl, MeOH/THF, rt, 4h, 50% yield (b) CH_3COCl, DCM, rt, 16h, 85% yield (c) CH_3I, 2,6 lutidine, DMF, rt, 16h, 49% yield.

The other series of amide containing compounds was synthesized by coupling commercially available 5-chlorosalisylic acid with various aniline derivatives. A methyl ester derivative **5a** was synthesized via PCl_3 coupling. Ester hydrolysis with LiOH produced carboxylic acid analogue **6** which was intended to serve as a scaffold to produce a small library of amide analogues. (**Figures 4.3** and **4.4**).

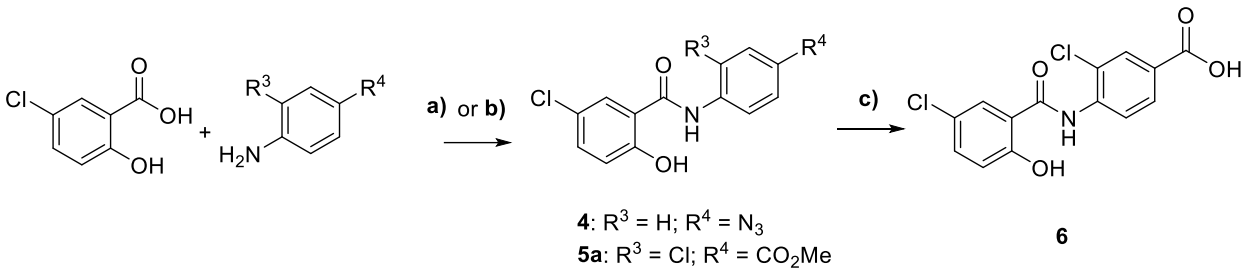

Figure 4.3. Synthesis of azide, ester and carboxylic acid derivatives of niclosamide. (a) EDC, THF, rt, 5h, 73% yield (b) PCl_3, xylenes, reflux 4h, 55% yield (c) LiOH (aq), THF/MeOH, rt, 2h, 98% yield.

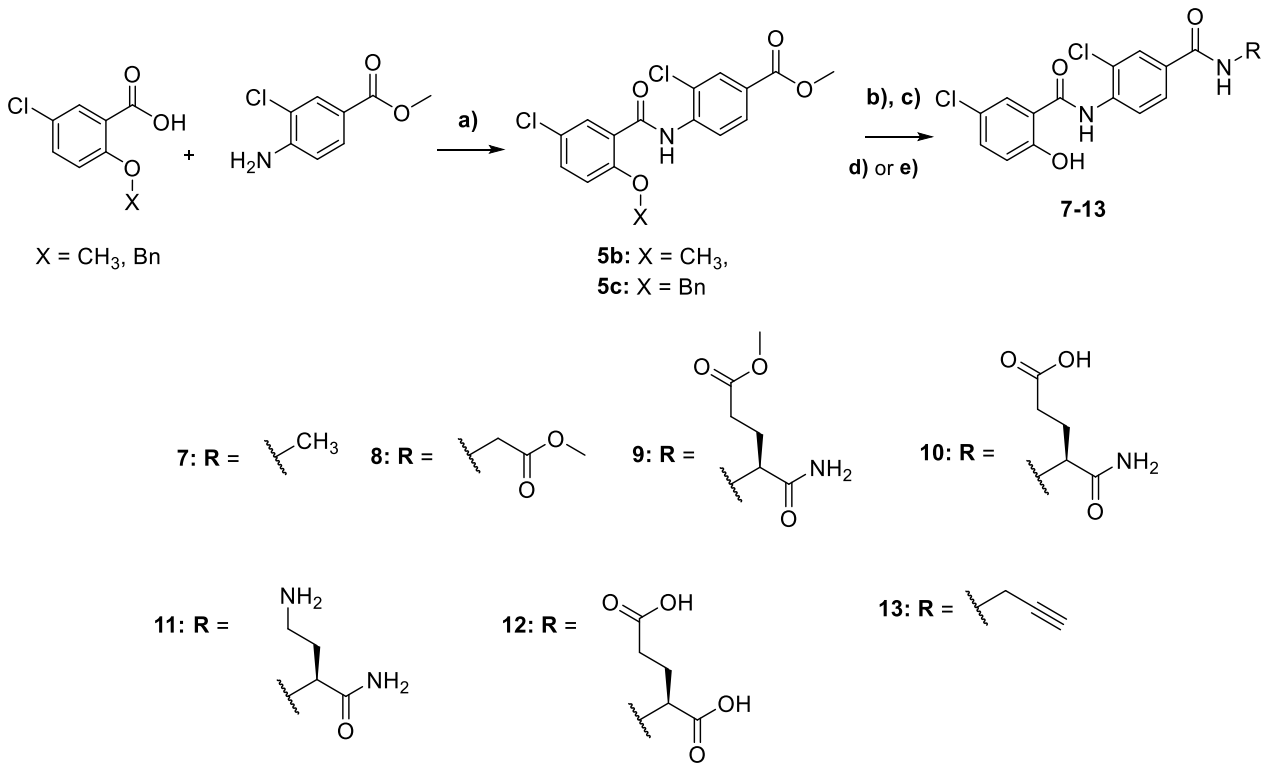

Figure 4.4. Synthesis of amide derivatives of niclosamide (a) PCl_3/xylenes, reflux, 4h, 73% yield; (b) LiOH (aq), THF/MeOH, rt, 2h, 98% yield; (c) TBTU, NMM, DMF, NH_2-R^4 rt, 2h, 55-86% yield (d) BBr_3, DCM, 0°C, 16h, 65-83% yield (e) H_2 Pd/C, MeOH/THF, rt, 2h, 87% yield.

Two phenol protecting group strategies were developed to overcome this challenge: a methyl ether protecting group that could be deprotected using BBr_3 and a benzyl protecting group that could be deprotected with catalytic hydrogenolysis. The role of the phenol functional group was also explored using intermediate **5b**, analogous to **5a** but with a methyl ether protected phenol. These protecting group strategies enabled the development of amide derivatives **7-12** which allowed for the introduction of a variety of functional groups. (**Figure 4.4**).

An azide derivative **4** was also prepared by reacting 5-chlorosalisylic acid with 4-azidoaniline in the presence of 1-ethyl-3-(3-dimethylaminopropyl)carbodiimide (EDC). Attempts to synthesize

an ethynylaniline derivative with an alkyne at the same position as the azide group proved unsuccessful, so an alternative strategy to install the alkyne group was utilized. Compound **13**, a propargylamide derivative, was coupled to various azide-containing fragments via copper-assisted azide-alkyne cycloaddition (CuAAC)[16] in **Figure 4.5** to explore the effects of a triazole moiety in compounds **14-17**.

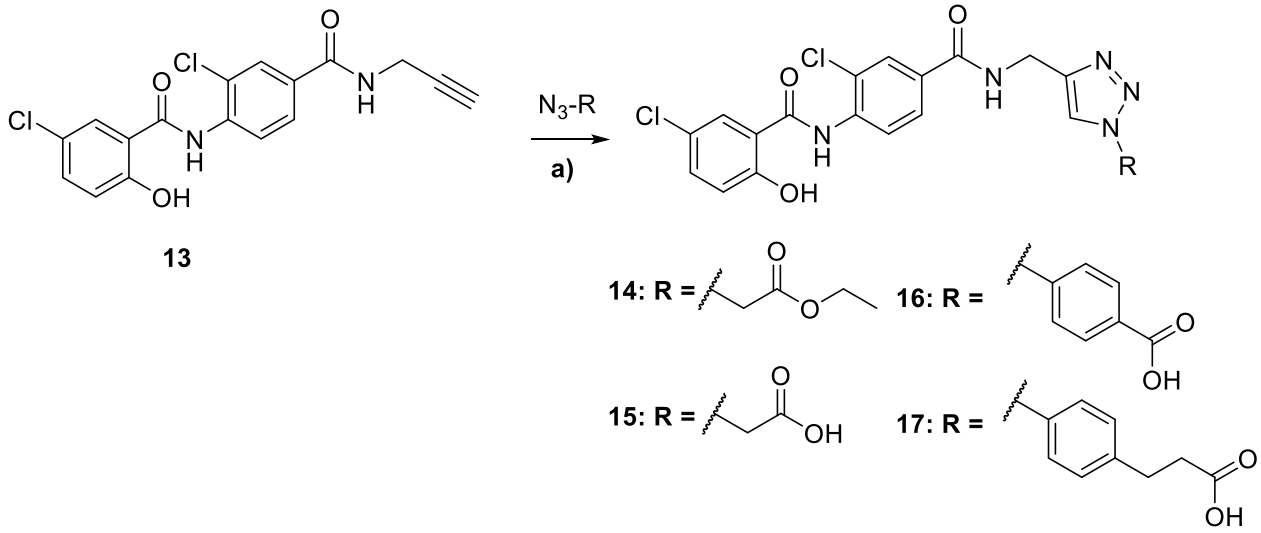

Figure 4.5. Synthesis of triazole derivatives of niclosamide (a) CuI·P(OEt)$_3$, *i*Pr$_2$Net, DMF, rt, 2 h., 33-86% yield

Lastly, a series of polyphenol derivatives were synthesized (**Figure 4.6**). Since the phenol group on niclosamide was previously shown to be essential for its activity as a protonophore[17] and thus its synergy with colistin[13], we wanted to explore the effect of installing additional phenol groups. The salicylic acid ring of niclosamide was modified with additional hydroxyl groups (**18**, **19**) and the previously described amide coupling method was used to produce polyphenol analogs **20** and **21**.

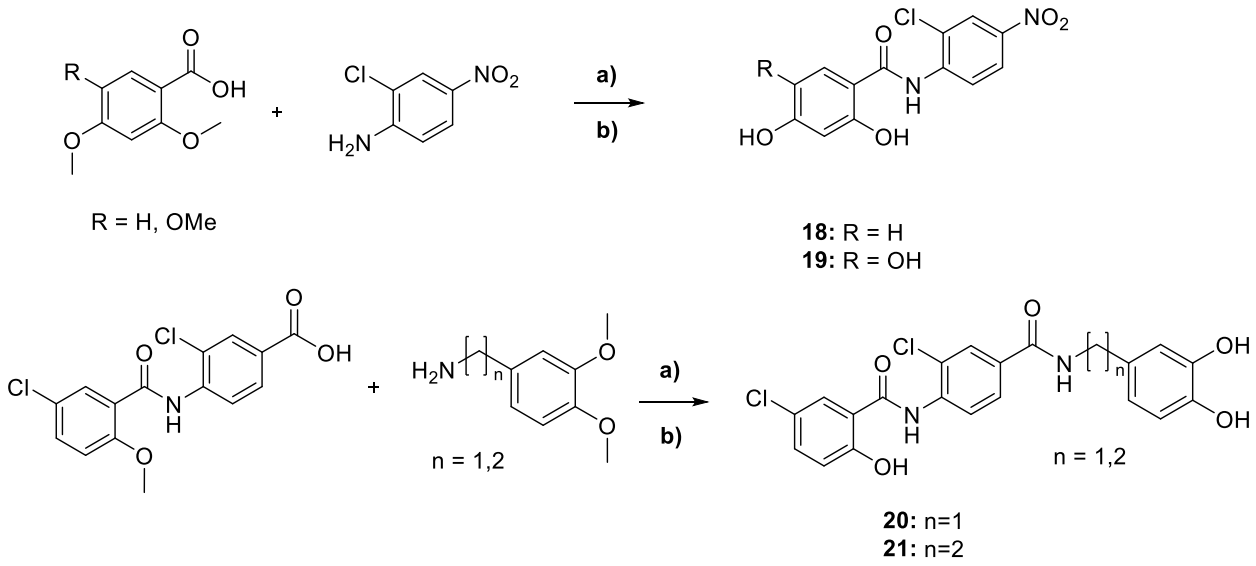

Figure 4.6. Synthesis of polyphenol derivatives of niclosamide. (a) PCl_3, xylenes, reflux, 4hr, 68-85% yield (b) BBr_3, DCM, 0°C, 16hr, 65-83% yield.

4.3.2 Initial screen for synergy with colistin and SAR

The initial screen of our study aimed to evaluate the ability of compounds **1-21** to synergize with colistin. For the initial screen, two colistin-resistant clinical isolates of *Klebsiella pneumoniae* (KP113250 and KP113254) and *Escherichia coli* (EC94393 and EC94474) were chosen. The two *K. pneumoniae* strains were chosen as they are highly colistin-resistant with minimum inhibitory concentrations (MIC) for colistin of 256 μg/mL. The two *E. coli* strains were selected as they were known to harbor the *mcr-1* gene[18] which confers colistin resistance via phosphoethanolamine transferase.[19] Colistin had MICs of 8 μg/mL in EC94394 and 16 μg/mL in EC94474.

To ensure any biological activity seen was due to colistin potentiation and not to any innate activity of the newly synthesized compounds, we first screened all compounds for standalone antibacterial activity against these four strains (**Table S1**). The lowest concentration of each compound able to inhibit bacterial growth was determined to be the MIC. Similar to niclosamide,

all compounds displayed poor antibacterial activity with MIC values of ≥128 μg/mL and were then further evaluated for synergy with colistin.

To perform the initial screen, we used a fixed concentration of 4 μM of compound and determined the MIC of colistin in combination against each strain. As a comparison, niclosamide was shown to drastically enhance the antibacterial activity of colistin in all four strains, consistent with previous reports.[9] At 4 μM, niclosamide was able to lower the MIC of colistin by 512-fold against KP113250, 1024-fold against KP113254, and 32-fold against both *E. coli* strains. The prominent colistin MIC reduction by niclosamide provided a baseline of potentiating activity to which the novel derivatives could be compared. At first, we investigated colistin potentiation for compounds **1**-**3** at 4 mM (**Table 4.1**)**.** We observed that the conversion of the nitro group to an amine moiety (**1**) resulted in comparable potentiation of colistin in *E. coli* strains. However, reduced potentiation was observed against *K. pneumoniae*. Further modifying the amine with acylation (**2**) or alkylation (**3**) led to a complete loss of colistin-potentiating activity against both bacteria (**Table 4.1**).

Table 4.1. Colistin MIC in combination with 4 μM of compounds 1-3 against four colistin-resistance strains of GNB. KP = Klebsiella pneumoniae, EC = Escherichia coli.

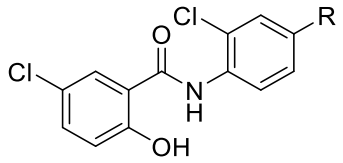

Compound	R	Colistin MIC with 4 μM compound (μg/mL)			
		KP113250	**KP113254**	**EC94393**	**EC94474**
Niclosamide	**NO_2**	**0.25**	**0.5**	**0.25**	**0.5**
1	**NH_2**	**16**	**32**	**0.5**	**2**
2		256	256	8	16
3		256	256	8	16
Colistin MIC alone		256	256	8	16

We next replaced the nitro group on niclosamide with an azide (**4**), a methyl ester (**5a)**, a carboxylic acid (**6**), various amide moieties (**7**-**12)** and triazole fragments (**14**-**17**) (**Table 4.2**). We observed that the azide and methyl ester derivatives retained synergy with colistin against all strains tested, indicating that these modifications are compatible with the colistin potentiation of niclosamide. Compound **4** displayed prominent potentiating activity against the two *E. coli* strains, reducing the MIC of colistin to 0.016 μg/mL against EC94393 (a 16-fold higher reduction compared to niclosamide). As **4** also contains hydrogen at R^1 instead of a chlorine atom, it appears that the chlorine at this position is not necessary for synergy with colistin. Compound **5a**, in combination with colistin, displayed a comparable synergy profile relative to niclosamide in all tested strains.

Interestingly, compound **5b**, which differs from **5a** only by a methylated phenol group, lost all synergy with colistin (**Table S2)**. This demonstrates the necessity of the phenol in niclosamide's ability to potentiate colistin. Unfortunately, further modification of the methyl ester moiety by converting it to a carboxylic acid (**6**) or an amide (**7**-**12**) completely abolished all synergy with colistin. The triazole analogs **14**-**17** were not able to potentiate colistin in all tested strains. Nonetheless, these findings demonstrated that the nitro group on niclosamide can be replaced with a variety of substituents while still retaining synergy with colistin.

Table 4.2. Colistin MIC in combination with 4 μM of compounds **4**-**12** and **14**-**17** against four colistin-resistance strains of GNB. KP = *Klebsiella pneumoniae,* EC = *Escherichia coli*.

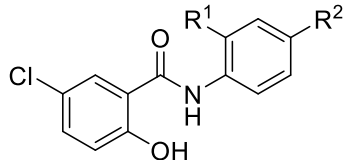

			Colistin MIC with 4 μM compound (μg/mL)			
Compound	**R^1**	**R^2**	**KP113250**	**KP113254**	**EC94393**	**EC94474**
Niclosamide	Cl	NO_2	0.25	0.5	0.25	0.5
4	H	N_3	0.25	0.5	0.016	0.25
5a	Cl		1	1	0.25	1
6	Cl		256	256	8	16
7	Cl		256	256	8	16
8	Cl	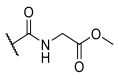	256	256	8	16
9	Cl	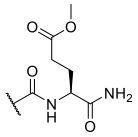	256	256	8	16
10	Cl	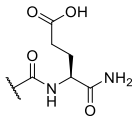	256	256	8	16
11	Cl	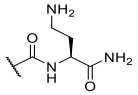	256	256	8	16
12	Cl	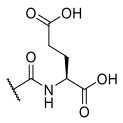	256	256	8	16
14	Cl	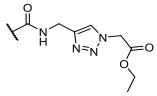	256	256	8	16
15	Cl	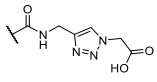	256	256	8	16

16	Cl	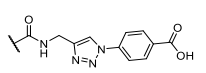	256	256	8	16
17	Cl	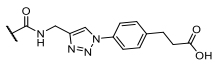	256	256	8	16
Colistin MIC alone			256	256	8	16

Given the demonstrated importance of the phenol moiety within the salicylanilide scaffold, we wondered how the installation of additional phenol groups, as in compounds **18**-**21**, would affect niclosamide's ability to potentiate colistin (**Table 4.3)**. We observed that the addition of even one additional phenol group on the salicylic acid ring (**18**) resulted in a complete loss of synergy with colistin. The amide-containing polyphenol compounds **20** and **21** were also inactive. These results suggest that while the phenol group is necessary, the addition of multiple phenol groups reduces colistin-potentiating activity.

Table 4.3. Colistin MIC in combination with 4 μM of polyphenol compounds **18-21** against four colistin-resistance strains of GNB. KP = *Klebsiella pneumoniae,* EC = *Escherichia coli*.

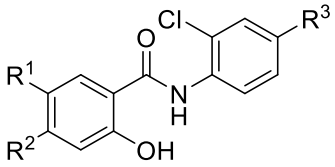

				Colistin MIC with 4 μM compound (μg/mL)			
Compound	**R^1**	**R^2**	**R^3**	**KP113250**	**KP113254**	**EC94393**	**EC94474**
Niclosamide	Cl	H	NO_2	0.25	0.5	0.25	0.5
18	H	OH	NO_2	256	256	8	16
19	OH	OH	NO_2	256	256	8	16
20	Cl	H	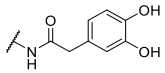	256	256	8	16
21	Cl	H	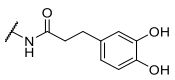	256	256	8	16
Colistin MIC alone				256	256	8	16

Overall, the results of this SAR led to us conclude that the nitro group in niclosamide can be replaced with an azide, a methyl ester, and (to a lesser extent) an amine while still retaining synergy with colistin against GNB. We also show that further modification of the amine or ester groups abolishes synergistic activity. The phenol group was shown to be necessary for synergy with colistin as methylation resulted in complete loss of colistin potentiation (compound **5b**, **Table S2**).

Finally, we compared the colistin potentiation of hit compounds **1**, **4** and **5a** to niclosamide in a panel of colistin-resistant and colistin-susceptible GNB using the checkerboard assay (**Figure 4.6**). The fractional inhibitory concentration index (FICI) for each combination was determined to assess interactions between the two components. FICI values of ≤ 0.5, $0.5 < x \leq 4$, and >4 were interpreted as synergistic, additive, and antagonistic interactions, respectively. We observed that compound **4** was overall superior to niclosamide (lowest FICI value), especially in *E. coli.* Compound **5a** was comparable to niclosamide, while compound **1** showed synergy with colistin only in *E. coli* and *K. pneumoniae* but not in *Pseudomonas aeruginosa.* Despite the promising colistin-potentiating activity of **4**, the high synthetic cost as well as concerns over the stability of the aryl azide led to us selecting the methyl ester compound **5a** for further screening against clinical isolates of *P. aeruginosa* and *Acinetobacter baumannii*.

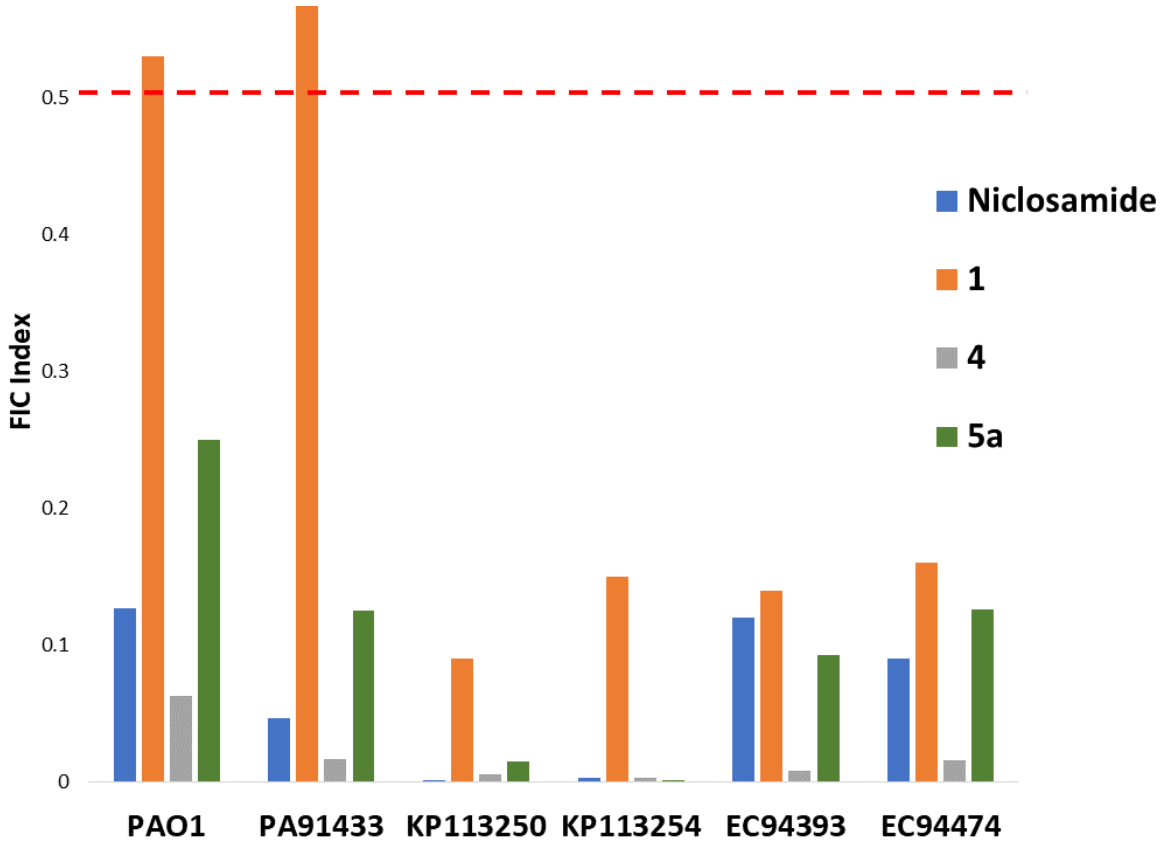

Figure 4.6. Synergy comparison between compounds **1**, **5a** or **4** and niclosamide PA = *Pseudomonas aeruginosa*, KP = *Klebsiella pneumoniae,* EC = *Escherichia coli*. Red dotted line denotes FICI of 0.5. FICI values were obtained at a concentration of 4 µM for each compound.

*4.3.3 Synergy between **5a** and colistin against P. aeruginosa and A. baumannii*

We further evaluated the therapeutic potential of lead compound **5a** in combination with colistin against a panel of multidrug-resistant (MDR) clinical isolates of *P. aeruginosa* and *A. baumannii* (**Tables 4.4** and **4.5**). Compound **5a** was able to synergize with colistin in 8 out of 10 strains of *P. aeruginosa.* Synergy was only not observed in PA259 and PA260, which were already highly susceptible to colistin (MIC of 0.25 µg/mL). Analog **5a** was able to drastically reduce colistin's MIC against all colistin-resistant isolates (PA91433, PA101243, PA262 and PA101885). The combination of **5a** and colistin against PA101243 was of particular note, with 1 µg/mL of **5a**

lowering the MIC of colistin from 1024 μg/mL to 0.5 μg/mL, a 2048-fold reduction. In all strains tested, **5a** was able to lower the MIC of colistin to 0.5 μg/mL or less (**Table 4.4**).

Table 4.4. Synergy between compound **5a** and colistin against a panel of wild-type and clinical isolates of *P. aeruginosa.*

Strain	MIC_{Col}	MIC_{Combi}	MIC_{5a}	MIC_{Combi}	FICI	Interpretation
PAO1	1	0.25	>256	0.25	0.250<x<0.251	Synergy
PA095	0.25	0.016	>256	16	0.063<x<0.125	Synergy
PA259	0.25	0.25	>256	1	1.000<x<1.004	Additive
PA260	0.25	0.125	>256	1	0.500<x<0.504	Additive
PA264	1	0.25	>256	0.5	0.250<x<0.252	Synergy
PA262	4	0.25	>256	1	0.063<x<0.066	Synergy
PA100036	2	0.25	>256	1	0.125<x<0.129	Synergy
PA101885	4	0.5	>256	1	0.125<x<0.129	Synergy
PA91433	4	0.5	>256	0.25	0.125<x<0.126	Synergy
PA101243	1024	0.5	>256	1	0.0005<x<0.0045	Synergy

Similar synergystic activity was observed for *A. baumannii* (**Table 4.5**). Synergy was observed in four out of five isolates, LAC-4 (colistin MIC of 0.25 μg/mL) being the only exception. Compound **5a** was able to lower the MIC of colistin to 0.5 μg/mL or below in all strains tested, including against highly resistant AB027 (colistin MIC of 1024 μg/mL).

Table 4.5. Synergy between compound **5a** and colistin against a panel of wild-type and clinical isolates of *A. baumannii.*

Strain	MIC_{Col}	MIC_{Combi}	MIC_{5a}	MIC_{Combi}	FICI	Interpretation
***A. baumannii* ATCC**	1	0.25	>256	0.25	0.250<x<0.251	Synergy
***A baumannii* 1190193**	4	0.5	>256	0.25	0.125<x<0.126	Synergy
AB027	1024	0.5	>256	1	0.0005<x<0.004	Synergy
AB031	0.25	0.015625	>256	16	0.063<x<0.125	Synergy
LAC-4	0.25	0.25	>256	1	1.000<x<1.004	Additive

Overall, these results show that a combination of colistin and **5a** is effective against *K. pneumonia, E. coli, P. aeruginosa* and *A. baumannii.* Replacing the nitro group of niclosamide with a methyl ester led to the development of a novel derivative that synergized with colistin in nearly all clinical isolates tested, and restored colistin activity against every colistin-resistant isolate.

*4.3.4 Cytotoxicity of **1** and **5a** against eukaryotic cells*

Toxicity against eukaryotic cells is a major challenge for repurposing niclosamide as an antibacterial agent. To test whether the modification of the nitro group may be a potential avenue for reducing toxicity, the toxic effects of compounds **1** and **5a** were investigated on two ovarian cancer cell lines OVCAR-3 and COV362, and compared to niclosamide which has been shown to possess potent antitumor effects against ovarian cancer cells[20]. The results of experiments with the three compounds using the CyQuant assay[21] are displayed in **Figure 4.7**. After 48 h incubation, the cell number for the controls increased by about 26% for OVCAR-3 and 89% for COV362 relative to the initial cell number (day 0).

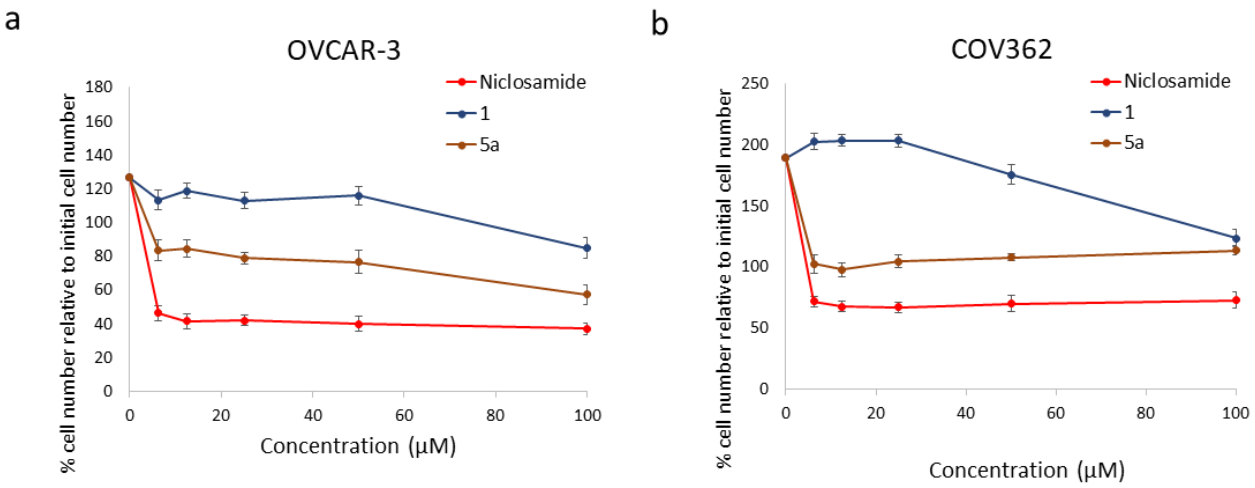

Figure 4.7: Effect of niclosamide, compound **1** and compound **5a** (0-100 µM) on ovarian cancer cell lines a) OVCAR-3 and b) COV362 cells. Cell numbers from representative wells were determined on day 0 before the addition of the compound. After 48 h incubation (day 2), cells were counted again to determine the increase in cell number over day 0 cell count. The overall increase in cell number for control after 48 h incubation was found to be around 26% and 89% relative to the initial cell number (day 0) for OVCAR-3 and COV362 cells, respectively. Each concentration of the drug tested is represented as a percent of that cell growth relative to the initial cell number. The results represent the mean ± standard deviation of two independent experiments with four wells for each concentration.

Incubation with 6-100 µM niclosamide after 48 h showed a toxic effect on both the cell lines, killing around 60% (OVCAR-3) and 30% (COV362) of the initial cell number before drug treatment. Incubation of cells with compound **5a** at 6-50 µM killed only 20% of OVCAR-3 cells while it had a cytostatic effect (no significant change in initial cell number) in the same concentration range in COV362 cells. On the other hand, compound **1** at 6-50 µM showed slight inhibition of proliferation (around 13%) in OVCAR-3 cells relative to the control whereas under the same incubation conditions at 6-25 µM in COV362 cells, it stimulated proliferation and increased the cell number by 14% more than the control. Thus, in both OVCAR-3 and COV362

cells, incubation with compound **1** resulted in cell numbers higher than the initial cell number indicating a non-cytotoxic effect in the range of 6-25 μM.

Compound **5a** and compound **1** at 100 μM killed 43% and 15% of OVCAR-3 cells, respectively. At the same concentration, in COV362 cells, compound **5a** and compound **1** showed 75% and 66% inhibition of proliferation relative to the control but the cell numbers were still higher than the initial cell number indicating an antiproliferative rather than a cytotoxic effect. Taken together, the results demonstrate that compounds **1** and **5a** are less cytotoxic than niclosamide at all concentrations tested. Since the results of the microbiological studies demonstrate that compound **5a** was able to synergize with colistin to eradicate colistin-resistant GNB strains tested at concentrations of 1μg/mL (~0.3 μM), these results are very promising as an initial demonstration of reduced cytotoxicity. Overall, these results show that the replacement of the nitro group in niclosamide is a viable strategy to reduce toxicity against eukaryotic cells while retaining synergy with colistin.

4.5: Conclusions

A series of niclosamide analogs were synthesized to perform an SAR with an overall goal of replacing the nitro group of niclosamide to reduce toxicity while maintaining the ability of niclosamide to synergize with colistin against GNB. A small library of compounds was produced and their ability to synergize with colistin was observed. It was found that the nitro group on niclosamide can be replaced by an amine, a methyl ester, or an azide while still retaining colistin-potentiating activity. We also showed that the phenol group of niclosamide was necessary for synergy with colistin, but that the addition of multiple phenols led to a complete loss of synergy. The methyl ester analog (**5a**) was assessed against a panel of MDR clinical isolates and was shown

to reduce colistin MIC to below CLSI breakpoint values, even against highly resistant isolates. The amine and methyl ester compounds were also found to be less toxic to eukaryotic cells. One significant challenge that needs to be overcome is the likely metabolic instability of the ester in compound **5a**, as esters are known to be prone to hydrolysis *in vivo*[22], especially given that the carboxylic acid derivative **6** displayed no synergy with colistin. Nonetheless, this work provides important insights into synthetic strategies for the future development of novel niclosamide derivatives, and that modification to the nitro group of niclosamide may be a viable strategy of reducing toxicity.

4.6: Experimental

4.5.1. Materials

Reagents and solvents were purchased from commercially available suppliers such as Sigma-Aldrich, AK Scientific, Fisher Scientific, and Bachem and were used without further purification. Air- and moisture-sensitive reactions were performed with dry solvents under inert nitrogen atmosphere. Reaction progress was monitored using thin-layer chromatography (TLC) plates visualized with UV light. Column chromatography was performed to purify the compounds using SiliaFlash P60 (40–63 μm) 60 Å silica gel from Silicycle. The chemical structures of all final products used for biological testing were characterized by nuclear magnetic resonance spectroscopy (^{1}H NMR and ^{13}C NMR) on a Bruker AMX NMR 300 MHz and 500 MHz spectrometer. Electrospray ionization mass spectrometry (ESI-MS) data was obtained using a Varian 320-MS LC/MS.

4.5.2. Synthetic methods

General synthetic procedures

General procedure A: Benzanilide coupling using PCl_3

The appropriate benzoic acid derivative (1 equiv.) and aniline derivative (1 equiv.) were dissolved in dry xylenes (2 mL per mmol of reactants) and heated to reflux. PCl_3 (0.4 equiv.) was added dropwise upon which a precipitate formed. Solution was refluxed for 4 h. The mixture was cooled to rt and filtered, after which the precipitate was washed with ethyl acetate.

General procedure B: LiOH Ester hydrolysis

The appropriate carboxylic acid was dissolved in a THF (5 mL per mmol) and MeOH (5 mL per mmol) mixture. A solution of 2M LiOH in water (10 mL per mmol) was added and the reaction was stirred at rt for 2 h. The reaction was neutralized with concentrated HCl at 0°C upon which the product precipitated, was filtered and washed with water (3×10mL).

General procedure C: Amide coupling using TBTU

The appropriate carboxylic acid (1 equiv.), *N*-methylmorpholine (3 equiv.), and O-(Benzotriazol-1-yl)-N,N,N',N'-tetramethyluronium tetrafluoroborate (TBTU) (1.1 equiv.) were dissolved in anhydrous DMF (3 mL per mmol of carboxylic acid) and stirred at rt for 15 min under N_2. The appropriate amine (1.2 equiv.) was added and the reaction was stirred for 4 h at rt. Solution was concentrated *in vacuo* and the residue was collected in DCM, washed with 1M HCl (× 3), saturated $NaHCO_3$ (× 3) and brine. The organic layer was concentrated and the product was purified using flash chromatography (0-10% MeOH in DCM).

General procedure D: Methoxy deprotection

The appropriate methoxy protected intermediate (1 equiv.) was dissolved in anhydrous DCM at 0°C. A 1M solution of BBr_3 in DCM (1.5 equiv. BBr_3 per methoxy group) was added dropwise and the reaction was slowly warmed to rt. Solution was stirred overnight. Reaction was cooled to 0°C and quenched with the careful addition of MeOH (5 mL per mmol) followed by stirring for 15 min. Reaction mixture was concentrated *in vacuo* and the product was purified using flash chromatography (0-10% MeOH in DCM).

General procedure E: Benzyl deprotection

The appropriate benzyl protected intermediate (1 equiv.) was dissolved in MeOH (3 mL per mmol) and THF (1 mL per mmol) Palladium on carbon (0.1 equiv.) was then added followed by H_2 gas (balloon). The solution was stirred for 2 h at rt, filtered over celite and concentrated *in vacuo*. The product was purified using flash chromatography (0-10% MeOH in DCM).

General procedure F: Copper-assisted azide-alkyne cycloaddition (CuAAC)

The appropriate azide (1 equiv.) and alkyne (1 equiv.) and $CuI{\cdot}P(OEt)_3$ (0.3 equiv.) were dissolved in anhydrous DMF (3 mL) and treated with iPr_2NEt (2 equiv.) The reaction was stirred under N_2 at rt for 2 h. The reaction mixture was concentrated under vacuum, dissolved in water and extracted with DCM (× 3) The organic layers were combined, dried over anhydrous Na_2SO_4, and concentrated *in vacuo*. The product was purified using flash chromatography (0-10% MeOH in DCM).

(1) N-(4-amino-2-chlorophenyl)-5-chloro-2-hydroxybenzamide

Niclosamide (1.435g, 4.38 mmol) was suspended in 25 mL MeOH, followed by the addition of 10mL of saturated NH_4Cl (aq). Zinc dust (3g, 45.89 mmol) was slowly added into the solution at 0°C. The reaction was warmed to RT and stirred for 4 hours, after which TLC indicated that the starting material was completely consumed. The solution was filtered over celite to remove

excess zinc and the resulting filtrate was concentrated *in vacuo*. The crude residue was dissolved in 30 mL ethyl acetate and washed with water (3 x 10 mL) and brine (3 x 5 mL). The organic layer was concentrated and purified by flash chromatography (0-10% MeOH in DCM) yielding 649.5mg (2.19 mmol, 49.9%) of compound **1** as a pale yellow solid. ^{1}H NMR (500 MHz, Methanol-d_4) δ 8.64 (d, J = 8.9 Hz, 1H), 8.02 (d, J = 2.7 Hz, 1H), 7.56 (d, J = 2.5 Hz, 1H), 7.41 – 7.37 (m, 2H), 6.97 (d, J = 8.8 Hz, 1H). ^{13}C NMR (126 MHz, Methanol-d_4) δ 163.49, 155.16, 136.00, 133.39, 130.08, 126.86, 124.82, 124.55, 123.72, 123.19, 122.03, 119.42, 118.14. ESI-MS: *m/z* $[M+H]^+$ 297.0193

(2) N-(4-acetamido-2-chlorophenyl)-5-chloro-2-hydroxybenzamide

Compound **1** (88mg, 0.3 mmol) was dissolved in 3mL DCM followed by the addition of Et_3N (125 µL, 0.9 mmol) and acetyl chloride (25 µL, 0.36 mmol). Solution was stirred at RT overnight and concentrated *in vacuo*. The crude residue was dissolved in 5 mL ethyl acetate and washed with saturated $NaHCO_3$ (3 x 5 mL) and brine (3 x 3 mL). The organic layer was dried over anhydrous Na2SO4, concentrated and purified by flash chromatography (0-10% MeOH in DCM) yielding 86.6 mg (0.25 mmol, 84.8%) off-white powder.^{1}H NMR (500 MHz, DMSO-d_6) δ 10.88 (s, 1H), 10.76 (s, 1H), 8.24 (d, J = 8.9 Hz, 1H), 8.01 (d, J = 2.3 Hz, 1H), 7.97 (d, J = 2.8 Hz, 1H), 7.58 (dd, J = 9.0, 2.4 Hz, 1H), 7.47 (dd, J = 8.8, 2.8 Hz, 1H), 7.32 (d, J = 8.8 Hz, 1H), 2.07 (s, 3H). ^{13}C NMR (126 MHz, DMSO- d_6) δ 169.14, 163.02, 156.37, 137.21, 133.54, 130.32, 129.98, 123.99, 123.57, 123.51, 119.99, 119.75, 119.59, 118.44, 24.37. ESI-MS: *m/z* $[M+H]^+$ 339.0312

(3) 3-chloro-4-(5-chloro-2-hydroxybenzamido)-*N*,*N*,*N*-trimethylanilinium

Compound **1** (250mg, 0.85 mmol) was dissolved in 5mL DMF. 2,6 lutidine (186 µL, 1.6 mmol) was added followed by iodomethane (211 µL, 3.4 mmol). Solution was stirred at RT overnight and 20 mL ethyl acetate was added to facilitate precipitation. Product was washed on-filter with ethyl acetate (3x 5mL), acetone (3x 5mL) and DCM (3x 5mL) yielding 142mg (0.41 mmol, 49%) **4** as a dark brown solid. ^{1}H NMR (500 MHz, DMSO-d_6) δ 11.17 (s, 1H), 8.24 (d, J = 8.9 Hz, 1H), 8.01 (d, J = 2.3 Hz, 1H), 7.97 (d, J = 2.8 Hz, 1H), 7.58 (dd, J = 9.0, 2.4 Hz, 1H), 7.47 (dd, J = 8.8, 2.8 Hz, 1H), 7.32 (d, J = 8.8 Hz, 1H), 2.07 (s, 3H). ^{13}C NMR (126 MHz, DMSO-d_6) δ 169.14, 163.02, 156.37, 137.21, 133.54, 130.32, 129.98, 123.99, 123.57, 123.51, 119.99, 119.75, 119.59, 118.44, 24.37. ESI-MS: *m/z* $[M]^+$ 339.0661

(4) *N*-(4-azidophenyl)-5-chloro-2-hydroxybenzamide

5-Chlorosalicylic acid (45 mg, 0.293 mmol) and EDC (112 mg, 0.586 mmol) were dissolved in tetrahydrofuran (2 mL) at room temperature and stirred for 15 minutes. 4-Azidoaniline (51 mg, 0.299 mmol) was added and the reaction mixture was stirred at rt for 5 hours over which time the solution gradually turned from clear to yellow. The reaction was concentrated under vacuo and dissolved in 12 mL ethyl acetate, washed with 1 M HCl (3 × 5 mL), saturated sodium bicarbonate solution (3 × 5 mL) and brine (3 × 5 mL), dried over anhydrous Na_2SO_4 and concentrated *in vacuo*. The crude material was purified using flash chromatography using DCM

as a solvent system to afford **5** as a brown solid (61 mg, 73%) ^{1}H NMR (500 MHz, DMSO-d_6) δ 11.81 (s, 1H), 10.47 (s, 1H), 7.93 (d, J = 2.6 Hz, 1H), 7.76 (dd, J = 9.0, 2.9 Hz, 2H), 7.48 (dd, J = 8.8, 2.6 Hz, 1H), 7.16 – 7.13 (m, 2H), 7.02 (d, J = 8.8 Hz, 1H). ^{13}C NMR (126 MHz, DMSO-d_6) δ 177.32, 165.42, 157.41, 143.04, 135.53, 133.49, 128.77, 122.63, 122.60, 119.67, 119.63.

(5a) methyl 3-chloro-4-(5-chloro-2-hydroxybenzamido)benzoate

Compound **5a** was synthesized following general procedure A starting from 5-Chlorosalicylic acid (928mg, 5.38 mmol) and methyl 4-amino-3-chlorobenzoate (1g, 5.38 mmol) and purified by flash chromatography (0-10% MeOH in DCM) resulting in 748mg (2.2 mmol, 41%) **5a** as a white solid. ^{1}H NMR (500 MHz, DMSO-d_6) δ 12.37 (s, 1H), 11.14 (s, 1H), 8.67 (d, J = 8.7 Hz, 1H), 8.01 (d, J = 2.0 Hz, 1H), 7.98 – 7.92 (m, 2H), 7.50 (dd, J = 8.7, 2.8 Hz, 1H), 7.08 (d, J = 8.8 Hz, 1H), 3.85 (s, 3H). ^{13}C NMR (126 MHz, DMSO-d_6) δ 165.15, 162.85, 155.55, 139.79, 134.15, 130.46, 130.35, 129.55, 125.99, 124.14, 122.81, 121.53, 120.09, 119.53, 52.75. ESI-MS: *m/z* $[M+H]^+$ 340.0148

(5b) methyl 3-chloro-4-[(5-chloro-2-methoxybenzoyl)amino]benzoate

Compound **5b** was synthesized following general procedure A starting from 5-Chloro-2-methoxybenzoic Acid (558mg, 3 mmol) and methyl 4-amino-3-chlorobenzoate (516g, 3 mmol) resulting in 840mg (2.4 mmol, 82%) of **5b** as a white solid. ^{1}H NMR (300 MHz, Chloroform-*d*) δ 10.80 (s, 1H), 8.81 (d, J = 8.8 Hz, 1H), 8.29 (d, J = 2.8 Hz, 1H), 8.12 (d, J = 2.0 Hz, 1H), 8.05 – 7.94 (m, 1H), 7.50 (dd, J = 8.9, 2.8 Hz, 1H), 7.02 (d, J = 8.9 Hz, 1H), 4.12 (s, 3H), 3.94 (s, 3H). ^{13}C NMR (75 MHz, Chloroform-*d*) δ 165.69, 162.19, 155.90, 139.56, 133.55, 132.37, 130.48, 129.49, 127.19, 125.90, 122.47, 120.84, 113.11, 56.77, 52.33. ESI-MS: *m/z* $[M+H]^+$ 354.0292

(5c) methyl 4-{[2-(benzyloxy)-5-chlorobenzoyl]amino}-3-chlorobenzoate

Compound **5a** (100mg, 0.3mmol) was dissolved in 3mL anhydrous DMF under N_2 at 0 °C. NaH (13mg, 0.32 mmol) as a 60% dispersion in mineral oil was added and the solution was stirred at 0 °C for 15 mins. Benzyl bromide (39 µL, 0.32 mmol) was added dropwise and the solution was warmed to RT and stirred for 4 hours. Reaction was quenched with 10 mL 1M HCl (aq) at 0 °C which caused the product to precipitate. The precipitate was filtered and washed with 3x5 mL hexanes yielding 107mg of **6c** as a pale-yellow solid (0.25 mmol, 83%) which was used without further purification.

(6) 3-chloro-4-(5-chloro-2-hydroxybenzamido)benzoic acid

Compound **6** was obtained using general procedure B starting from **5a** (708mg, 2.1 mmol) in 98% (667 mg) yield as a white powder. ^{1}H NMR (300 MHz, DMSO-d_6) δ 11.38 (s, 1H), 8.61 (d, J = 8.6 Hz, 1H), 7.95 (d, J = 1.9 Hz, 1H), 7.91 – 7.86 (m, 2H), 7.53 – 7.45 (m, 2H). ^{13}C NMR (75 MHz, DMSO-d_6) δ 166.09, 163.06, 156.65, 139.29, 133.87, 130.44, 130.13, 129.57, 123.32, 122.61, 121.43, 120.09, 119.86. ESI-MS: *m/z* $[M+H]^+$ 327.1365

(6b) 3-chloro-4-[(5-chloro-2-methoxybenzoyl)amino]benzoic acid

Compound **6b** was obtained using general procedure B starting from **5b** (820mg, 2.3 mmol) in 96% (779 mg) yield as a white powder which was used without further purification.

(6c) 3-chloro-4-{[2-(benzyloxy)-5-chlorobenzoyl]amino}- benzoic acid

Compound **6c** was obtained using general procedure B starting from **5c** (107mg, 0.25 mmol) in 96% (100mg) yield as a white powder which was used without further purification.

(7) 5-chloro-*N*-[2-chloro-4-(methylcarbamoyl)phenyl]-2-hydroxybenzamide

Compound **7** was obtained using general procedure C starting from **6b** (200mg, 0.6 mmol) and methylamine HCl, followed by general procedure D resulting in 119mg (0.35 mmol) of white powder (58% over 2 steps). ^{1}H NMR (500 MHz, DMSO-d_6) δ 12.33 (s, 1H), 11.05 (s, 1H), 8.54 (dd, J = 22.9, 7.1 Hz, 2H), 8.05 – 7.96 (m, 2H), 7.86 (d, J = 8.7 Hz, 1H), 7.52 (dd, J = 8.7, 2.5 Hz, 1H), 7.09 (d, J = 8.8 Hz, 1H), 2.79 (d, J = 4.2 Hz, 3H). ^{13}C NMR (126 MHz, DMSO-d_6) δ 165.19, 162.96, 155.68, 137.82, 134.11, 131.29, 130.40, 128.56, 127.31, 124.11, 123.10, 121.85, 120.16, 119.59, 26.75. ESI-MS: *m/z* $[M+H]^+$ 339.0287

(8) methyl [3-chloro-4-(5-chloro-2-hydroxybenzamido)benzamido]acetate

Compound **8** was obtained using general procedure C starting from **6b** (200mg, 0.6 mmol) and glycine methyl ester HCl, followed by general procedure D resulting in 132 mg (0.33 mmol) of white powder (55% over 2 steps). ^{1}H NMR (500 MHz, DMSO-d_6) δ 12.36 (s, 1H), 11.10 (s, 1H), 9.06 (t, J = 5.8 Hz, 1H), 8.61 (d, J = 8.6 Hz, 1H), 8.03 (m, 2H), 7.92 (dd, J = 8.6, 2.1 Hz, 1H), 7.53 (dd, J = 8.7, 2.8 Hz, 1H), 7.10 (d, J = 8.7 Hz, 1H), 4.03 (s, 2H), 3.67 (s, 3H). ^{13}C NMR (126 MHz, DMSO-d_6) δ 170.74, 165.25, 162.97, 155.67, 138.30, 134.14, 130.42, 130.26, 128.78, 127.61, 124.13, 123.09, 121.82, 120.15, 119.59, 52.25, 41.72. ESI-MS: *m/z* $[M+H]^+$ 397.0324

(9) methyl (4*S*)-5-amino-4-[3-chloro-4-(5-chloro-2-hydroxybenzamido)benzamido]-5-oxopentanoate

Compound 9 was obtained using general procedure C starting from **6b** (200mg, 0.6 mmol) and L-Glutamic Acid γ-Methyl Ester α-Amide Hydrochloride followed by general procedure D resulting in 146 mg (0.31 mmol) of white powder (52% over 2 steps). ^{1}H NMR (500 MHz, DMSO-d_6) δ. 12.42 (s, 1H), 11.09 (s, 1H), 8.51 (m, 2H), 8.09 (s, 1H), 7.92 (m, 2H), 7.42 (m, 2H), 6.09 (m, 2H) 4.32 (m, 1H), 3.52 (s, 1H), 2.23 (m, 2H), 1.98 (m, 1H), 1.78 (m, 1H). ^{13}C NMR (126 MHz, DMSO-d_6) δ 173.61, 173.32, 165.05, 163.04, 155.90, 138.07, 134.11, 130.78, 130.39, 129.03, 124.94, 123.98, 122.90, 121.66, 120.15, 119.65, 53.18, 51.80, 30.77, 27.28. ESI-MS: *m/z* $[M+H]^+$ 468.0712

(10) (4*S*)-5-amino-4-[3-chloro-4-(5-chloro-2-hydroxybenzamido)benzamido]-5-oxopentanoic acid

Compound **10** was obtained using general procedure B starting from **9** (100mg, 0.21 mmol) resulting in 78 mg (0.17 mmol) of off-white powder (81%). ^{1}H NMR (500 MHz, Methanol-d_4) δ 8.65 (d, J = 8.6 Hz, 1H), 8.05 (d, J = 2.7 Hz, 1H), 8.02 (d, J = 2.0 Hz, 1H), 7.86 (dd, J = 8.7, 2.0 Hz, 1H), 7.41 (dd, J = 8.7, 2.8 Hz, 1H), 6.98 (d, J = 8.7 Hz, 1H), 4.58 (dd, J = 9.2, 5.0 Hz, 1H), 2.48 (t, J = 7.4 Hz, 2H), 2.26 – 2.20 (m, 1H), 2.12 – 2.05 (m, 1H). ^{13}C NMR (126 MHz, Methanol-d_4) δ 175.29, 175.07, 166.73, 163.32, 155.04, 138.27, 133.35, 130.22, 129.86, 128.44, 126.60, 124.87, 123.16, 121.17, 119.70, 118.10, 53.27, 30.06, 26.79. ESI-MS: *m/z* $[M+H]^+$ 454.0515

(11) 5-chloro-*N*-(4-{[(2*S*)-1,4-diamino-1-oxobutan-2-yl]carbamoyl}phenyl)-2-hydroxybenzamide

Compound **11** was obtained using general procedure C starting from **6c** (100mg, 0.3 mmol) and L-diaminobutyric acid γ- Carbobenzoxy-α-Amide hydrochloride followed by general procedure E resulting in 43 mg (0.10 mmol) of brown powder (34% over 2 steps). 1H NMR (500 MHz, DMSO-d_6) δ 12.52 – 12.43 (m, 1H), 11.12 (s, 1H), 8.71 (d, J = 7.8 Hz, 1H), 8.60 (d, J = 8.4 Hz, 1H), 8.14 (s, 1H), 7.99 (d, J = 2.3 Hz, 1H), 7.95 (d, J = 8.7 Hz, 1H), 7.77 – 7.69 (m, 3H), 7.57 – 7.50 (m, 2H,), 7.23 (s, 1H, 12-b), 7.12 (d, J = 8.6 Hz, 1H), 4.51 – 4.46 (m, 1H), 2.92 – 2.85 (m, 2H), 2.11 (dd, J = 14.1, 6.8 Hz, 1H), 1.96 (dd, J = 14.6, 7.3 Hz, 1H). 13C NMR (126 MHz, DMSO-d_6) δ 173.09, 165.18, 163.00, 155.72, 138.15, 134.17, 130.62, 130.38, 129.09, 128.02, 124.09, 122.87, 121.64, 120.12, 119.62, 51.44, 36.97, 29.97 ESI-MS: *m/z* $[M+H]^+$ 425.0761

(12) (2*S*)-2-[3-chloro-4-(5-chloro-2-hydroxybenzamido)benzamido]pentanedioic acid

Compound **12** was obtained using general procedure C starting from **6c** (100mg, 0.3 mmol) and Di-tert-butyl (S)-2-Aminopentanedioate hydrochloride followed by general procedure E and then general procedure B resulting in 22 mg (0.05 mmol) of white powder (15% over 3 steps).^{1}H NMR (500 MHz, Methanol-d_4) δ 8.73 (d, J = 8.8 Hz, 1H), 8.02 (d, J = 2.1 Hz, 1H), 7.86 – 7.79 (m, 2H), 7.08 (dd, J = 8.8, 3.1 Hz, 1H), 6.67 (d, J = 8.9 Hz, 1H), 4.39 (dd, J = 8.3, 4.4 Hz, 1H), 2.35 – 2.21 (m, 3H), 2.13 – 2.08 (m, 1H). ^{13}C NMR (126 MHz, Methanol-d_4) δ 180.97, 177.83, 168.80, 167.48, 166.23, 139.73, 132.64, 129.31, 128.45, 128.32, 128.25, 125.99, 123.53, 120.97, 119.21, 116.99, 56.06, 34.39, 29.03. ESI-MS: *m/z* $[M+Na]^+$ 477.0291

(13) 5-chloro-*N*-{2-chloro-4-[(prop-2-yn-1-yl)carbamoyl]phenyl}-2-hydroxybenzamide

Compound **13** was obtained using general procedure C starting from **6b** 500mg, 1.5 mmol) and propargylamine followed by general procedure D resulting in 267 mg (0.74 mmol) of white powder (49% over 2 steps) which was used without further purification.

(14) methyl {4-[({3-chloro-4-[(5-chloro-2-hydroxybenzoyl)amino]benzoyl}amino)ethyl]-1*H*-1,2,3-triazol-1-yl}acetate

Compound **14** was obtained using general procedure F starting from **13** (55mg, 0.15 mmol) and ethyl 2-azidoacetate resulting in 23 mg (0.05 mmol) of off-white powder (33%).^{1}H NMR (300 MHz, DMSO-d_6) δ 12.35 (s, 1H), 11.08 (s, 1H), 9.16 (t, J = 5.8 Hz, 1H), 8.58 (d, J = 8.7 Hz, 1H), 8.08 (d, J = 2.0 Hz, 1H), 8.00 – 7.88 (m, 3H), 7.53 (dd, J = 8.7, 2.8 Hz, 1H), 7.10 (d, J = 8.8 Hz, 1H), 5.35 (s, 2H), 4.54 (d, J = 5.7 Hz, 2H), 4.17 (q, J = 7.1 Hz, 2H), 1.22-1.18 (m, 3H). ^{13}C NMR

(126 MHz, DMSO-d_6) δ 167.72, 164.75, 162.95, 155.66, 145.45, 138.06, 134.13, 130.81, 130.40, 128.77, 127.59, 124.93, 124.11, 123.04, 121.76, 120.14, 119.58, 61.88, 50.74, 35.33, 14.44. ESI-MS: *m/z* $[M+H]^+$ 492.0779

(15) {4-[({3-chloro-4-[(5-chloro-2-hydroxybenzoyl)amino]benzoyl}amino)methyl]-1*H*-1,2,3-triazol-1-yl}acetic acid

Compound **15** was obtained using general procedure B starting from **13** (15mg, 0.03 mmol) resulting in 12 mg (0.025 mmol) of off-white powder (86%).^{1}H NMR (500 MHz, DMSO-d_6) δ 11.29 (s, 1H), 9.17 (t, *J* = 5.8 Hz, 1H), 8.59 (d, *J* = 8.7 Hz, 1H), 8.08 (d, *J* = 2.0 Hz, 1H), 7.97 (d, *J* = 3.1 Hz, 2H), 7.92 (dd, *J* = 8.6, 2.0 Hz, 1H), 7.50 (dd, *J* = 8.7, 2.9 Hz, 1H), 7.11 (dd, *J* = 9.2, 5.0 Hz, 1H), 5.21 (s, 2H), 4.53 (d, *J* = 5.7 Hz, 2H). ^{13}C NMR (126 MHz, DMSO-d_6) δ 164.81, 163.13, 156.33, 145.34, 138.19, 134.03, 130.68, 130.31, 128.77, 127.57, 124.86, 123.63, 122.97, 121.68, 119.79, 53.08, 35.33. ESI-MS: *m/z* $[M+H]^+$ 464.0523

(16) {4-[({3-chloro-4-[(5-chloro-2-hydroxybenzoyl)amino]benzoyl}amino)methyl]-1*H*-1,2,3-triazol-1-yl}benzoic acid

Compound **16** was obtained using general procedure F starting from **13** (55mg, 0.15 mmol) and 4-azido benzoic acid resulting in 42 mg (0.08 mmol) of off-white powder (53%). ^{1}H NMR (500 MHz, DMSO-d_6) δ 13.20 (s, 1H), 12.52 (s, 1H), 11.12 (s, 1H), 9.23 (s, 1H), 8.82 (d, *J* = 7.1 Hz, 1H), 8.59 (d, *J* = 8.5 Hz, 1H), 8.16 – 8.06 (m, 5H), 8.03 – 7.93 (m, 2H), 7.52 (d, *J* = 8.4 Hz, 1H), 7.19 (d, *J* = 8.4 Hz, 1H), 4.63 (d, *J* = 5.5 Hz, 2H). ^{13}C NMR (126 MHz, DMSO-d_6) δ 166.83, 164.96, 164.87, 138.09, 134.09, 131.55, 131.52, 130.94, 130.35, 128.87, 127.72, 124.00, 122.96, 121.85, 121.69, 121.19, 120.13, 35.38. ESI-MS: *m/z* $[M+H]^+$ 526.0617

(17) 3-{4-[({3-chloro-4-[(5-chloro-2-hydroxybenzoyl)amino]benzoyl}amino)methyl]-1*H*-1,2,3-triazol-1-yl-phenyl}propionic acid

Compound **17** was obtained using general procedure F starting from **13** (55mg, 0.15 mmol) and 3-(4-Azidophenyl)propanoic acid resulting in 51 mg (0.09 mmol) of off-white powder (61%). ^{1}H NMR (500 MHz, DMSO-d_6) δ 12.36 (s, 1H), 12.17 (s, 1H), 11.09 (s, 1H), 9.17 (t, *J* = 5.6 Hz, 1H), 8.66 (s, 1H), 8.59 (d, *J* = 8.7 Hz, 1H), 8.11 (d, *J* = 1.9 Hz, 1H), 8.02 – 7.93 (m, 2H), 7.81 (d, *J* = 8.1 Hz, 2H), 7.53 (dd, *J* = 8.9, 2.8 Hz, 1H), 7.44 (d, *J* = 8.1 Hz, 2H), 7.10 (d, *J* = 8.7 Hz, 1H), 4.62 (d, *J* = 5.4 Hz, 2H), 2.90 (t, *J* = 7.6 Hz, 2H), 2.60 (t, *J* = 7.6 Hz, 2H). ^{13}C NMR (126 MHz, DMSO-d_6) δ 174.07, 164.81, 162.96, 155.67, 146.37, 141.97, 138.04, 135.33, 134.12, 130.86, 130.39, 130.07, 130.07, 128.85, 127.69, 124.10, 123.02, 121.74, 121.61, 120.38, 120.37, 120.14, 119.58, 35.40, 35.36, 30.24. ESI-MS: *m/z* $[M+H]^+$ 554.0965

(18) *N*-(2-chloro-4-nitrophenyl)-2,4-dihydroxybenzamide

Compound **18** was obtained using general procedure A starting from 2,4-Dimethoxybenzoic acid (182mg, 1 mmol) and 2-chloro-4-nitro aniline (172mg, 1 mmol) followed by general procedure D, resulting in 120mg (0.39 mmol) pale orange powder (39% over 2 steps)^{1}H NMR (500 MHz, DMSO-d_6) δ 11.99 (s, 1H), 11.21 (s, 1H), 10.31 (s, 1H), 8.86 (d, *J* = 9.2 Hz, 1H), 8.42 (d, *J* = 2.6 Hz, 1H), 8.28 (dd, *J* = 9.3, 2.6 Hz, 1H), 7.89 (d, *J* = 8.6 Hz, 1H), 6.49 – 6.43 (m, 2H). ^{13}C NMR

(126 MHz, DMSO-d_6) δ 164.27, 163.42, 158.44, 142.44, 142.38, 133.45, 125.23, 124.35, 122.32, 120.77, 110.04, 109.17, 103.10. ESI-MS (negative mode): *m/z* $[M-H]^-$ 307.0388

(19) *N*-(2-chloro-4-nitrophenyl)-2,4,5-trihydroxybenzamide

Compound **19** was obtained using general procedure A starting from 2,4,5-Trimethoxybenzoic acid (212mg, 1 mmol) and 2-chloro-4-nitro aniline (172mg, 1 mmol) followed by general procedure D, resulting in 175mg (0.54 mmol) pale yellow powder (54% over 2 steps) ^{1}H NMR (500 MHz, DMSO-d_6) δ 11.26 (s, 2H), 9.88 (s, 1H), 8.83 – 8.80 (m, 2H), 8.35 (d, J = 2.6 Hz, 1H), 8.21 (dd, J = 9.3, 2.7 Hz, 1H), 7.36 (s, 1H), 6.45 (s, 1H). ^{13}C NMR (126 MHz, DMSO-d_6) δ 164.25, 152.17, 150.86, 142.52, 142.24, 139.69, 125.21, 124.33, 122.04, 120.49, 116.63, 108.86, 104.09 ESI-MS (negative mode): *m/z* $[M-H]^-$ 323.0201

(20) 3-chloro-4-[(5-chloro-2-hydroxybenzoyl)amino]-*N*-(3,4-dihydroxybenzyl)benzamide

Compound **20** was obtained using general procedure C starting from **6b** (100mg, 0.3 mmol) and 1-(3,4-dimethoxyphenyl)methanamine followed by general procedure D resulting in 52 mg (0.12 mmol) of white powder (39% over 2 steps).^{1}H NMR (500 MHz, DMSO-d_6) δ 12.37 (s, 1H), 11.11 (s, 1H), 8.98 (t, *J* = 6.0 Hz, 1H), 8.84 (s, 1H), 8.71 (s, 1H), 8.58 (d, *J* = 8.7 Hz, 1H), 8.14 – 8.06 (m, 1H), 7.99 (d, *J* = 2.9 Hz, 1H), 7.93 (d, *J* = 8.8 Hz, 1H), 7.53 (dd, *J* = 8.8, 2.9 Hz, 1H), 7.10 (d, *J* = 8.7 Hz, 1H), 6.73 (s, 1H), 6.67 (d, *J* = 8.0 Hz, 1H), 6.58 (d, *J* = 8.0 Hz, 1H), 4.31 (d, *J* = 5.8 Hz, 2H). ^{13}C NMR (126 MHz, DMSO-d_6) δ 164.50, 162.98, 155.77, 145.54, 144.64, 137.93, 134.11, 131.20, 130.70, 130.38, 128.71, 127.54, 124.03, 123.06, 121.80, 120.14, 119.61, 118.76, 115.77, 115.38, 42.83. ESI-MS: *m/z* $M+H]^+$ 447.0510

(21) 3-chloro-4-[(5-chloro-2-hydroxybenzoyl)amino]-*N*-[2-(3,4-dihydroxyphenyl)ethyl]benzamide

Compound **21** was obtained using general procedure C starting from **6b** (100mg, 0.3 mmol) and 2-(3,4-dimethoxyphenyl)ethan-1-amine followed by general procedure D resulting in 67 mg (0.15 mmol) of white powder (50% over 2 steps).^{1}H NMR (500 MHz, DMSO-d_6) δ 12.37 (s, 1H), 11.09 (s, 1H), 8.76 (s, 1H), 8.70 – 8.53 (m, 3H), 8.00 (d, *J* = 14.3 Hz, 2H), 7.87 (d, *J* = 8.7 Hz, 1H), 7.52 (d, *J* = 8.7 Hz, 1H), 7.10 (d, *J* = 8.8 Hz, 1H), 6.70 – 6.58 (m, 2H), 6.48 (d, *J* = 8.0 Hz, 1H), 3.41 (s, 2H), 2.66 (t, *J* = 7.5 Hz, 2H). ^{13}C NMR (126 MHz, DMSO-d_6) δ 164.62, 162.96, 155.76, 145.53, 144.00, 137.84, 134.08, 131.37, 130.66, 130.38, 128.61, 127.39, 124.04, 123.04, 121.78, 120.14, 119.70, 119.59, 116.46, 115.96, 41.85, 35.03. ESI-MS: *m/z* $[M+H]^+$ 461.0597

NMR spectra can be found in supplementary material.

4.5.3 Antimicrobial susceptibility assay

Bacterial isolates used in this study were obtained from the American Type Culture Collection (ATCC), the Canadian National Intensive Care Unit (CAN-ICU) surveillance study[23] and the Canadian Ward (CANWARD) surveillance study.[24] Clinical isolates belonging to the CAN-ICU and CANWARD surveillance studies were recovered from patients suffering presumed infectious diseases entering or admitted in a participating medical center across Canada during the time of study. The in vitro antibacterial activities of the compounds were assessed the using microbroth dilution method according to the Clinical and Laboratory Standards Institute (CLSI) guidelines.[25] Bacterial cultures were grown overnight and diluted in saline to achieve a 0.5 McFarland turbidity, followed by 1:50 dilution in Cation-adjusted Mueller-Hinton broth (CAMHB) for inoculation to a final concentration of approximately 5×10^5 colony forming units per mL. Experiments were performed on 96-well plates. The tested agents were 2-fold serially diluted in CAMHB and incubated with equal volumes of bacterial inoculum at 37°C for 18 h. The MIC was determined as the lowest concentration to inhibit visible bacterial growth in the form of visible turbidity, which was confirmed using an EMax Plus microplate reader (Molecular Devices, USA) at a wavelength of 590 nm. CAMHB with or without bacterial cells were used as positive or negative controls, respectively.

4.5.4 Checkerboard assay

The assay was performed on 96-well plates as previously described.[26] One agent was 2-fold serially diluted along the x-axis, while the other agent was 2-fold serially diluted along the y-axis to create a matrix in which each well contained a combination of both agents at different concentrations. Bacterial cultures grown overnight were diluted in saline to 0.5 McFarland turbidity, followed by 1:50 dilution in CAMHB and inoculation of each well to a final concentration of approximately 5×10^5 colony forming units per mL. Wells consisting of only

CAMHB with or without bacterial cells were used as positive or negative controls, respectively. Plates were incubated for 18 h at 37°C and inspected for visible turbidity, which was confirmed using EMax Plus microplate reader (Molecular Devices, USA) at a wavelength of 590 nm. Fractional inhibitory concentration (FIC) of each agent was calculated by dividing the MIC of the compound in the presence of colistin by the MIC of the compound alone. Likewise, the FIC of colistin was calculated via dividing the MIC of colistin in the presence of each compound by the MIC of colistin alone. The FIC index was obtained by the summation of both FIC values. The FIC indices were interpreted as synergistic, indifferent or antagonistic for values of ≤ 0.5, $0.5 < x \leq 4$ or >4, respectively.

4.5.4 Cell proliferation assay

Cell proliferation was assessed by quantifying changes in cell numbers using the CyQuant cell proliferation assay (Invitrogen), essentially as described by the manufacturer. OVCAR-3 and COV362 cells were seeded in 96-well plates (7500 cells/well) in a volume of 100 µL. Wells with only media and no cells served as blanks. The plates were maintained in a 5% CO_2 incubator at 37°C. Two additional plates with cells and blank wells were prepared as control plates (did not receive the drug treatment) for determination of the cell numbers on the day of the addition of the drugs (day 0) and after the 48h incubation absolute cell numbers from representative wells from these plates were determined with a Coulter ZM counter, while the remainder wells were processed for the CyQuant assay as described below. When cells were in the log phase, drug solutions were added to the test plates to yield final concentrations of 0-100 µM. The control plates received the media with the vehicle. After 48 h incubation, the media was removed, and the plates were placed at -80°C for 7 days. The plates were allowed to thaw to room temperature, and CyQuant reagent

in lysis buffer (200 µL) was added to each well. Fluorescence was measured on a SpectraMax M2 microplate reader (Molecular Devices USA) at excitation and emission wavelengths of 480 and 520 nm, respectively. The results were expressed as percent cell number relative to initial cell number for each concentration.

Declaration of Competing Interest

The authors declare no conflicts of interest.

Acknowledgements

This work was supported by the Natural Sciences and Engineering Research Council of Canada (NSERC) in the form of a discovery grant (2018-06047). L.B. acknowledges support from the University of Manitoba in the form of a University of Manitoba Graduate Fellowship.

4.7: References

1. Theuretzbacher, U. *Curr Opin Microbiol* **2017**, *39*, 106–112.
2. Brown, E. D.; Wright, G. D. *Nature* **2016**, *529* (7586), 336–343.
3. Todd, R.; Kiehlbauch, J.; Chen, L.; Walters, M.; Kallen, A. *MMWR Morb Mortal Wkly Rep* **2017**, *66* (1), 33.
4. Prasad, V.; Mailankody, S. *JAMA Intern Med* **2017**, *177* (11), 1569.
5. Fernandes, P.; Martens, E. *Biochem Pharmacol* **2017**, *133*, 152–163.
6. Ejim, L.; Farha, M. A.; Falconer, S. B.; Wildenhain, J.; Coombes, B. K.; Tyers, M.; Brown, E. D.; Wright, G. D. *Nat Chem Biol* **2011**, *7* (6), 348–350.
7. Rajamuthiah, R.; Fuchs, B. B.; Conery, A. L.; Kim, W.; Jayamani, E.; Kwon, B.; Ausubel, F. M.; Mylonakis, E. *PLoS One* **2015**, *10* (4), e0124595.
8. Imperi, F.; Massai, F.; Pillai, C. R.; Longo, F.; Zennaro, E.; Rampioni, G.; Visc, P.; Leoni, L. *Antimicrob Agents Chemother* **2013**, *57* (2), 996–1005.

9. Domalaon, R.; Malaka De Silva, P.; Kumar, A.; Zhanel, G. G.; Schweizer, F. *Antimicrob Agents Chemother* **2019**, *63* (4), e02574-18.

10. Jara, M. O.; Warnken, Z. N.; Sahakijpijarn, S.; Thakkar, R.; Kulkarni, V. R.; Christensen, D. J.; Koleng, J. J.; Williams, R. O. *Pharmaceutics* **2022**, *14* (12).

11. Chen, W.; Mook, R. A.; Premont, R. T.; Wang, J. *Cell Signal* **2018**, *41*, 89–96.

12. Li, H.; Mattingly, A. E.; Jania, L. A.; Smith, R.; Melander, R. J.; Ernst, R. K.; Koller, B. H.; Melander, C. *ACS Infect Dis* **2021**, *7* (12), 3303–3313.

13. Copp, J. N.; Pletzer, D.; Brown, A. S.; Van der Heijden, J.; Miton, C. M.; Edgar, R. J.; Rich, M. H.; Little, R. F.; Williams, E. M.; Hancock, R. E. W.; Tokuriki, N.; Ackerley, D. F. *mBio* **2020**, *11* (5), 1–14.

14. Ngai, T. W.; Elfar, G. A.; Yeo, P.; Phua, N.; Hor, J. H.; Chen, S.; Ho, Y. S.; Cheok, C. F. *Int J Mol Sci* **2021**, *22* (19).

15. Domalaon, R.; Okunnu, O.; Zhanel, G. G.; Schweizer, F. *J Antibiot (Tokyo)* **2019**.

16. Huisgen, R. *Angew.Chem.,Int.Ed.Engl.* **1963**, *2* (10), 565–598.

17. Mook, R. A.; Ren, X.-R.; Wang, J.; Piao, H.; Barak, L. S.; Lyerly, H. K.; Chen, W. *Bioorg Med Chem* **2017**, *25* (6), 1804–1816.

18. Walkty, A.; Karlowsky, J. A.; Adam, H. J.; Lagace-Wiens, P.; Baxter, M.; Mulvey, M. R.; McCracken, M.; Poutanen, S. M.; Roscoe, D.; Zhanel, G. G. *CMAJ Open* **2016**, *4* (4), E641–E645.

19. Liu, Y. Y.; Wang, Y.; Walsh, T. R.; Yi, L. X.; Zhang, R.; Spencer, J.; Doi, Y.; Tian, G.; Dong, B.; Huang, X.; Yu, L. F.; Gu, D.; Ren, H.; Chen, X.; Lv, L.; He, D.; Zhou, H.; Liang, Z.; Liu, J. H.; Shen, J. *Lancet Infect Dis* **2016**, *16* (2), 161–168.

20. Shangguan, F.; Liu, Y.; Ma, L.; Qu, G.; Lv, Q.; An, J.; Yang, S.; Lu, B.; Cao, Q. *J Cancer* **2020**, *11* (12), 3454–3466.

21. Bittman, R.; Li, Z.; Samadder, P.; Arthur, G. *Cancer Lett* **2007**, *251* (1), 53–58.

22. Wang, D.; Zou, L.; Jin, Q.; Hou, J.; Ge, G.; Yang, L. *Acta Pharm Sin B* **2018**, *8* (5), 699–712.

23. Zhanel, G. G.; DeCorby, M.; Adam, H.; Mulvey, M. R.; McCracken, M.; Lagacé-Wiens, P.; Nichol, K. A.; Wierzbowski, A.; Baudry, P. J.; Tailor, F.; Karlowsky, J. A.; Walkty, A.; Schweizer, F.; Johnson, J.; Hoban, D. J. *Antimicrob Agents Chemother* **2010**, *54* (11), 4684–4693.

24. Hoban, D. J.; Zhanel, G. G. *J Antimicrob Chemother* **2013**, *68 Suppl 1*, i3-5.

25. Clinical and Laboratory Standards Institute. 28th ed.; Clin. Lab. Stand Institute: Wayne, PA, 2018.

26. Berry, L.; Brizuela, M.; Jackson, G.; Schweizer, F. *RSC Med Chem* **2021**, *12* (9), 1565–1573.

CHAPTER FIVE:
A Niclosamide-Tobramycin hybrid adjuvant potentiates cefiderocol against P. aeruginosa

The work presented in this chapter has been published in:

Berry, L.; Brizuela, M.; Jackson, G.; Schweizer, F. *RSC Med Chem* **2021**, *12* (9), 1565–1573.

5.1: Preface

The following chapter expands upon the SAR presented in chapter 4, using the azide analog of niclosamide to produce a niclosamide-tobramycin hybrid adjuvant. One approach that our group has previously used to combat antibiotic-resistant infections was the use of tobramycin-based hybrid adjuvants. We have reported several examples of tobramycin-based hybrid adjuvants that are able to potentiate a wide variety of antibiotics, primarily acting through membrane destabilization and inhibition of efflux. The objection of this study was to repurpose the pleiotropic biological effects of niclosamide to unlock new activities for this tobramycin scaffold.

Although one of the objectives presented in chapter 3 was the synthesis of a niclosamide-colistin hybrid molecule via solid-phase peptide synthesis, the lack of activity for all amide analogs presented in chapter 4 indicated that the proposed amide linkage would be unviable. As tobramycin and colistin are both large polybasic molecules, the niclosamide-tobramycin conjugate described herein also shares many chemical properties with a niclosamide-colistin hybrid.

The niclosamide-tobramycin hybrid lost the ability to potentiate colistin but was able to potentiate a wide variety of other antibiotics against multidrug-resistant Gram-negative bacteria. Notably, the hybrid was able to significantly enhance the activity of cefiderocol, a recently approved siderophore cephalosporin. Overall, these results show that derivatives of niclosamide can display a wide range of antibacterial effects, and synergize with antibiotics other than colistin.

5.2: Abstract

There is an urgent need for new therapies to overcome antimicrobial resistance (AMR) especially against Gram-negative bacilli (GNB). Multicomponent therapy combining antibiotics with enhancer molecules known as adjuvants is an emerging strategy to combat AMR. We have previously reported tobramycin-based adjuvants which are able to potentiate various antibiotics. In order to expand the repertoire of tobramycin hybrid adjuvants, a new hybrid containing niclosamide, an FDA approved anthelmintic which has recently demonstrated a variety of interesting biological effects, was synthesized. It was found that this conjugate can potentiate several antibiotics against multidrug-resistant GNB, including the recently approved siderophore cephalosporin cefiderocol. 8 μg/ml of the niclosamide-tobramycin hybrid in combination therapy against a pandrug-resistant strain of *P. aeruginosa* was able to lower the cefiderocol MIC 32-fold, from 8 μg/ml to 0.25 μg/ml in iron-rich media where siderophore uptake is reduced. These results indicate that a niclosamide-tobramycin hybrid adjuvant can serve to potentiate a newly approved antibiotic.

5.3: Introduction

Rising rates of multidrug-resistant (MDR) and extensively drug-resistant (XDR) bacterial infections represents one of the largest threats to global health.[1] MDR Gram-negative bacteria (GNB) are particularly hard to treat due to their highly restrictive dual membrane system which limits the entry of many antibiotics into the cell.[2] Even amongst GNB, some organisms such as *Pseudomonas aeruginosa* possess extremely restrictive membranes which severely limits effective treatment options. *P. aeruginosa* infections display troubling rates of antimicrobial resistance, are commonly hospital acquired and typically target immunocompromised patients.[3] In light of the ongoing COVID-19 pandemic, ventilator associated pneumonia (VAP) caused by

bacterial co-infection is a major concern.[4] *P. aeruginosa* is notable for causing VAP and MDR isolates of *P. aeruginosa* have been isolated from COVID-19 patients leading to increased levels of antibiotic usage and potentially increased rates of resistance.[5]

As a result of the difficulty in treating MDR *P. aeruginosa,* new therapies against this pathogen are currently being developed. One such example is cefiderocol, a recently approved siderophore cephalosporin antibiotic with a novel method of cell entry.[6] Cefiderocol is able to chelate iron and hijack the siderophore uptake mechanism that bacteria use to acquire iron from the environment, allowing it to bypass the outer membrane. Cefiderocol also displays enhanced stability towards b-lactamases and efficacy against a variety of MDR Gram-negative bacteria. Cefiderocol is used to treat complicated urinary tract infections and was approved by the FDA in September 2020 for the treatment of VAP and hospital-acquired pneumonia caused by GNB that are resistant to other antibiotics.[7] Despite the promising efficacy of this antibiotic, antimicrobial resistance remains a concern. Clinical isolates have already been reported with cefiderocol resistance, presumably mediated through reduced expression of the *pirA* siderophore receptor gene.[8] In order to maintain the clinical effectiveness of cefiderocol in light of reduced siderophore uptake, it may be advantageous to explore other methods of bypassing the outer membrane. Screening for compounds which enhance cefiderocol activity in iron-rich media where siderophore uptake is reduced may be one method of overcoming this problem.

Another approach to tackling antimicrobial resistance is the use of adjuvants. Adjuvants are molecules that possess little or no antimicrobial activity but are able to enhance the efficacy of partner antibiotics when used in combination therapy.[9] We have recently reported several examples of tobramycin-based hybrid adjuvants that are able to potentiate a wide variety of antibiotics.[10,11] These compounds are composed of a tobramycin antibiotic attached covalently to

a partner antibiotic via an aliphatic hydrocarbon tether. We have previously demonstrated that these adjuvants are able to permeabilize the outer membrane of GNB as well as dissipate the proton motive force to de-energize efflux pumps.[12] An interesting feature associated with these hybrids is that selection of the partner moiety modulates the potentiation effect and breadth of antibiotics synergized.[13] In an effort to explore new combinations of antibiotics and tobramycin hybrid adjuvants, a niclosamide-tobramycin hybrid was synthesized. Niclosamide is an FDA approved non-antibiotic drug that is used to treat tapeworm infections but has recently been shown to display a wide variety of other biological effects.[14] It is currently in several clinical trials for cancer therapy[15], and also demonstrates potent activity against Gram-positive bacteria[16]. Although not active against GNB, niclosamide has been shown to disrupt quorum sensing and the secretion of virulence factors against *P. aeruginosa*[17], as well as reverse colistin-resistance in combination therapy.[18,19] Despite the plethora of biological interactions, niclosamide suffers from poor bioavailability and water solubility which limits its use as a systemic agent.

A niclosamide-tobramycin hybrid molecule was synthesized, in part, to overcome the poor water solubility of niclosamide as well as to expand the repertoire of tobramycin-based antibiotic adjuvants due to niclosamide's diverse biological properties. Copper-assisted azide-alkyne cycloaddition (CuAAC)[20] was chosen as the ligation method to join an azide derivative of niclosamide with a tobramycin derivative incorporating a 1-hexyne aliphatic tether. The resulting hybrid was found to potentiate a variety of antibiotics against wild-type *Pseudomonas aeruginosa*, *Acinetobacter baumannii*, and *Escherichia coli.* Notably, cephalosporins including cefiderocol were potentiated. The niclosamide-tobramycin hybrid was shown to synergize with cefiderocol against MDR/XDR clinical isolates of *P. aeruginosa* via checkerboard assay as well as with time-kill kinetics. Interestingly, it was also found that synergy with cefiderocol was lost

under iron-depleted conditions. Overall, this report shows that a niclosamide-tobramycin adjuvant may be able to synergize with even the most potent antibiotics, increasing their effectiveness against resistant phenotypes.

5.4: Results and discussion

5.3.1 Synthesis of niclosamide-tobramycin hybrid

Niclosamide-tobramycin hybrid **7** was designed based on our previous studies with tobramycin hybrid adjuvants as outlined in **Fig 5.1.**[13] A 1,4-disubstituted 1,2,3-triazole linkage was recently demonstrated to retain the adjuvant activity of a tobramycin homodimer[21] and thus CuAAC was chosen to link the two units. An azide containing analog of niclosamide (compound **3**) was synthesized via 1-Ethyl-3-(3-dimethylaminopropyl)carbodiimide (EDC) coupling between 5-chlorosalicylic acid **1** and 4-azidoaniline **2**. 3 was evaluated for microbiological activity to verify that the modification of the niclosamide scaffold would not result in a loss of activity (Table S1 and S2) and the results were comparable to our previously reported activity for niclosamide. Tobramycin **4** was N-Boc and O-TBDMS protected following previously established protocol[21], yielding **5** which contained a free OH at the C-5 position of the deoxystreptamine ring. Previous studies have shown that modifying this position results in tobramycin derivatives that lack the ribosomal binding activity characteristic of aminoglycosides but display enhanced membrane interaction.[10] Alkylation with 6-iodohexyne followed by deprotection of the hydroxyl groups afforded amphiphilic tobramycin **6.** A 6-carbon aliphatic tether was chosen as this alkyne fragment was shown to be effective for the above-mentioned tobramycin homodimer. Although previous tobramycin-fluoroquinolone hybrids utilized a 12-carbon tether, niclosamide is relatively more hydrophobic than ciprofloxacin and moxifloxacin, thus, a shorter alkyl chain was considered appropriate. Compounds **3** and **6** were coupled using a

copper(I) catalyst followed by deprotection with trifluoroacetic acid (TFA) resulting in compound **7** which contained a niclosamide fragment attached to an amphiphilic tobramycin fragment via a triazole linkage.

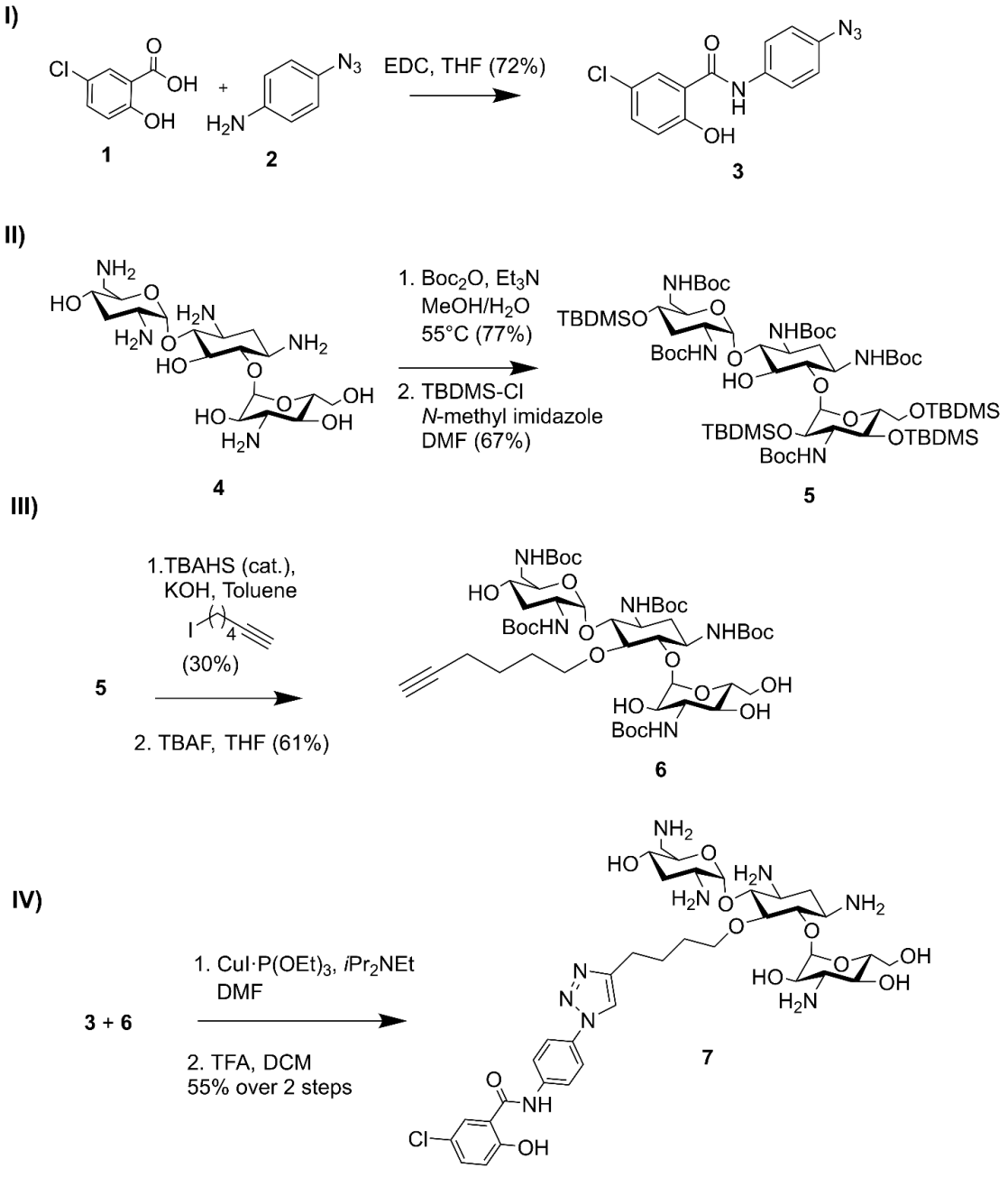

Figure 5.1. Synthesis of niclosamide tobramycin hybrid **7**. 1) amide coupling of **3**, II) tobramycin protection, III) alkylation followed by OTBDMS deprotection, IV) CuACC followed by N-Boc deprotection

5.3.2 Niclosamide-tobramycin hybrid 7 lacks intrinsic antibacterial activity

The antibacterial activity of **7** was initially evaluated against a panel of wild-type bacteria and compared to niclosamide and tobramycin (Table 5.1). As expected, niclosamide displayed potent activity against the Gram-positive organisms tested while tobramycin was active against Gram-negative organisms, *Staphylococcus aureus* and *Staphylococcus epidermis*. Compound **7** displayed very high MICs (≥ 64 μg/ml) against all organisms tested confirming the expected loss of tobramycin ribosomal binding. The lack of intrinsic antibacterial activity of **7** also suggested that niclosamide's mechanism of action against Gram-positive bacteria was also lost. Many adjuvants lack stand-alone activity despite being able to synergize with other antibiotics.[22] We therefore assessed the ability of **7** to potentiate various antibiotics in combination therapy.

Table 5.1. Antimicrobial activity of **7**, niclosamide and tobramycin against wild-type bacteria

	Minimum Inhibitory Concentration (μg/ml)		
Organism	**7**	Niclosamide	Tobramycin
P. aeruginosa PAO1	64	>128	0.5
A. baumannii ATCC 17978	>128	>128	0.5
E. coli ATCC 25922	>128	>128	2
S. aureus ATCC 29213	>128	1	0.5
MRSA ATCC 33592	>128	0.25	2
MRSE 61589	128	1	8
E. faecalis ATCC 29212	>128	2	8
E. faecium ATCC 27270	>128	2	16

5.3.3 Compound 7 potentiates different classes of antibiotics against Gram-negative bacteria

In order to assess the adjuvant capabilities of **7**, we next studied the synergistic activity of hybrid **7** with 21 different antibiotics from various classes against wild-type *P. aeruginosa*, *A. baumannii* and *E. coli.* For the initial screening, a fixed concentration of 8 μg/mL of hybrid **7** in combination with each antibiotic was evaluated for the ability to inhibit bacterial growth prior to further analysis via checkerboard assay. The fold-potentiation was calculated by comparing the MIC of the antibiotic alone to the MIC in combination with the adjuvant. A decrease of the MIC in combination with **7** by at least 4-fold was interpreted as significant due to the inherent 2-fold margin of error in the microbroth dilution technique used to determine MIC.[23] From the initial screen, compound **7** appeared to be more active against *P. aeruginosa*, and *E. coli*, with limited potentiation in wild-type *A. baumannii* (Fig 5.2). Several classes of antibiotics were potentiated including efflux-susceptible antibiotics (fluoroquinolones, tetracyclines, and chloramphenicol) as well as antibiotics which have difficulty crossing the outer membrane (rifampicin, novobiocin). In addition, **7** was found to synergize with niclosamide, consistent with previous reports that show synergy between niclosamide and membrane-active agents.[19] This also indicates the original mode of action of niclosamide is lost in hybrid **7**.[19] Based on the spectrum of antibiotics potentiated, it appears that compound **7** is most likely an adjuvant with a mechanism of action consistent with previously reported tobramycin hybrids (outer membrane destabilization and efflux pump inhibition).

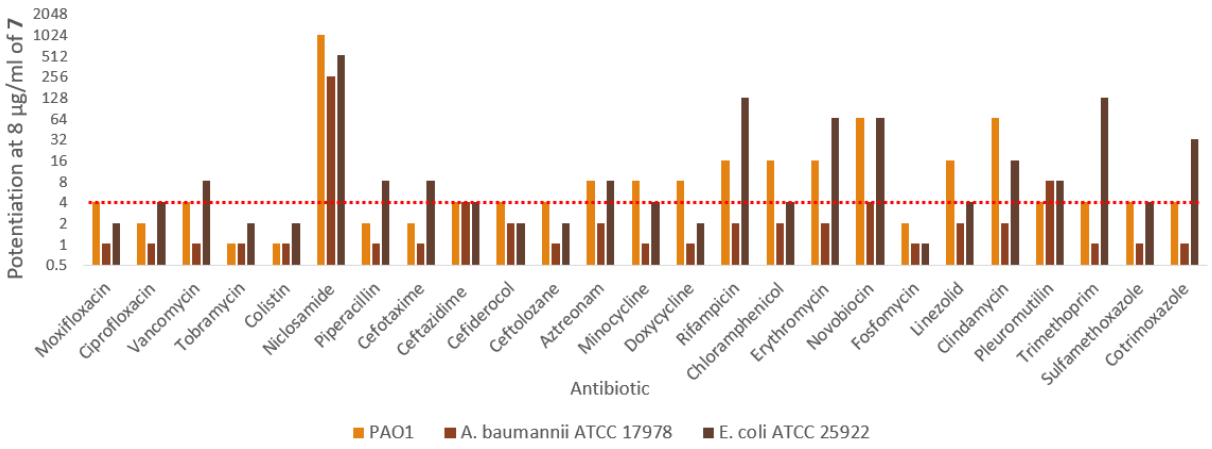

Figure 5.2. Fold potentiation of various antibiotics in combination with 8 µg/ml **7** against wild-type Gram-negative bacteria, red dotted line denotes a 4-fold potentiation. Values at or above this line were determined to be significant due to the 2-fold margin of error inherent to MIC assays.

Interestingly, **7** was also found to potentiate several generations of cephalosporins against PAO1. This effect was interesting as cephalosporins are one of the few classes of antibiotics effective against *P. aeruginosa*.[24] We elected to further explore the synergy of hybrid **7** with various cephalosporins including cefotaxime, ceftazidime, cefiderocol and ceftolozane against MDR cephalosporin-resistant *P. aeruginosa* clinical isolates (Fig. 3). Significant potentiation was observed when 8 µg/ml **7** was combined with cefiderocol against all isolates tested. Of particular note is the 32-fold potentiation seen in PA259, an XDR isolate resistant to all currently approved classes of antibiotics with the exception of colistin. As previously mentioned, this result was very promising since cefiderocol is approved to treat highly resistant *P. aeruginosa* infections. The combination of **7** and cefiderocol was chosen for a more detailed synergy evaluation against an expanded panel of clinical isolates.

In order to demonstrate that neither niclosamide nor tobramycin alone was responsible for the observed synergy with cefiderocol, a checkerboard assay of each antibiotic was performed against PAO1. As expected, tobramycin or niclosamide alone were unable to change

the MIC of cefiderocol in combination therapy, resulting in additive interactions for both agents (Table S4). This shows that the adjuvant properties of **7** are unique to the hybrid structure which matches our previously established reports for tobramycin hybrid adjuvants.

It should also be noted that the media used for this assay was Mueller-Hinton broth (MHB). Due to cefiderocol's unique siderophore uptake mechanism, *in vitro* MIC values have been shown to differ depending on the level of iron present in the medium.[6] Under iron-depleted conditions bacteria are believed to over-express siderophore secretion and uptake which enhances cefiderocol's outer membrane penetration. For this reason, current guidelines indicate that cefiderocol should be assessed using iron-depleted cation-adjusted Mueller-Hinton broth (ID-CAMHB) instead of the standard MHB used for microbroth dilution assays. However, to the best of our knowledge, the suitability of ID-CAMHB for assessing membrane-active adjuvants has yet to be determined. In addition, the interplay between siderophore uptake and membrane permeabilization would serve to further complicate the analysis. Thus, the initial synergy assay was performed in MHB in order to uncouple enhancing membrane penetration from siderophore uptake. This may limit the clinical relevance of the results obtained in MHB to situations where siderophore uptake is unavailable, such as in isolates with reduced expression of the *pirA* gene or in cases of hemochromatosis resulting in host iron overload conditions.[25] The ability of hybrid **7** to potentiate cefiderocol in iron-replete media where cefiderocol faces reduced uptake was therefore assessed.

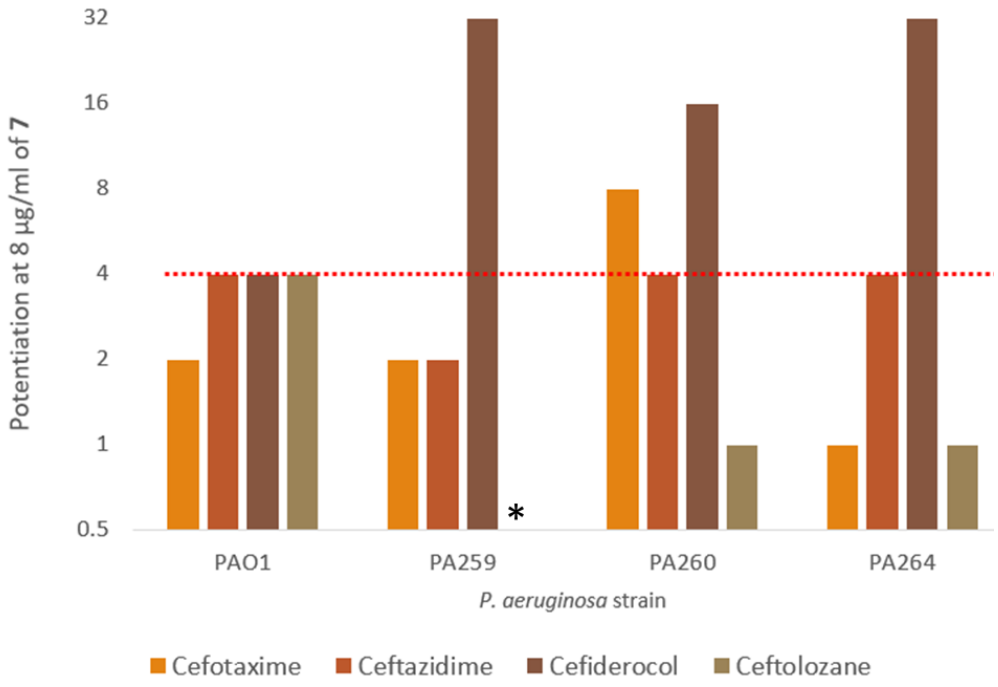

Figure 5.3. Fold potentiation of cephalosporins in combination with 8 µg/ml **7** against wild-type and MDR clinical isolates of *P. aeruginosa* in MHB. Red dotted line denotes a 4-fold potentiation. *The combination of **7** and ceftolozane against PA259 was not evaluated

5.3.4 Hybrid 7 synergizes with cefiderocol against P. aeruginosa

To further confirm the observed synergy with cefiderocol against *P. aeruginosa,* a checkerboard assay was performed. The fractional inhibitory concentration (FIC) index for each isolate was calculated to assess the interactions between each agent. FIC for cefiderocol was calculated by dividing the MIC of cefiderocol in combination by the MIC of cefiderocol alone. Similar calculations were performed to obtain the FIC of **7**. The FIC index was then calculated by adding the FIC indices of cefiderocol and the adjuvant. FIC index values of ≤ 0.5, $0.5 < x \leq 4$, and > 4 were interpreted as synergistic, additive, and antagonistic interactions, respectively.[23] As shown in Table 2, synergy was observed in most clinical isolates, but not in PA100036,

PA86052, PA88949 and PA114228, which appeared extremely susceptible to cefiderocol (MIC ≤ 0.125 μg/ml). Of particular note were strains PA259, PA101885 and PA109084 which had cefiderocol MIC values between 4-8 μg/ml. In combination with **7** the MIC of cefiderocol in all of these strains was lowered significantly to ≤ 0.25 μg/ml. In addition, synergy was observed in 2 out of 3 colistin-resistant clinical isolates tested. As the polybasic antibiotic colistin also exerts antimicrobial activity through membrane destabilization and cell lysis, colistin resistance is primarily mediated through modification of the negatively charged lipopolysaccharide (LPS) embedded in the outer membrane of GNB.[26] Despite this, **7** retained adjuvant activity against these strains suggesting that LPS modification may not reduce its effectiveness as an adjuvant. Adjuvant activity was also compared to the well-known outer membrane permeabilizer polymyxin B nonapeptide (PMBN) (Table S6). 8 μg/ml of PMBN was also able to potentiate cefiderocol in 3 out of 9 *P. aeruginosa* strains although **7** was superior overall.

Table 5.2. Checkerboard assay of **7** in combination with cefiderocol. **7** potentiates cefiderocol in 10 out of 14 multidrug-resistant clinical isolates of *P. aeruginosa* tested in MHB.

Strain	MIC_{FDC}[$MIC_{Combinati}$ (μg/ml)	MIC_{7}[$MIC_{Combinatio}$ (μg/ml)	FIC index
PAO1	0.125[0.031]	64[0.5]	0.258
PA259	8[0.25]	>128[4]	0.031<x<0.063
PA260	1[0.063]	>128[0.125]	0.063<x<0.063
PA262	1[0.25]	>128[1]	0.25<x<0.258
PA264	0.5[0.031]	>128[0.125]	0.125<x<0.126
PA100036	0.063[0.063]	>128[0.25]	1<x<1.002
PA101885	4[0.063]	>128[2]	0.017<x<0.031
PA86052	0.031[0.031]	>128[0.25]	1<x<1.001
PA88949	0.016[0.016]	>128[0.25]	1<x<1.002
PA108590	2[0.031]	>128[4]	0.016<x<0.047
PA109084	4[0.016]	>128[0.5]	0.004<x<0.008
PA91433*	0.25[0.016]	>128[1]	0.016<x<0.023
PA101243*	0.5[0.063]	>128[2]	0.125<x<0.141
PA114228*	0.125[0.063]	32[16]	1

*denotes colistin-resistant isolates of *P. aeruginosa*.

To gain insight into the bacterial killing kinetics caused by the combination of niclosamide-tobramycin hybrid **7**, a time-kill curve was generated for PA259 (Fig 5.4). PA259 was chosen as it is XDR and showed the highest cefiderocol MIC. 4 μg/ml of cefiderocol was bacteriostatic after 24 hours while 8 μg/ml of **7** displayed little effect on bacteria growth. However, when 8 μg/ml of **7** was administered in combination with 4 μg/ml of cefiderocol, complete eradication was observed after 8 hours. This indicates that combinations of **7** and cefiderocol display bactericidal activity (defined as >3 log reduction in CFU/mL) and further

demonstrates how the activity of cefiderocol can be enhanced in combination therapy. Overall, these results indicate that even in iron-replete media where siderophore uptake is reduced, the activity of cefiderocol can be enhanced in combination therapy. This shows that hybrid **7** reverses the effect of reduced uptake caused by the presence of iron in the media and that membrane destabilization may serve to overcome reduced siderophore uptake.

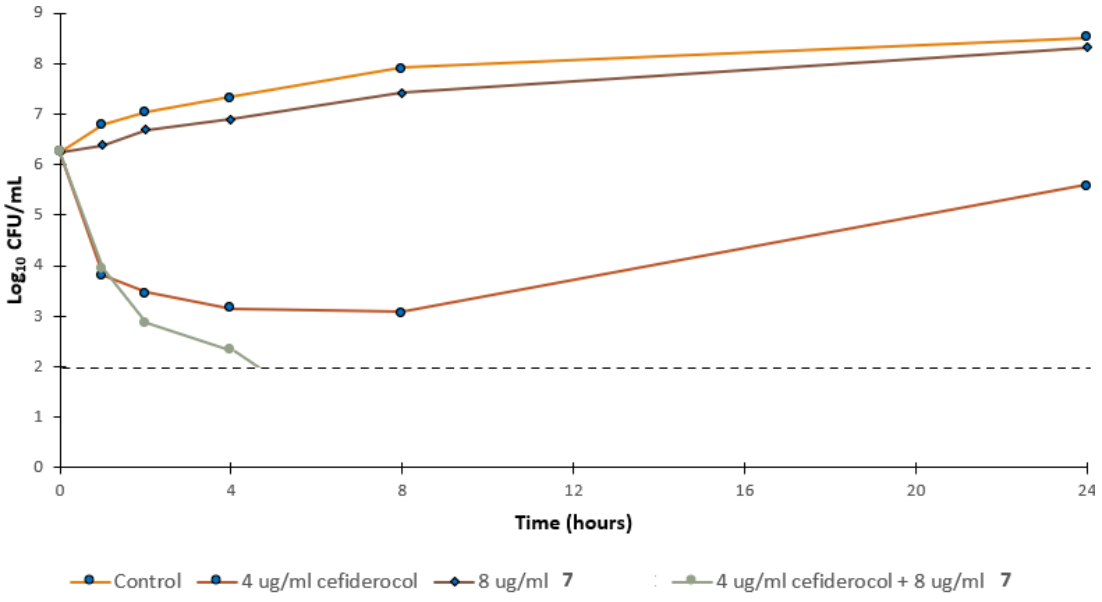

Figure 5.4. Time-kill kinetics of **7** in combination with ½ MIC of cefiderocol against PA259 in MHB. CFU/mL = colony forming units/mL

5.3.5 Synergy with cefiderocol was reduced against other Gram-negative species

We next evaluated whether the potentiation of cefiderocol was unique to *P. aeruginosa* or could also be observed in other GNB. Checkerboard assays against *A. baumannii* (Table 5.4) and Enterobacteriaceae (*E. coli, Klebsiella pneumoniae* and *Enterobacter cloacae*, Table 5.5)

revealed an overall reduction in synergy when compared to *P. aeruginosa*. Synergy was observed in wild-type *A. baumannii* ATCC 179781 but not in MDR clinical isolates. Synergy was also observed in 2 out of 4 strains of *E. coli* and 1 out of 3 strains of *K. pneumoniae*. Although some synergistic combinations were observed they were all limited to a 4-fold potentiation of cefiderocol, and no synergy was observed in *E. cloacae*. Overall, there appears to be a drastic reduction in synergy against Gram-negative organisms other than *P. aeruginosa*, indicating that the synergistic effects of **7** and cefiderocol appear to be *P. aeruginosa* specific. This may be a result of the inherently more restrictive outer membrane of *P. aeruginosa* compared to other Gram-negative organisms[3] where cefiderocol faces fewer permeability challenges.

Table 5.4. Checkerboard assay of **7** in combination with cefiderocol against *A. baumannii* in MHB.

Strain	MIC_{FDC}[$MIC_{Combination}$ (μg/ml)	MIC_{7}[$MIC_{Combination}$] (μg/ml)	FIC index
A. baumannii ATCC	1[0.25]	>128[16]	0.25<x<0.375
A. baumannii AB031	1[0.5]	>128[0.25]	0.5<x<0.502
A. baumannii AB92247	0.25[0.125]	>128[8]	0.5<x<0.563
A. baumannii LAC-4	4[4]	>128[0.25]	1<x<1.002

Table 5.5. Checkerboard assay of **7** in combination with cefiderocol against Enterobacteriaceae in MHB.

Strain	MIC_{FDC}[$MIC_{Combination}$ (μg/ml)	MIC_{7}[$MIC_{Combination}$] (μg/ml)	FIC index
E. coli ATCC 25922	0.125[0.063]	>128[0.25]	0.5<x<0.502
E. coli 107115	1[0.5]	>128[0.25]	0.5<x<0.502
E. coli 94393	1[0.25]	>128[1]	0.25<x<0.258
E. coli 94474	1[0.25]	>128[8]	0.25<x<0.313
KP113250	1[0.25]	>128[4]	0.25<x<0.281
KP113254	1[0.5]	>128[1]	0.5<x<0.508
KP116381	0.25[0.125]	>128[0.25]	0.5<x<0.502
E. cloacae 117029	1[0.5]	>128[4]	0.5<x<0.531
E. cloacae 118564	2[2]	>128[0.25]	1<x<1.002
E. cloacae 121187	2[2]	>128[0.25]	1<x<1.002

5.3.6 Synergy was lost under iron-depleted conditions

As previously mentioned, ID-CAMHB is typically used to assess the activity of cefiderocol rather than MHB in order to maximize siderophore uptake. Unfortunately, when the synergy between **7** and cefiderocol again *P. aeruginosa* was assessed in ID-CAMHB a reduction in synergy was observed in all strains with the exception of wild-type PAO1 (Fig 5). This may indicate that compound **7** would only be useful under conditions where siderophore uptake is unavailable (such as in resistant strains with reduced *pirA* expression). Increased membrane

permeability may not confer any advantage to cefiderocol when siderophore uptake already serves to bypass the restrictive outer membrane of GNB. Alternatively, as this is the first reported instance of a membrane-active adjuvant being assessed in ID-CAMHB, this media may not be suitable for assessing the activity of similar compounds. Future work will explore the suitability of using ID-CAMHB to assess synergy of cefiderocol with membrane-active adjuvants. In addition, although a reduction in cefiderocol MIC against *P. aeruginosa* was seen in ID-CAMHB, PA259 still maintained a relatively high MIC of 4 μg/ml which according to the FDA and EUCAST guidelines indicates cefiderocol resistance.[27] Overall, the 32-fold reduction in MIC observed in PA259 may still demonstrate the utility of adjuvant therapy in overcoming cefiderocol resistance despite the loss of synergy in ID-CAMHB, particularly in situations where siderophore uptake is limited.

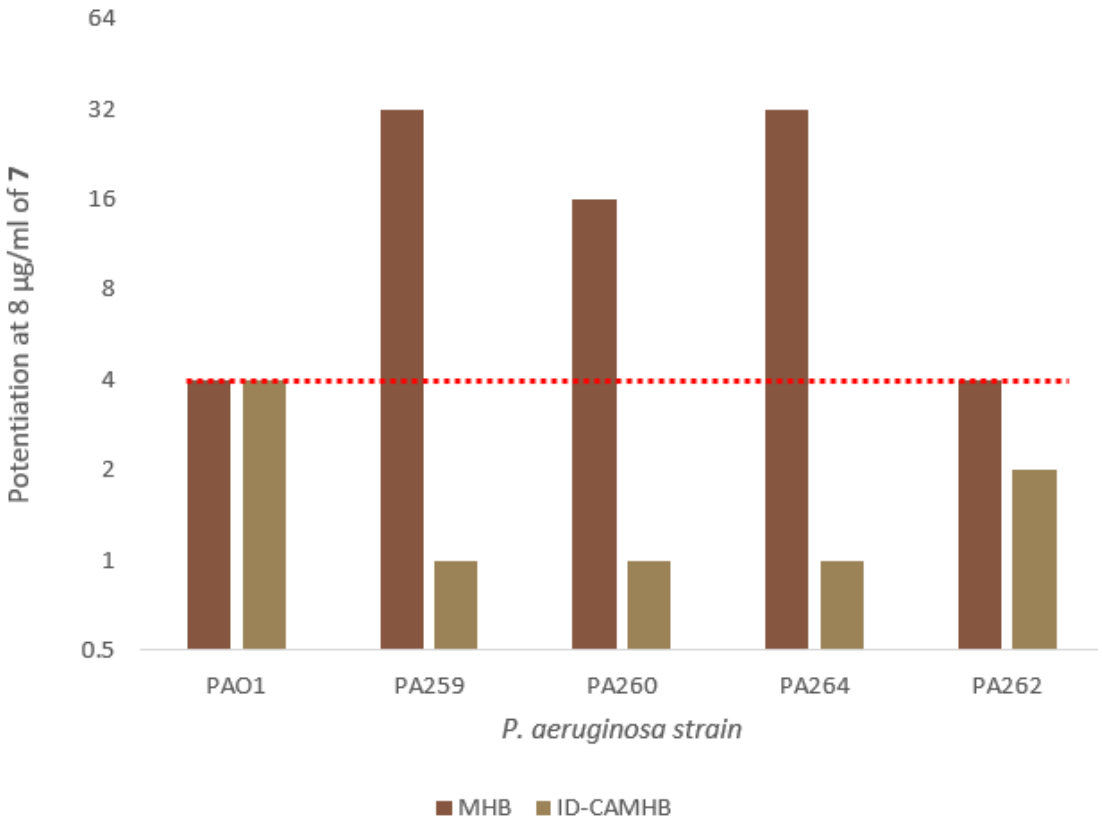

Figure 5.5. Fold-potentiation of 8 µg/ml **7** in MHB compared to ID-CAMHB. Red dotted line denotes a 4-fold potentiation.

5.5: Conclusions

A niclosamide-tobramycin hybrid **7** was successfully synthesized via CuAAC and assessed for synergy against several classes of antibiotics against GNB. It was found that **7** was able to potentiate a variety of antibiotics against wild-type *P. aeruginosa* and *E. coli* with limited activity against *A. baumannii*. Potent synergy was observed with cefiderocol against nearly all MDR clinical isolates of *P. aeruginosa* tested under iron-replete conditions and time-kill kinetics revealed complete bacterial killing at ½ MIC after 8 hours. Synergy observed appeared to be relatively specific to *P. aeruginosa* when compared to other GNB species. An overall loss of

synergy was observed under ID-CAMHB conditions. Overall, this study indicates that a tobramycin-niclosamide hybrid can potentiate cefiderocol under iron-replete conditions. This is the first report on the potentiation of cefiderocol with an antibiotic adjuvant.

5.6: Experimental

5.5.1 Synthesis

Tobramycin was purchased from AK Scientific Inc. (CA, USA) and all other reagents were purchased from Sigma-Aldrich (Oakville, ON, Canada) and were used without further purification. Air- and moisture-sensitive reactions were performed with dry solvents under inert nitrogen atmosphere. Reaction progress was monitored using thin-layer chromatography (TLC) plates visualized with UV light and staining with ninhydrin solution. Final compound **7** was fully characterized using 1-dimensional (^{1}H and ^{13}C) and 2-dimensional nuclear magnetic resonance (NMR) experiments as well as mass spectrometry. All NMR measurements were recorded on AMX-500 (500 MHz) Bruker instrument (Germany). High-resolution matrix-assisted laser desorption ionization mass spectrometry (MALDI-MS) experiments were done on a Bruker Ultraflextreme mass spectrometer (Germany) coupled to a time-of-flight mass analyzer.

N-(4-azidophenyl)-5-chloro-2-hydroxybenzamide (3)

5-chlorosalicylic acid **1** (45 mg, 0.293 mmol) and EDC (112 mg, 0.586 mmol) were dissolved in tetrahydrofuran (2 mL) at room temperature and stirred for 15 minutes. 4-azidoaniline **2** (51mg, 0.299 mmol) was added and the reaction mixture was stirred at rt for 5 hours over which time the solution gradually turned from clear to yellow. The reaction was concentrated under vacuo and

dissolved in 12 mL ethyl acetate, washed with 1M HCl (3 x 5 mL), saturated sodium bicarbonate solution (3 x 5 mL) and brine (3 x 5 mL), dried over anhydrous Na_2SO_4 and concentrated in vacuo. The crude material was purified using flash chromatography using DCM as a solvent system to afford **3** as a brown solid (61mg, 73%) 1H NMR (500 MHz, DMSO-d6) δ 11.81 (s, 1H), 10.47 (s, 1H), 7.93 (d, J = 2.6 Hz, 1H), 7.76 (dd, J = 9.0, 2.9 Hz, 2H), 7.48 (dd, J = 8.8, 2.6 Hz, 1H), 7.16 – 7.13 (m, 2H), 7.02 (d, J = 8.8 Hz, 1H).

13C NMR (126 MHz, DMSO-d6) δ 165.4, 157.3, 136.7, 135.5, 135.3, 133.5, 128.7, 123.2, 122.8, 122.6, 122.5, 119.8, 119.5.

1,3,2′,6′,3″-Penta-*N*-Boc-4′,2″,4″,6″-tetra-*O*-TBDMS-tobramycin (5). Commercial tobramycin **4** (4.00 g, 8.56 mmol) was dissolved in a 2:1 mixture of methanol and water (150 mL) and treated with Boc_2O (14.25 g, 65.29 mmol) in the presence of Et_3N (8.0 mL, 57.4 mmol). The reaction mixture was stirred under reflux (at 55 °C) overnight (~ 20 h), concentrated under vacuo, and thoroughly dried under high vacuum for 24 h to afford a white powdery solid (6.38 g, 77%). The dried crude penta-N-boc-protected tobramycin (1.13 g, 1.16 mmol) was dissolved in anhydrous DMF (6.0 mL) and treated with tert-butyldimethylsilyl chloride, TBDMSCl (1.13 g, 7.49 mmol), and N-methylimidazole (0.6 mL, 7.49 mmol). The reaction was stirred at rt for 4 days under nitrogen gas atmosphere, and the resulting mixture was poured into water (50.0 mL) and extracted with DCM (50 mL, × 3). The organic layer was dried over anhydrous Na_2SO_4, concentrated in vacuo, and purified by flash chromatography using gradient elution (hexanes/ethyl acetate, 15:1 to 8:1, v/v) to afford **5** (1.1 g, 67%) as a white solid. NMR data was consistent with a previous report.[21]

5-O-Hexyne-1,3,2′,6′,3″-penta-*N*-Boc-tobramycin (6)

A solution of **5** (1.1g, 0.78mmol) in 4 mL toluene was treated with KOH (131mg, 2.34 mmol) 2, 6-iodohexyne (0.2 mL, 1.55mmol), and a catalytic amount of tetrabutylammonium hydrogen sulfate (TBAHS). The reaction was stirred at rt overnight, dispersed in 40 mL water and extracted with ethyl acetate (3 x 40 mL). The organic layers were combined, washed with brine (1 x 40 mL), dried over anhydrous Na_2SO_4, concentrated in vacuo, and purified by flash chromatography using gradient elution (hexanes/ethyl acetate, 15:1 to 8:1, v/v) to afford the alkylated product (331 mg, 30%) as a white solid. TBDMS deprotection of the hydroxyl groups was performed by dissolving 190 mg of the alkylated product in 2.5 mL anhydrous THF. The solution was treated with 0.1 mL tetrabutylammonium fluoride (TBAF) and stirred under nitrogen for 2 hours at rt. The reaction mixture was concentrated in vacuo, dissolved in 40 mL water and extracted with DCM (3 x 40 mL). The organic layers were combined, dried over anhydrous Na_2SO_4, concentrated in vacuo, and purified by flash chromatography using gradient elution (DCM/methanol, 25:1 to 20:1, v/v) to afford **6** (72 mg, 61%) NMR data was consistent with a previous report.[21]

Tobramycin-Niclosamide Hybrid 7

3 (8.2 mg, 0.027 mmol) and **6** (28.0 mg, 0.027 mmol) and $CuI{\cdot}P(OEt)_3$ (15mg, 0.054 mmol) were dissolved in anhydrous DMF (3 mL) and treated with *i*Pr_2NEt (7.2 µL, 0.054 mmol). The reaction was stirred under nitrogen gas at rt for 2h. The reaction mixture was concentrated under vacuum, dissolved in water (5 mL), and extracted with DCM (3 x 5 mL). The organic layers were combined, dried over anhydrous Na_2SO_4, concentrated in vacuo and the crude Boc-protected material was used in the next step without further purification. The crude residue was dissolved in 1 mL DCM and was treated with trifluoracetic acid (1 mL), stirred at rt for 2 hours and concentrated in vacuo. Purification by reverse-phase flash chromatography using gradient

elution (methanol/water with 0.1% TFA, 20% methanol to 80% methanol, **7** eluted at 45% methanol) yielded off-white **7** (12.5mg, 55%) 1H NMR (500 MHz, D2O) δ 7.91 (s, 1H, C*H* of triazole), 7.64 – 7.30 (m, 5H, Niclosamide-Ph), 7.11 – 6.99 (m, 1H, Niclosamide-Ph), 6.73 – 6.61 (m, 1 H, Niclosamide-Ph), 5.18 (d, *J* = 2.6 Hz, 1H, anomeric H-1'), 4.99 (d, *J* = 3.5 Hz, 1H, anomeric H-1"), 4.08 (dt, *J* = 8.5, 3.8 Hz, 1H, H-5'), 3.97 (t, *J* = 9.8 Hz, 1H, H-5"), 3.88 – 3.51 (m, 10H, H-5, H-6, H-4, H-2', H-4, H-2", H-4", O-CH_2 of linker), 3.51 – 3.46 (m, 1H, H-6"), 3.46 – 3.33 (m, 3H, H-1, H-3, H-3"), 3.22 – 3.14 (m, 1H, H-6'), 3.10 – 3.01 (m, 1H, H-6'), 2.66 – 2.52 (m, 2H, Triazole-CH_2 of linker), 2.37 (dt, *J* = 12.6, 4.4 Hz, 1H, H-2), 2.07 – 1.92 (m, 2H, H-3'), 1.77 (q, *J* = 12.6 Hz, 1H, H-2), 1.68 – 1.45 (m, 4H, CH_2 of linker). 13C NMR (126 MHz, D2O) δ 155.1 (Niclosamide-*C*ONH), 148.4, 137.5, 134.9, 134.9, 133.6, 128.8, 124.4 (*C*H of triazole), 122.0, 120.8, 120.3, 118.6, 117.6, 115.3, 101.3 (C-1"), 92.7 (C-1'), 82.0 (C-4"), 81.8 (C-5), 76.8 (C-5"), 75.9 (C-5'), 73.2 (C-4), 73.1 (O-*C*H_2 of linker), 68.5 (C-2"), 64.8 (C-6), 63.1 (C-4'), 59.3 (C-6"), 54.8 (C-3"), 49.7 (C-1), 48.4 (C-3), 48.4, 47.2 (C-2'), 38.4 (C-6"), 28.8 (*C*H_2 of linker), 28.0 (C-3'), 27.7 (C-2), 25.1 (*C*H_2 of linker), 24.4 (Triazole-*C*H_2 of linker). MALDI-TOF-MS *m/z* calcd for $C_{37}H_{54}ClN_9NaO_{11}^+$ monoisotopic peak $(M+Na)^+$: 858.352 found: 858.360

5.5.2 Antimicrobial susceptibility assay

Bacterial isolates used in this study were obtained from the American Type Culture Collection (ATCC) [reference strains], the Canadian National Intensive Care Unit (CAN-ICU) surveillance study[28] and the Canadian Ward (CANWARD) surveillance study.[29] Clinical isolates belonging to the CAN-ICU and CANWARD surveillance studies were recovered from patients suffering presumed infectious diseases entering or admitted in a participating medical center across Canada during the time of study. The in vitro antibacterial activities of the conjugates were assessed the using microbroth dilution method according to the Clinical and Laboratory

Standards Institute (CLSI) guidelines.[30] Bacterial cultures were grown overnight and diluted in saline to achieve a 0.5 McFarland turbidity, followed by 1 : 50 dilution in Mueller-Hinton broth (MHB) for inoculation to a final concentration of approximately 5×10^5 colony forming units per mL. Experiments were performed on 96-well plates. The tested agents were 2-fold serially diluted in MHB and incubated with equal volumes of bacterial inoculum at 37 °C for 18 h. The MIC was determined as the lowest concentration to inhibit visible bacterial growth in the form of visible turbidity, which was confirmed using an EMax Plus microplate reader (Molecular Devices, USA) at a wavelength of 590 nm. MHB with or without bacterial cells were used as positive or negative controls, respectively.

5.5.3 Checkerboard assay

The assay was performed on 96-well plates as previously described.[31] The antibiotic was 2-fold serially diluted along the x axis, while the adjuvant was 2-fold serially diluted along the y axis to create a matrix in which each well contained a combination of both agents at different concentrations. Bacterial cultures grown overnight were diluted in saline to 0.5 McFarland turbidity, followed by 1 : 50 dilution in MHB and inoculation of each well to a final concentration of approximately 5×10^5 colony forming units per mL. Wells consisting of only MHB with or without bacterial cells were used as positive or negative controls, respectively. Plates were incubated for 18 h at 37 °C and inspected for visible turbidity, which was confirmed using EMax Plus microplate reader (Molecular Devices, USA) at a wavelength of 590 nm. Fractional inhibitory concentration (FIC) of antibiotic was calculated by dividing the MIC of antibiotic in the presence of conjugates by the MIC of antibiotic alone. Likewise, the FIC of conjugates was calculated via dividing the MIC of conjugates in the presence of antibiotic by the MIC of conjugates alone. The FIC index was obtained by the summation of both FIC values. The

FIC indices were interpreted as synergistic, indifferent or antagonistic for values of ≤ 0.5, 0.5 < x ≤ 4 or >4, respectively. ID-CAMHB was prepared from MHB as previously described. [32]

Acknowledgments

This work was supported by the Canadian Institutes of Health Research (CIHR) in the form of a pilot project (162159) and the Natural Sciences and Engineering Research Council of Canada (NSERC) in the form of a discovery grant (DG 2018-06047). LB acknowledges support from the University of Manitoba in the form of a University of Manitoba Graduate Fellowship.

Author contributions

LB: Conceptualization, investigation, writing - original draft, MB: Investigation (microbiology assays), GJ: Investigation (synthesis of **6**), FS: Conceptualization, project administration, supervision, writing – review & editing.

Conflicts of interest

There are no conflicts to declare

5.7: References

1. Brown, E. D.; Wright, G. D. *Nature*. **2016**, 336–343.
2. Zgurskaya, H. I.; López, C. A.; Gnanakaran, S. *ACS Infect Dis* **2016**, *1* (11), 512–522.
3. Pang, Z.; Raudonis, R.; Glick, B. R.; Lin, T. J.; Cheng, Z. *Biotechnol Adv* **2019**, *37* (1), 177–192.
4. Póvoa, H. C. C.; Chianca, G. C.; Iorio, N. L. P. P. *Infect Dis Ther* **2020**, *9* (3), 417–420.
5. Gregorova, M.; Morse, D.; Brignoli, T.; Steventon, J.; Hamilton, F.; Albur, M.; Arnold, D.; Thomas, M.; Halliday, A.; Baum, H.; Rice, C.; Avison, M. B.; Davidson, A. D.; Santopaolo, M.; Oliver, E.; Goenka, A.; Finn, A.; Wooldridge, L.; Amulic, B.; Boyton, R. J.; Altmann, D. M.;

Butler, D. K.; McMurray, C.; Stockton, J.; Nicholls, S.; Cooper, C.; Loman, N.; Cox, M. J.; Rivino, L.; Massey, R. C. *Elife* **2020**, *9*, 1–13.

6. Zhanel, G. G.; Golden, A. R.; Zelenitsky, S.; Wiebe, K.; Lawrence, C. K.; Adam, H. J.; Idowu, T.; Domalaon, R.; Schweizer, F.; Zhanel, M. A.; Lagacé-Wiens, P. R. S.; Walkty, A. J.; Noreddin, A.; Lynch III, J. P.; Karlowsky, J. A. *Drugs* **2019**, *79* (3), 271–289.

7. Yusuf, E.; Bax, H. I.; Verkaik, N. J.; van Westreenen, M. *Journal of Clinical Medicine*. **2021**, 1068.

8. Malik, S.; Kaminski, M.; Landman, D.; Quale, J. *Antimicrob Agents Chemother* **2020**, *64* (11), e01221-20.

9. Wright, G. D. *Trends Microbiol* **2016**, *24* (11), 862–871.

10. Gorityala, B. K.; Guchhait, G.; Goswami, S.; Fernando, D. M.; Kumar, A.; Zhanel, G. G.; Schweizer, F. *J Med Chem* **2016**, *59* (18), 8441–8455.

11. Domalaon, R.; Idowu, T.; Zhanel, G. G.; Schweizer, F. *Clin Microbiol Rev* **2018**, *31* (2), e00077-17.

12. Yang, X.; Goswami, S.; Gorityala, B. K.; Domalaon, R.; Lyu, Y.; Kumar, A.; Zhanel, G. G.; Schweizer, F. *J Med Chem* **2017**, *60* (9), 3913–3932.

13. Idowu, T.; Ammeter, D.; Brizuela, M.; Jackson, G.; Alam, S.; Schweizer, F. *Bioorg Med Chem Lett* **2020**, *30* (21), 127575.

14. Chen, W.; Mook, R. A.; Premont, R. T.; Wang, J. *Cell Signal* **2018**, *41*, 89–96.

15. Burock, S.; Daum, S.; Keilholz, U.; Neumann, K.; Walther, W.; Stein, U. *BMC Cancer* **2018**, *18* (1), 297.

16. Rajamuthiah, R.; Fuchs, B. B.; Conery, A. L.; Kim, W.; Jayamani, E.; Kwon, B.; Ausubel, F. M.; Mylonakis, E. *PLoS One* **2015**, *10* (4), e0124595.

17. Imperi, F.; Massai, F.; Pillai, C. R.; Longo, F.; Zennaro, E.; Rampioni, G.; Visc, P.; Leoni, L. *Antimicrob Agents Chemother* **2013**, *57* (2), 996–1005.

18. Ayerbe-Algaba, R.; Gil-Marqués, M. L.; Jiménez-Mejías, M. E.; Sánchez-Encinales, V.; Parra-Millán, R.; Pachón-Ibáñez, M. E.; Pachón, J.; Smani, Y. *Front Cell Infect Microbiol* **2018**, *8*, 348.

19. Domalaon, R.; Malaka De Silva, P.; Kumar, A.; Zhanel, G. G.; Schweizer, F. *Antimicrob Agents Chemother* **2019**, *63* (4), e02574-18.

20. Huisgen, R. *Angewandte Chemie International Edition* **1963**, *2* (10), 565–598.

21. Idowu, T.; Ammeter, D.; Rossong, H.; Zhanel, G. G.; Schweizer, F. *J Med Chem* **2019**, *62* (20), 9103–9115.

22. Douafer, H.; Andrieu, V.; Phanstiel, O.; Brunel, J. M. *J Med Chem* **2019**, *62* (19), 8665–8681.

23. Odds, F. C. *Journal of Antimicrobial Chemotherapy* **2003**, *52* (1), 1.

24. Yaneja, N.; Kaur, H. *Microbiol Insights* **2016**, *9*, 29459.

25. Kidd, J. M.; Abdelraouf, K.; Nicolau, D. P. *Antimicrob Agents Chemother* **2019**, *64* (1), e01767-19.

26. Jeannot, K.; Bolard, A.; Plésiat, P. *Int J Antimicrob Agents* **2017**, *49* (5), 526–535.

27. Simner, P. J.; Patel, R. *J Clin Microbiol* **2020**, *59* (1), e00951-20.

28. Zhanel, G. G.; DeCorby, M.; Laing, N.; Weshnoweski, B.; Vashisht, R.; Tailor, F.; Nichol, K. A.; Wierzbowski, A.; Baudry, P. J.; Karlowsky, J. A.; Lagacé-Wiens, P.; Walkty, A.; McCracken, M.; Mulvey, M. R.; Johnson, J.; Canadian Antimicrobial Resistance Alliance (CARA), T. C. A. R. A.; Hoban, D. J. *Antimicrob Agents Chemother* **2008**, *52* (4), 1430–1437.

29. Hoban, D. J.; Zhanel, G. G. *J Antimicrob Chemother* **2013**, *68 Suppl 1*, i3-5.

30. Clinical and Laboratory Standards Institute. 28th ed.; Clin. Lab. Stand Institute: Wayne, PA, 2018.

31. Berry, L.; Domalaon, R.; Brizuela, M.; Zhanel, G. G.; Schweizer, F. *Medchemcomm* **2019**, *10* (4), 517–527.

32. Hackel, M. A.; Tsuji, M.; Yamano, Y.; Echols, R.; Karlowsky, J. A.; Sahm, D. F. *Antimicrob Agents Chemother* **2018**, *62* (2), e01968-17.

CHAPTER SIX:
Sulfonamide bioisosteres of niclosamide enhance antibacterial activity of colistin and bacitracin

The work presented in this chapter has been submitted for publication in:

Liam Berry, Danyel Ramirez, Ronald Domalaon, Frank Schweizer, *J. Antibiotics.* **2023**

6.1: Preface

The following chapter extends the SAR previously discussed in chapter 4, by reporting a series of niclosamide analogs with the central amide replaced by a sulfonamide group. The insights gained in chapter 4, demonstrating that the nitro group of niclosamide is a viable site for further modifications, guided the SAR in this chapter. The aniline ring of the sulfonamide derivatives was modified with various electron donating and withdrawing substituents, to explore the influence of electronic effects on colistin potentiation. As chapter 4 also demonstrated the necessity of the phenol group on niclosamide's ability to potentiate colistin, the phenol was not modified in this study.

This chapter also explores for the first time the utility of triple combination therapy by adding bacitracin to combinations of niclosamide and colistin. Synergy between niclosamide and bacitracin against Gram-positive organisms was also discovered, further expanding the spectrum of antibacterial activity of niclosamide derivatives. Overall, this study builds upon the SAR in the previous chapters, showing that sulfonamide bioisosteres of niclosamide can further increase synergy with colistin. It also demonstrates that niclosamide and its analogs can synergize with antibiotics other than colistin, potentially unlocking new therapeutic approaches for future development.

6.2: Abstract

Multicomponent therapy combining antibiotics with enhancer molecules known as adjuvants is an emerging strategy to combat antimicrobial resistance. Niclosamide is a clinically relevant anthelmintic drug with potential to be repurposed for its inherent antibacterial activity against Gram-positive bacteria and its ability to potentiate the antibacterial activity of colistin against susceptible and resistant Gram-negative bacteria. Herein, sulfonamide analogs of niclosamide were prepared and found to enhance colistin activity against Gram-negative bacteria. The ability of niclosamide and the new sulfonamide analogs to synergize with bacitracin against vancomycin-resistant *Enterococcus faecium* was also discovered.

6.3: Introduction

The emergence of multidrug-resistant (MDR) bacterial infections has led to a lack of effective antibiotics in the clinic.[1,2] Additionally, limited success of drug development programs to develop new classes of antibiotics[3] has led to the re-introduction of antibiotics such as colistin (COL) as drugs of last resort.[4] However, rising rates of COL resistance are rendering even last-resort drugs ineffective against MDR bacteria, and thus new therapeutic options are being explored. Given the lack of antibiotic development in recent decades [3], clinicians have been forced to utilize a variety of therapeutic approaches. Combination therapy, where two or more antibiotics are administered simultaneously, is one such approach.[5] Another form of combination therapy that has gained prominence in recent years is the inclusion of adjuvants.

Adjuvants are enhancer molecules that increase the activity of other antibiotics when used in combination therapy, and several classes of adjuvants for various antibiotics have been reported.[6] Several adjuvants for COL have been explored to try to overcome COL resistance[7–9] including the anthelminthic salicylanilide drug niclosamide (NIC). NIC has been shown to

possess antibacterial activity against Gram-positive bacteria (GPB)[10], inhibit quorum sensing in Gram-negative bacteria[11](GNB), and synergize with COL in eradicating GNB[12,13] & prevent the development of COL resistance. Previously, we have studied the structure-activity relationships (SAR) of NIC-based adjuvants enhance COL activity against GNB. This study demonstrated that the phenol group of NIC was necessary COL potentiation, but the addition of multiple phenol groups resulted in complete loss of COL potentiation. Moreover, the same study indicated that the nitro group in NIC can be replaced by electron withdrawing groups.[14] Given a recent report by Li et al[15] that demonstrated the amide moiety of NIC is not essential for salicylanilides to act as COL adjuvants and can be replaced with a benzimidazole bioisostere, we sought to replace the amide with a sulfonamide in order to explore the effects on COL potentiation.

Eight sulfonamide analogs of NIC, containing various substituents on the aniline ring, were synthesized based on previous SAR findings[14]. We showed that electron-withdrawing substituents are necessary for the sulfonamides to enhance COL activity, and sulfonamide **7** displayed the highest increase in COL activity. To examine potential beneficial interactions with other antibiotics, we also found that adding bacitracin (BAC) to combinations of COL and compound **7** or NIC, in a triple combination, further increased antibacterial activity. Given that BAC is typically used against GPB[16] and NIC has previously demonstrated activity against GPB[10,17], we explored combinations of NIC and BAC against *Enterococcus faecium*. For the first time, antibacterial synergy between NIC and BAC was discovered, further expanding the scope of NIC as an antibiotic adjuvant.

6.4: Results and Discussion

6.3.1 Synthesis and initial antibacterial screening of sulfonamides

Sulfonamides **1-8** were synthesized by coupling 5-chloro-2-methoxybenzenesulfonyl chloride with various commercially available aniline derivatives in pyridine, followed by deprotection with boron tribromide. Anilines containing electron donating or withdrawing groups were chosen to determine the role of electronic effects on COL potentiation (**Figure 6.1**).

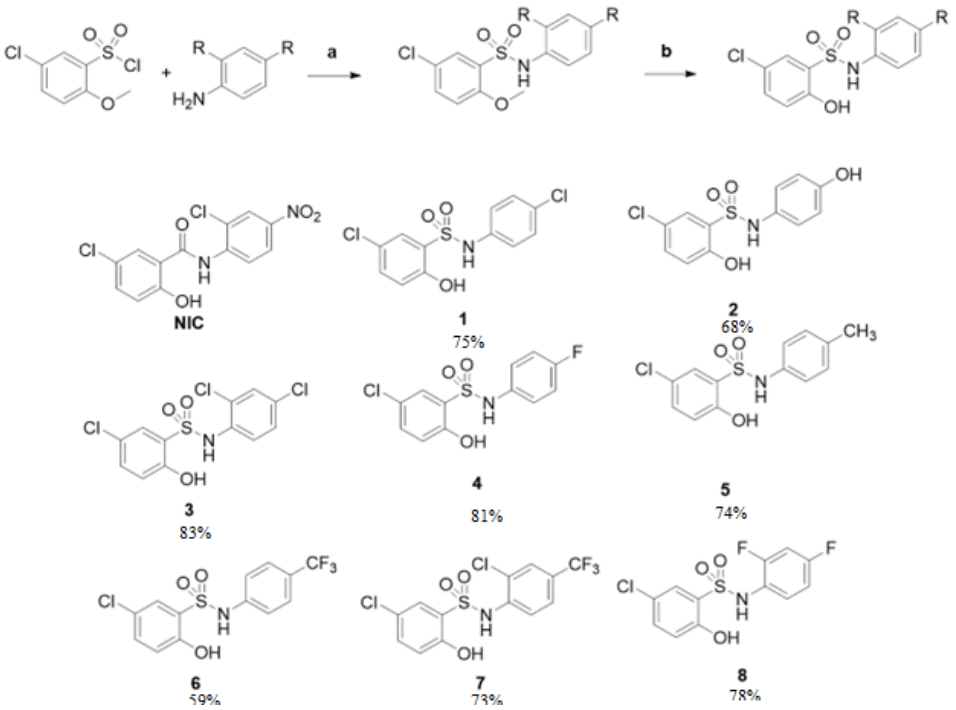

Figure 6.1. Synthesis of sulfonamides **1-8**. a) Pyridine, rt, 2-4 h; b) BBr_3, DCM, 0°C, overnight. NIC = niclosamide

We first evaluated the ability of compounds **1-8** to enhance COL activity against COL-resistant GNB. For the initial screen, two COL-resistant clinical isolates of *Klebsiella pneumoniae* (KP113250 and KP113254) and *Escherichia coli* (EC94393 and EC94474) were chosen. To ensure any biological activity seen was due to COL potentiation and not to any innate activity of the newly synthesized compounds, we first screened all compounds for stand-alone antibacterial activity against these four strains (**Table S1**). The lowest concentration of each compound able to inhibit bacterial growth was determined to be the minimum inhibitory concentration (MIC). Similar to

NIC, all compounds displayed poor antibacterial activity with MIC values of ≥128 μg/mL and were then further evaluated for synergy with COL. To perform the initial screen, we used a fixed concentration of 8 μg/mL of compounds **1-8** and NIC and determined the MIC of COL in combination against each strain. (**Table 6.1**).

Table 6.1. Colistin (COL) MIC in combination with 8 μg/mL of compounds **1-8** against four COL-resistant strains of GNB. KP = *Klebsiella pneumoniae,* EC = *Escherichia coli*.

	COL MIC with 8 μg/mL compound (in μg/mL)			
Compound	**KP113250**	**KP113254**	**EC94393**	**EC94474**
NIC	0.25	0.5	0.25	0.5
1	64	16	0.5	0.5
2	128	128	8	16
3	2	2	1	4
4	128	128	8	16
5	128	128	8	16
6	2	1	1	2
7	1	1	0.5	0.5
8	128	128	8	16
COL alone	128	128	8	16

NIC showed strong enhancement of COL activity, consistent with previous reports.[12,13] At 8 μg/mL, NIC was able to lower the MIC of COL from 128 μg/mL to 0.25 μg/mL against KP113250 and 0.5 μg/mL against KP113254, from 8 μg/mL to 0.25 μg/mL against EC94393, and from 16 μg/mL to 0.5 μg/mL against EC94474. Several sulfonamides containing electron-withdrawing groups were also able to potentiate COL in combination therapy. Compound **1**, which contained a

single chlorine substitution on the aniline ring, displayed comparable COL-potentiation to NIC against *E. coli* but only attained subpar reduction of COL MIC against *K. pneumoniae*. Compound **3**, containing two chlorine substituents, displayed a 32- and 8-fold increase in COL potentiation against KP113250 and KP113254, respectively compared to **1**. Compound **6**, which contained a trifluoromethyl substituent, had comparable adjuvant activity to compound **3** with a 2-fold increase in COL potentiation against KP113254 and EC94474. Adding an additional chlorine substituent in compound **7** further increased COL activity in combination. Compound **7** was the most potent sulfonamide tested, with comparable adjuvant activity to NIC, demonstrating that the amide in NIC can be replaced with a sulfonamide while retaining synergy with COL.

An overall trend emerged amongst compounds that displayed antibacterial synergism with COL, wherein the sulfonamide with the most electron-withdrawn aniline ring (**7**) displayed the highest potentiation of COL and the sulfonamide with the least withdrawn ring (**1**) displayed the lowest. This trend was also consistent with the complete lack of synergy with COL shown in compounds that contained electron-donating groups **2** (containing a hydroxyl group) and **5** (containing a methyl group). Fluorine-containing compounds **4** and **8** were an exception to this trend since both compounds displayed no meaningful COL potentiation against tested bacteria. A similar result was observed in *Li et al*'s benzimidazole analogs, wherein the most potent benzimidazoles contained trifluoromethyl groups and di-fluorinated benzimidazoles did not synergize with COL to eradicate bacteria.[15] The most potent compound **7** was selected for further evaluation via checkerboard assay against other GNB.

6.3.2 Further evaluation of compound 7 and COL

We next evaluated the COL potentiation of lead compound **7** against a panel of COL-resistant and COL-susceptible GNB using the checkerboard assay (**Table 6.2**). The fractional

inhibitory concentration index (FICI)[18] for each combination was determined to assess interactions between the two components. FICI values of ≤0.5, 0.5 < x ≤ 4, and >4 was interpreted as synergistic, additive, and antagonistic interactions, respectively.[18]

Table 6.2. Synergy between compound **7** and COL against a panel of GNB. PA = *P. aeruginosa*, AB = *A. baumannii,* KP = *K. pneumoniae,* EC = *E. coli*.

Strain	MIC_{Col}	MIC_{Combi}	MIC_{7}	MIC_{Combi}	FICI	Interpretation
PAO1	1	0.5	>256	0.25	0.500<x<0.501	Additive
PA264	1	0.25	>256	0.5	0.250<x<0.252	Synergy
PA262	4	0.25	>256	4	0.063<x<0.079	Synergy
PA100036	2	0.25	>256	1	0.125<x<0.129	Synergy
PA101885	4	0.5	>256	2	0.125<x<0.133	Synergy
PA91433	4	0.5	>256	4	0.125<x<0.141	Synergy
PA101243	1024	0.5	>256	1	0.001<x<0.005	Synergy
ABATCC 17978	1	0.25	>256	2	0.250<x<0.251	Synergy
AB1190193	4	0.5	>256	0.5	0.125<x<0.126	Synergy
AB027	1024	0.5	>256	4	0.001<x<0.016	Synergy
AB031	0.25	0.031	>256	8	0.124<x<0.155	Synergy
KP113250	128	1	>256	8	0.031<x<0.035	Synergy
KP113254	128	1	>256	4	0.016<x<0.019	Synergy
EC94393	8	0.5	>256	2	0.125<x<0.133	Synergy
EC94474	16	0.5	>256	8	0.063<x<0.093	Synergy

Compound **7** was able to potentiate COL activity against 6 out of 7 strains of *Pseudomonas aeruginosa* and all 4 strains of *Acinetobacter baummanni.* Synergism was only not observed in wild-type PAO1, which was already susceptible to COL. Sulfonamide **7** was able to drastically reduce COL's MIC against all COL-resistant isolates (PA91433, PA101243, PA262,

PA101885, AB027, and *A. baumannii* 110193). The highest COL potentiation was seen in PA101243 and AB027, where compound **7** showed a 2048-fold reduction in COL MIC. The same COL potentiation against KP113250, KP113254, EC94393, and EC 94474 shown in the initial screen was confirmed via checkerboard assay. Compound **7** synergized with COL against nearly all strains tested and was able to lower COL's MIC to 1 μg/mL or lower, even against highly COL-resistant strains (**Table 6.2**).

6.3.3 Adding BAC to combinations of COL and NIC or compound 7 further improves COL activity

We next explored ways to enhance COL activity even further against COL-resistant EC94474, EC94393, KP113254, and KP113250. Commercially available polymyxin combinations include the topical ointment Polysporin, which has various formulations of polymyxin B in combination with other agents.[19] Polymyxin B has been combined with the peptide antibiotics BAC and gramicidin, and the aminoglycoside neomycin.[19] We elected to add BAC to the combination of COL and NIC or **7** to assess if COL's antibacterial activity could be further augmented in combination. A concentration of 128 μg/mL was chosen, as a previous study which reported triple combinations of miconazole, BAC, and polymyxin B saw potent antibacterial activity at similar concentrations of BAC.[20] Triple combinations of NIC or compound **7** with COL and BAC displayed greater activity than without BAC present (**Figure 6.2**).

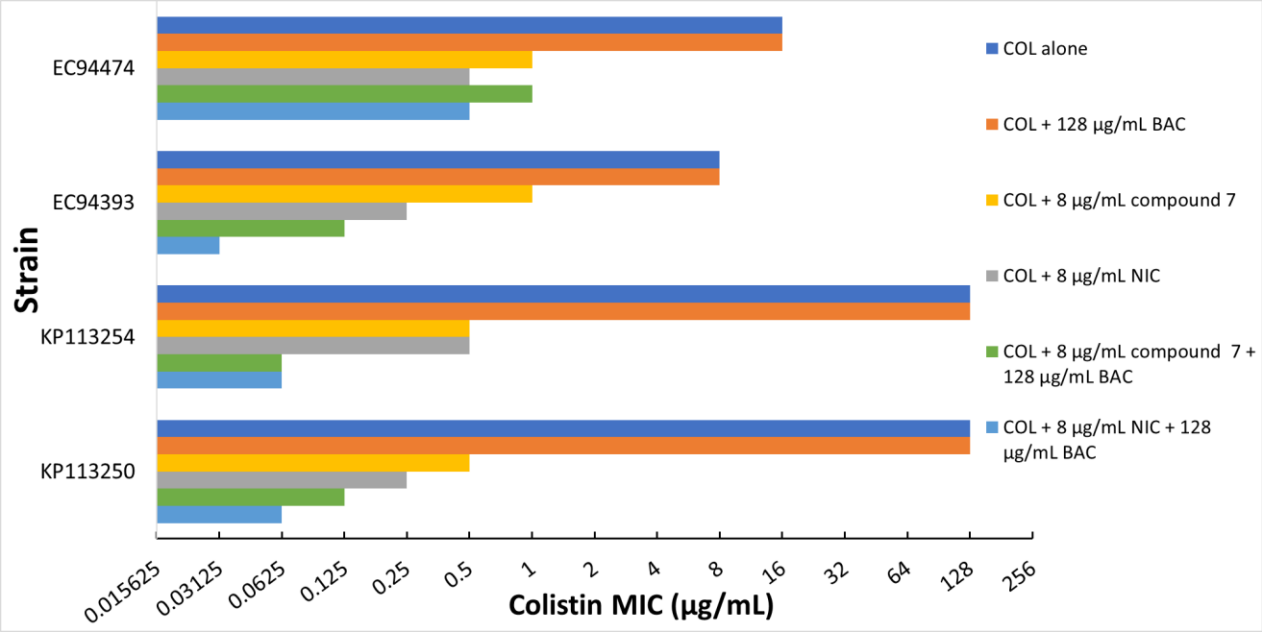

Figure 6.2. Dual and triple combinations of COL, BAC, and NIC or **7** against four COL-resistant strains of GNB. COL = COL, BAC = bacitracin, NIC = NIC, KP = *K. pneumoniae,* EC = *E. coli*.

First, the dual combination of COL and BAC was tested against the four previously mentioned strains. No change in COL MIC was observed in combination with 128 µg/mL BAC compared to COL alone. However, adding BAC to a combination of NIC and COL was able to further lower COL's MIC against three out of four strains tested. 8 µg/mL of NIC lowered COL's MIC from 8 µg/mL to 0.25 µg/mL against EC94393 and adding 128 µg/mL BAC was able to lower the MIC an additional 8-fold down to 0.0313 µg/mL. An 8-fold reduction in COL MIC was also observed in KP113254 after augmenting the COL/NIC combination with 128 µg/mL BAC, and a 4-fold reduction was seen in KP113250 (**Figure 6.2**).

Triple combinations of COL, BAC, and compound **7** also showed superior antibacterial activity compared to dual combinations of COL and **7**. No change in COL MIC was observed against EC94474 when comparing the triple and dual combinations, but adding BAC lowered COL's MIC against the other three strains tested. The addition of BAC resulted in an 8-fold

reduction in COL MIC against EC94393 and KP113254, and a 4-fold reduction in MIC against KP113250. (**Figure 6.2**)

Overall, adding BAC and either NIC or **7** to COL resulted in higher activity than dual combinations of either component. The sulfonamide analog **7** displayed similar activity to NIC, further confirming that the sulfonamide replacement was a viable strategy for retaining NIC activity against GNB. Future work will explore triple combinations with other agents. These results were interesting, as BAC is typically only active against GPB.[21] Since both NIC and BAC have previously been demonstrated to have antibacterial activity against Gram-positive *Enterococcus faecium*[10,16], we next explored combinations of BAC and NIC or compound **7** against *E faecium*.

6.3.4. Synergy with BAC against E. faecium

Although NIC has been studied extensively as an adjuvant for COL[12,13] against GNB and as a stand-alone agent against GPB[10,17], no efforts to explore antibacterial synergism between NIC and GPB-active antibiotics have been reported. Given the promising results of the triple combination against GNB, we next assessed synergy between BAC and NIC or compound **7** against *E. faecium*.

Nine BAC-resistant clinical isolates of vancomycin-resistant *E. faecium* were selected, with BAC MICs between 128 and 512 μg/mL. NIC showed strong stand-alone activity with MICs between 1 and 4 μg/mL. NIC and BAC were synergistic in 6 out of 9 strains, with BAC MICs between 4- and 8-fold lower in combination with NIC (**Table 6.3**). In comparison, compound **7** had higher stand-alone MICs (2 to 8 μg/mL), it synergized with BAC in 8 out of 9 strains. In addition, BAC had lower MICs in combination with **7** than in combination with NIC

(**Table 6.4**). The greatest difference in activity was seen against *E. faecium* 131553, where NIC was additive in combination with BAC, but compound **7** was synergistic with an FIC index of 0.313. (**Figure 6.3**)

Table 6.3. Synergy between NIC (NIC) and bacitracin (BAC) against clinical isolates of *E. faecium*.

Strain	MIC_{BAC}	MIC_{Comb}	MIC_{NIC}	MIC_{Combi}	FICI	Interpretation
***E. faecium* 108175**	512	64	1	0.25	0.375	Synergy
***E. faecium* 110023**	128	16	1	0.25	0.375	Synergy
***E. faecium* 117263**	512	128	1	0.25	0.5	Synergy
***E. faecium* 125877**	256	64	1	0.25	0.5	Synergy
***E. faecium* 126572**	512	64	2	0.5	0.375	Synergy
***E. faecium* 129206**	256	64	1	0.5	0.75	Additive
***E. faecium* 130546**	512	128	2	0.5	0.5	Synergy
***E. faecium* 131553**	512	256	2	0.25	0.625	Additive
***E. faecium* 133746**	512	256	4	1	0.75	Additive

Table 6.4. Synergy between compound **7** and bacitracin (BAC) against clinical isolates of *E. faecium*.

Strain	MIC_{BAC}	MIC_{Comb}	MIC_{7}	MIC_{Combi}	FICI	Interpretation
***E. faecium* 108175**	512	64	4	1	0.375	Synergy
***E. faecium* 110023**	128	8	4	1	0.375	Synergy
***E. faecium* 117263**	512	64	4	1	0.5	Synergy
***E. faecium* 125877**	256	16	2	0.5	0.313	Synergy
***E. faecium* 126572**	512	64	4	0.5	0.313	Synergy
***E. faecium* 129206**	256	32	4	1	0.375	Synergy
***E. faecium* 130546**	512	64	4	1	0.375	Synergy
***E. faecium* 131553**	512	32	8	2	0.313	Synergy
***E. faecium* 133746**	512	256	2	0.125	0.563	Additive

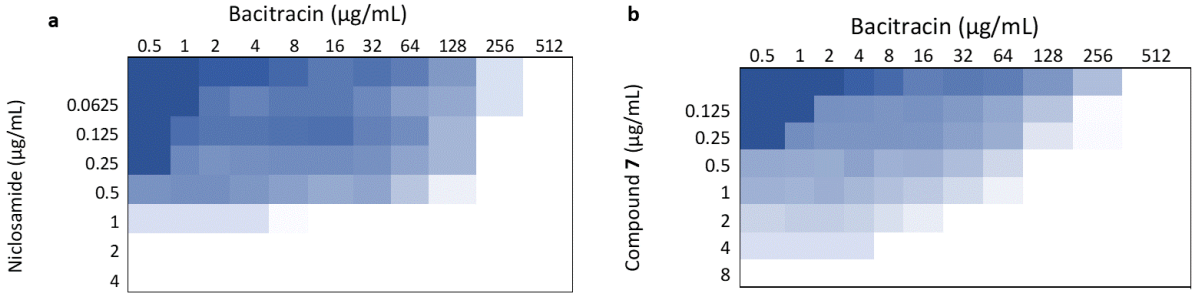

Figure 6.3. Checkerboard assays of NIC (**a**) and compound **7** (**b**) in combination with BAC against *E. faecium* 131553. Darker shading corresponds to higher cell density.

These results demonstrate synergy between NIC and BAC for the first time against *E. faecium*, and sulfonamide derivative **7** displayed even higher synergy. Although BAC is

primarily used in topical formulations, combinations of NIC with other antibiotics against GPB may be a future strategy that can be explored.

6.5: Experimental

6.4.1 Materials

Reagents and solvents were purchased from commercially available suppliers such as Sigma-Aldrich, AK Scientific, Fisher Scientific, and Bachem, and were used without further purification. Air- and moisture-sensitive reactions were performed with dry solvents under inert nitrogen atmosphere. Reaction progress was monitored using thin-layer chromatography (TLC) plates visualized with UV light. Column chromatography was performed to purify the compounds using SiliaFlash P60 (40–63 μm) 60 Å silica gel from Silicycle. The chemical structures of all final products used for biological testing were characterized by nuclear magnetic resonance spectroscopy (^{1}H NMR and ^{13}C NMR) on a Bruker AMX NMR 300 MHz and 500 MHz spectrometer. Electrospray ionization mass spectrometry (ESI-MS) data was obtained using a Varian 320-MS LC/MS.

6.4.2 Synthesis of compounds 1-8

General sulfonamide coupling procedure

The appropriate aniline derivative (1.1 equiv.) and 5-Chloro-2-methoxybenzenesulfonyl chloride (1 equiv.) were dissolved in dry pyridine (2 mL per mmol of reactants) and stirred at rt for 2-4 h. Ice-cold water (5 mL per mmol) was added, and the resulting precipitate was collected and washed with water. The crude precipitate was collected in DCM, washed with 1M HCl (× 3), saturated $NaHCO_3$ (× 3) and brine. The organic layer was concentrated, and the product was purified using flash chromatography (0-10% MeOH in DCM).

General methoxy deprotection procedure

The appropriate methoxy protected intermediate (1 equiv.) was dissolved in anhydrous DCM at 0°C. A 1M solution of BBr_3 in DCM (1.5 equiv. BBr_3) was added dropwise and the reaction was slowly warmed to rt. Solution was stirred overnight. Reaction was cooled to 0°C and quenched with the careful addition of MeOH (5 mL per mmol) followed by stirring for 15 min. Reaction mixture was concentrated *in vacuo* and the product was purified using flash chromatography (0-10% MeOH in DCM).

4′-Chloro-5-chloro-2-hydroxybenzenesulfonanilide (**1**)

^{1}H NMR (500 MHz, Acetone-d_6) δ 7.64 (d, J = 2.7 Hz, 1H), 7.38 (dd, J = 8.8, 2.7 Hz, 1H), 7.31 – 7.26 (m, 2H), 7.25 – 7.22 (m, 2H), 7.20 (d, J = 8.8 Hz, 1H). ^{13}C NMR (126 MHz, Acetone-d_6) δ 154.17, 153.99, 136.35, 134.45, 129.53, 129.07, 129.02, 125.84, 123.29, 122.57, 122.56, 119.08. ESI-MS: *m/z* $[M+H]^+$ 316.9657

4′-Hydroxy-5-chloro-2-hydroxybenzenesulfonanilide (**2**)

^{1}H NMR (500 MHz, DMSO-d_6) δ 11.17 (s, 1H), 9.48 (s, 1H), 9.25 (s, 1H), 7.57 – 7.36 (m, 2H), 6.97 (d, J = 8.6 Hz, 1H), 6.91 – 6.88 (m, 2H), 6.62 – 6.51 (m, 2H).
^{13}C NMR (126 MHz, DMSO) δ 155.17, 154.71, 134.49, 129.35, 129.35, 128.79, 126.70, 124.11, 124.05, 122.22, 119.35, 115.87. ESI-MS: *m/z* $[M+H]^+$ 299.0024

2′,4′-Dichloro-5-chloro-2-hydroxybenzenesulfonanilide (**3**)

^{1}H NMR (500 MHz, $CDCl_3$) δ 8.32 (s, 1H), 7.53 (dd, J = 8.5, 2.9 Hz, 1H), 7.47 (d, J = 2.6 Hz, 1H), 7.42 – 7.36 (m, 1H), 7.33 (d, J = 2.6 Hz, 1H), 7.28 (d, J = 9.5 Hz, 1H), 7.03 (s, 1H), 6.93 (dd, J = 8.9, 3.0 Hz, 1H). ^{13}C NMR (126 MHz, $CDCl_3$) δ 153.81, 136.11, 132.72, 130.75, 129.55, 128.47, 127.73, 127.65, 125.47, 125.22, 122.58, 120.49. ESI-MS: *m/z* $[M+H]^+$ 350.9290

4′-Fluoro-5-chloro-2-hydroxybenzenesulfonanilide (**4**)

^{1}H NMR (500 MHz, $CDCl_3$) δ 7.52 (d, J = 3.1 Hz, 1H), 7.35 (dd, J = 8.6, 2.4 Hz, 1H), 7.29 (s, 1H), 7.08 – 7.04 (m, 2H), 6.97 – 6.91 (m, 3H).^{13}C NMR (126 MHz, $CDCl_3$) δ 162.44, 160.47, 153.41, 135.63, 128.10, 126.17, 126.10, 125.48, 122.92, 120.02, 116.56, 116.38. ESI-MS: *m/z* $[M+H]^+$ 300.9975

4′-Methyl-5-chloro-2-hydroxybenzenesulfonanilide (**5**)

^{1}H NMR (500 MHz, $CDCl_3$) δ 8.48 – 8.34 (m, 1H), 7.49 (d, J = 2.6 Hz, 1H), 7.35 (dd, J = 8.8, 2.6 Hz, 1H), 7.09 (d, J = 8.0 Hz, 2H), 6.97 – 6.93 (m, 2H), 6.90 (d, J = 8.8 Hz, 1H), 6.68 (s, 1H),

2.31 (s, 3H). ^{13}C NMR (126 MHz, $CDCl_3$) δ 153.75, 137.27, 135.46, 131.93, 130.18, 127.80, 125.24, 124.09, 122.92, 120.21, 20.94. ESI-MS: *m/z* $[M+H]^+$ 297.0221

4′-Trifluoromethyl-5-chloro-2-hydroxybenzenesulfonanilide (**6**)

^{1}H NMR (500 MHz, $CDCl_3$) δ 7.57 (d, *J* = 8.4 Hz, 2H), 7.54 (d, *J* = 2.6 Hz, 1H), 7.40 (dd, *J* = 8.8, 2.6 Hz, 1H), 7.19 (d, *J* = 8.3 Hz, 2H), 6.96 (d, *J* = 8.9 Hz, 1H). ^{13}C NMR (126 MHz, $CDCl_3$) δ 153.69, 138.38, 136.05, 128.48, 128.22, 127.70, 126.97, 125.73, 124.73, 122.71, 122.56, 121.53, 120.59. ESI-MS: *m/z* $[M+H]^+$ 350.9943

2′-Chloro-4′-trifluoromethyl-5-chloro-2-hydroxybenzenesulfonanilide (**7**)

^{1}H NMR (500 MHz, $CDCl_3$) δ 7.68 (d, *J* = 8.5 Hz, 1H), 7.61 (d, *J* = 2.1 Hz, 1H), 7.56 (d, *J* = 2.1 Hz, 1H), 7.53 (d, *J* = 2.6 Hz, 1H), 7.41 (dd, *J* = 8.9, 2.6 Hz, 1H), 6.96 (d, *J* = 8.9 Hz, 1H). ^{13}C NMR (126 MHz, $CDCl_3$) δ 153.80, 136.37, 135.54, 127.68, 127.01, 125.76, 125.61, 125.28, 123.94, 122.53, 122.06, 121.78, 120.68. ESI-MS: *m/z* $[M+H]^+$ 384.9547

2′,4′-Difluoro-5-chloro-2-hydroxybenzenesulfonanilide (**8**)

^{1}H NMR (500 MHz, $CDCl_3$) δ 8.32 (s, 1H), 7.51 (d, *J* = 2.7 Hz, 1H), 7.49 – 7.43 (m, 1H), 7.37 (dd, *J* = 8.9, 2.6 Hz, 1H), 7.13 (s, 1H), 6.92 (d, *J* = 8.9 Hz, 1H), 6.89 – 6.83 (m, 1H), 6.81 – 6.71 (m, 1H). ^{13}C NMR (126 MHz, $CDCl_3$) δ 160.23, 154.99, 153.55, 135.87, 127.88, 127.73, 125.43, 122.90, 120.14, 118.90, 112.06, 104.55. ESI-MS: *m/z* $[M+H]^+$ 318.9874

NMR spectra for compounds **1-8** can be found in supplementary information.

6.4.3 Antimicrobial susceptibility assay

Bacterial isolates used in this study were obtained from the American Type Culture Collection (ATCC), the Canadian National Intensive Care Unit (CAN-ICU) surveillance study[22] and the Canadian Ward (CANWARD) surveillance study.[23] Clinical isolates belonging to the CAN-ICU and CANWARD surveillance studies were recovered from patients suffering presumed infectious diseases entering or admitted in a participating medical center across Canada during the time of study. The in vitro antibacterial activities of the compounds were assessed using the broth microdilution method according to the Clinical and Laboratory Standards Institute (CLSI)

guidelines.[24] Bacterial cultures were grown overnight and diluted in saline to achieve a 0.5 McFarland turbidity, followed by 1:50 dilution in Cation-adjusted Mueller-Hinton broth (CAMHB) for inoculation to a final concentration of approximately 5×10^5 colony forming units per mL. Experiments were performed on 96-well plates. The tested agents were 2-fold serially diluted in CAMHB and incubated with equal volumes of bacterial inoculum at 37°C for 18 h. The MIC was determined as the lowest concentration to inhibit visible bacterial growth in the form of visible turbidity, which was confirmed using an EMax Plus microplate reader (Molecular Devices, USA) at a wavelength of 590 nm. CAMHB with or without bacterial cells were used as positive or negative controls, respectively.

6.4.4. Checkerboard assay

The assay was performed on 96-well plates as previously described.[25] One agent was 2-fold serially diluted along the x-axis, while the other agent was 2-fold serially diluted along the y-axis to create a matrix in which each well contained a combination of both agents at different concentrations. Bacterial cultures grown overnight were diluted in saline to 0.5 McFarland turbidity, followed by 1:50 dilution in CAMHB and inoculation of each well to a final concentration of approximately 5×10^5 colony forming units per mL. Wells consisting of only CAMHB with or without bacterial cells were used as positive or negative controls, respectively. Plates were incubated for 18 h at 37°C and inspected for visible turbidity, which was confirmed using EMax Plus microplate reader (Molecular Devices, USA) at a wavelength of 590 nm. Fractional inhibitory concentration (FIC) of each agent was calculated by dividing the MIC of the compound in the presence of COL by the MIC of the compound alone. Likewise, the FIC of coilstin was calculated via dividing the MIC of COL in the presence of each compound by the MIC of COL alone. The FIC index was obtained by the summation of both FIC values. The FIC

indices were interpreted as synergistic, indifferent, or antagonistic for values of ≤ 0.5, 0.5 < x ≤ 4, or >4, respectively.[18] For triple combinations, the third agent at a fixed concentration is added in the culture media.

6.6: Conclusions

A series of sulfonamide bioisosteres of NIC, with various substituents on the aniline ring were synthesized and assessed for their ability to potentiate COL. It was found that electron-withdrawing substituents are necessary for synergy with COL, and sulfonamide **7** which contained chloro- and trifluoromethyl substituents displayed the most potent activity. We also found that adding BAC to combinations of COL and compound **7** or NIC further increased COL activity. Triple combinations showed that BAC can reduce COL MIC by up to an additional 8-fold compared to just NIC or compound **7**. We also showed that combinations of NIC or compound **7** are synergistic with BAC against *E. faecium*. Overall, this work expands the potential landscape of applications for NIC and its derivatives as antibacterial agents.

6.7: References

1. Theuretzbacher, U. *Curr Opin Microbiol* **2017**, *39*, 106–112.
2. Brown, E. D.; Wright, G. D. *Nature* **2016**, *529* (7586), 336–343.
3. Fernandes, P.; Martens, E. *Biochem Pharmacol* **2017**, *133*, 152–163.
4. Li, J.; Nation, R. L.; Turnidge, J. D.; Milne, R. W.; Coulthard, K.; Rayner, C. R.; Paterson, D. L. *Lancet Infect Dis* **2006**, *6* (9), 589–601.
5. Tyers, M.; Wright, G. D. *Nature Reviews Microbiology*. **2019**, 141–155.
6. Douafer, H.; Andrieu, V.; Phanstiel, O.; Brunel, J. M. *J Med Chem* **2019**, *62* (19), 8665–8681.
7. Ghirga, F.; Stefanelli, R.; Cavinato, L.; Lo Sciuto, A.; Corradi, S.; Quaglio, D.; Calcaterra, A.; Casciaro, B.; Loffredo, M. R.; Cappiello, F.; Morelli, P.; Antonelli, A.; Rossolini, G. M.;

Mangoni, M.; Mancone, C.; Botta, B.; Mori, M.; Ascenzioni, F.; Imperi, F. *Journal of Antimicrobial Chemotherapy* **2020**, *75* (9), 2564–2572.

8. Minrovic, B. M.; Hubble, V. B.; Barker, W. T.; Jania, L. A.; Melander, R. J.; Koller, B. H.; Melander, C. *ACS Med Chem Lett* **2019**, *10* (5), 828–833.

9. Diletta, C.; Alessandra, F.; Paolo, V.; Francesco, I.; Giordano, R.; Livia, L. *Microbiol Spectr* **2023**, *11* (2), e04275-22.

10. Mohammad, H.; AbdelKhalek, A.; Abutaleb, N. S.; Seleem, M. N. *Int J Antimicrob Agents* **2018**, *51* (6), 897–904.

11. Imperi, F.; Massai, F.; Pillai, C. R.; Longo, F.; Zennaro, E.; Rampioni, G.; Visc, P.; Leoni, L. *Antimicrob Agents Chemother* **2013**, *57* (2), 996–1005.

12. Domalaon, R.; Malaka De Silva, P.; Kumar, A.; Zhanel, G. G.; Schweizer, F. *Antimicrob Agents Chemother* **2019**, *63* (4), e02574-18.

13. Ayerbe-Algaba, R.; Gil-Marqués, M. L.; Jiménez-Mejías, M. E.; Sánchez-Encinales, V.; Parra-Millán, R.; Pachón-Ibáñez, M. E.; Pachón, J.; Smani, Y. *Front Cell Infect Microbiol* **2018**, *8*, 348.

14. Berry, L.; Neale, Q.; Arora, R.; Ramirez, D.; Brizuela, M.; Domalaon, R.; Arthur, G.; Schweizer, F. *Manuscript submitted for publication* **2023**.

15. Li, H.; Mattingly, A. E.; Jania, L. A.; Smith, R.; Melander, R. J.; Ernst, R. K.; Koller, B. H.; Melander, C. *ACS Infect Dis* **2021**, *7* (12), 3303–3313.

16. O'Donovan, C. A.; Fan-Havard, P.; Tecson-Tumang, F. T.; Smith, S. M.; Eng, R. H. K. *Diagn Microbiol Infect Dis* **1994**, *18* (2), 105–109.

17. Tharmalingam, N.; Port, J.; Castillo, D.; Mylonakis, E. *Sci Rep* **2018**, *8* (1), 3701.

18. Berenbaum, M. C. *Pharmacol Rev* **1989**, *41* (2), 93.

19. Edge, R.; Argáez, C. In *CADTH Rapid Response Report*; CADTH Rapid Response Reports; Canadian Agency for Drugs and Technologies in Health, Ottawa (ON), 2017.

20. Cornelissen, F.; Van den Bossche, H. *Chemotherapy* **2009**, *29* (6), 419–427.

21. Johnson, B. A.; Anker, H.; Meleney, F. L. *Science (1979)* **1945**, *102* (2650), 376–377.

22. Zhanel, G. G.; DeCorby, M.; Adam, H.; Mulvey, M. R.; McCracken, M.; Lagacé-Wiens, P.; Nichol, K. A.; Wierzbowski, A.; Baudry, P. J.; Tailor, F.; Karlowsky, J. A.; Walkty, A.; Schweizer, F.; Johnson, J.; Hoban, D. J. *Antimicrob Agents Chemother* **2010**, *54* (11), 4684–4693.

23. Hoban, D. J.; Zhanel, G. G. *J Antimicrob Chemother* **2013**, *68 Suppl 1*, i3-5.

24. Clinical and Laboratory Standards Institute. 28th ed.; Clin. Lab. Stand Institute: Wayne, PA, 2018.

25. Berry, L.; Brizuela, M.; Jackson, G.; Schweizer, F. *RSC Med Chem* **2021**, *12* (9), 1565–1573.

CHAPTER SEVEN:
Conclusions and Future Work

7.1 Conclusions

Considering the looming threat of antibacterial resistance, humanity desperately needs novel solutions. Colistin resistance represents the possibility that we may soon lack any effective antibiotics to treat challenging infections. Niclosamide shows great promise for drug repurposing efforts as an adjuvant for colistin but has significant challenges. In order for niclosamide to succeed as a colistin adjuvant, novel derivatives must be synthesized, solving challenges such as toxicity and poor water solubility. This thesis represents an important contribution towards solving some of these challenges and understanding the medicinal chemistry of niclosamide as a colistin adjuvant.

In chapter 4, a series of niclosamide analogs were synthesized to perform an SAR with an overall goal of replacing the nitro group of niclosamide to reduce toxicity while maintaining the ability of niclosamide to synergize with colistin. A small library of compounds was produced and their ability to synergize with colistin was observed. It was found that the nitro group on niclosamide can be replaced by an amine, a methyl ester, or an azide while still retaining colistin-potentiating activity. We also showed that the phenol group of niclosamide was necessary for synergy with colistin, but that the addition of multiple phenols led to a complete loss of synergy. A methyl ester analog was assessed against a panel of MDR clinical isolates and was shown to reduce colistin MIC to below CLSI breakpoint values, even against highly resistant isolates. The amine and methyl ester compounds were also found to be less toxic to eukaryotic cells. One significant challenge that needs to be overcome is the likely metabolic instability of the ester, as esters are known to be prone to hydrolysis *in vivo*, especially given that the carboxylic acid derivative displayed no synergy with colistin. This work provided important insights into synthetic strategies for the future development of novel niclosamide derivatives, and that modification to the nitro group of niclosamide is a viable strategy of reducing toxicity.

In chapter 5, the niclosamide-hybrid approach was studied. Although the original objectives for this thesis included synthesizing a niclosamide-colistin hybrid, all amino acid derivatives of niclosamide in chapter 4 lost synergy with colistin. Therefore, our efforts were instead focused on synthesizing the niclosamide-tobramycin hybrid molecule, to examine how attaching niclosamide to a tobramycin fragment could expand the activity of the tobramycin-based hybrid adjuvant scaffold. A niclosamide-tobramycin hybrid was successfully synthesized via CuAAC and assessed for synergy against several classes of antibiotics against GNB. It was found

that the hybrid was able to potentiate a variety of antibiotics against wild-type *P. aeruginosa* and *E. coli* with limited activity against *A. baumannii*. This was the first report on the potentiation of cefiderocol with an antibiotic adjuvant and demonstrated that attaching niclosamide to the tobramycin scaffold imparts novel biological activity. However, given the lack of colistin potentiation displayed by the tobramycin-niclosamide hybrid, it appears that attaching large polybasic molecules to niclosamide will result in a loss of activity. A niclosamide-colistin hybrid molecule would share similar structural features and is thus unlikely to be a promising candidate for further exploration.

In chapter 6, a series of sulfonamide bioisosteres of niclosamide, with various substituents on the aniline ring were synthesized and assessed for their ability to potentiate colistin. It was found that electron-withdrawing substituents are necessary for synergy with colistin, and a sulfonamide which contained chloro- and trifluoromethyl substituents displayed the most potent activity. We also found that adding bacitracin to combinations of colistin and niclosamide or its sulfonamide analogs further increased colistin activity. Triple combinations showed that bacitracin can reduce colistin MIC by up to an additional 8-fold compared to just dual combinations. We also showed that combinations of niclosamide and sulfonamide analogs are synergistic with bacitracin against *E. faecium*. Overall, this work expands the potential landscape of applications for niclosamide and its derivatives as antibacterial agents.

Overall, several key insights were gained towards understanding the SAR of niclosamide as a colistin adjuvant:

- The phenol group on niclosamide is essential for synergy with colistin.
    - Modifying this group with even a methyl substituent completely abolishes colistin potentiation.
- Electron-withdrawing groups on the aniline are necessary for synergy with colistin.
    - Chapter 6 demonstrates that a certain threshold of electron-withdrawing substituents is necessary for activity, and a clear trend was observed where derivatives with the strongest electron-withdrawing groups were the most active.
- Modifying niclosamide with hydrophilic substituents completely abolishes activity and is not a viable method to enhance water solubility of niclosamide.

    - The amide and triazole derivatives bearing both acidic and basic moieties in chapter 4 and the niclosamide-tobramycin hybrid in chapter 5 lost all colistin potentiation.
- Replacing the nitro group on niclosamide is a viable method to reduce toxicity to eukaryotic cells.
    - The nitro group must be replaced by an electron-withdrawing substituent in order to retain synergy with colistin
- The central amide group in niclosamide is not necessary for activity and can be replaced with a sulfonamide.

This thesis has provided important insights into how niclosamide can be modified for use as an antibacterial adjuvant. The chemistry of synthesizing novel niclosamide derivatives has been optimized, modifying the nitro group on niclosamide has proven to be a viable strategy to reduce toxicity, and potentiation of colistin has been enhanced. Several limitations for using niclosamide analogs as an antibacterial agent still exist. Although several water-soluble derivatives have been synthesized, every derivative with enhanced water solubility lacked synergy with colistin. Future work should expand on the insights contained herein to design new derivatives with improved solubility, while maintaining the improvements already demonstrated. In addition, the lead compound in chapter 4 contains a methyl ester which is highly susceptible to hydrolysis *in vivo*. Future derivatives of niclosamide should replace this group with an isostere that is more metabolically stable.

7.2 Future Work

Several challenges for repurposing niclosamide as a colistin adjuvant have been solved, but others remain. Future work should combine the insights discussed in chapter 4 and chapter 6, to produce derivatives of niclosamide with improved drug-like properties. Another important insight which has only briefly been mentioned thus far is the solubility improvements of the sulfonamide compounds listed in chapter 6. No quantitative solubility data has been produced, but qualitative insights show that the sulfonamides display greatly improved solubility in organic solvents. This will greatly increase synthetic output for future derivatives, as one challenge involved in synthesizing niclosamide analogs is its poor solubility in organic solvents. The sulfonamide analogs were easier to purify via flash chromatography and could be analyzed using

deuterated chloroform instead of dimethyl sulfoxide as an NMR solvent. Therefore, future work should build upon the sulfonamide scaffold, while taking insights from the SAR in chapter 4. The methyl ester analogue of niclosamide shown in chapter 4 was the most potent and least toxic analogue produced thus far, so an interesting future molecule would combine the sulfonamide replacement with the methyl ester substitution. Further optimization should involve replacing the ester moiety with a bioisostere, to overcome the inherent instability of esters *in vivo*. **Figure 7.1** outlines several proposed new niclosamide analogs, incorporating these insights.

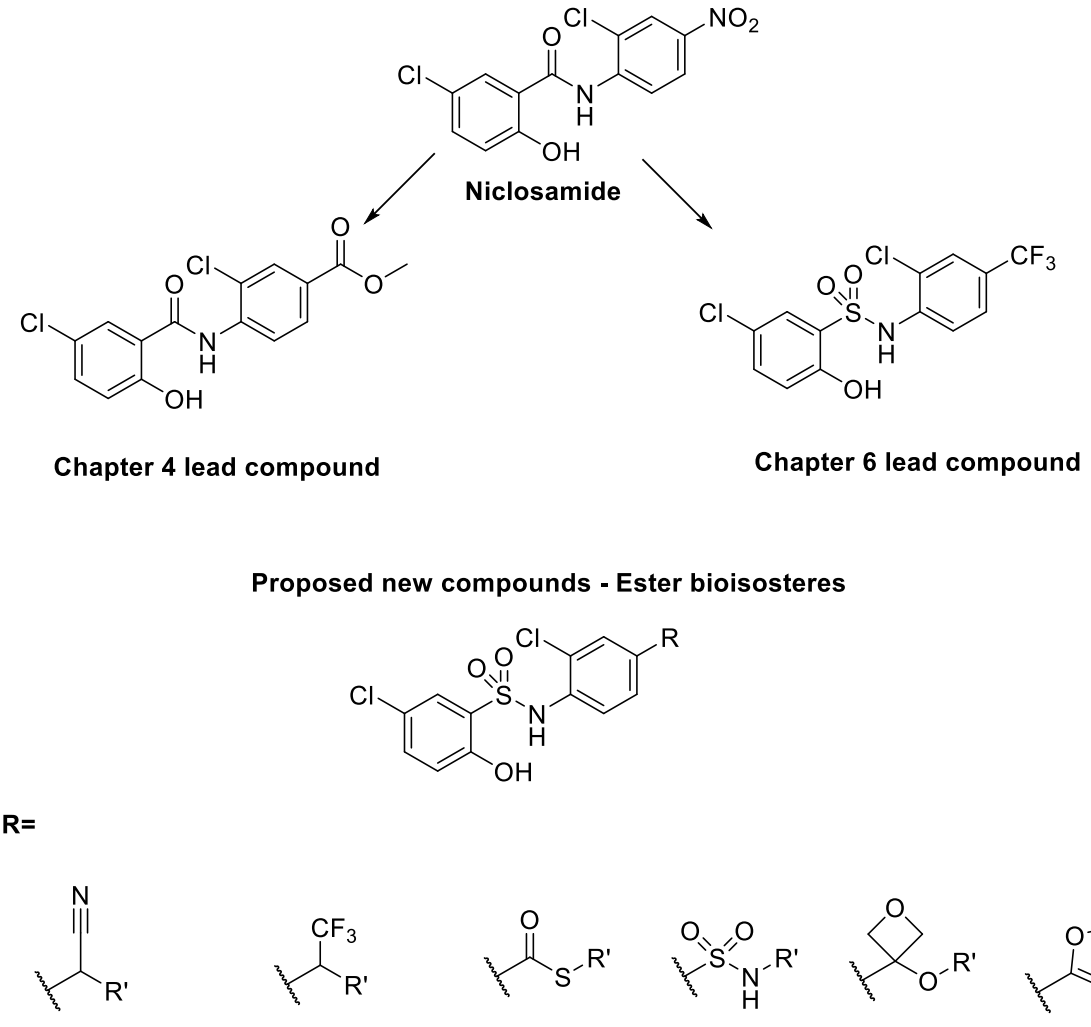

Figure 7.1 Proposed new compounds for future work. The sulfonamide approach from chapter 6 will be combined with bioiosteres for the methyl ester compound in chapter 4. The new derivatives should contain electron-withdrawing groups on the aniline ring.

In addition, future work should seek to uncover novel biological activity of new niclosamide analogs. The results in chapters 5 and 6 indicate that niclosamide derivatives can

display a wide variety of antibacterial activity, especially as adjuvants for antibiotics other than colistin. A detailed study of the mechanism of action of niclosamide as an adjuvant for colistin and other antibiotics should be performed, to help guide future drug discovery efforts. Lastly, the promising *in vitro* results in this thesis should be confirmed with *in vivo* experiments. Overall, this work has uncovered a promising starting point for designing novel niclosamide analogs as adjuvants for colistin.

APPENDIX A:
Supplementary material for chapter 4

Supplementary information for Chapter 4: Exploring structure-activity relationships of niclosamide-based colistin potentiators in colistin-resistant Gram-negative bacteria

Contents

NMR Spectra of compounds used for biological testing

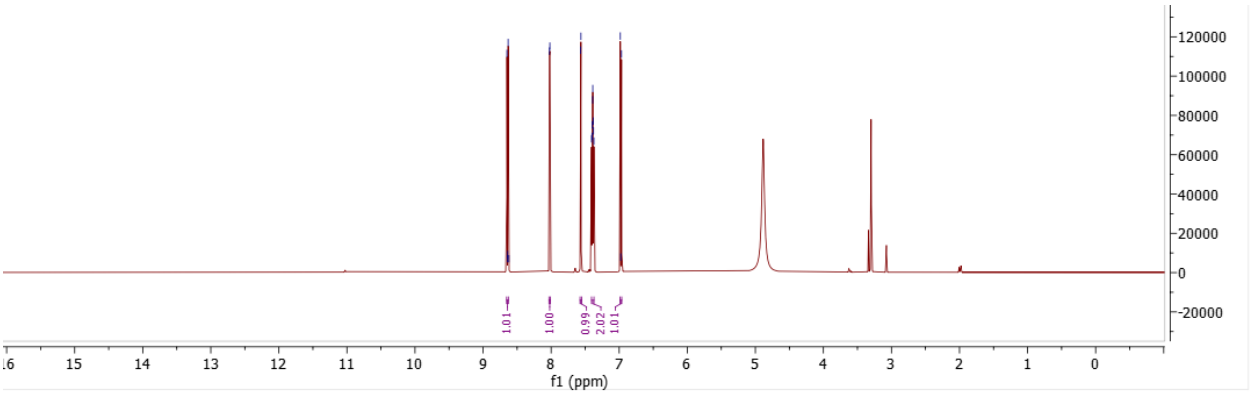

Figure S1 ^{1}H NMR spectrum of compound **1**

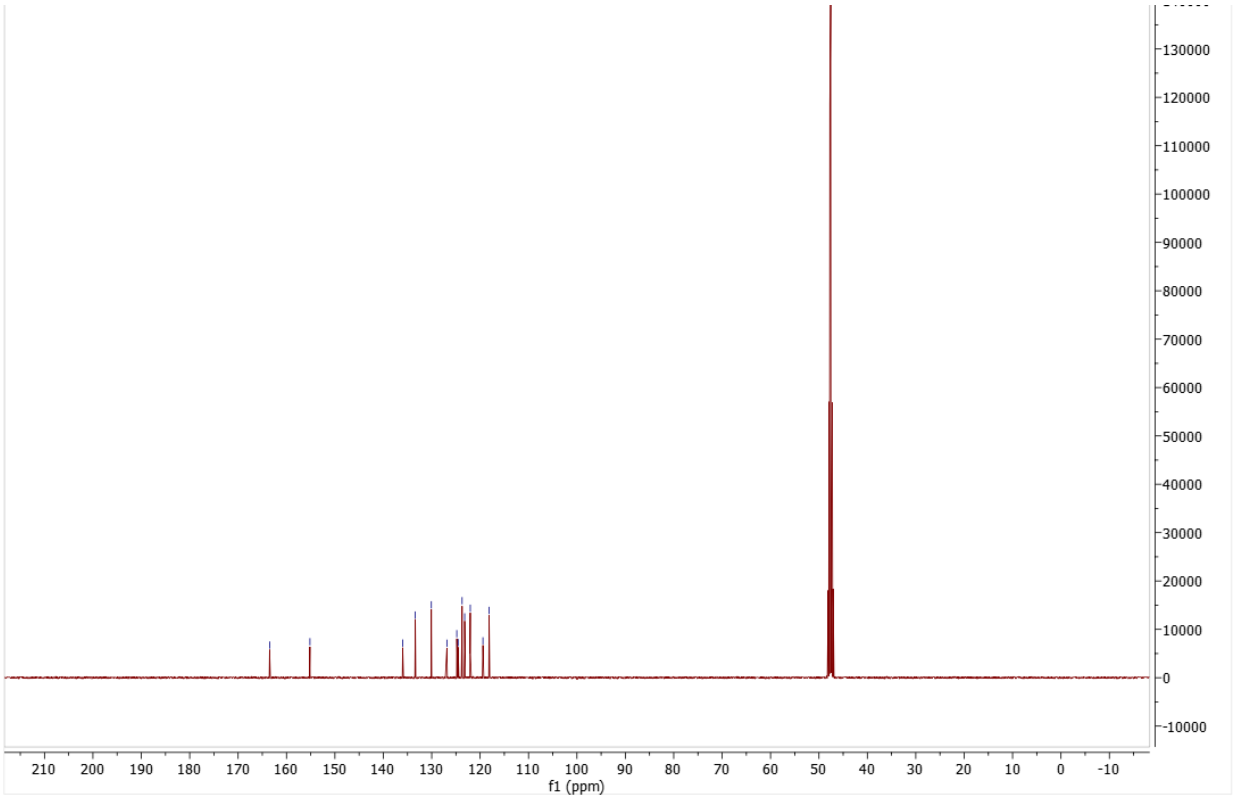

Figure S2 ^{13}C NMR spectrum of compound **1**

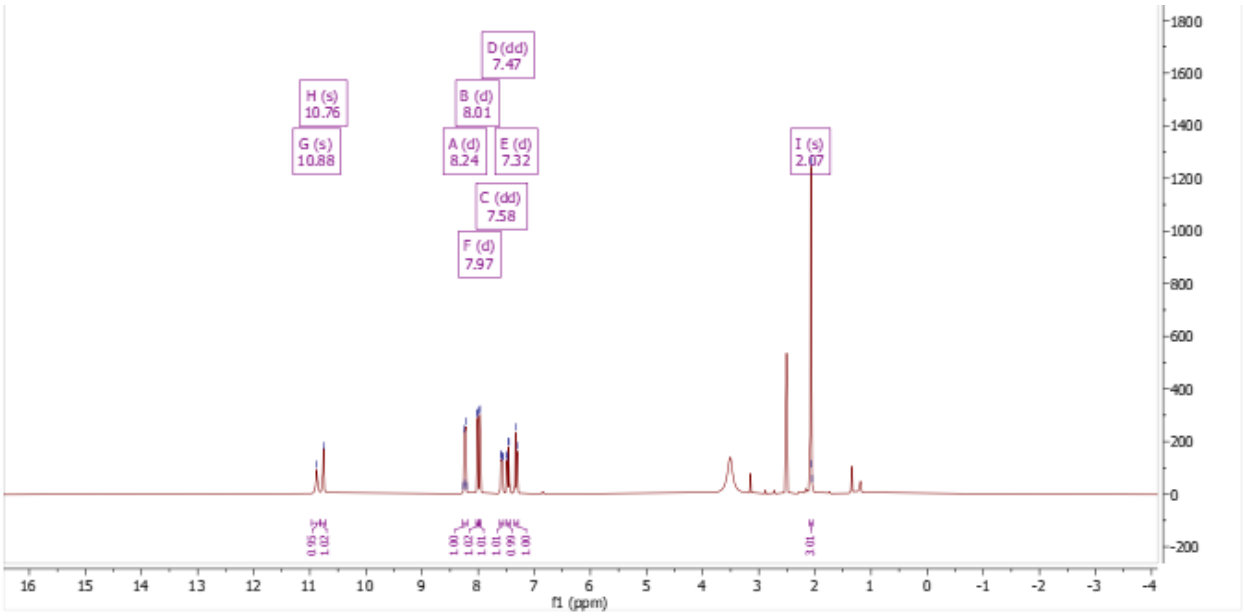

Figure S3 ^{1}H NMR spectrum of compound **2**

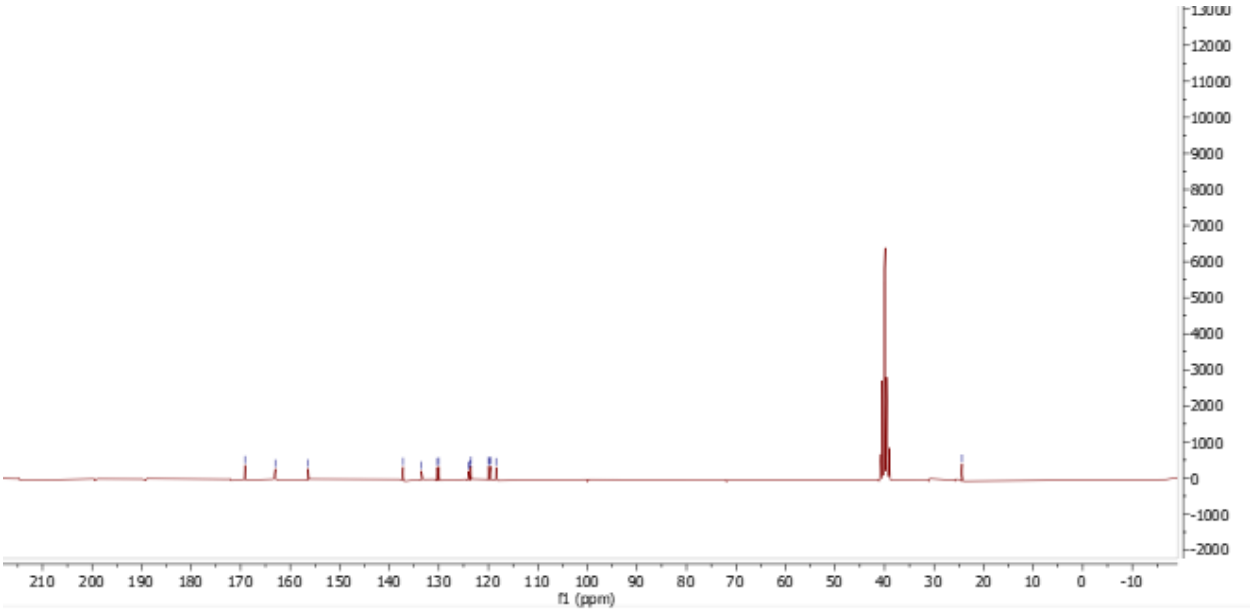

Figure S4 ^{13}C NMR spectrum of compound **2**

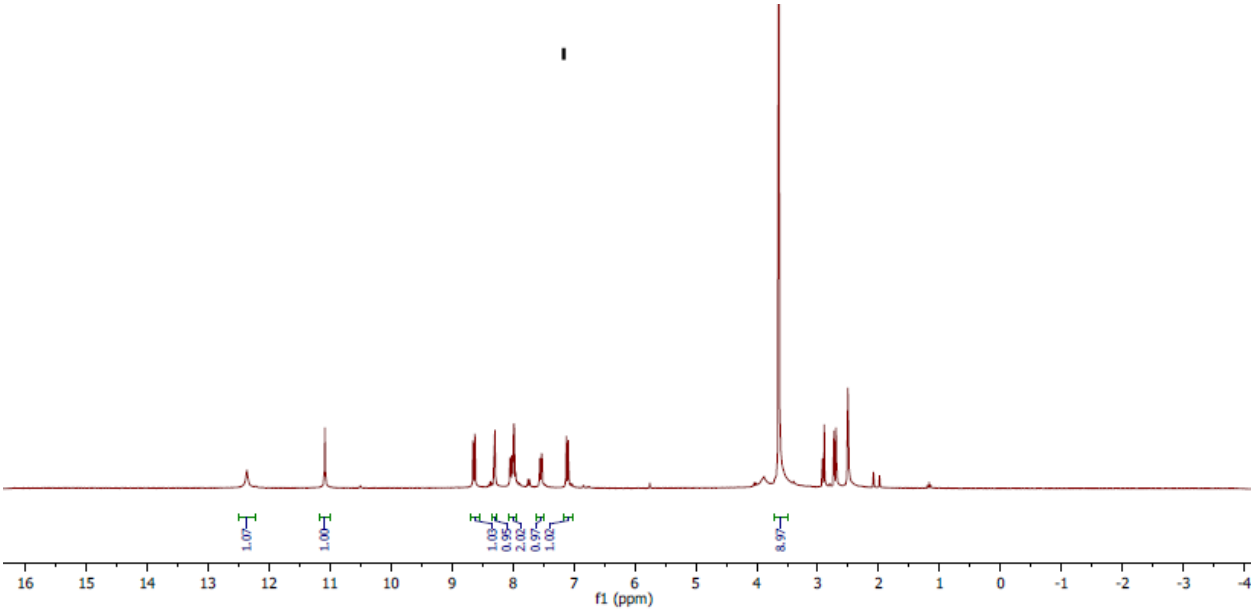

Figure S5 ^{1}H NMR spectrum of compound **3**

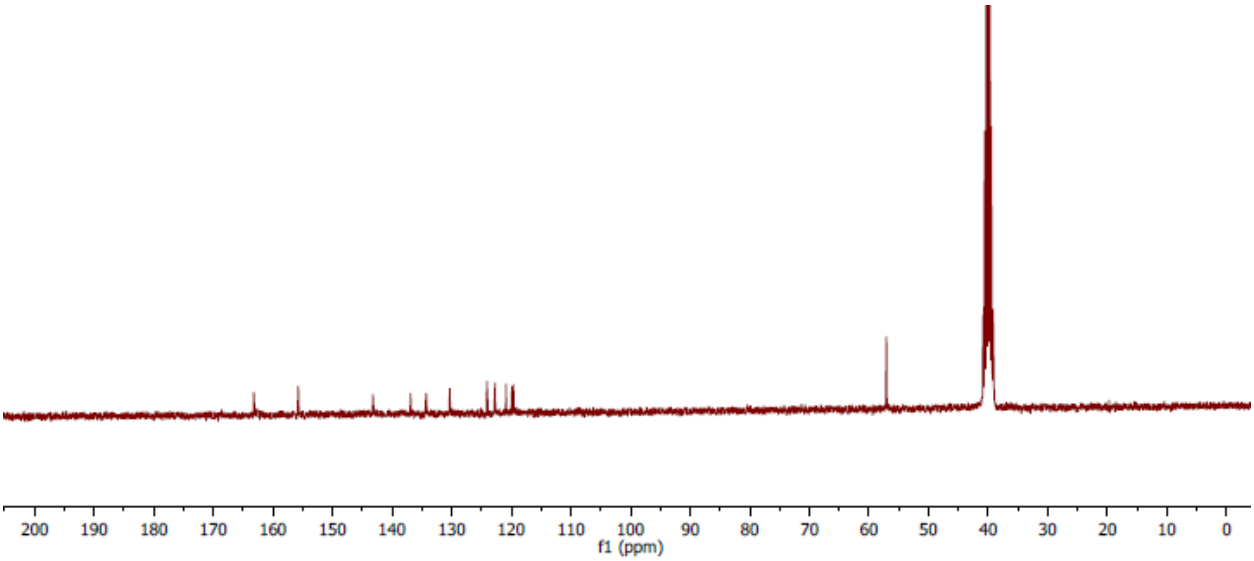

Figure S6 ^{13}C NMR spectrum of compound **3**

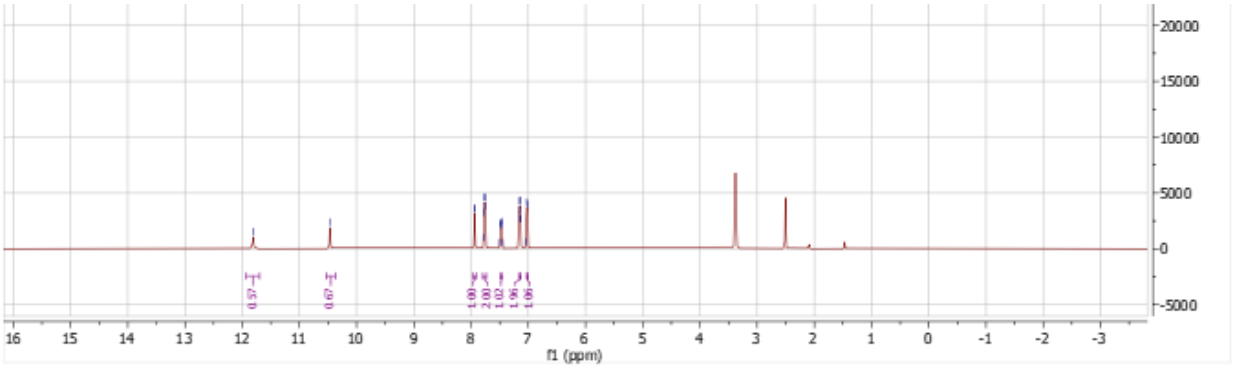

Figure S7 ^{1}H NMR spectrum of compound **4**

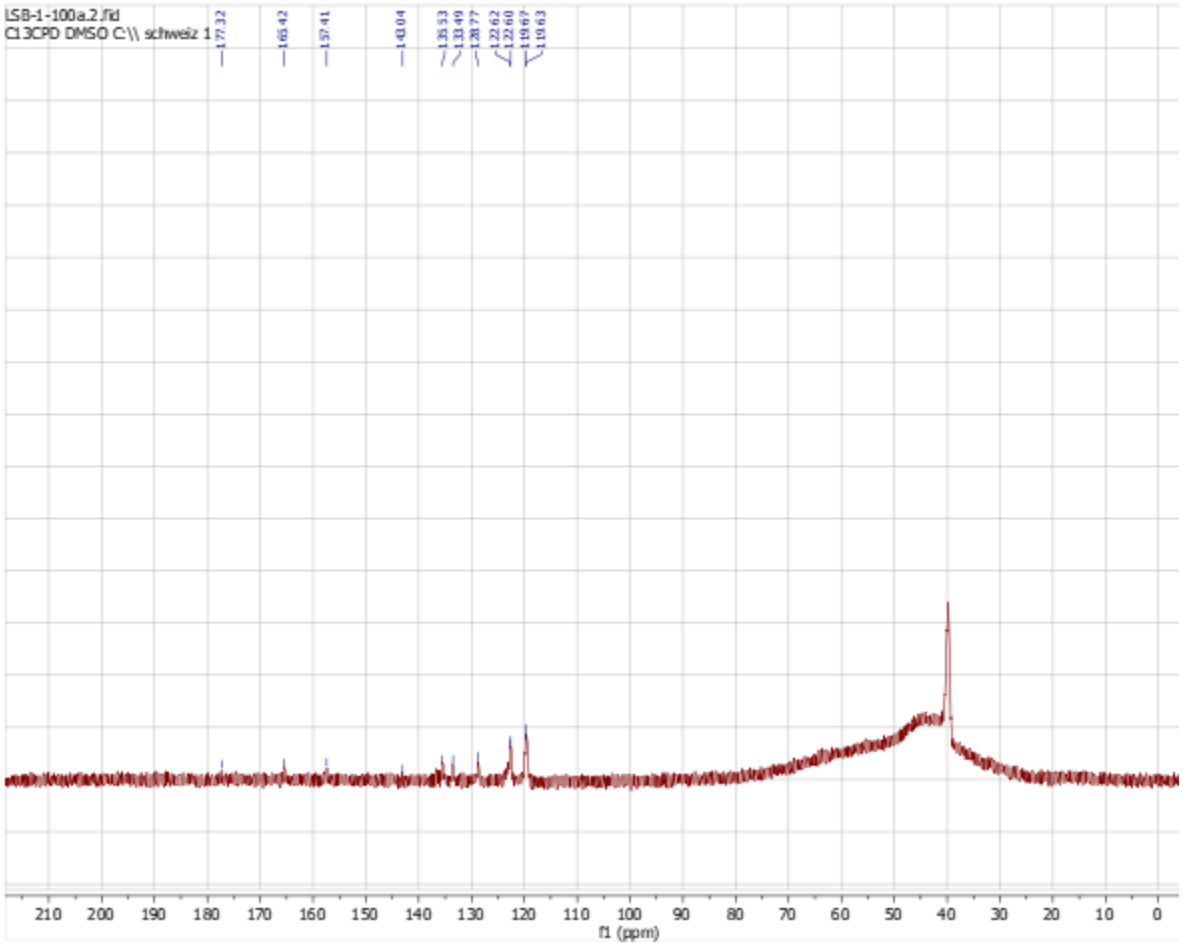

Figure S8 ^{13}C NMR spectrum of compound **4**

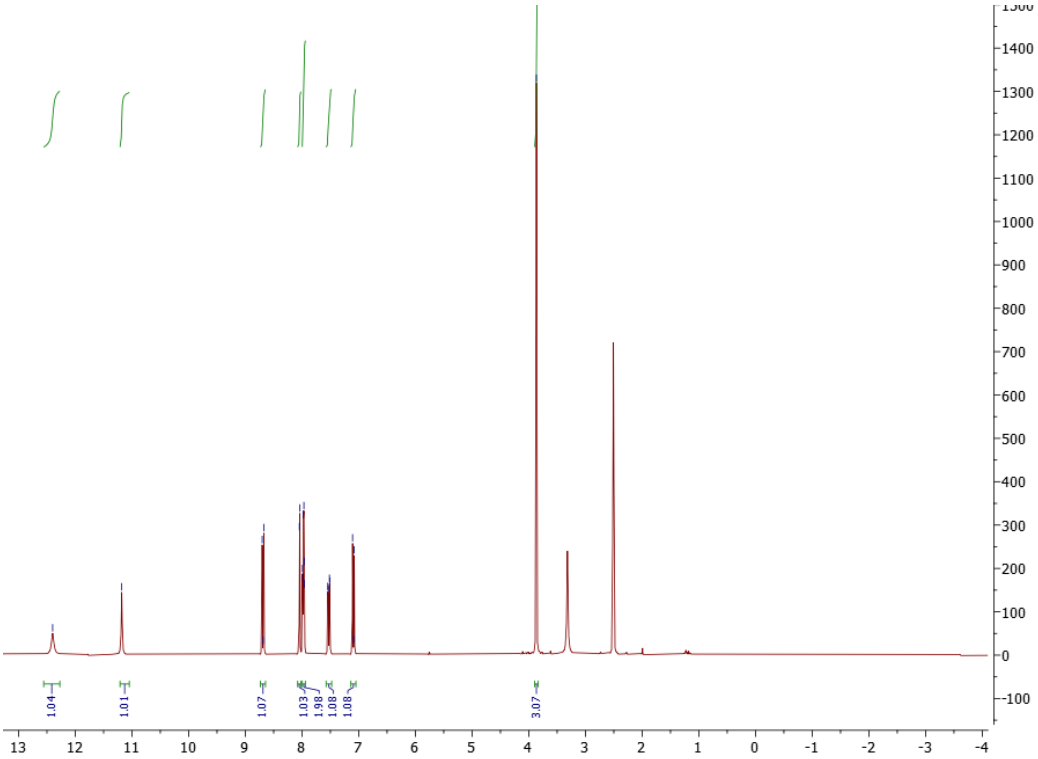

Figure S9 ^{1}H NMR spectrum of compound **5a**

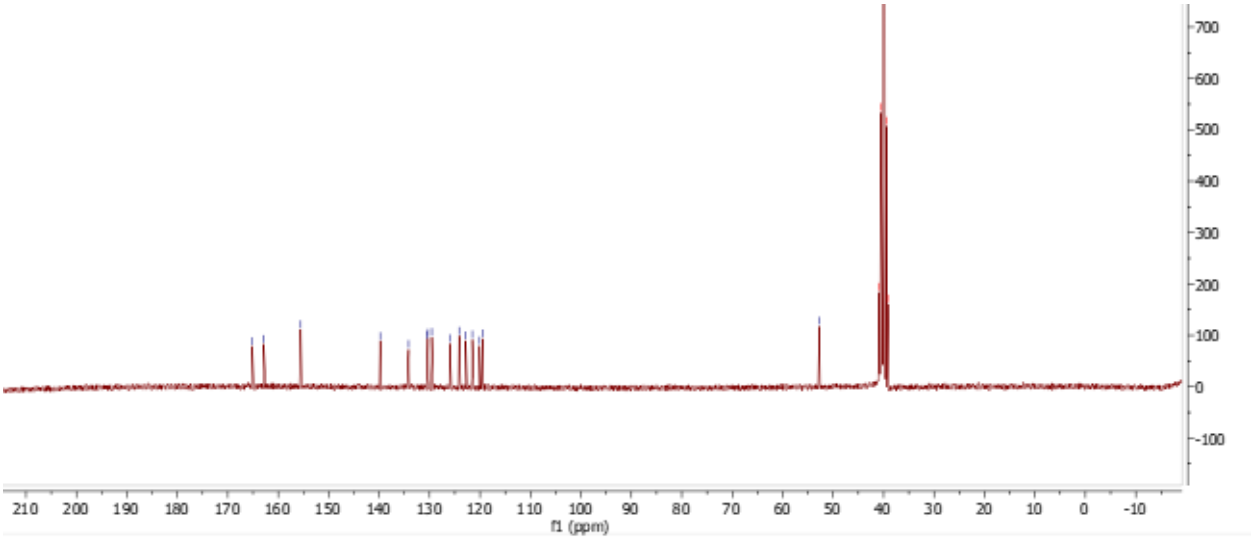

Figure S10 ^{13}C NMR spectrum of compound **5a**

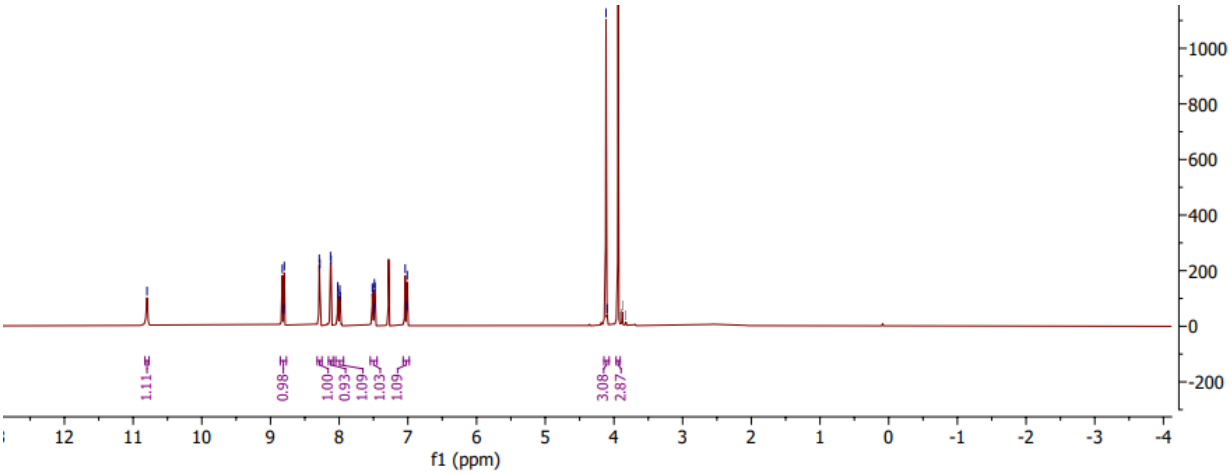

Figure S11 ^{1}H NMR spectrum of compound **5b**

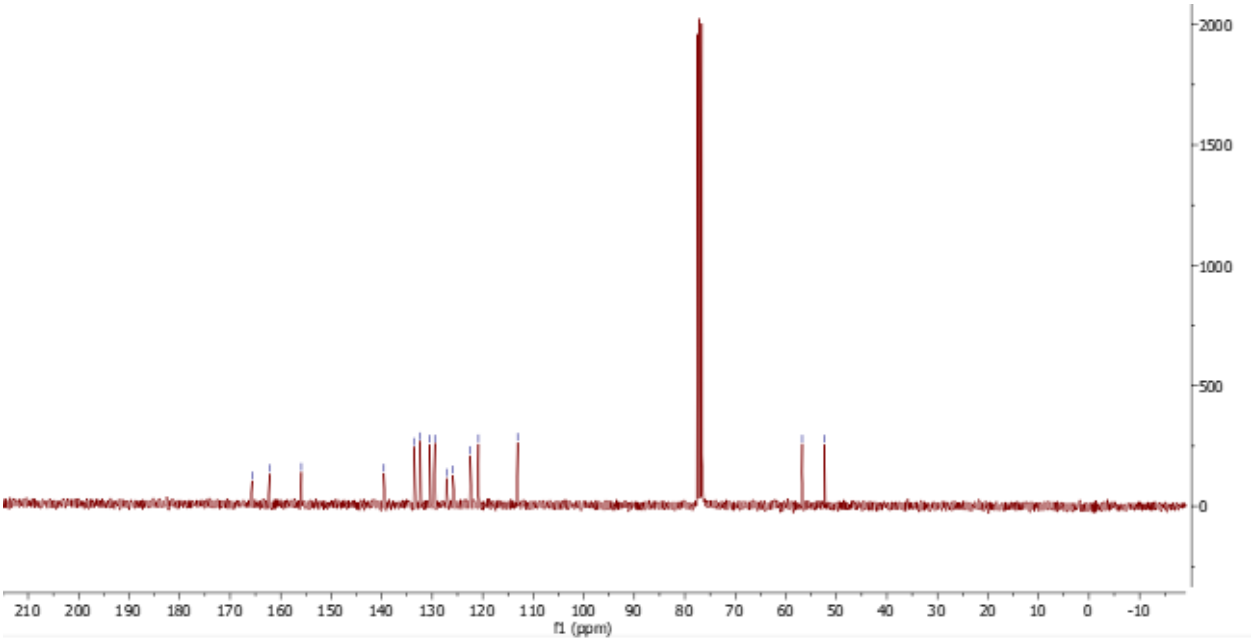

Figure S12 ^{13}C NMR spectrum of compound **5b**

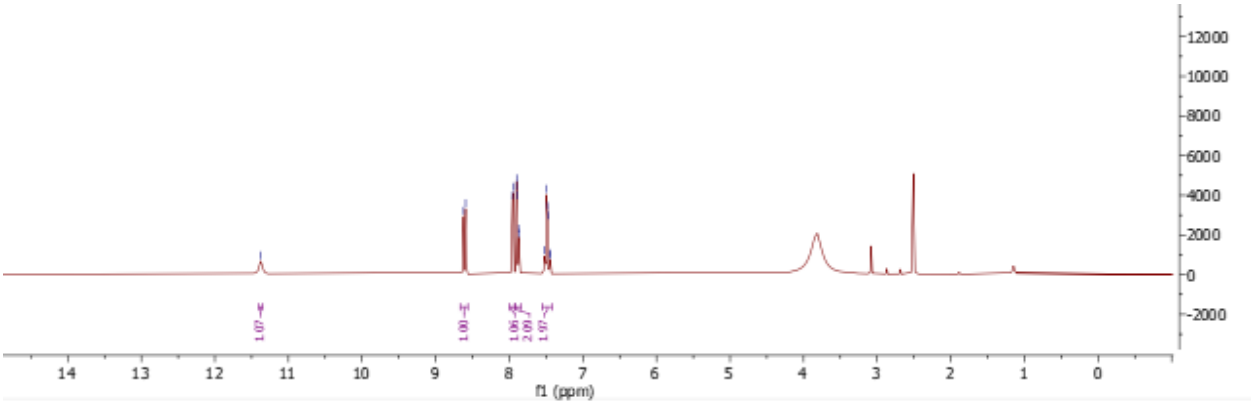

Figure S13 ^{1}H NMR spectrum of compound **6**

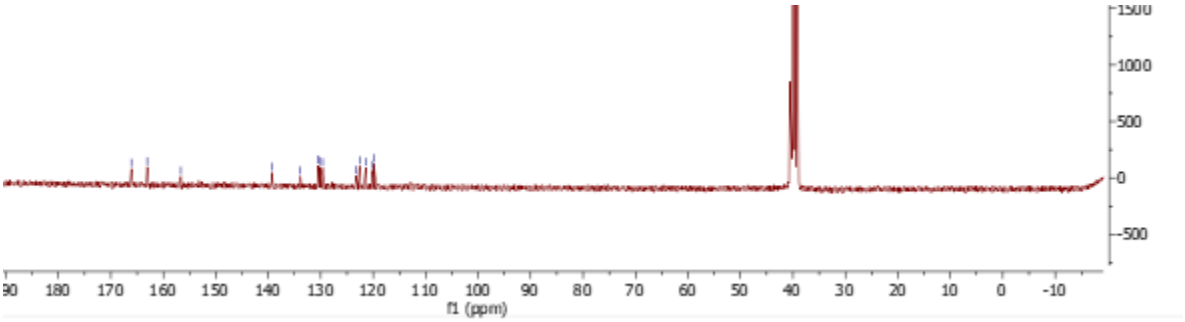

Figure S14 ^{13}C NMR spectrum of compound **6**

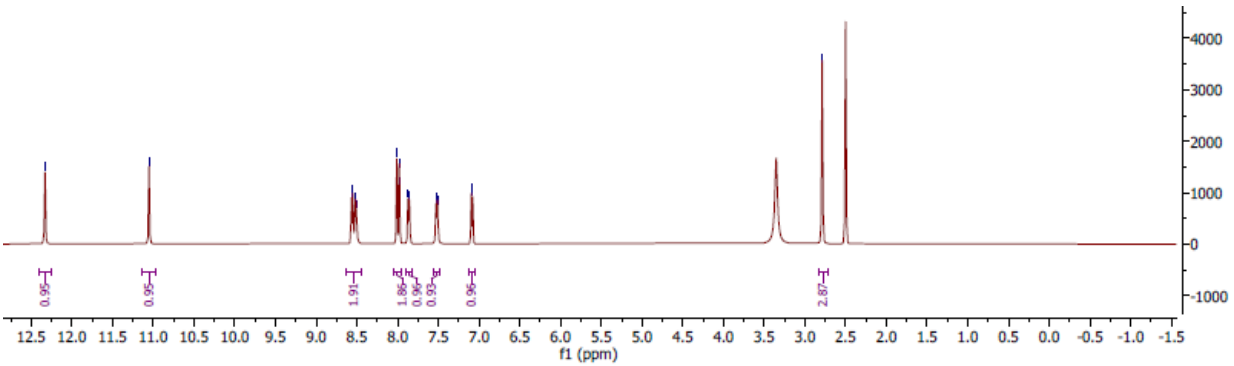

Figure S15 [1]H NMR spectrum of compound **7**

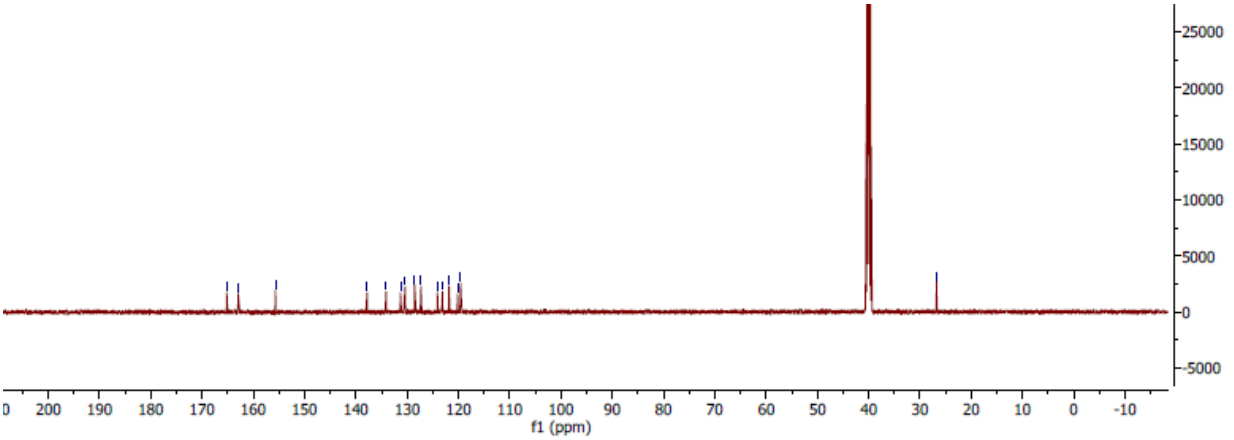

Figure S16 [1]H NMR spectrum of compound **7**

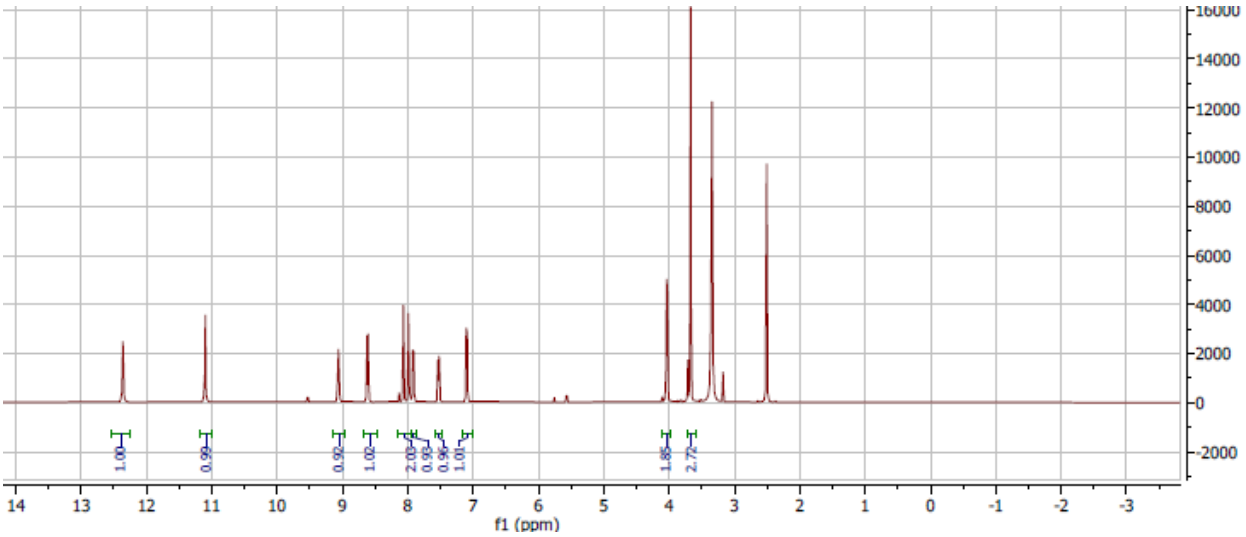

Figure S17 [1]H NMR spectrum of compound **8**

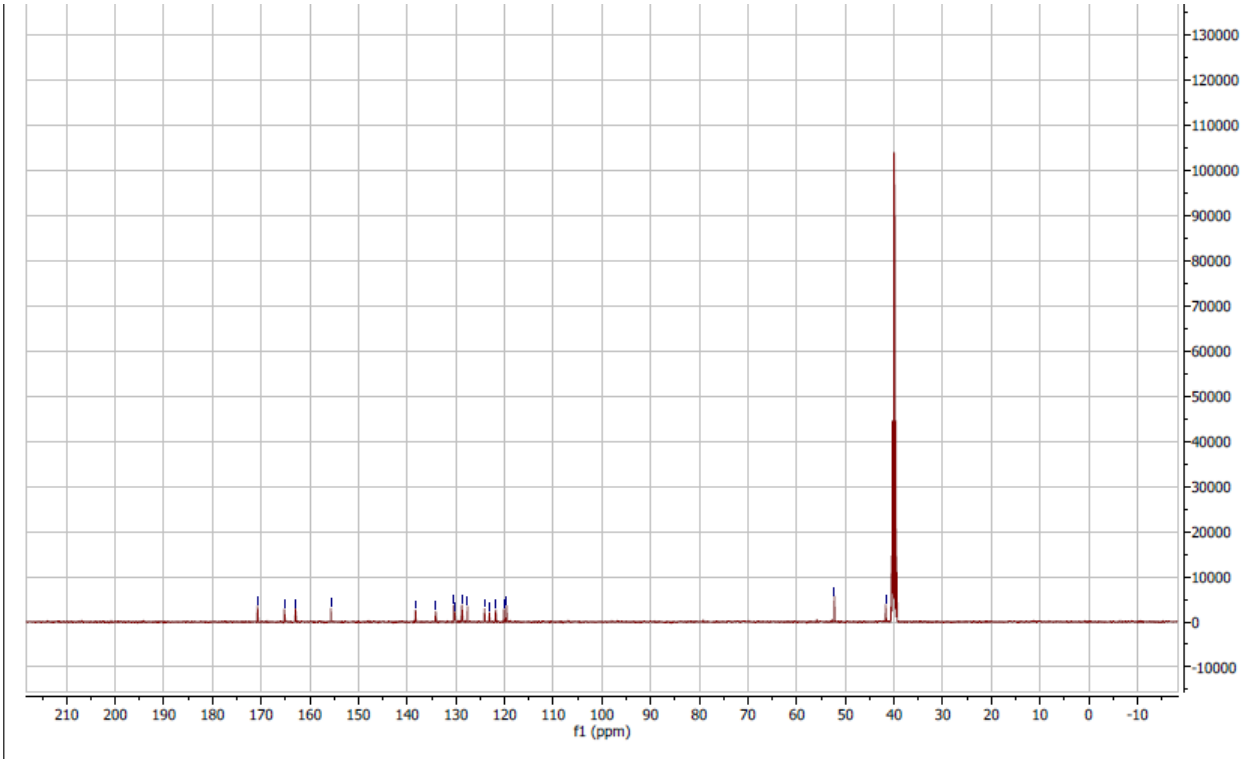

Figure S18 ^{13}C NMR spectrum of compound **8**

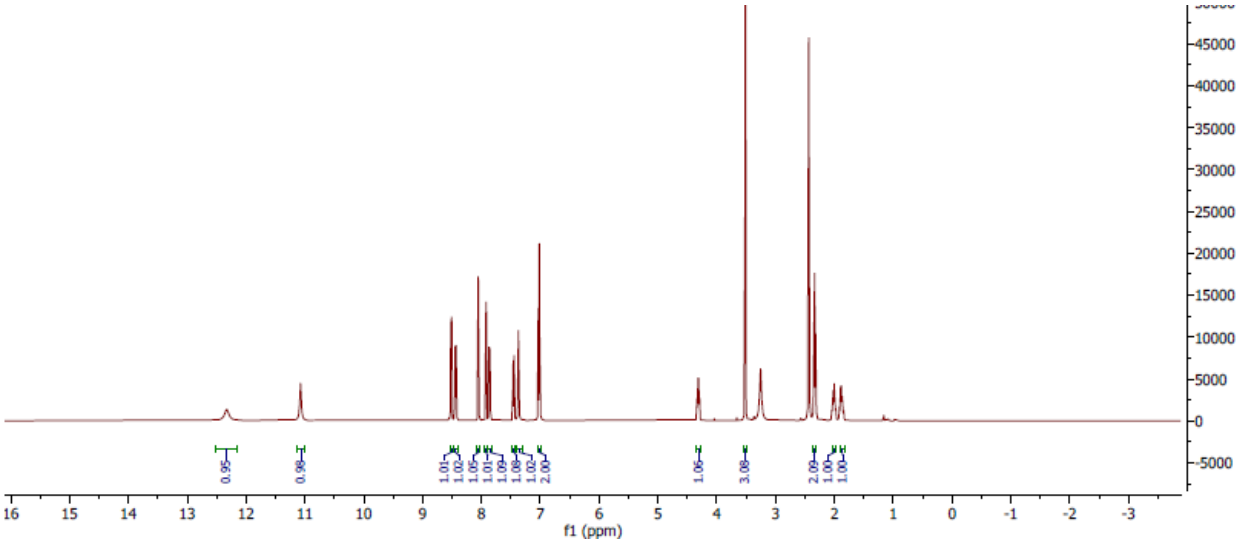

Figure S19 ^{1}H NMR spectrum of compound **9**

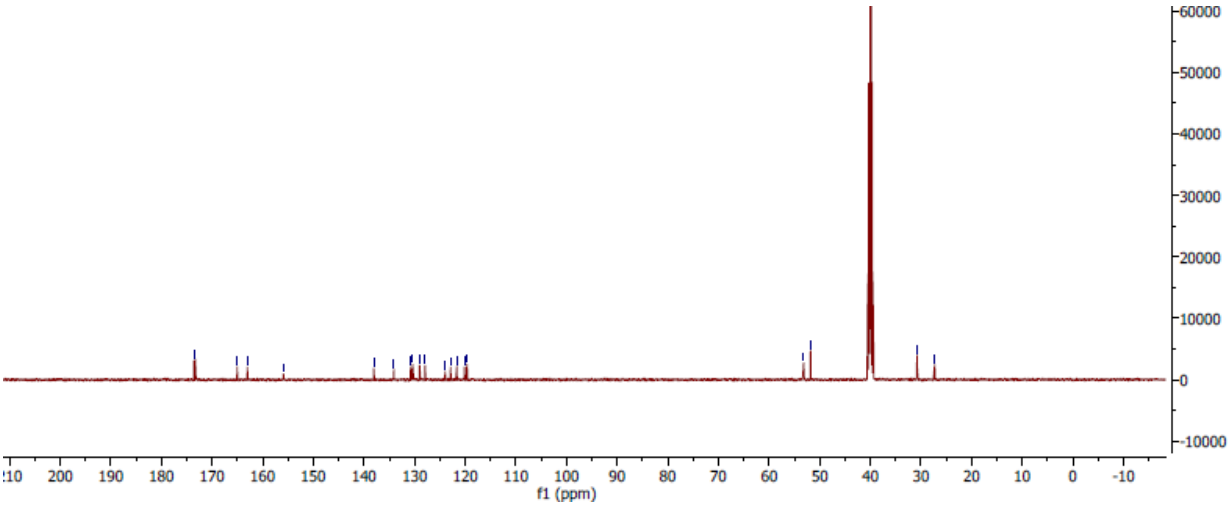

Figure S20 ^{13}C NMR spectrum of compound **9**

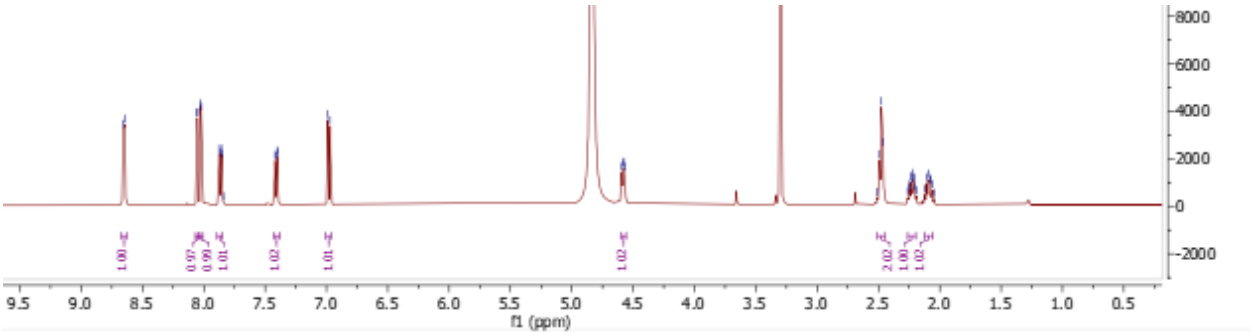

Figure S21 ^{1}H NMR spectrum of compound **10**

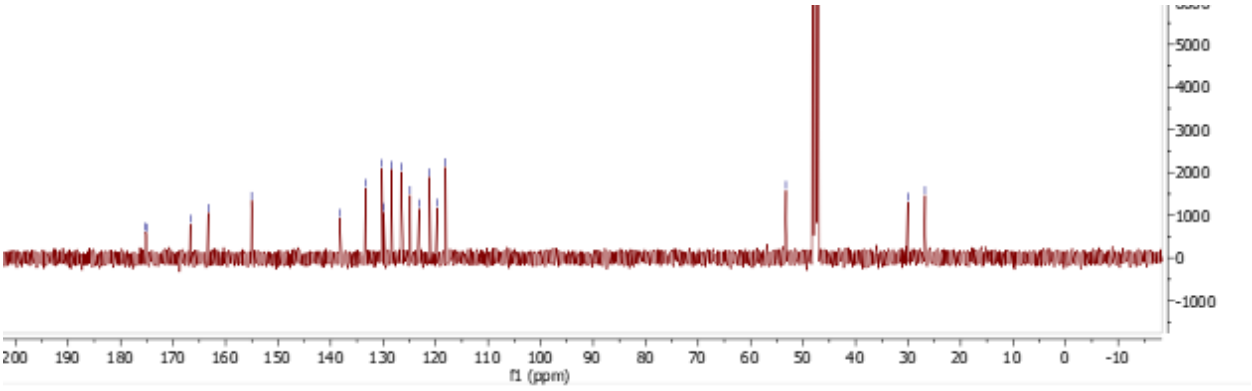

Figure S22 ^{13}C NMR spectrum of compound **10**

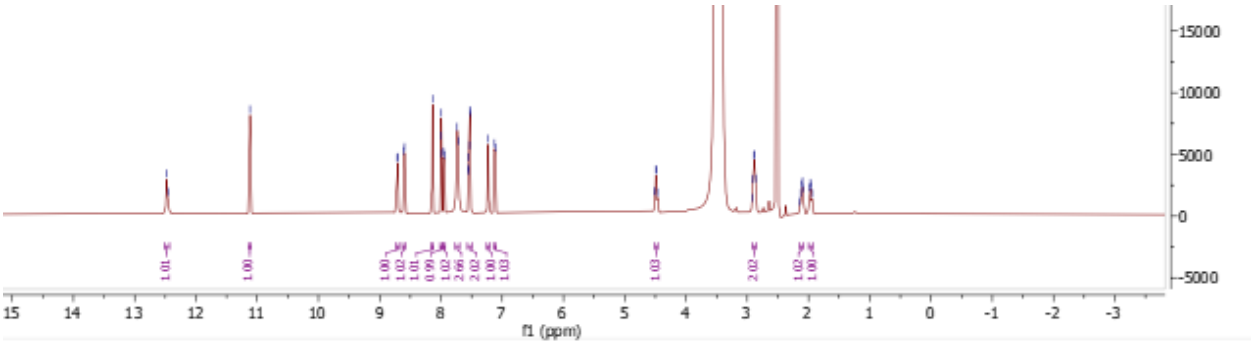

Figure S23 [1]H NMR spectrum of compound **11**

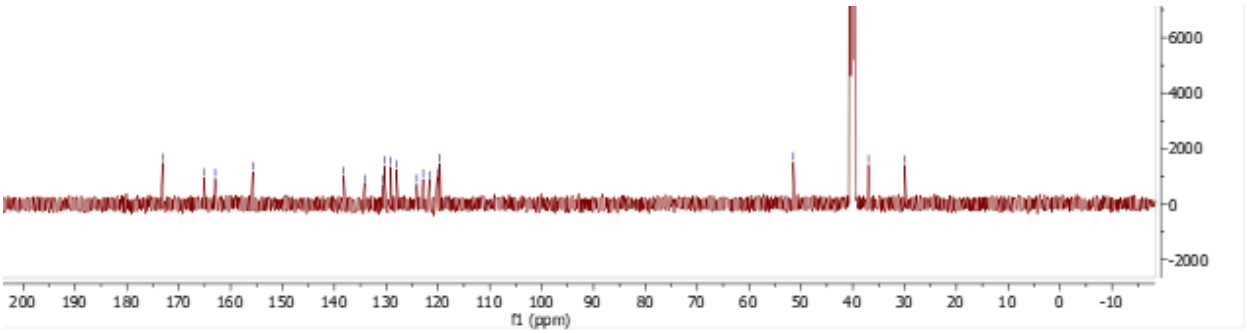

Figure S24 [13]C NMR spectrum of compound **11**

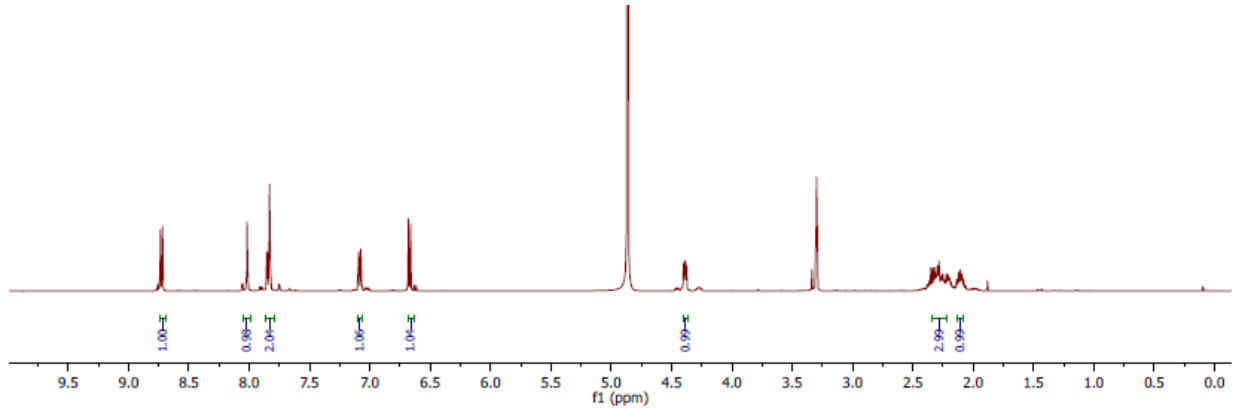

Figure S25 [1]H NMR spectrum of compound **12**

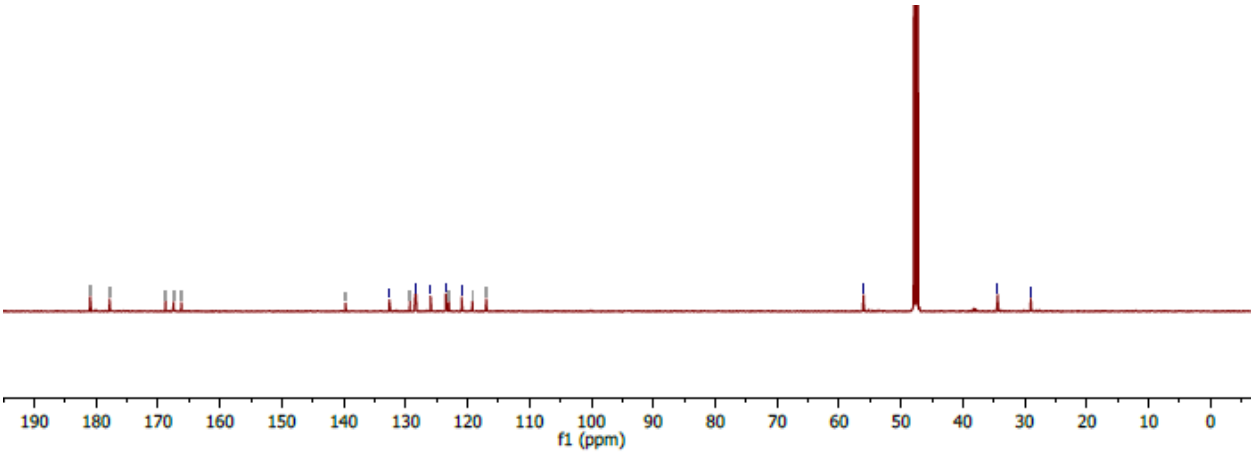

Figure S26 ^{13}C NMR spectrum of compound **12**

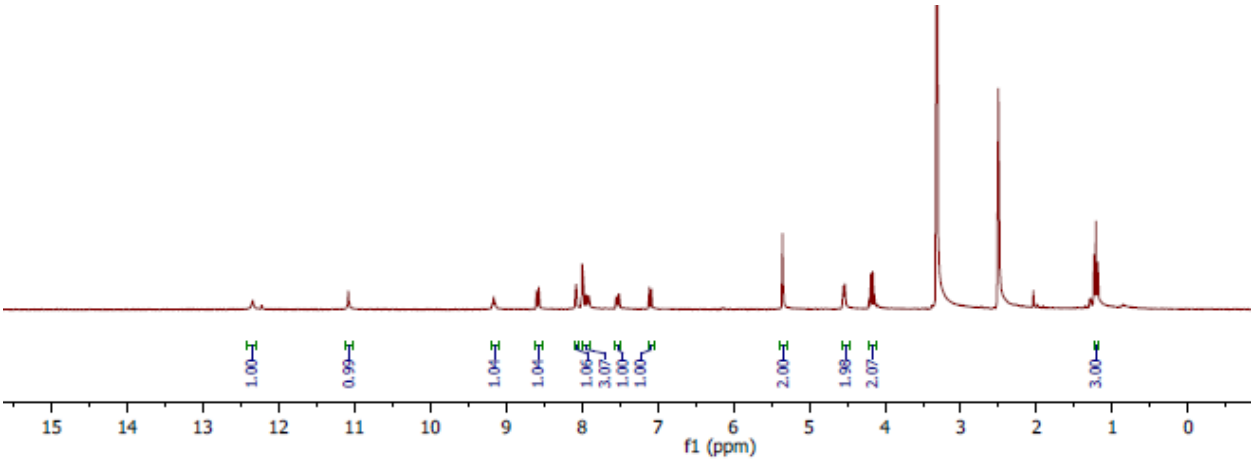

Figure S27 ^{1}H NMR spectrum of compound **14**

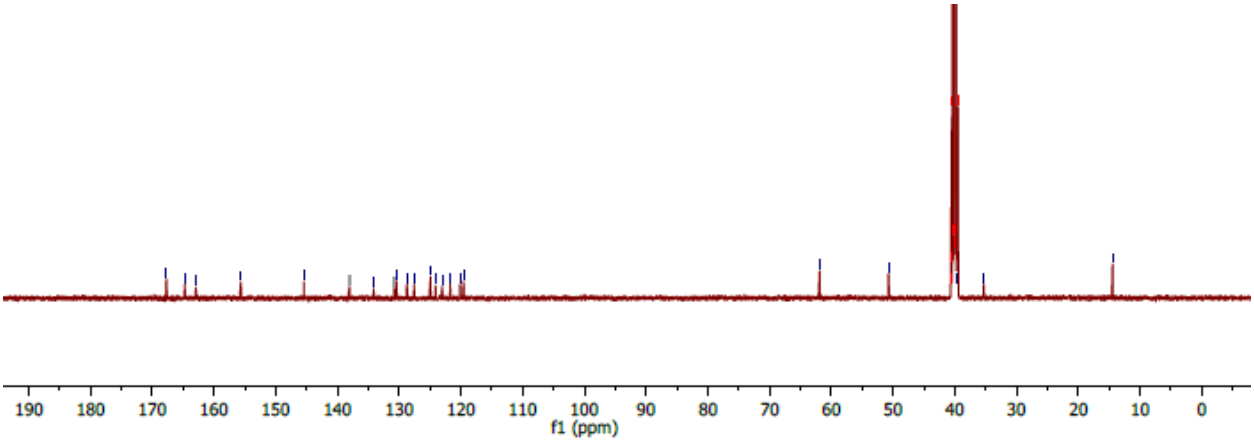

Figure S28 ^{13}C NMR spectrum of compound **14**

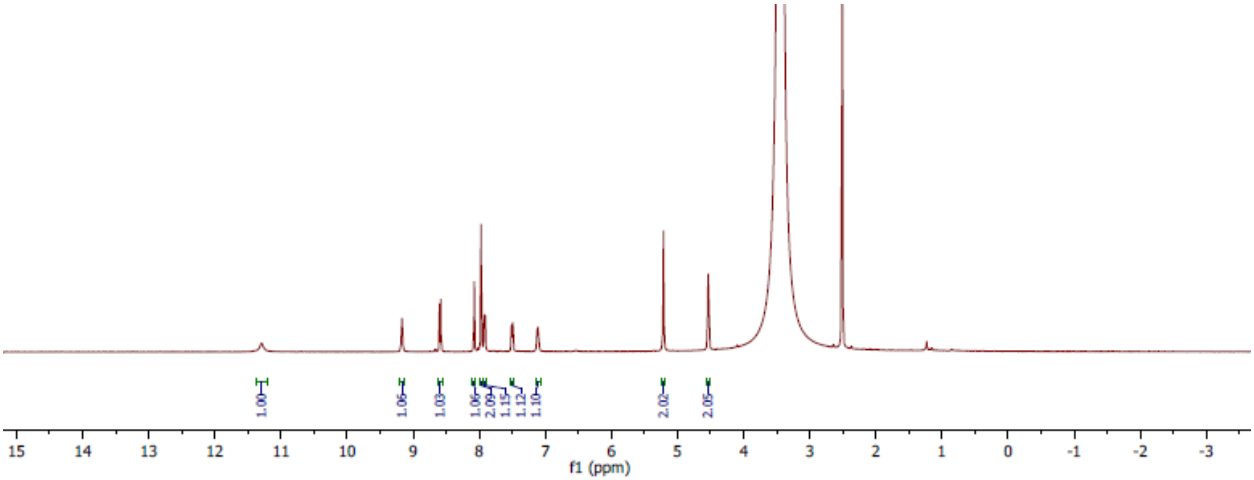

Figure S29 ^{1}H NMR spectrum of compound **15**

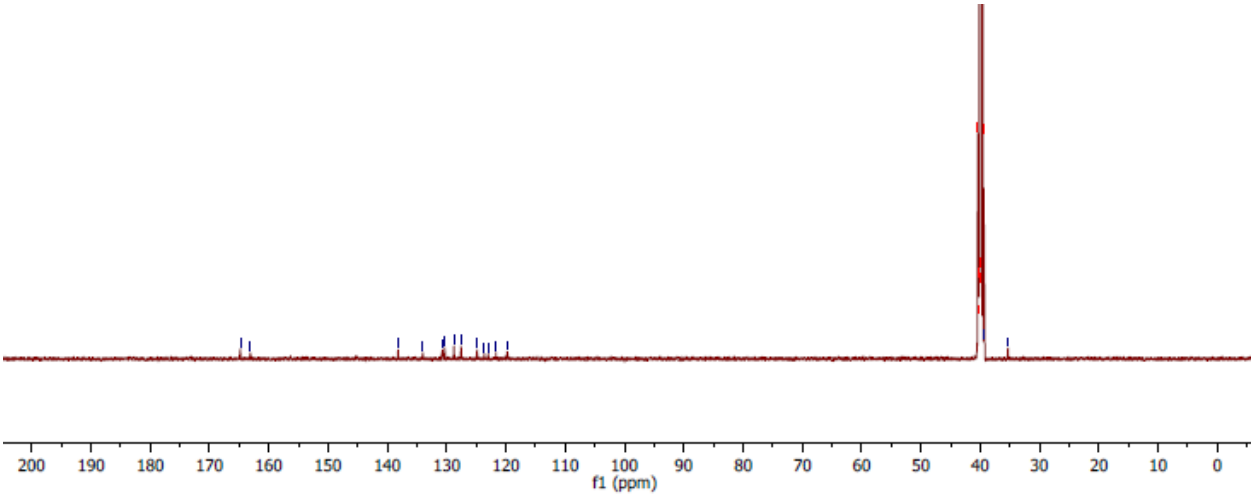

Figure S30 ^{13}C NMR spectrum of compound **15**

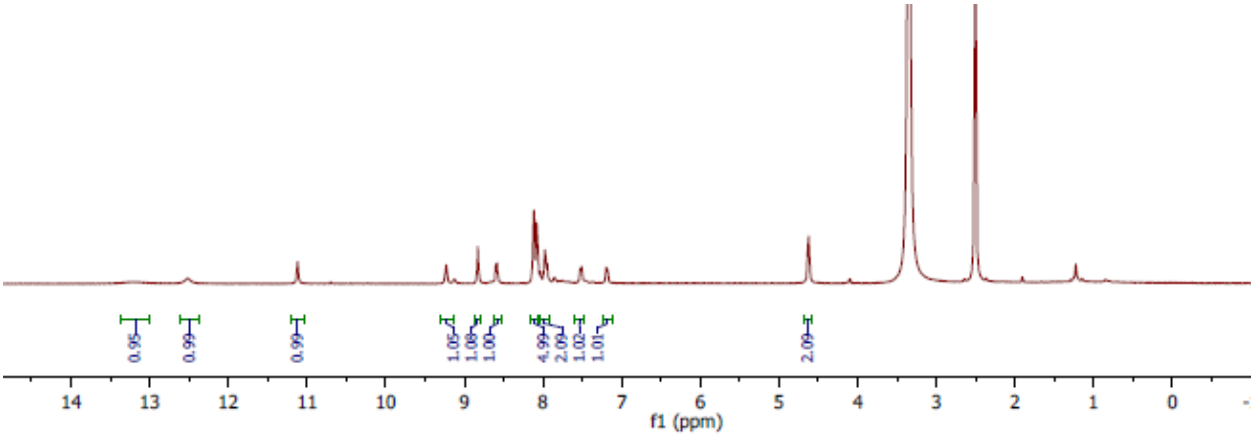

Figure S31 ^{1}H NMR spectrum of compound **16**

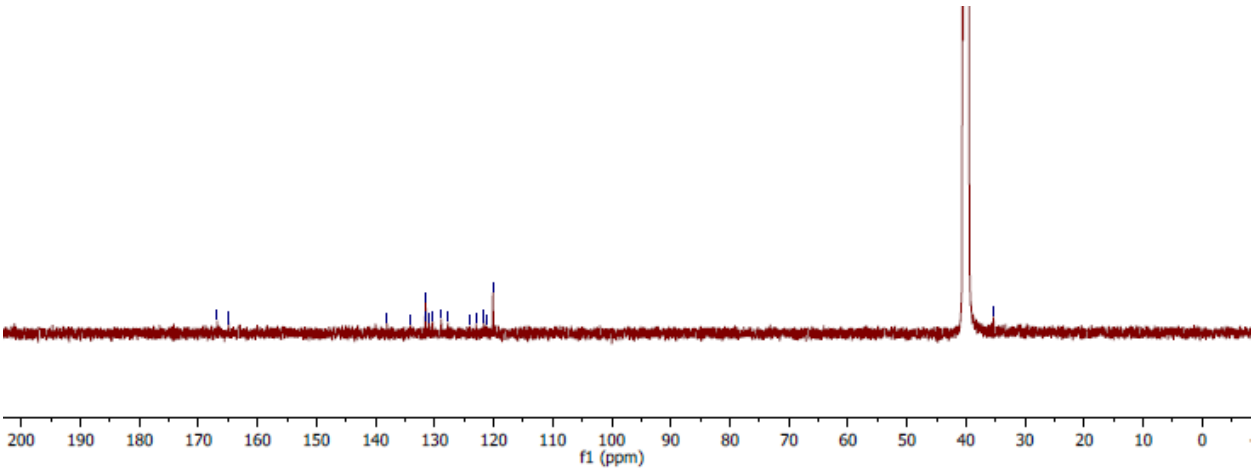

Figure S32 ^{13}C NMR spectrum of compound **16**

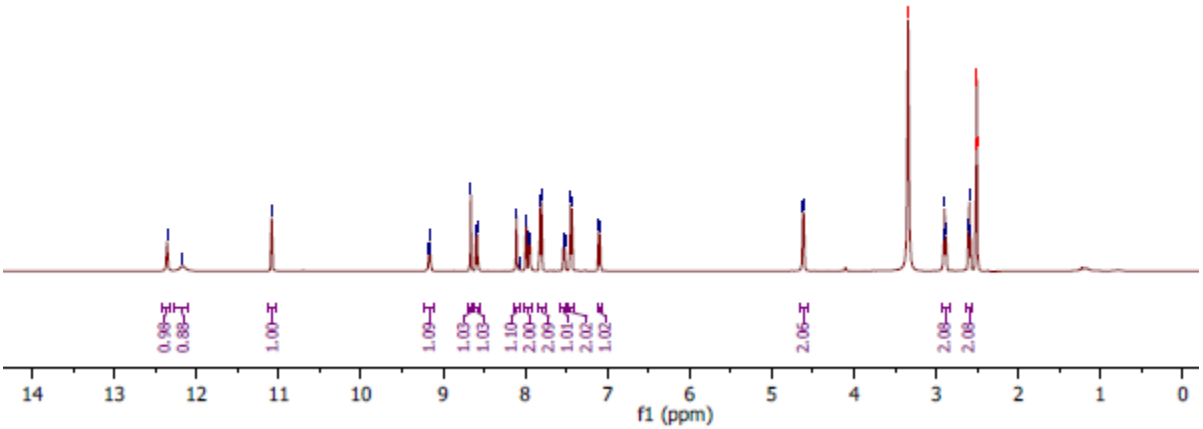

Figure S33 [1]H NMR spectrum of compound **17**

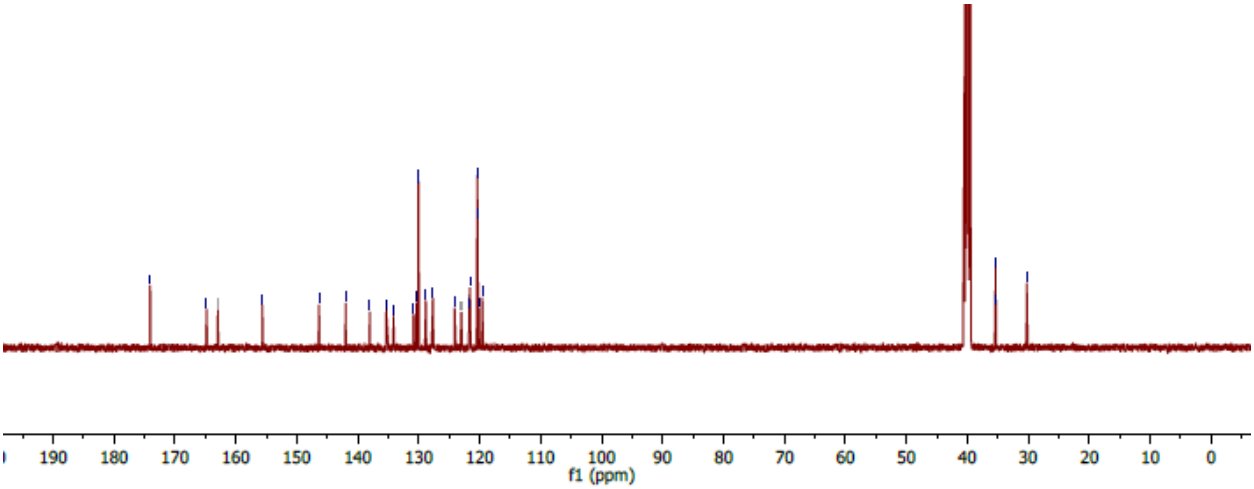

Figure S34 [13]C NMR spectrum of compound **17**

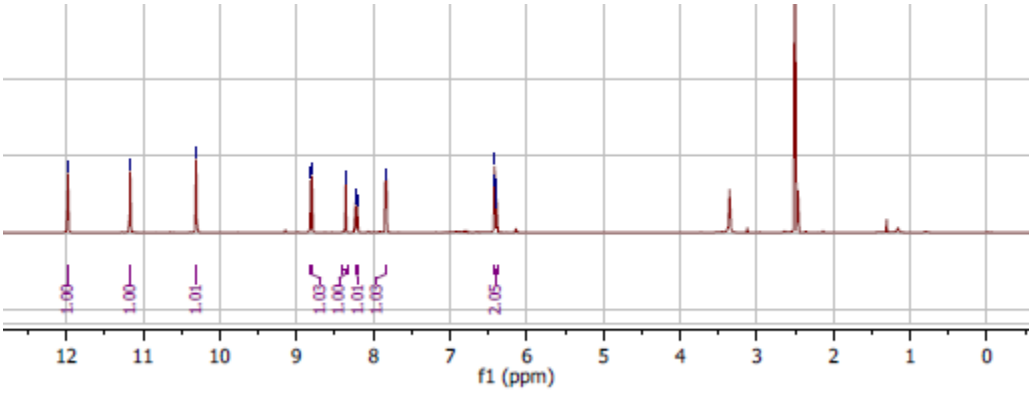

Figure S35 [1]H NMR spectrum of compound **18**

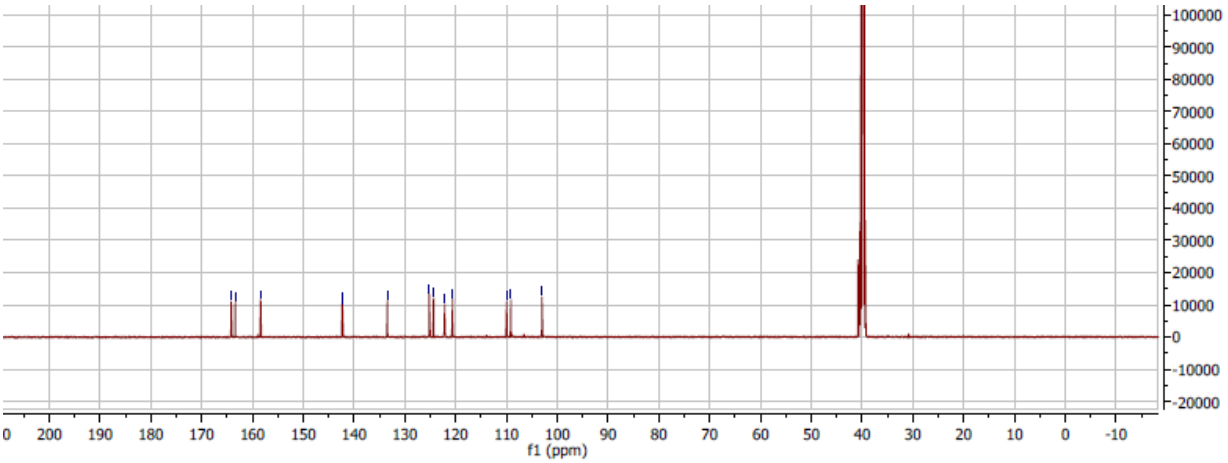

Figure S36 ^{13}C NMR spectrum of compound **18**

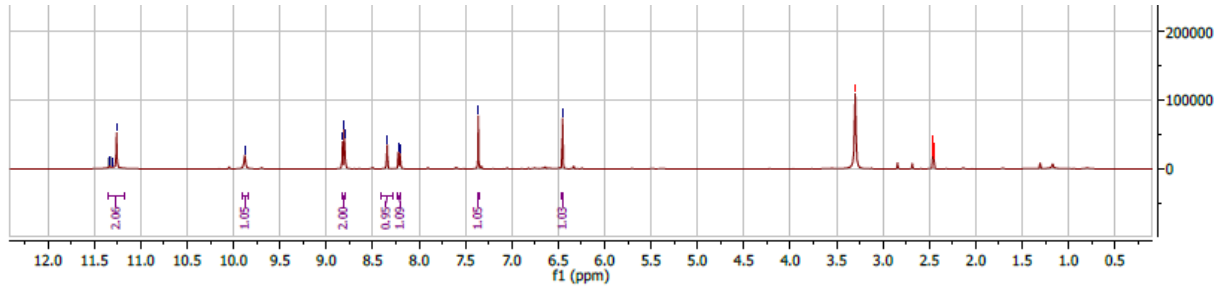

Figure S37 ^{1}H NMR spectrum of compound **19**

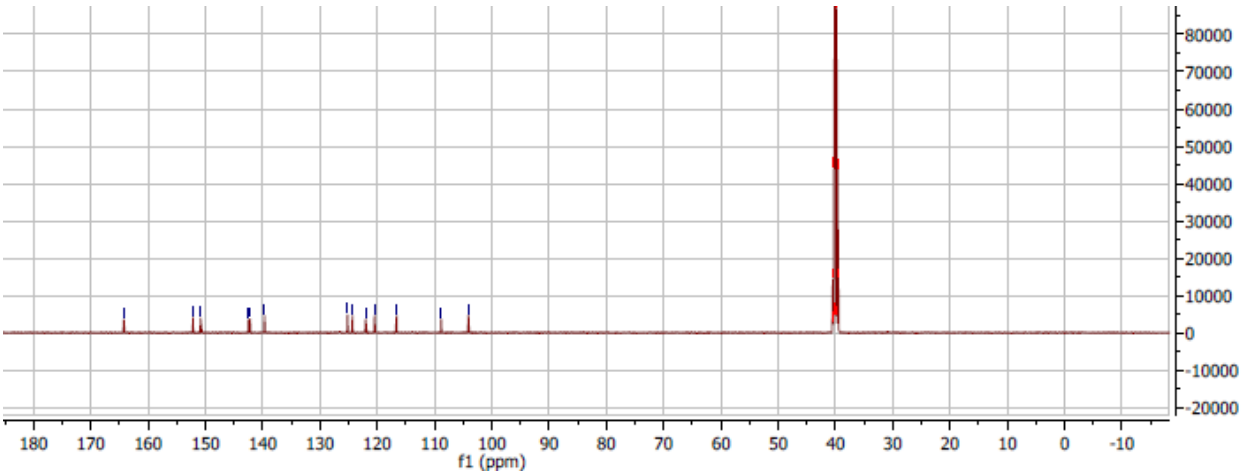

Figure S38 ^{13}C NMR spectrum of compound **19**

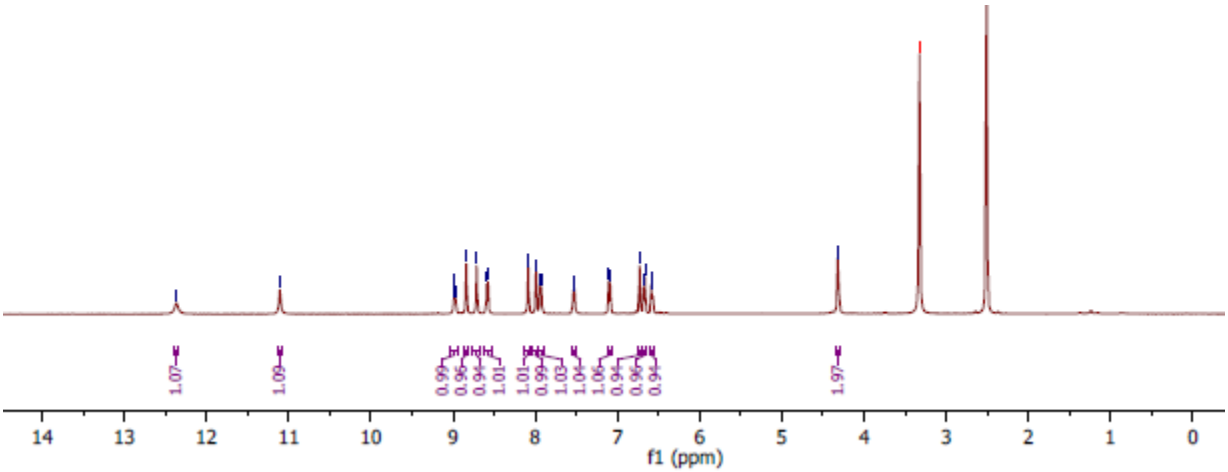

Figure S39 [1]H NMR spectrum of compound **20**

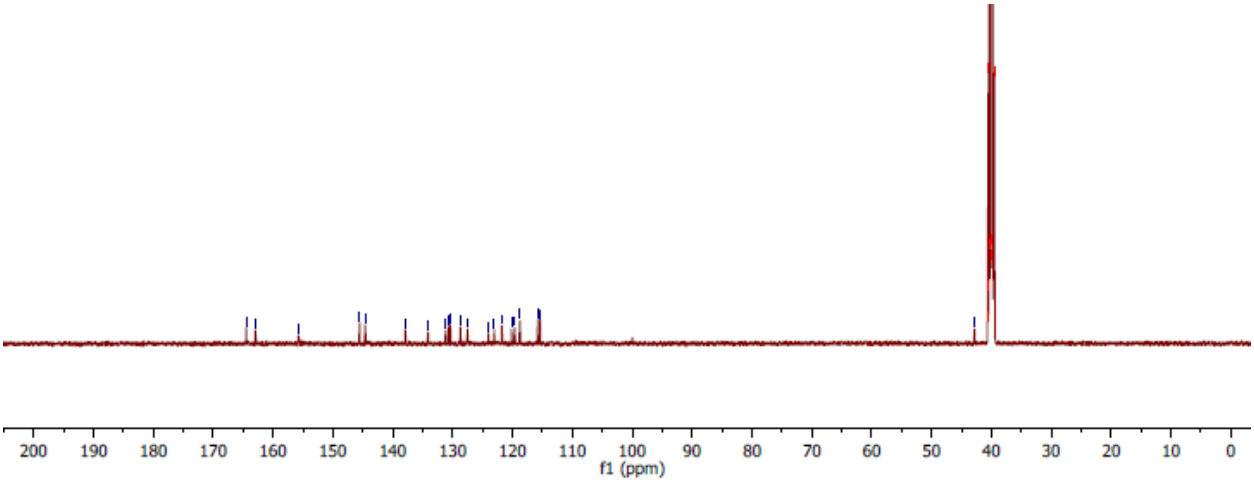

Figure S40 [13]C NMR spectrum of compound **20**

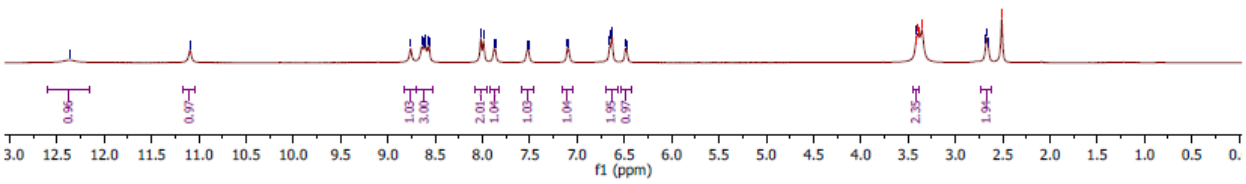

Figure S41 [1]H NMR spectrum of compound **21**

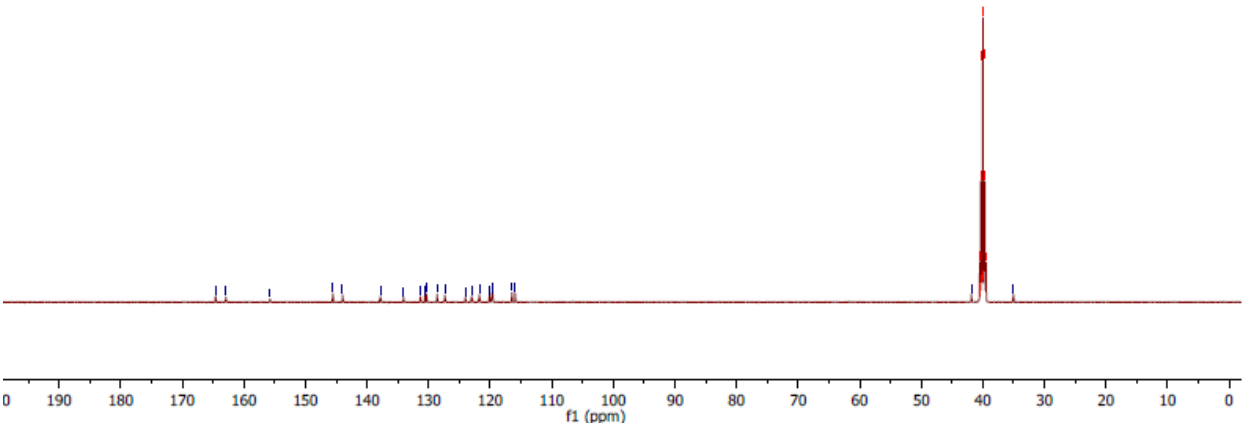

Figure S42 ^{13}C NMR spectrum of compound **21**

Extended Biological Data

Table S1 Minimum inhibitory concentration (MIC) in μg/mL of compounds **1-21** against 4 colistin-resistant strains of GNB. KP = *Klebsiella pneumoniae,* EC = *Escherichia coli*.

Compound	KP113250	KP113254	EC94393	EC94474
1	>128	>128	>128	>128
2	>128	>128	>128	>128
3	>128	>128	>128	>128
4	>128	>128	>128	>128
5a	>128	>128	>128	>128
5b	>128	>128	>128	>128
6	>128	>128	>128	>128
7	>128	>128	>128	>128
8	>128	>128	>128	>128
9	>128	>128	>128	>128
10	>128	>128	>128	>128
11	>128	>128	>128	>128
12	>128	>128	>128	>128
14	>128	>128	>128	>128
15	>128	>128	>128	>128
16	>128	>128	>128	>128
17	>128	>128	>128	>128
18	>128	>128	>128	>128
19	>128	>128	>128	>128
20	>128	>128	>128	>128
21	>128	>128	>128	>128

Table S2. Colistin minimum inhibitory concentration (MIC) in combination with 4 μM of compound **5b** and niclosamide against 4 colistin-resistant strains of GNB. KP = *Klebsiella pneumoniae,* EC = *Escherichia coli*.

	Colistin MIC with 4 μM compound (μg/mL)			
Compound	**KP113250**	**KP113254**	**EC94393**	**EC94474**
Niclosamide	0.25	0.5	0.25	0.5
5b	256	256	8	16
Colistin alone	256	256	8	16

APPENDIX B:
Supplementary materials for Chapter 5

Supplementary information for Chapter 5: A Niclosamide-Tobramycin hybrid adjuvant potentiates cefiderocol against *P. aeruginosa*

Contents

NMR spectra

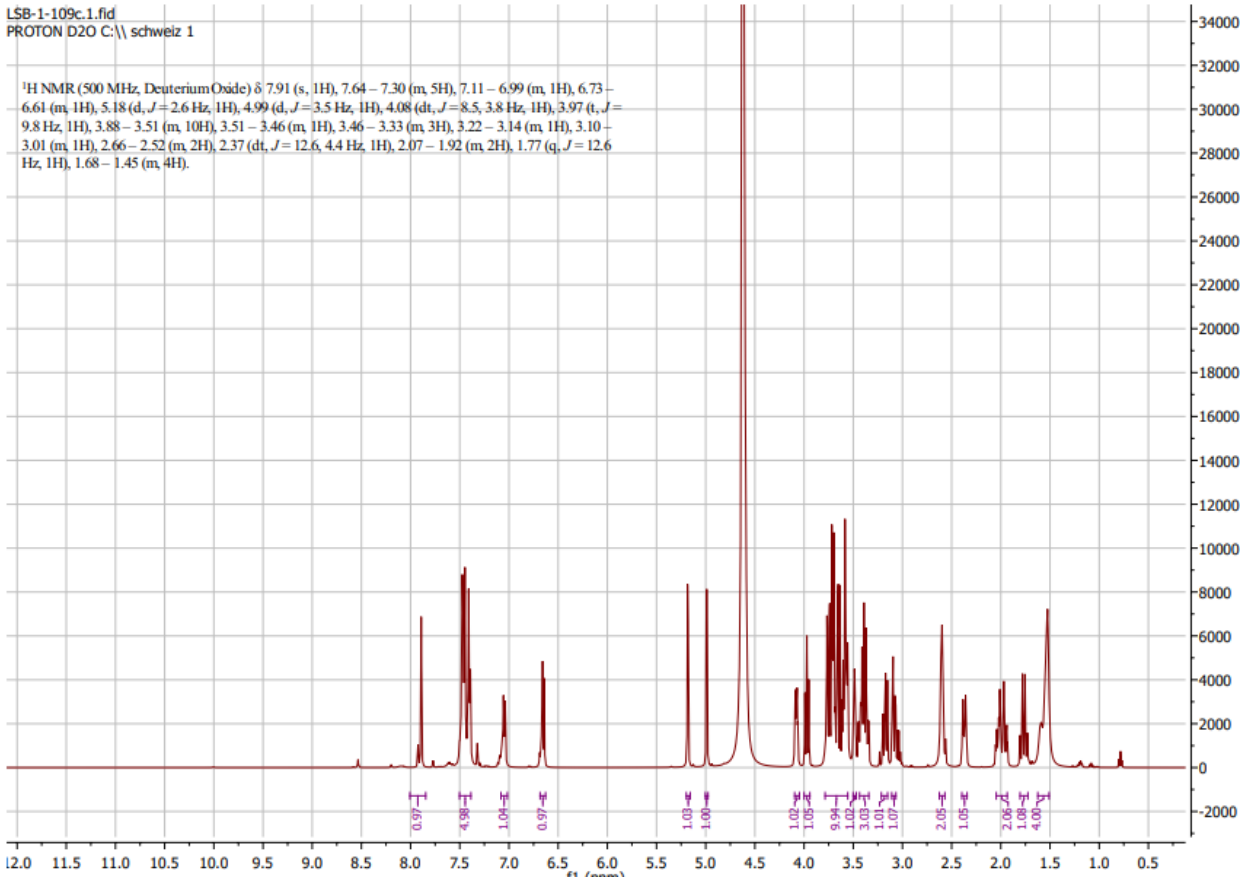

Figure S1. Hybrid **7** ^{1}H NMR spectrum

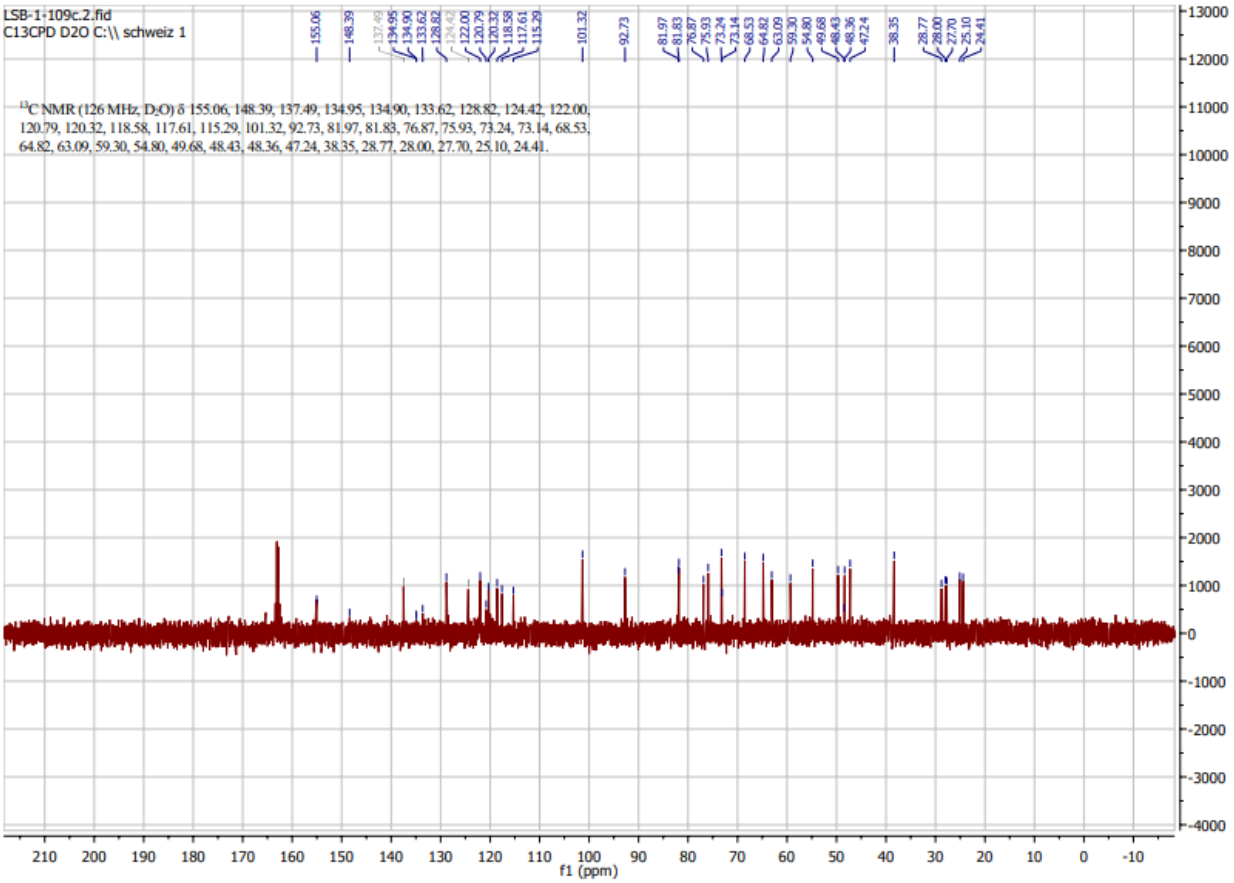

Figure S2. Hybrid **7** ^{13}C NMR spectrum

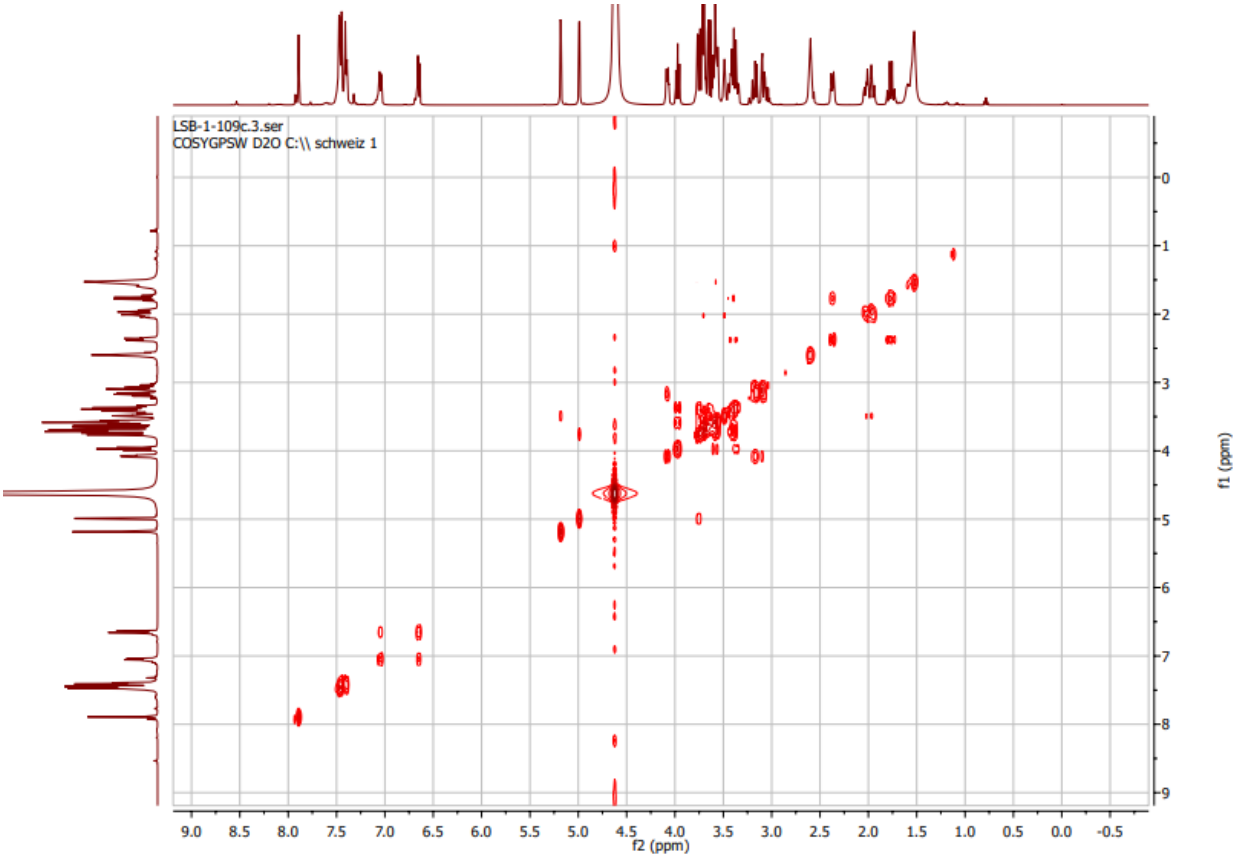

Figure S3. Hybrid **7** COSY NMR spectrum

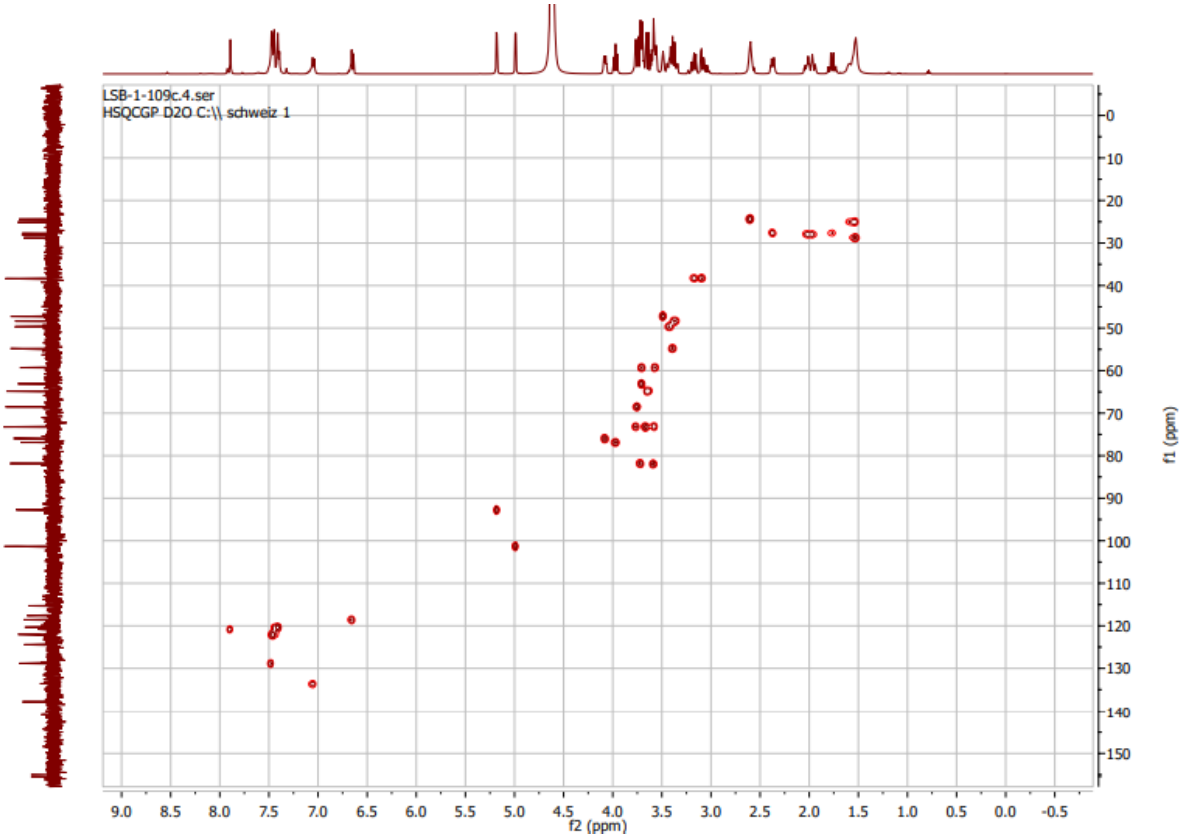

Figure S4. Hybrid **7** HSQC NMR spectrum

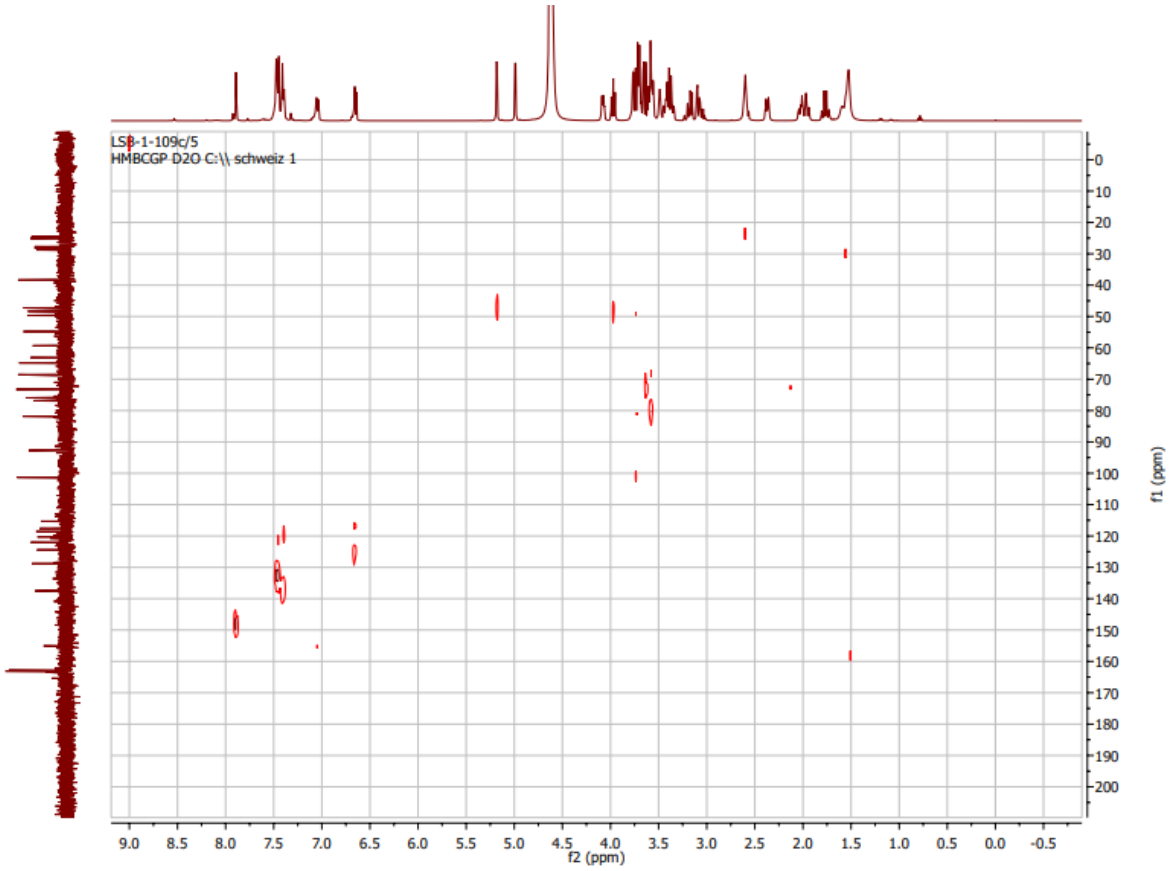

Figure S5. Hybrid **7** HMBC NMR spectrum

Biological Data

Table S1. Activity of niclosamide and niclosamide-azide analog (**3**) against Gram-negative and Gram-positive bacteria

Strain	**Minimum Inhibitory Concetration** (μg/ml)

	Niclosamide	**3**
PAO1	512	>256
A. baumannii ATCC 17978	512	>256
E. coli ATCC 25922	1024	>256
S. aureus ATCC 29213	1	2
MRSA ATCC 33592	≤0.25	1
MRSE 61589	≤0.25	0.5
E. faecalis ATCC 29212	2	64
E. faecium ATCC 27270	2	16

Table S2. Checkerboard studies of colistin and **3** against wild-type *P. aeruginosa* PAO1 and colistin-resistant clinical isolates

Strain	$MIC_{Colistin}$	MIC_{Combi}	MIC_3	MIC_{Combi}	FIC index	Interpretation
PAO1	1	0.125	>256	1	0.063<x<0.067	Synergy
PA91433	16	0.25	>256	1	0.016<x<0.019	Synergy
K. pneumoniae 113250	256	0.25	>256	2	0.002<x<0.010	Synergy

K. pneumoniae 113254	256	0.5	>256	1	0.002<x<0.006	Synergy
E. coli 94393	4	0.015625	>256	4	0.004<x<0.020	Synergy
E. coli 94474	16	0.25	>256	2	0.016<x<0.018	Synergy

Table S3. Potentiation of antibiotics with adjuvant **7** against *P. aeruginosa* PAO1 in MHB

Drug	MIC_{Drug}	MIC at 8 ug/ml of **7**	Potentiation at 8 ug/ml of **7**
Moxifloxacin	1	0.25	4
Ciprofloxacin	0.25	0.125	2
Vancomycin	256	64	4
Tobramycin	2	2	1
Colistin	1	1	1
Niclosamide	512	0.5	1024
Piperacillin	8	4	2
Cefotaxime	16	8	2
Ceftazidime	4	1	4
Cefiderocol	0.125	0.0313	4
Ceftolozane	0.5	0.125	4
Aztreonam	4	0.5	8
Minocycline	16	2	8
Doxycycline	8	1	8

Rifampicin	16	1	16
Chloramphenicol	32	2	16
Erythromycin	256	16	16
Novobiocin	1024	16	64
Fosfomycin	64	32	2
Linezolid	1024	64	16
Clindamycin	1024	256	64
Pleuromutilin	512	128	4
Trimethoprim	128	16	4
Sulfamethoxazole	256	64	4
Cotrimoxazole	2:38	0.25:4.75	4

Table S4. Potentiation of antibiotics with adjuvant **7** against *A. baumannii* ATCC 17978 in MHB

Drug	MIC_{Drug}	MIC at 8 ug/ml of **7**	Potentiation at 8 ug/ml of **7**
Moxifloxacin	0.0313	0.033	1
Ciprofloxacin	1	1	1
Vancomycin	128	128	1
Tobramycin	1	1	1
Colistin	0.5	0.5	1
Niclosamide	512	2	256
Piperacillin	64	64	1
Cefotaxime	16	16	1
Ceftazidime	4	1	4
Cefiderocol	1	0.5	2
Ceftolozane	2	2	1
Aztreonam	64	32	2
Minocycline	0.25	0.25	1
Doxycycline	0.125	0.125	1

Rifampicin	2	1	2
Chloramphenicol	128	64	2
Erythromycin	16	8	2
Novobiocin	8	2	4
Fosfomycin	128	128	1
Linezolid	256	128	2
Clindamycin	512	256	2
Pleuromutilin	1024	128	8
Trimethoprim	64	64	1
Sulfamethoxazole	>608	>608	1
Cotrimoxazole	32:608	32:608	1

Table S5. Potentiation of antibiotics with adjuvant **7** against *E. coli* ATCC 25922 in MHB

Drug	MIC_{Drug}	MIC at 8 ug/ml of **7**	Potentiation at 8 ug/ml of **7**
Moxifloxacin	0.016	0.008	2
Ciprofloxacin	0.016	0.004	4
Vancomycin	128	16	8
Tobramycin	2	1	2
Colistin	0.25	0.125	2
Niclosamide	512	1	512
Piperacillin	2	0.25	8
Cefotaxime	0.25	0.0313	8

Ceftazidime	0.25	0.063	4
Cefiderocol	0.125	0.063	2
Ceftolozane	1	0.5	2
Aztreonam	0.25	0.063	4
Minocycline	1	0.25	4
Doxycycline	0.5	0.25	2
Rifampicin	4	0.031	128
Chloramphenicol	4	1	4
Erythromycin	32	1	32
Novobiocin	32	0.5	64
Fosfomycin	16	16	1
Linezolid	128	32	4
Clindamycin	64	4	16
Pleuromutilin	64	8	8
Trimethoprim	256	1	256
Sulfamethoxazole	304	76	4
Cotrimoxazole	8:152	0.5:9.5	16

Table S6. Neither niclosamide nor tobramycin alone potentiate cefiderocol against wild-type *P. aeruginosa* PAO1 in MHB

$Drug_1$	MIC_{Drug1}	MIC_{Combi}	$Drug_2$	MIC_{Drug2}	MIC_{Combi}	FIC index
Cefiderocol	0.125	0.125	Tobramycin	1	0.5	1.5
Cefiderocol	0.125	0.125	Niclosamide	512	0.25	$1.031<x<1.063$

Table S7. Checkerboard studies of cefotaxime and **7** against wild-type and multidrug-resistant *P. aeruginosa* strains in MHB

Strain	MIC_{Drug}	MIC_{Combi}	$MIC_{Adjuvant}$	MIC_{Combi}	FIC index
PAO1	16	4	64	16	0.5
PA259	2048	1024	>128	1	0.5<x<0.508
PA260	1024	128	>128	8	0.125<x<0.188
PA264	2048	1024	>128	16	0.5<x<0.625

Table S8. Checkerboard studies of ceftazidime and **7** against wild-type and multidrug-resistant *P. aeruginosa* strains in MHB

Strain	MIC_{Drug}	MIC_{Combi}	$MIC_{Adjuvant}$	MIC_{Combi}	FIC index
PAO1	4	0.5	64	16	0.375
PA259	512	256	>128	0.25	0.5<x<0.502
PA260	64	16	>128	8	0.25<x<0.313
PA264	128	32	>128	2	0.25<x<0.266

Table S9. Checkerboard studies of ceftolozane and **7** against wild-type and multidrug-resistant *P. aeruginosa* strains in MHB. ND = Not determined

Strain	MIC_{Drug}	MIC_{Combi}	$MIC_{Adjuvant}$	MIC_{Combi}	FIC index
PAO1	0.5	0.125	64	1	0.266

PA259	>16	ND	>128	ND	ND
PA260	1	0.5	>128	16	0.5<x<0.625
PA264	2	2	>128	0.25	1<x<1.002

Table S10. Checkerboard studies of cefiderocol and **7** against wild-type and multidrug-resistant *P. aeruginosa* strains in ID-CAMHB

Strain	MIC_{Drug}	MIC_{Combi}	$MIC_{Adjuvant}$	MIC_{Combi}	FIC index	Interpretation	Potentiation at 8 µg/ml of adjuvant
PAO1	0.0313	0.008	64	2	0.281	Synergy	4
PA259	4	4	>128	0.5	1<x<1.002	Additive	1
PA260	0.063	0.063	>128	0.25	1<x<1.002	Additive	1

PA262	0.0313	0.0156	>128	0.25	0.5<x<0.502	Additive	2
PA264	0.0156	0.0156	>128	0.25	1<x<1.002	Additive	1

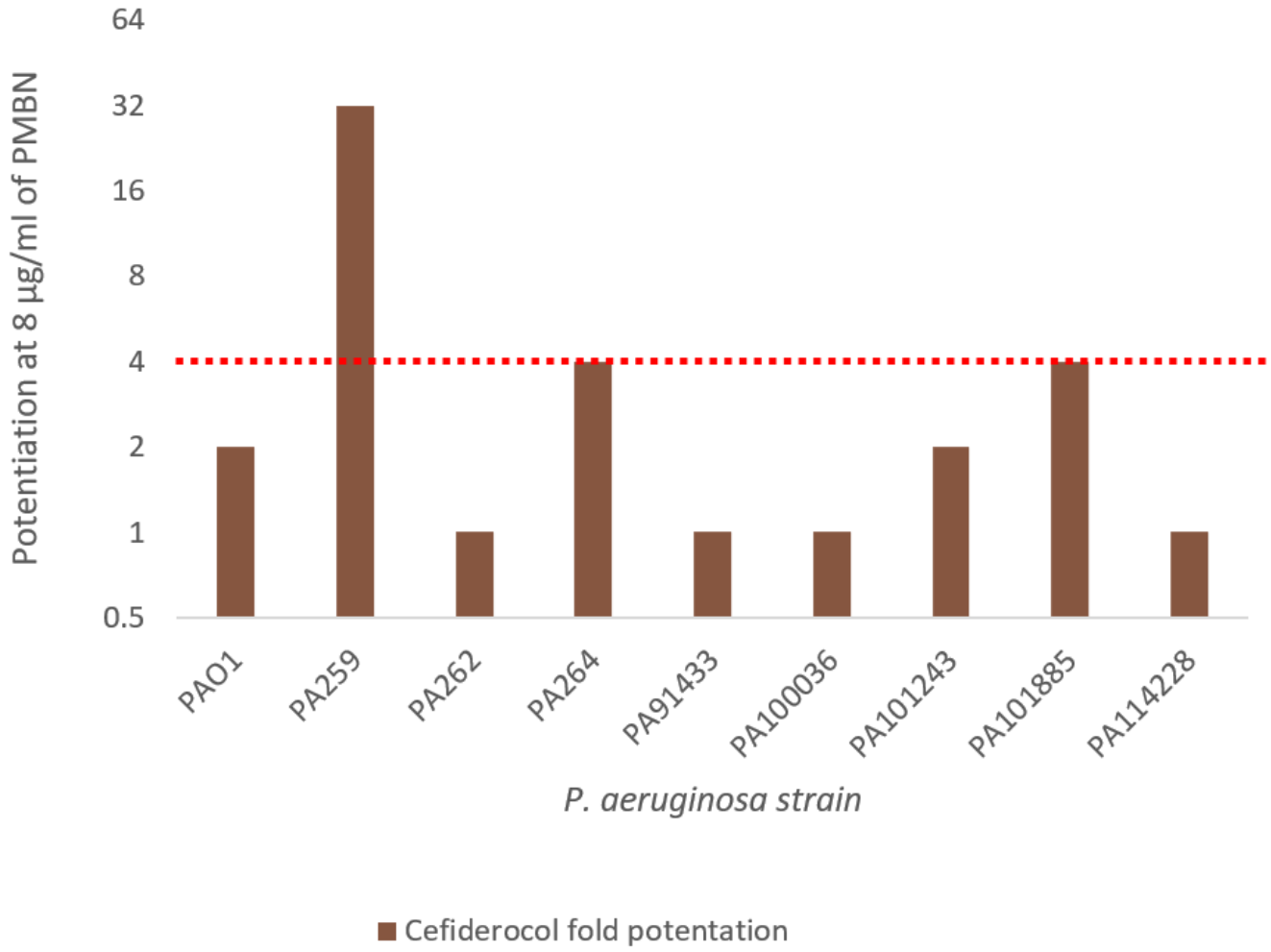

Figure S6. Fold potentiation of cefiderocol in combination with 8 µg/ml PMBN against wild-type and MDR clinical isolates of *P. aeruginosa* in MHB. Red dotted line denotes a 4-fold potentiation.

Table S11. MICs (in μg/mL) of various antibiotics against MDR clinical isolates.*

a) *Pseudomonas aeruginosa* isolates

P. aeruginosa	PTZ	A/C	AZT	FOX	CFZ	CTR	CPM	CTX	CAZ	IMI	MER	DOR	ETP	CIP	LEV	MOX	TOB	GEN	AMK	TGC	MIN	DOX	ERC
259-96918	64	>32	32	>32	>128	>64	>64	2048	512	32	1024	>1024	>32	>16	256	>16	256	>32	>64	32	32	32	8
262-101856	64	>32	32	>32	>128	64	32	128	16	32	32	16	>32	>16	64	>16	1024	>32	>64	32	64	1024	8
264-104354	256	>32	64	>32	>128	>64	32	2048	128	32	64	16	>32	>16	64	>16	128	>32	8	32	32	64	8
91433	64	>32	512	>32	>128	>64	16	1024	1024	32	16	16	>32	2	ND	16	16	32	>32	32	16	32	16
114228	ND	ND	>32	ND	ND	ND	ND	128	8	ND	8	8	ND	ND	ND	ND	2	ND	ND	ND	32	16	8

b) *Acinetobacter baumannii* isolates

A. baumannii	PTZ	FOX	CFZ	CPM	CTX	CAZ	C/T	IMI	MER	CIP	LEV	MOX	TOB	GEN	AMK	TGC	MIN	DOX	ERC	OMC
AB027	512	ND	>128	>128	>256	ND	>16	32	16	>16	8	8	ND	32	>64	4	0.25	ND	0.5	1
AB031	4	ND	>128	4	16	ND	>16	0.25	1	0.25	0.25	0.12	ND	<0.5	2	8	0.25	ND	0.25	2
LAC-4	ND	ND	ND	ND	8	>16	8	<1	<1	>4	2	ND	>4	>4	4	<4	4	<4	0.06	1
92247	<1	32	128	4	ND	ND	2	ND	4	≤0.06	ND	ND	ND	ND	<1	0.25	0.125	ND	ND	ND

c) *Escherichia coli* isolates

E. coli	PTZ	A/C	AZT	FOX	CFZ	CPM	CAZ	C/T	IMI	MER	ETP	CIP	LEV	MOX	TOB	GEN	AMK	TGC	MIN	DO
94393 (mcr-1 +)	≤1	4	≤0.12	4	1	≤0.25	≤0.25	0.25	0.25	≤0.03	≤0.03	0.5	1	1	≤0.5	≤0.5	2	0.25	2	4
94474 (mcr-1 +)	16	>32	≤0.12	16	4	≤0.25	0.5	0.5	0.25	≤0.03	≤0.03	>16	32	16	32	16	2	1	64	>32
107115	>512	>32	>64	>32	>128	>64	>32	>6	8	32	>32	>16	32	16	8	>32	2	0.25	32	>32

d) *Klebsiella pneumoniae* isolates

K. pneumoniae	PTZ	A/C	AZT	FOX	CFZ	CPM	CAZ	C/T	IMI	MER	ETP	CIP	LEV	MOX	TOB	GEN	AMK	TGC	MIN	DO
113250	4	4	≤0.12	1	1	1	0.5	2	0.25	≤0.03	≤0.03	≤0.06	0.125	≤0.06	≤0.5	≤0.5	≤1	ND	2	2
113254	<1	2	≤0.12	1	1	1	≤0.2	0.5	0.12	≤0.03	≤0.03	≤0.06	0.0625	≤0.06	≤0.5	≤0.5	≤1	ND	2	2
116381	8	16	16	16	>128	16	8	1	0.5	≤0.03	0.12	>16	128	>16	4	≤0.5	≤1	1	64	>2

e) *E cloacae* isolates

E. cloacae	PTZ	A/C	AZT	FOX	CFZ	CPM	CAZ	C/T	IMI	MER	ETP	CIP	MOX	TOB	GEN	AMK	TGC	MIN	DOX	ERC
117029	2	16	≤0.12	>32	>128	≤0.25	0.5	0.25	0.25	≤0.03	≤0.03	≤0.06	≤0.06	2	≤0.5	2	0.5	32	>32	0.5
118564	2	>32	≤0.12	>32	>128	0.25	0.5	ND	ND	0.12	ND	0.06	0.12	1	1	2	ND	ND	4	ND
121187	1	8	≤0.12	>32	32	0.25	0.5	ND	ND	0.06	ND	0.25	1	32	>32	1	ND	ND	>32	ND

* Complete susceptibility data was not available for all isolates used. PTZ: piperacillin-tazobactam, A/C: amoxicillin-clavulanic acid, AZT: aztreonam, FOX: cefoxitin, CFZ: cefazolin, CTR: ceftriaxone, CPM: cefepime, CTX: cefotaxime, CAZ: ceftazidime, C/T: ceftolozane-tazobactam, IMI: imipenem, MER: meropenem, DOR: doripenem, ETP: ertapenem, CIP: ciprofloxacin, LEV: levofloxacin, MOX: moxifloxacin, TOB: tobramycin, GEN: gentamicin, AMK: amikacin, TGC: tigecycline, MIN: minocycline, DOX: doxycycline, ERC: eravacycline, OMC: omadacyline, CST: colistin, CAM: chloramphenicol, ND: not determined.

APPENDIX C:
Supplementary materials for Chapter 6

Supplementary information for Chapter 6: Sulfonamide bioisosteres of niclosamide enhance antibacterial activity of colistin and bacitracin

Contents

NMR Spectra of compounds used for biological testing

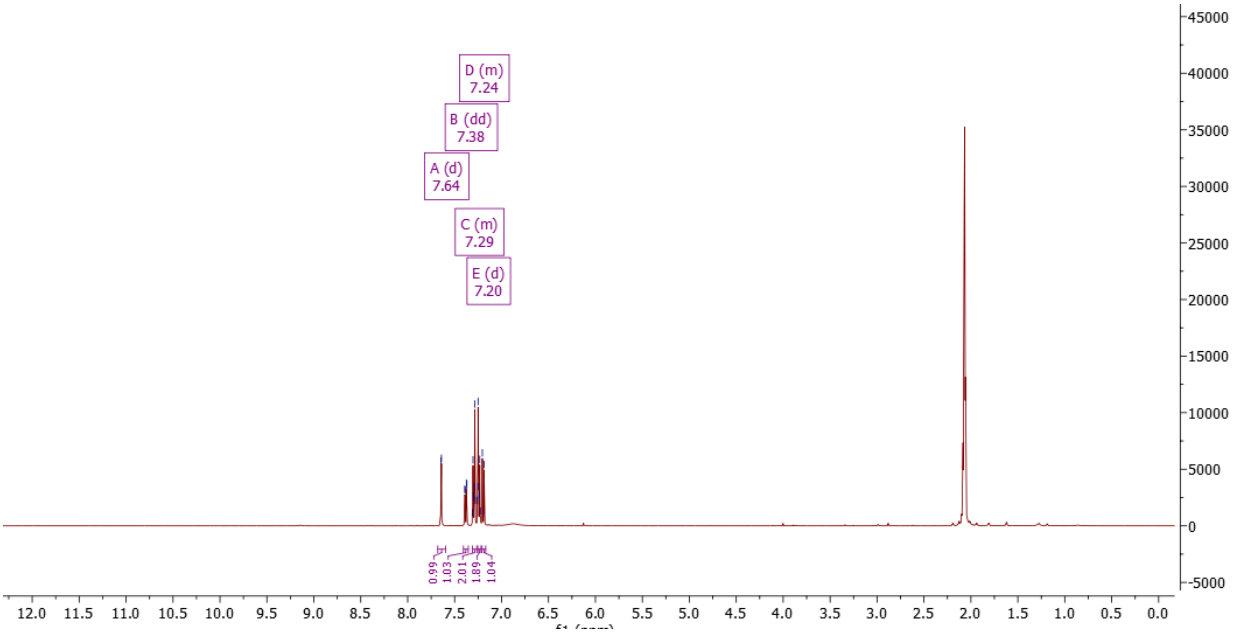

Figure S1 ^{1}H NMR spectrum of compound **1**

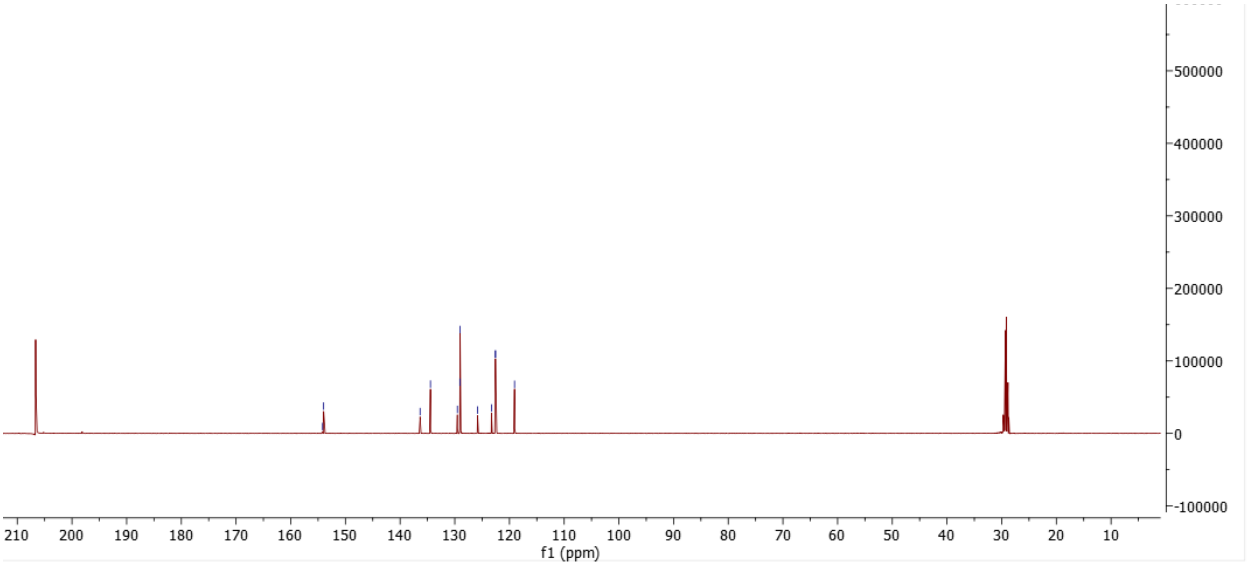

Figure S2 ^{13}C NMR spectrum of compound **1**

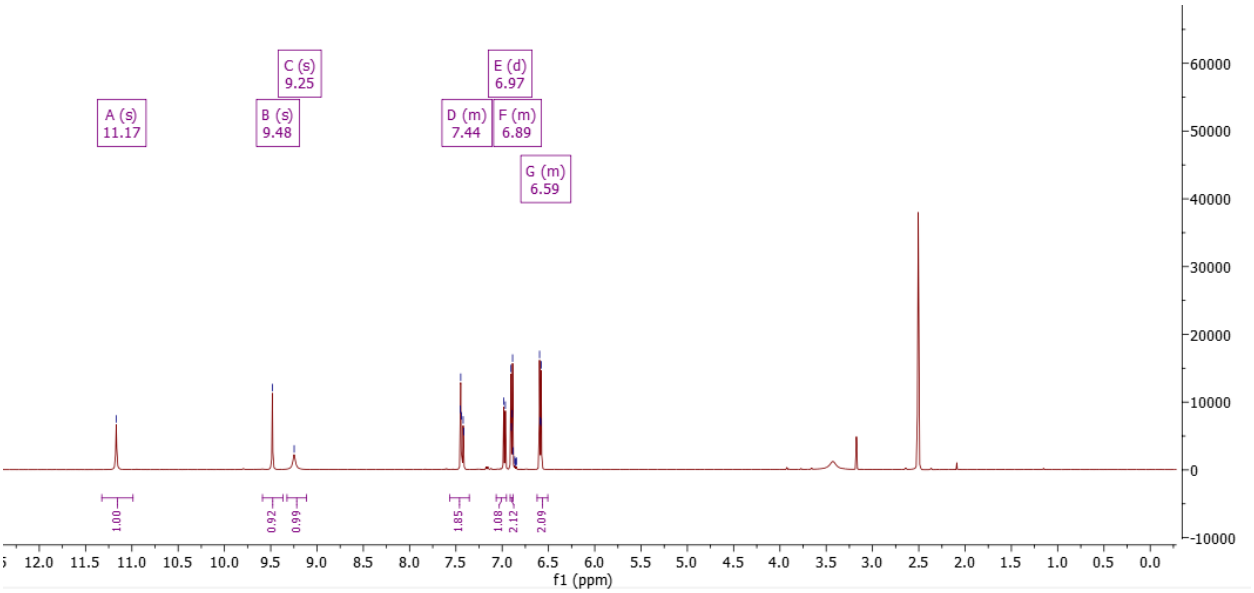

Figure S3 ^{1}H NMR spectrum of compound **2**

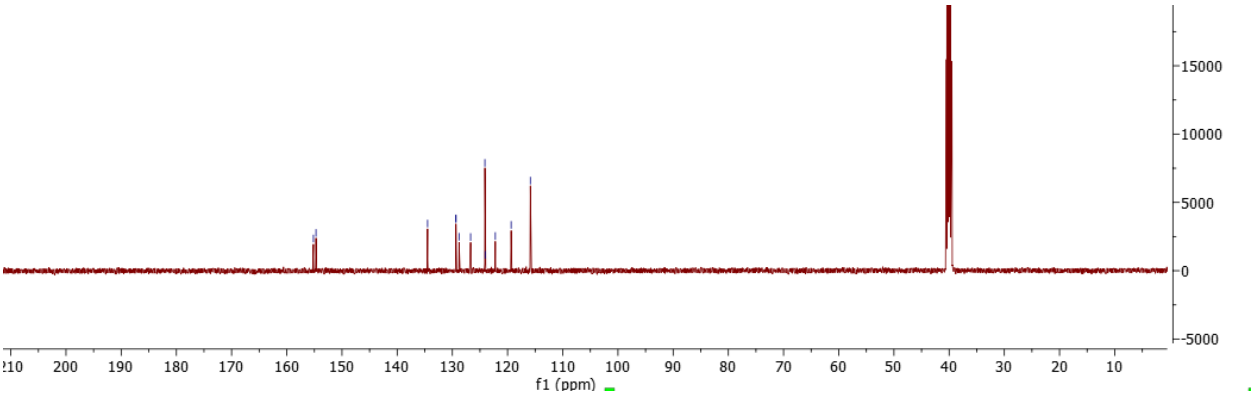

Figure S4 ^{13}C NMR spectrum of compound **2**

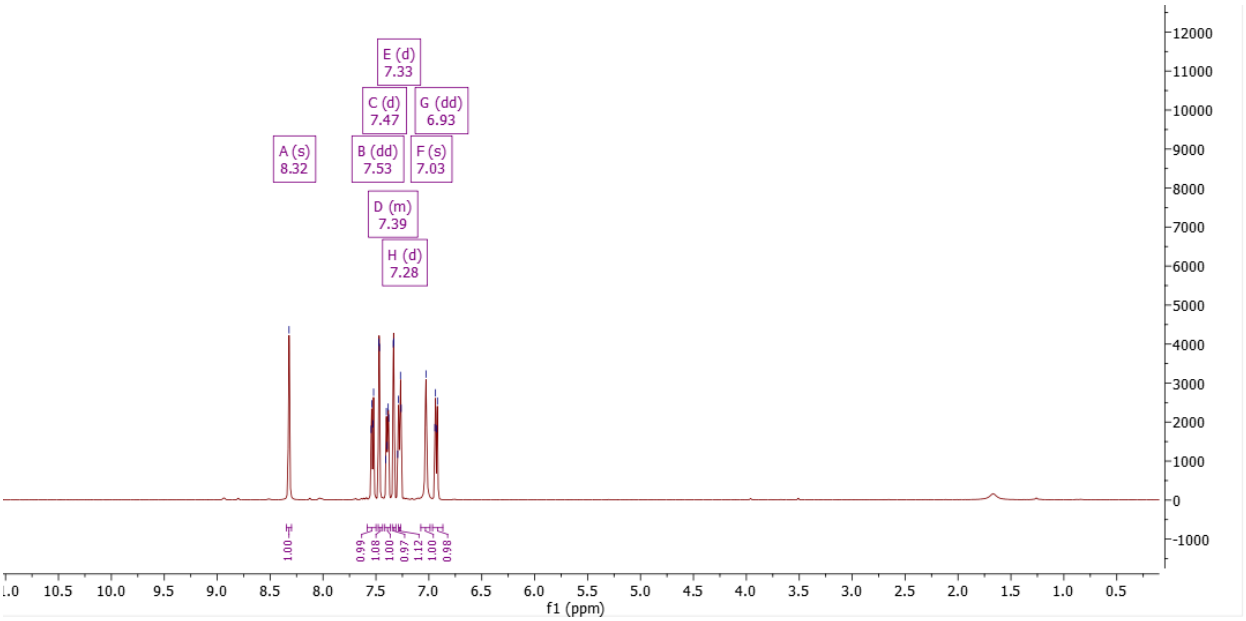

Figure S5 [1]H NMR spectrum of compound **3**

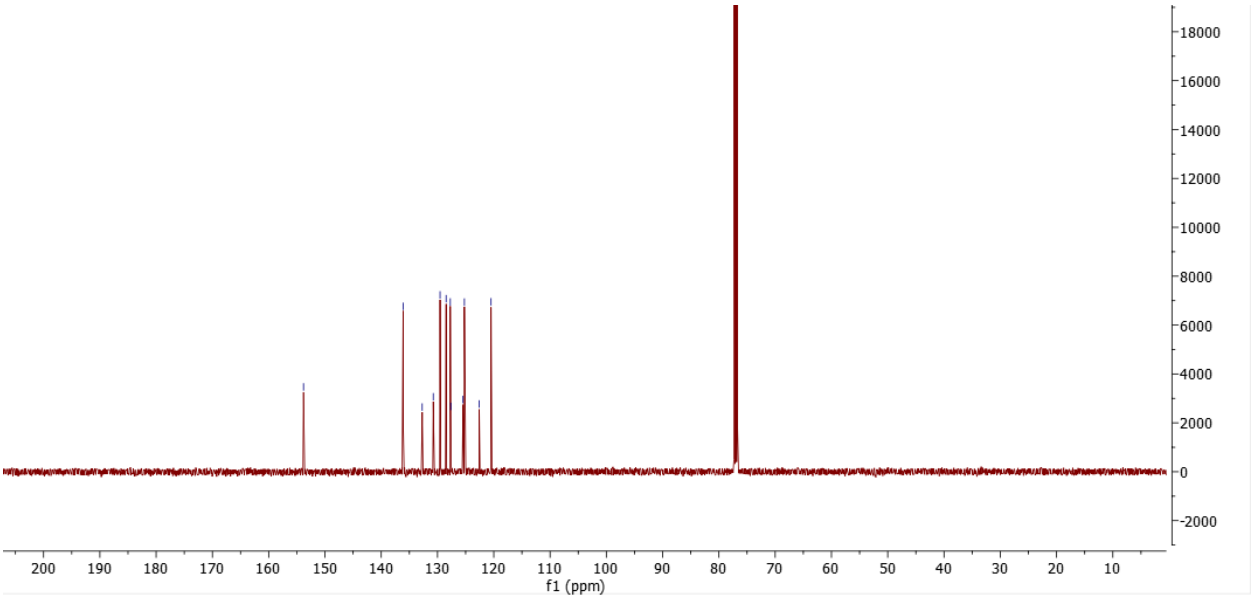

Figure S6 [13]C NMR spectrum of compound **3**

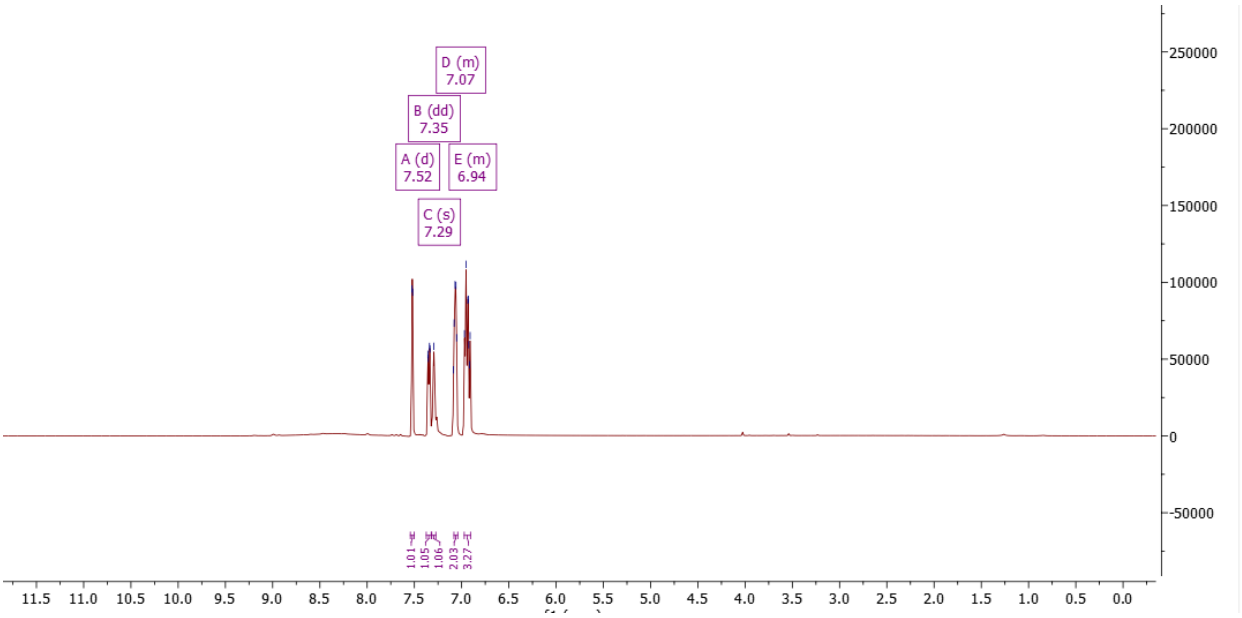

Figure S7 ^{1}H NMR spectrum of compound **4**

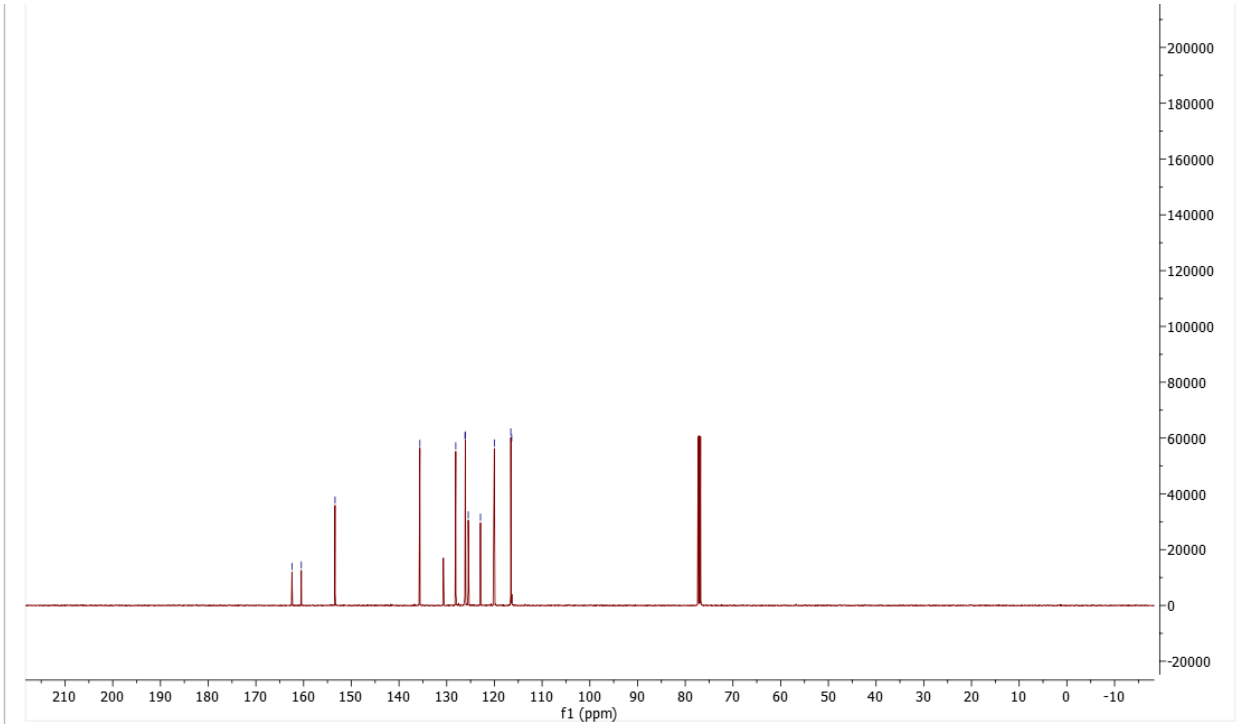

Figure S8 ^{13}C NMR spectrum of compound **4**

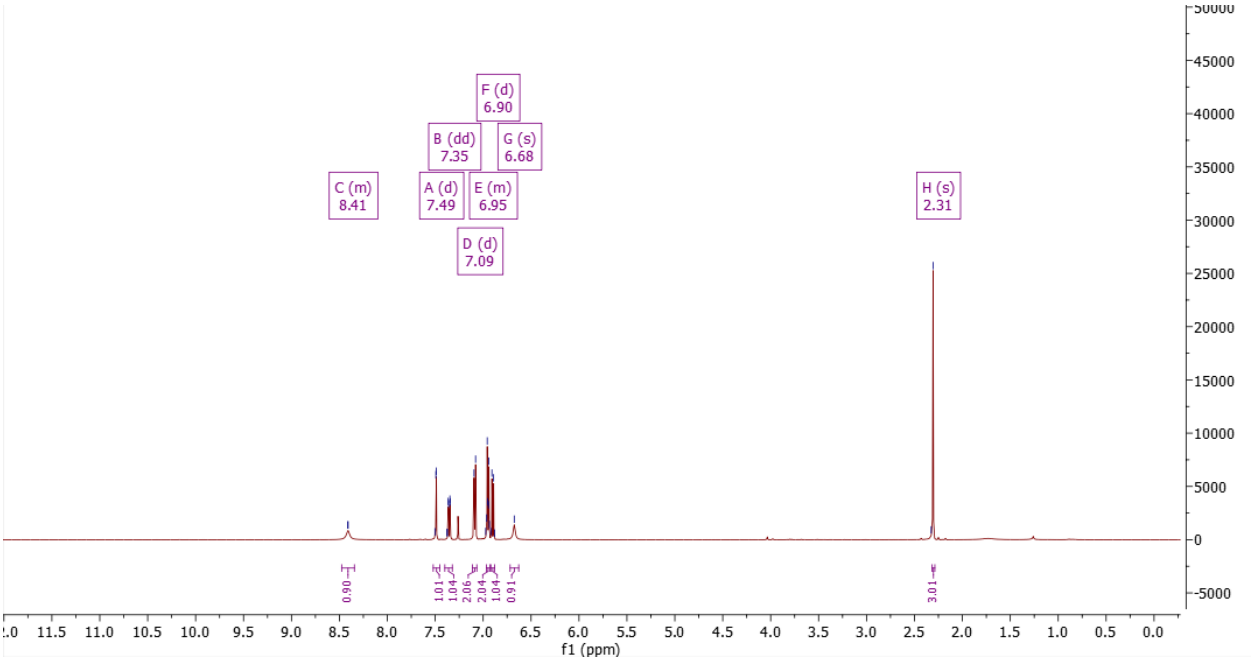

Figure S9 ^{1}H NMR spectrum of compound **5**

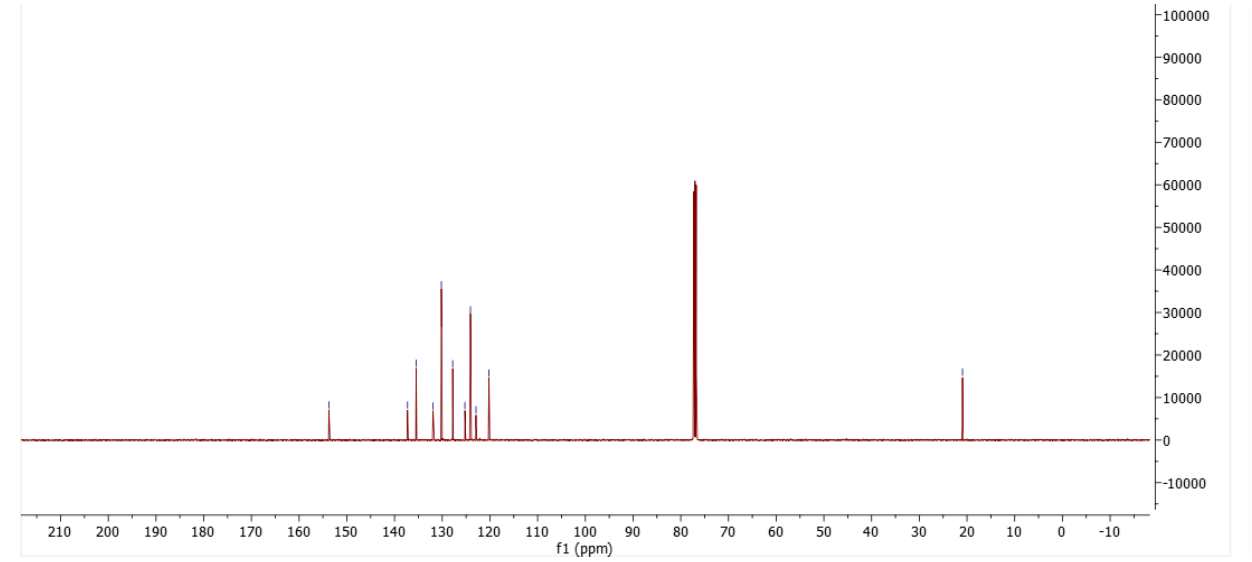

Figure S10 ^{13}C NMR spectrum of compound **5**

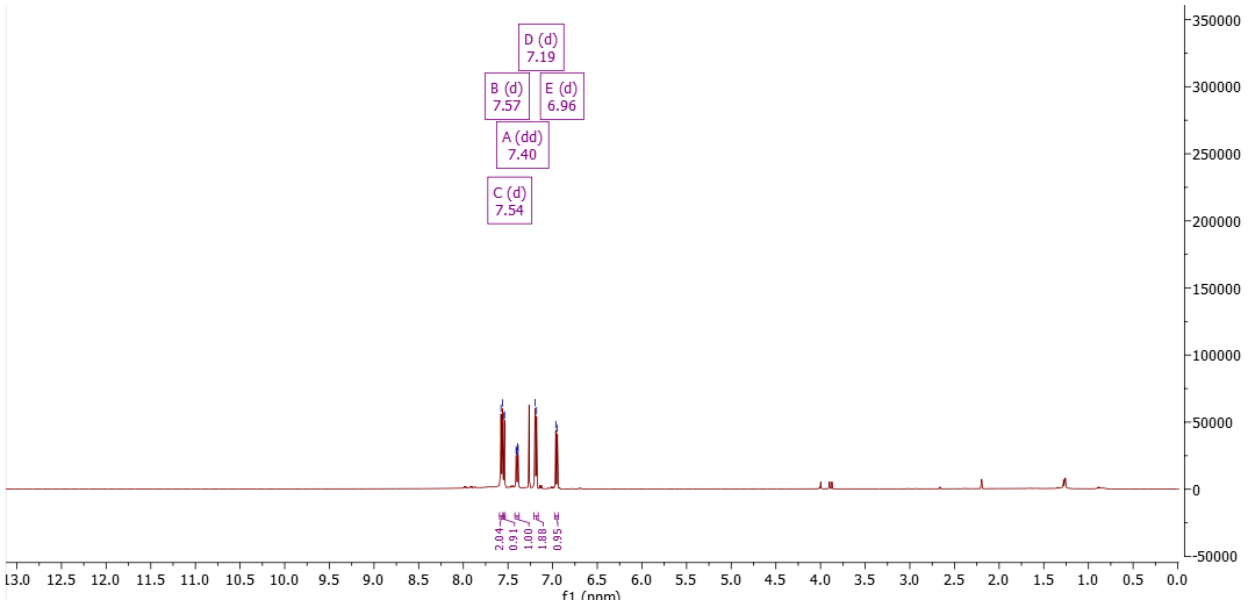

Figure S11 ^{1}H NMR spectrum of compound **6**

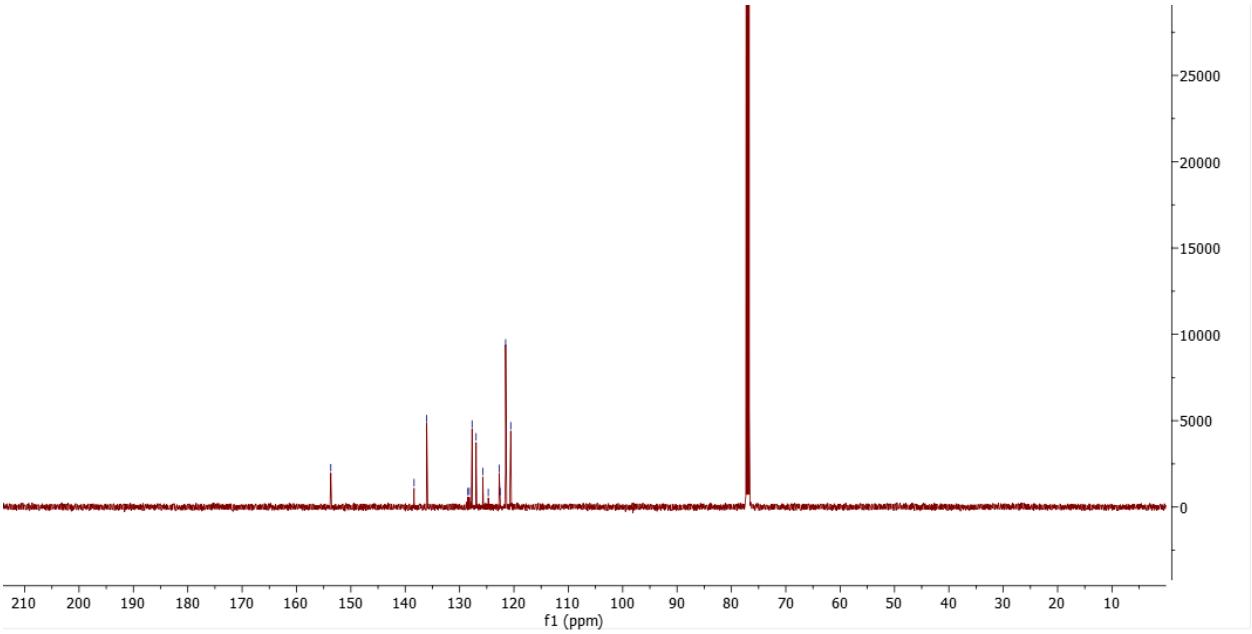

Figure S12 ^{13}C NMR spectrum of compound **6**

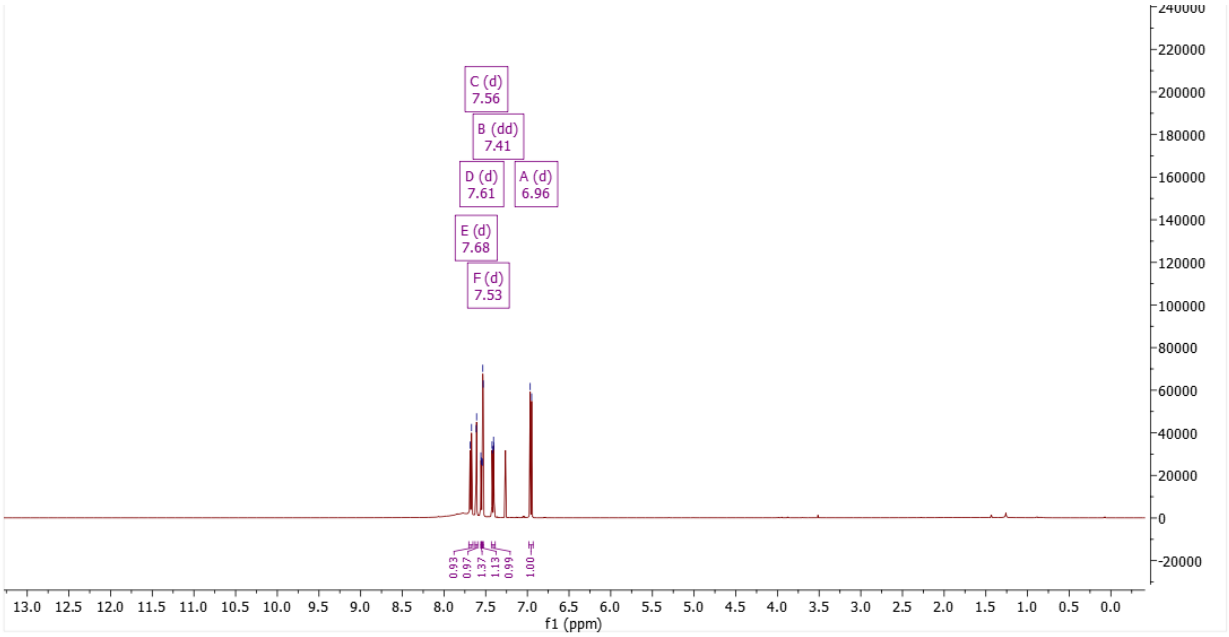

Figure S13 [1]H NMR spectrum of compound **7**

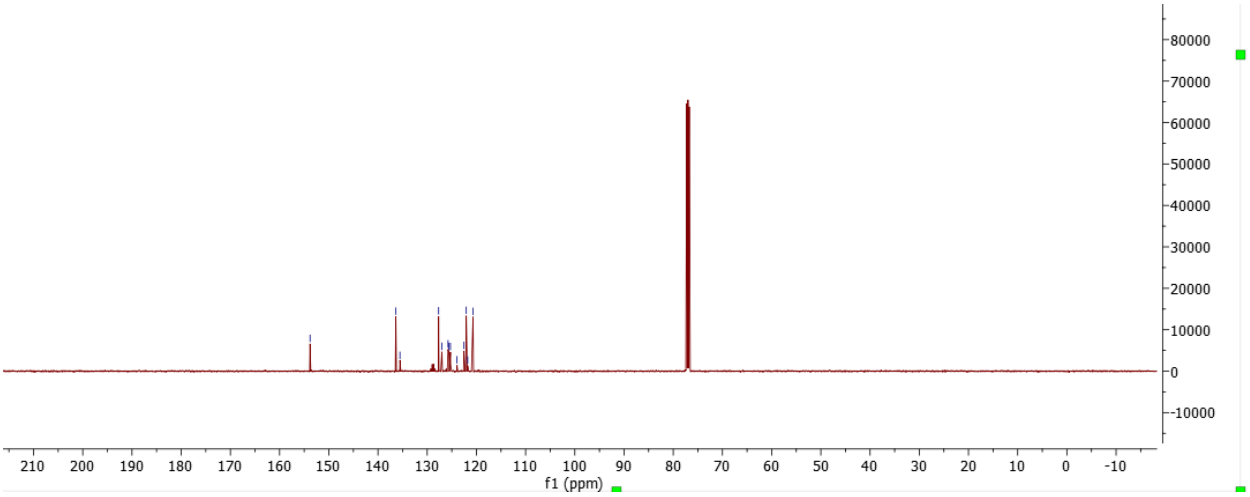

Figure S14 [13]C NMR spectrum of compound **7**

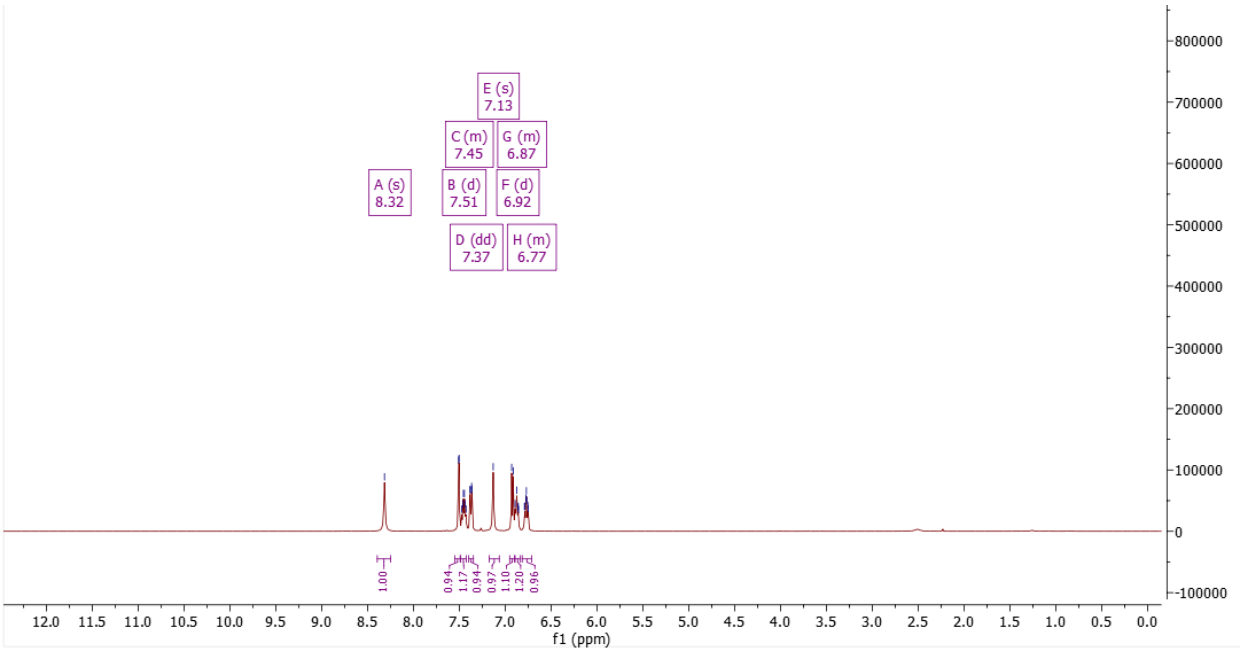

Figure S15 ^{1}H NMR spectrum of compound **8**

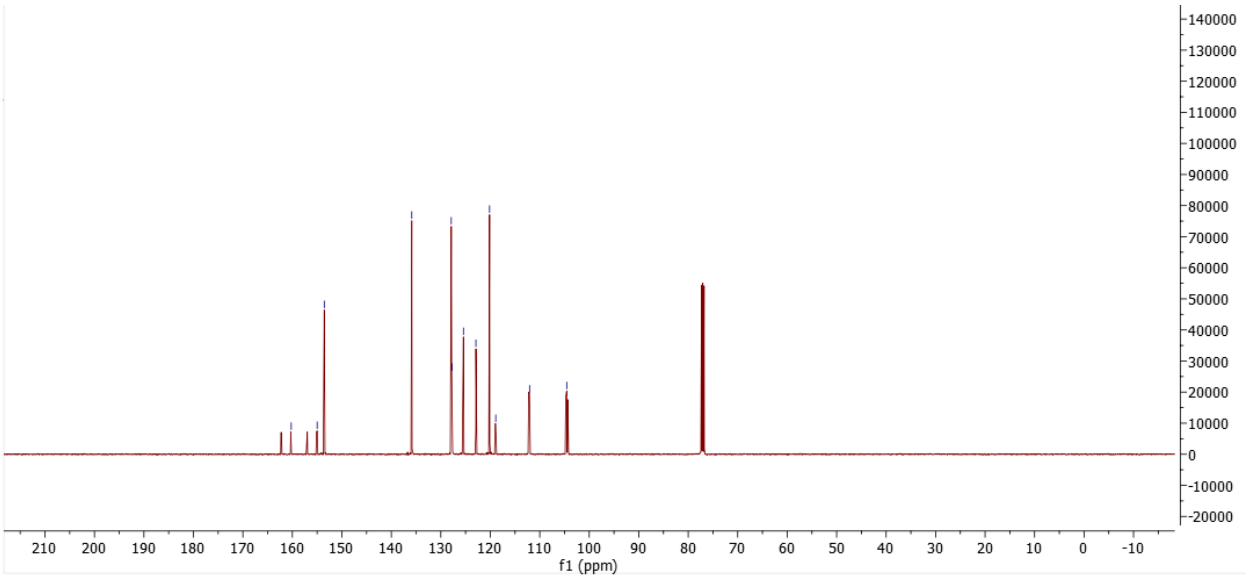

Figure S16 ^{1}H NMR spectrum of compound **8**

Extended Biological Data

Table S1 Minimum inhibitory concentration (MIC) in μg/mL of compounds **1-8** against 4 colistin-resistant strains of GNB. KP = *Klebsiella pneumoniae,* EC = *Escherichia coli*.

Compound	KP113250	KP113254	EC94393	EC94474
1	>128	>128	>128	>128
2	>128	>128	>128	>128
3	>128	>128	>128	>128
4	>128	>128	>128	>128
5	>128	>128	>128	>128
6	>128	>128	>128	>128
7	>128	>128	>128	>128
8	>128	>128	>128	>128